Iron and Lead Corrosion in WIPP-Relevant Conditions: Six Month Results

Gregory T. Roselle

Repository Performance Dept. 6712
Sandia National Laboratories
Carlsbad Programs Group
Carlsbad, NM 88220

WIPP:1.4.2.2:TD:QA-L:Recert:546084

APPROVAL PAGE

Author:	Gregory T. Roselle, 6712	10/7/2009 Date
Technical Reviewer:	Je-Hun Jang, 6712	10/7/09 Date
QA Reviewer:	Janis Trone, 6710	10/7/09 Date
Management Reviewer:	Christi Leigh, 6712	10/7/09 Date

TABLE OF CONTENTS

LIST OF FIGURES

LIST OF TABLES

DEFINITION OF ABREVIATIONS, ACRONYMS AND INITIALISMS

Abbreviation or Acronym	Definition
ASTM	American Society for Testing and Materials
CH	contact handled
CH_4	methane
CO_2	carbon dioxide
CPR	cellulosic, plastic, and rubber
CRA	compliance recertification application
DAS	data acquisition system
DI	de-ionized
DOE	Department of Energy
EDS	energy dispersive spectroscopy
EDTA	ethylenediaminetetraacetic acid
EPA	Environmental Protection Agency
ERDA-6	Energy Research and Development Administration (WIPP Well) 6. Synthetic Castile Formation brine
ES&H	Environmental Safety and Health
f_{CO2}	fugacity of carbon dioxide
FMT	Fracture-Matrix Transport, a geochemical speciation and solubility code
GWB	Generic Weep Brine, a synthetic Salado Formation brine.
H_2	hydrogen gas
H_2S	hydrogen sulfide
HSLA	high-strength, low-alloy
ISO	International Standards Organization
m	molal (mol/kg)

Abbreviation or Acronym	Definition
M	molar (mol/L)
MFGCS	mixed-flow gas control system
N_2	nitrogen gas
NACE	National Association of Corrosion Engineers
NP	Nuclear Waste Management Procedure
PA	performance assessment
QA	quality assurance
PABC	(WIPP) performance assessment baseline calculations
RH	remote handled
SEM	scanning electron microscopy
SNL	Sandia National Laboratories
TP	test plan
TRU	Transuranic
TSP	Trisodium phosphate
WIPP	Waste Isolation Pilot Plant
XRD	X-ray diffractometer

1 INTRODUCTION

The Waste Isolation Pilot Plant (WIPP) is a deep geologic repository developed by the U.S. Department of Energy (DOE) for the disposal of transuranic (TRU) radioactive waste. The WIPP repository is located within the bedded salts of the Permian Salado Formation, which consists of interbedded halite and anhydrite layers overlaying the Castile Formation. Containment of TRU waste at the WIPP is regulated by the U.S. Environmental Protection Agency (EPA) according to requirements set forth in Title 40 of the Code of Federal Regulations (CFR), Part 191. The DOE demonstrates compliance with containment requirements by means of performance assessment (PA). WIPP PA calculations are used to estimate the probability and consequence of radionuclide releases from the repository to the accessible environment for a regulatory period of 10,000 years after facility closure.

The WIPP PA includes modeling the consequences of future inadvertent human intrusions into the repository by drilling for resources. Such intrusions could lead to a postulated release of radionuclides to the accessible environment before the end of the 10,000 year regulatory period. To accomplish this, the DOE has examined different drilling scenarios, which involve the penetration of the repository by one or more drill holes; some of the scenarios also involve the possibility of the penetration of a pressurized Castile brine reservoir (U.S. DOE, 2009). The estimated quantity of radionuclides released to the accessible environment following penetration of the repository depends on the chemistry of these radioelements. For example, plutonium (Pu) is less soluble when it speciates in lower oxidation states, such as Pu(III) and Pu(IV), than in higher oxidation states, such as Pu(VI). Thus it follows that in order to minimize the release of such radionuclides from the repository it is desirable to maintain all such species in their least-soluble form (i.e., low oxidation states).

The nature of the environment within the WIPP following closure will, to a large extent, control the speciation of the radionuclides within the waste. More specifically, there are components contained within the waste that can impact the oxidative or reductive nature of the environment, such as metals undergoing active corrosion. If metals undergo active corrosion within the WIPP, the corrosion process will serve to maintain electrochemically reducing conditions. The predominant metals within the WIPP will be iron (Fe) in the form of low-carbon steel and lead (Pb). These metals are present within the waste itself, as well as the containers used to hold the waste during emplacement. The current inventory predicts that 280 and 599 kg/m^3 of Fe and Fe-base alloys will be present in the contact handled (CH) and remote handled (RH) wastes, respectively. Also 0.013 and 420 kg/m^3 of Pb will be present in the CH and RH wastes, respectively (Crawford 2005). The corrosion behavior of these materials, specifically the kinetics of the corrosion reaction, will be controlled by the availability of water (in brine) at the metal surface, as well as the internal atmosphere within the WIPP.

In addition to Fe and Pb, the waste disposed within WIPP contains significant quantities of cellulosic, plastic and rubber (CPR) materials. With time, microbial activity may consume some portion of the CPR materials, resulting in generation of significant quantities of carbon dioxide (CO_2), hydrogen sulfide (H_2S), hydrogen (H_2), nitrogen (N_2) and methane (CH_4). Some of these gasses, namely CO_2 and H_2S, may interact with the metallic Fe and Pb, altering their electrochemical behavior. Elevated concentrations of both gasses have been demonstrated to passivate Fe under certain conditions due to the formation of corrosion products on the surface of the metal (Telander and Westerman, 1993; 1997). If the Fe and Pb within the WIPP are passivated, the corrosion process will be stifled and electrochemically reducing conditions will no longer be maintained by the corrosion process. Under these conditions, Fe and Pb would not be available to prevent oxidation of the radionuclides, although other reductants may still be available.

The microbially-produced CO_2 also has the potential to significantly affect the mobility of actinides in other ways. The presence of CO_2 will acidify any brine present in the repository and increase the solubilities of the actinides (Appendix SOTERM, U.S. DOE, 2009). For this reason the DOE emplaces magnesium oxide (MgO) into the repository to buffer the f_{CO2} and pH within ranges that favor lower actinide solubilities. The f_{CO2} of the WIPP environment will be buffered by the MgO carbonation reaction:

$$5\ Mg(OH)_2\ (s) + 4\ CO_2\ (aq \text{ or } g) \Leftrightarrow Mg_5(CO_3)_4(OH)_2 \cdot 4\ H_2O\ (s) \quad (1)$$

where $Mg(OH)_2$ (brucite) is the main hydration product of the mineral periclase (MgO) expected in the WIPP and $Mg_5(CO_3)_4(OH)_2 \cdot 4\ H_2O$ is the form of the mineral hydromagnesite predicted by the repository models. The pH of brines possibly present in the WIPP is buffered by the brucite dissolution reaction:

$$Mg(OH)_2\ (s) \Leftrightarrow Mg^{2+}\ (aq) + 2\ OH^-\ (aq) \quad (2)$$

Laboratory and modeling studies (Appendix MgO, Table MgO-6, U.S. DOE, 2009) indicate that reaction (1) will buffer the f_{CO2} in the WIPP at a value of $10^{-5.50}$ atm and that reaction (2) will buffer pH in the WIPP at a value of 8.69 in Generic Weep Brine (GWB) and 8.94 in Energy Research and Development Administration (WIPP Well) 6 Synthetic Castile Formation brine (ERDA-6). The large quantities of Fe and Pb present in WIPP may also contribute to the consumption of microbially generated gases, primarily through the formation of carbonates and sulfides. After the limited concentration of O_2 trapped within the repository at the time of closure is depleted via the corrosion process and the aerobic microbial consumption of CPR materials, it has been hypothesized that anoxic corrosion of Fe and Pb will occur (Brush, 1990). The WIPP-specific experiments of Telander and Westerman (1993, 1997) have verified this hypothesis.

The experimental work reported in this document assesses the corrosion behavior of carbon steel and Pb alloys used to contain CH and RH waste under WIPP-relevant conditions. More specifically, the objective is to determine to what extent these alloys consume CO_2 through the formation of carbonates, potentially supporting MgO in its role of CO_2 sequestration. This work is being conducted under the test plan “Iron and Lead Corrosion in WIPP-Relevant Conditions, Test Plan TP 06-02”.

The following report documents the six month results from this multi-year experimental work. Additional reports will follow as more coupons are removed from the experiments at six month intervals.

2 EXPERIMENTAL APPROACH

The purpose of these experiments is to assess the corrosion behavior of carbon steel and Pb alloys used to contain CH and RH waste under WIPP-relevant conditions. Specifically, the experiments aim to determine the corrosion rates of these metals and the nature of the corrosion products that will form. The environmental conditions and samples used for this set of experiments are set up to be representative of the conditions that are expected in the WIPP following its closure. During these experiments steel and lead coupons will be immersed in different WIPP-relevant brines or hung in WIPP-relevant atmospheric conditions for a period of two years. A subset of samples will be removed from the experiments for analysis at six month intervals. The following subsections describe the types of metal coupons used and the environmental conditions employed in the experiments.

2.1 Test Coupons

In general, four different container forms are used to dispose of CH waste within the WIPP: drums (55, 85 and 100 gallons in size), standard waste boxes, ten drum overpacks and standard large boxes. These containers are constructed using a range of different carbon and high-strength, low alloy (HSLA) steels. Wall and Enos (2006) have shown that the majority of the steel present in the WIPP (from waste containers) will be of a composition defined either by ASTM A36, ASTM A1008 or ASTM A1011 with by far the largest quantity (approximately 94%) being defined by ASTM A1008, which is used for waste drums. The steels specified in A1008 and A1011 are similar with the exception of the method of production. A1008 is cold-rolled whereas A1011 is hot-rolled. While this will yield different mechanical properties, it has been shown by Telander and Westerman (1993, 1997) that the two will behave similarly in WIPP-relevant brine corrosion tests. ASTM A36 steels differ in composition from the other two in that they have higher C, Mn and Si contents, although A36 steels are still classified as low carbon steels. While it would be interesting to study the effects of brine corrosion over the entire range of steel compositions present in the WIPP, the number of coupons required would be prohibitive. Therefore, only one steel composition (ASTM A1008) was chosen for evaluation in this study. It should be noted that the use of only ASTM A1008 steel is a deviation from the test plan (TP 06-02), which calls for ASTM A36 to be used as well.

The ASTM A1008 steel coupons were obtained from a commercial vendor (Alabama Specialty Products, Inc., Munford, AL) under the Nuclear Waste Management Procedure (NP) 4-1. The certified composition of the steel coupons is given in Table 2-1. The coupons are 2 x 1.5 x 1/16 inches with a 3/16 inch diameter hole centered 0.25 inches from the end of the coupon. The coupon surfaces have been finished to 120 grit.

Table 2-1 Composition of ASTM A1008 Low-Carbon Steel

Element	Weight Percent
Al	0.026
C	0.050
Ca	0.001
Cr	0.040
Cu	0.110
Fe	balance
Mn	0.250
Mo	0.010
N	0.009
Nb	0.003
Ni	0.040
P	0.006
S	0.005
Si	0.010
Sn	0.007
Ti	0.002
V	0.002

Source: Material Test Report for AE960 (ERMS 551552)

The estimated quantity of Pb present in the repository from both the waste and its containers is 3.0 x 106 kg (Wall and Enos, 2006, Section 7.5.2). The vast majority of this Pb is contained in the lids of the packaging and not in the waste itself. Additionally, the DOE has proposed the use of shielded (Pb-lined) containers in the WIPP, which will dramatically increase the mass of Pb emplaced in the WIPP. If approved, the use of shielded containers could increase the mass of Pb by nearly ten-fold to 2.7 x 107 kg (Dunagan et al., 2008). The drawings for neither the current RH containers (Hertelendy, 1984) nor the proposed shielded containers (Sellmer, 2007) specify the Pb alloy to be used. Several specifications exist for Pb alloys. This includes the military specification QQ-L-171e, which in turn calls ASTM B29. This alloy is defined as chemical-copper lead and is nominally 99.9% Pb. The specific Pb alloy chosen for this study is the military specification Grade C, which is specified for chemical use. Lead coupons were obtained from Medi-Ray, Inc. (Tuckahoe, NY) also under NP 4-1. The certified composition of the lead coupons is given in Table 2-2. Lead coupon dimensions and surface finishing are the same as for the steel coupons.

Table 2-2 Composition of Chemical Lead (QQ-L-171e Grade C)

Element	Weight Percent
Ag	0.010
Bi	0.015
Cd	0.001
Cu	0.070
Fe	0.001
Ni	0.001
Pb	99.900
Sb+Sn+As	0.001
Zn	0.001

Source: Certificate Of Compliance and Inspection Metal Coupon, Lot 32829 (ERMS 551551)

2.2 Environmental Conditions

The environmental conditions used for this set of experiments are set up to be representative of the conditions that are expected in the WIPP following closure. These conditions include temperature, relative humidity, atmosphere and sample positioning.

The post-closure temperature within the waste disposal panels at WIPP is assumed to be 28°C. This is based on in-situ temperature measurements made within WIPP Room H (Munson et al., 1987). However, in the Fe/Pb corrosion experiments a temperature of 26°C is used because it is easier to control the relative humidity within the experiments at 26°C instead of 28°C. It is assumed that a 2°C reduction in the experimental temperature will have no effect on the corrosion rates in the experiments. Note that this is a deviation from the test plan, TP 06-02.

Brush (2005) conducted a series of FMT calculations for each of the brines expected in the WIPP. Those calculations show that the equilibrium relative humidity present in the headspace over each of these brines is effectively equivalent at 72%. Based on these calculations, the relative humidity in the Fe/Pb corrosion experiments will be maintained at 72% ±10%.

As stated previously the predicted atmosphere within the WIPP will be anoxic due to the consumption of O_2 by corrosion of metals within the WIPP. In addition, the microbial consumption of the CPR materials in the waste will produce a combination of inert (e.g. N_2 and

CH_4) and active (e.g. CO_2 and H_2S) gases. In the Fe/Pb corrosion experiments N_2 is substituted for CH_4 as the inert carrier gas to ease Environmental Safety and Health (ES&H) concerns. Although the test plan (TP 06-02) covering these experiments calls for the use of H_2S, no experiments are being conducted at this time with H_2S due to ES&H concerns. Four different atmospheric compositions are being used in these experiments to investigate the effect of CO_2 concentration on the corrosion rates. The four atmospheres are 0 ppm CO_2 (100% N_2), 350 ppm CO_2, 1500 ppm CO_2 and 3500 ppm CO_2. The O_2 concentration in each of the experimental lines is maintained to values less than 5 ppm.

Due to the limited quantity of brine that is predicted to permeate into the waste, it is reasonable to assume that not all of the material will come into contact with liquid brine. Thus, the two coupon types described in Section 2.1 will be evaluated while fully inundated by the brine, partially submersed in the brine and while exposed only to the humid atmosphere above the brine.

2.3 Experimental Brines

Two brines are predicted to come into contact with the waste over time. These brines are referred to as ERDA-6 and GWB. Both of these brines are synthetic in that they represent an average composition based on numerous brines collected from the field. ERDA-6 is representative of brines present in the Castile Formation, whereas GWB represents Salado Formation brines. Once either of these brines is introduced into the WIPP they will equilibrate with the engineered barrier (MgO) and the host rock (primarily halite and anhydrite). The compositions of GWB and ERDA-6 equilibrated with periclase (MgO), halite and anhydrite are given in the results of FMT calculations completed for the CRA 2005 PABC. The brines used in the Fe/Pb corrosion experiments were synthesized based on the predicted composition from FMT Runs 8 (GWB) and 12 (ERDA-6) (see Table 4 in Brush, 2005). The composition of the brines formulated for use in the experiments is given in Table 2-3.

Table 2-3 Synthesized Composition of GWB and ERDA-6 Brines Used in Steel/Pb Corrosion Studies

Chemical Species	GWB Concentration (molal)	ERDA-6 Concentration (molal)
Na^+	4.98	6.05
K^+	0.559	0.109
Li^+	5.05×10^{-3}	---
Ca^{2+}	1.24×10^{-2}	1.28×10^{-2}
Mg^{2+}	0.635	0.121
Cl^-	6.30	6.00
Br^-	3.18×10^{-2}	1.24×10^{-2}
SO_4^{2-}	0.209	0.191
$B_4O_7^{2-}$	4.73×10^{-2}	1.77×10^{-2}

Source: WIPP-FePb-3 p. 51 (ERMS 550783)

The WIPP waste will contain significant amounts of acetate, citrate, EDTA and oxalate at closure time. Brush and Xiong (2005) calculated the concentration of these ligands for the CRA 2005 PABC. These ligands are important to consider for the WIPP PA, as they influence the solubility of actinides in the WIPP. Additionally, there are indications in the literature that all of these organic ligands can have a significant impact on the electrochemical behavior of both Fe and Pb (e.g., Saltykov et al., 1989; Sankarapapavinasam et al., 1989a, 1989b; Kubal and Panacek, 1995; Pletcher et al., 2005). While none of these studies have evaluated the impact that low concentrations will have in WIPP relevant brines, they strongly suggest that the organic ligands may have an impact on the corrosion process.

Thus, the Fe/Pb corrosion experiments will also be done in GWB and ERDA-6 with organic ligand concentrations equal to those given in Brush and Xiong (2005) except for the oxalate species. The oxalate concentration given in Brush and Xiong (2005) was determined by taking the total mass of oxalate present in the waste and dividing by the minimum brine volume necessary for a release in the PA calculations. However, this value is above the solubility limit for oxalate, as predicted by the FMT calculations. Therefore, the oxalate concentration used in the Fe/Pb corrosion experiments was set equal to the predicted concentration in ERDA-6, which is lower than that predicted for GWB. Table 2-4 lists the concentrations of the brines synthesized with organic ligands that are used in this study. The major element compositions are slightly different from those in Table 2-3 because of the addition of the organic salts needed to synthesize these brines.

Table 2-4 Composition of GWB and ERDA-6 with Organic Ligands Synthesized for Use in Steel/Pb Corrosion Studies

Chemical Species	GWB Concentration (molal)	ERDA-6 Concentration (molal)
Na^+	4.99	5.96
K^+	0.563	0.109
Li^+	5.05×10^{-3}	---
Ca^{2+}	1.03×10^{-2}	1.22×10^{-2}
Mg^{2+}	0.663	0.179
Cl^-	6.24	5.98
Br^-	3.19×10^{-2}	1.24×10^{-2}
SO_4^{2-}	0.262	0.203
$B_4O_7^{2-}$	4.76×10^{-2}	1.77×10^{-2}
EDTA	8.85×10^{-6}	9.99×10^{-6}
Oxalate	3.38×10^{-4}	3.35×10^{-4}
Citrate	9.09×10^{-4}	9.04×10^{-4}
Acetate	1.19×10^{-2}	1.19×10^{-2}

Source: WIPP-FePb-3 p. 52 (ERMS 550783)

Test plan, TP 06-02 calls for the use of eight different brines in the Fe/Pb corrosion experiments. These eight brines include the four described above as well as the same brines without equilibration with MgO. In order to reduce the number of experiments to a more manageable number it was decided to only use those four brines that were equilibrated with MgO, which is a deviation from the original matrix in the test plan.

2.4 Experimental Test Matrix

The entire range of experimental variables is summarized in Table 2-5. This combination of experimental conditions, material types and time segments results in 288 unique experiments. In addition, three replicate coupons are used for each of the experimental conditions resulting in a total of 864 coupons (432 for lead and 432 for steel).

Table 2-5 Experimental Test Matrix

Condition	Variable	Matrix Identifier
Material Type	ASTM A1008 Steel	Fe
	QQ-L-171e Grade C Lead	Pb
Brine	GWB	G
	GWB with organics	Go
	ERDA-6	E
	ERDA-6 with organics	Eo
Sample Positioning	Fully Innundated	f
	Partially Submerged	p
	Humid Atmosphere	Atm
Atmosphere	0 ppm CO_2 (balance N_2)	0000
	350 ppm CO_2 (balance N_2)	0350
	1500 ppm CO_2 (balance N_2)	1500
	3500 ppm CO_2 (balance N_2)	3500
Time Segment	6 months	6
	12 months	12
	18 months	18
	24 months	24
Fixed Properties	Temperature – 26 °C	--
(constant for all experiments)	Relative Humidity – 75% ± 10%	--
	O_2 concentration < 5 ppm	--

Note: [2 Material types × 4 Brines × 2 Positions (wet) × 4 Atmospheres × 4 Time segments] + [2 Material type × 1 Position (humid) × 4 Atmospheres × 4 Time segments] = 288 experiments

Also shown in Table 2-5 are the matrix identifiers used in formulating unique sample numbers. The naming convention used follows this format: Aa-Bb-#### - X – Yz, where Aa is the material type, Bb the brine (or “Atm” for humid samples), #### the atmosphere, X the time segment, Y the replicate number (1 to 3) and z the sample position (left blank for humid position). Thus, sample number Fe-Go-1500-6-1f indicates the first replicate of a steel coupon fully inundated in GWB organic brine in a 1500 ppm CO_2 atmosphere for six months.

3 EXPERIMENTAL METHODS

3.1 Mixed Flow Gas Control System

Previous corrosion experiments (e.g., Telander and Westerman, 1993; 1997) have been conducted in closed systems in which the atmosphere in the experiments changes as a function of corrosion. This method uses measurements of the head gas composition to estimate the amount and type of corrosion occurring in the experiments. However, such experiments result in head space gas compositions that change over time and may not reflect the expected conditions in the WIPP after closure. Therefore, the current Fe/Pb corrosion experiments are being conducted in a continuous flow setup that allows the atmospheric composition to be fixed at constant values. A specially-built gas flow system known as the Mixed Flow Gas Control System (MFGCS) is being used to house the experiments. The MFGCS is a continuous flow system designed to create and maintain a controlled environment for the Fe/Pb corrosion experiments. The variables controlled by the MFGCS include the oxygen level, humidity level and N_2/CO_2 gas concentrations. The system is continuously monitored real time by a data acquisition system (DAS) to continuously assess various experimental and operational parameters. The MFGCS consists of three subsystems: 1) gas supply and automatic change over units; 2) gas distribution panel and flow controllers; and 3) saturation vessel, condensation flask, specimen test chambers and instrumentation. The specific details of the MFGCS can be found in MFGCS System Pressure Safety Package (Schuhen, 2007).

The gas supply and automatic change over units consists of three sections each supplying a different type of gas (see Figure 3-1). The first system is the pure N_2 supply, which uses a liquid nitrogen Dewar as the primary N_2 source. The primary N_2 source is backed up by a secondary N_2 supply consisting of three gas cylinders of pre-purified nitrogen. The primary and secondary gas supply lines are run through an automatic gas change over unit. The change over unit automatically switches from the primary to secondary gas source if the primary source is depleted during non-work hours. The second system is the CO_2/N_2 blend supply line, which is used to maintain the required experimental gas compositions. This system also contains primary and secondary gas sources that are plumbed through an automatic gas change over unit. Both the primary and secondary gas sources use 2.5% CO_2 gas cylinders. The third system is the calibration gas supply manifold. This system is only used when specific gases are needed to calibrate the CO_2 analyzer.

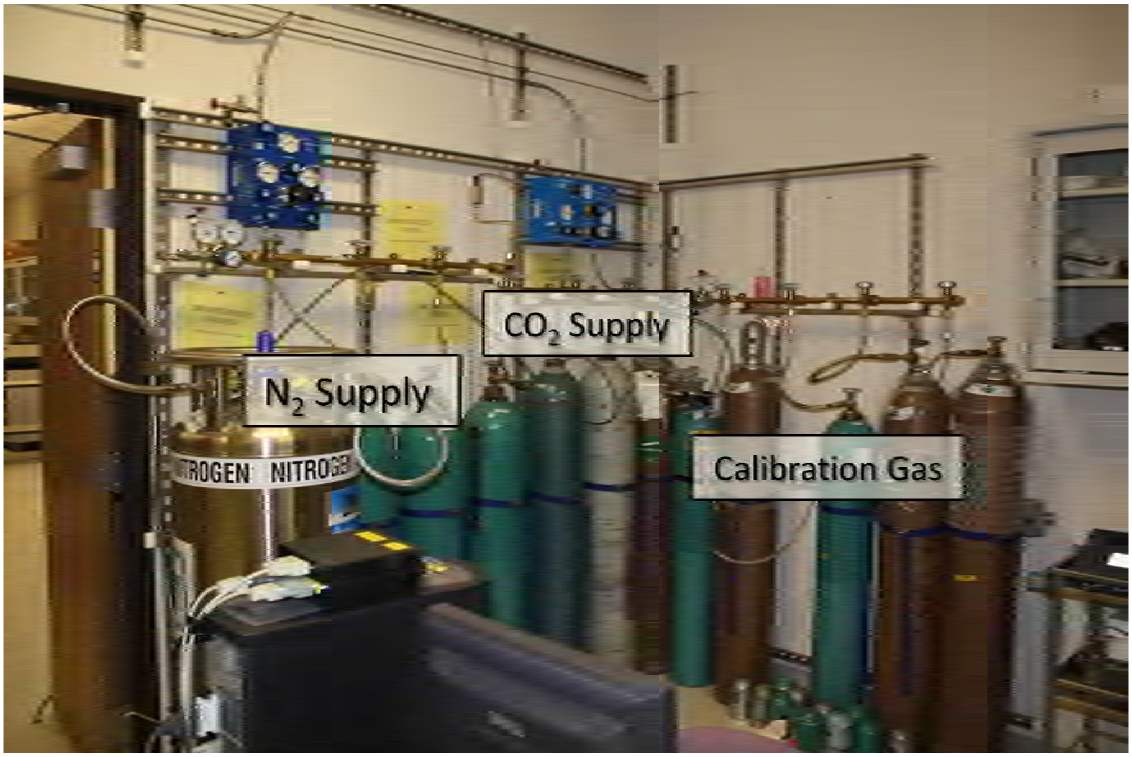

Figure 3-1 MFGCS Gas Supply and Automatic Change Over System. The three subsystems are (left to right): the N_2 supply, the CO_2/N_2 blend supply, and the calibration gas supply.

The second subsystem on the MFGCS is the gas distribution panel and flow controllers (see Figure 3-2). The gas distribution panel provides a centralized location for selecting and controlling the various gases from the gas supply and automatic change over system. The panel includes a set of oxygen traps for each gas stream. These traps will remove trace amounts of oxygen from the gas supplies upstream from the specimen chambers. The output of the gas distribution panel is routed to the various flow controllers located in an adjacent panel. The flow controllers are used to adjust flow rates of the gas streams thereby setting the composition of the gases in the experimental gas lines to the CO_2 concentrations required for the experiments. At this point the N_2 gas stream is split into two separate flow streams, which will be used for humid and dry gas in the third subsystem.

Figure 3-2 MFGCS Gas Distribution Panel (right) and Flow Controllers (bottom left).

The final subsystem for the MFGCS consists of the saturation vessels, condensation flasks, specimen test chambers and instrumentation. This subsystem includes all of the components between the output of the flow controllers through to the exhaust system. The three gas streams exiting the flow controllers are input into this subsystem. The first two streams, the mixed CO_2/N_2 and one of the N_2 streams, are routed directly from the flow controllers to a mixing chamber located inside an incubator. The third gas stream of N_2 is routed through saturation vessel into a condenser (located within the incubator) and then to the mixing chamber. The mixing chamber is where the dry N_2 and humid N_2 are mixed with the mixed CO_2/N_2 gas to produce a final gas stream with the desired relative humidity and CO_2 concentration. From the mixing chamber the gas stream is routed into the specimen test chamber. Each experimental line consists of 8 test chambers that are connected serially to the gas stream (see Figure 3-3). The test chambers were designed and built by SNL staff from acrylic tubing. The acrylic tubing used has a ½" wall thickness with an inside diameter of seven inches. Two end caps made of the same ½" acrylic material were machined to attach to the ends of the tubes using machine screws.

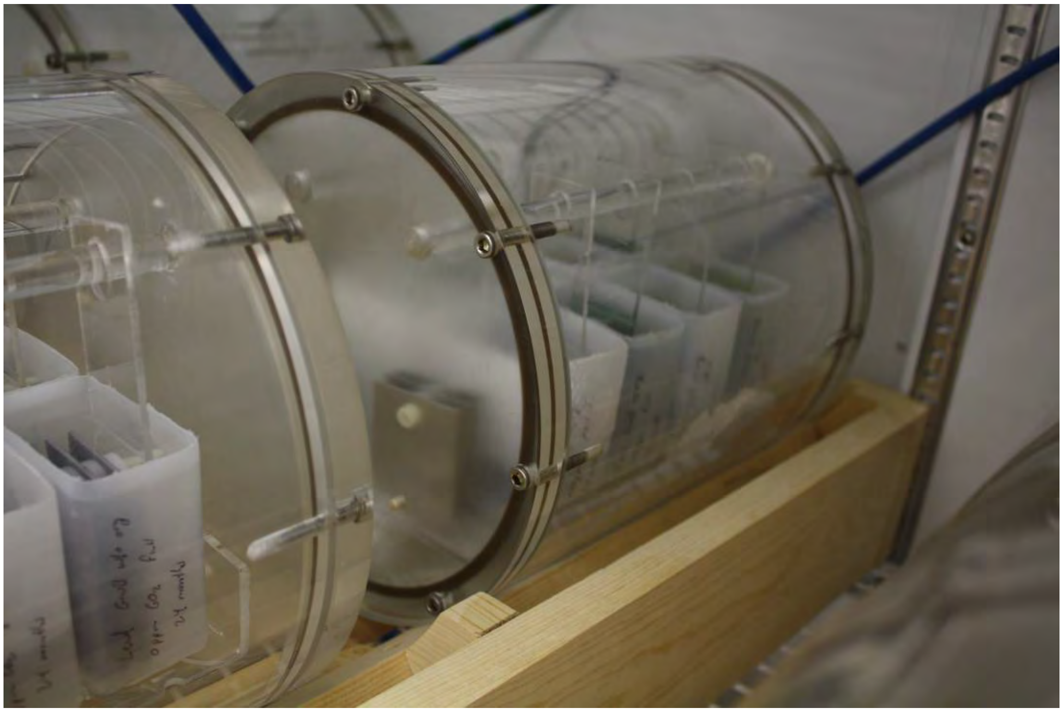

Figure 3-3 Specimen test Chambers inside the Incubator

After the gas stream exits the test chambers it is routed through a Protimeter chilled mirror sensor that will measure the relative humidity of the gas stream. Following the chilled mirror sensor, the gas is routed through an oxygen sensor manufactured by Delta F Corporation. From the oxygen sensor all of the process gas streams are plumbed into a solenoid valve manifold. These gas streams are then fed (one at a time) into a single California analytical CO_2 analyzer. Upon exiting the CO_2 analyzer the gas stream is vented to the outside.

3.2 Coupon Preparation

Prior to emplacement in the experiments each coupon was measured, cleaned and pre-weighed. All measurements were recorded in the appropriate scientific notebook. Coupons were measured using a Fowler digital caliper to an accuracy of ±0.025 mm. For each coupon three measurements of the width, length and thickness were made. The averages of these three measurements were then used to calculate the surface area for each coupon (see Appendix A). The pre-cleaning processes used for the steel and lead coupons were based on recommendations in ASTM G1-03 (ASTM, 2003). Steel coupons were cleaned by degreasing with a commercially available TSP (trisodium phosphate) substitute followed by rinsing with de-ionized (DI) water. Coupons were then rinsed with ethanol and allowed to air dry. Lead coupons were cleaned by degreasing with the TSP substitute solution and then immersed in a solution of boiling 1% acetic acid for two minutes. After boiling, the coupons were submerged in a beaker of DI water until all coupons had been cleaned in the acid solution. The beaker containing the submerged coupons was then placed into an anoxic glovebox. The lead coupons were then removed from the DI water and allowed to air dry under anoxic conditions. This step was necessary because air drying in the laboratory produced immediate oxidation of the lead coupons. Once the coupons were dry they could then be removed from the glovebox for further preparation. After cleaning, the mass of all coupons was determined to an accuracy of 0.0001 grams. Coupons were then photographed front and back. Figure 3-4 shows the typical appearance of steel and lead coupons after cleaning. All coupons were stored inside a desiccator in the anoxic glovebox until loaded in a sample test chamber.

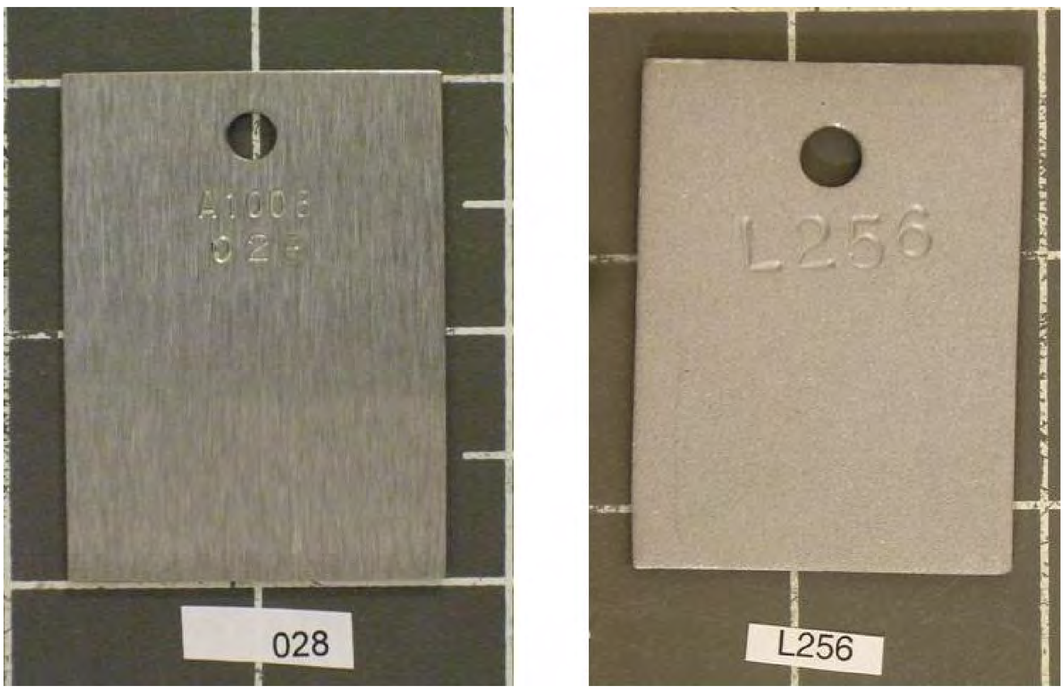

Figure 3-4 Typical appearance of steel (left) and lead (right) coupons after cleaning.

3.3 Sample Loading

After the preparation steps outlined in Section 3.2, the coupons are ready to be placed into the sample test chambers described in Section 3.1. The sample test chambers were placed into the anoxic glovebox with the coupons and all loading/unloading operations are done inside the glove box. There are eight sample chambers used for each of the four experimental gas streams (e.g. 0 ppm CO_2, 350 ppm CO_2, etc.): four chambers for Pb coupons (one for each of the four time segments) and four for steel coupons. Each test chamber includes eight HDPE containers for the brines (four for fully immersed and four for partially submerged coupons). The three replicate coupons for each setup are separated by nylon spacers and attached to an acrylic hanger with a nylon machine bolt. Each set of replicate coupons is placed into the same brine container. The brine containers are filled with approximately 120 mL of the appropriate brine for the fully immersed replicates and 75 mL of brine for the partially submerged replicate sets. The humid atmosphere set of replicates are hung from the top of the chamber at the end of the brine buckets. A typical setup of a sample test chamber is shown in Figure 3-5. Once the chamber has been loaded the end cap is sealed into place and the chamber is removed from the glove box and attached to the MFGCS.

Figure 3-5 Partially loaded sample chamber inside the anoxic glove box. A second row of brine containers will be placed into the chamber and then the humid atmosphere replicates will be hung at the end of the chamber.

3.4 Removal and Unloading of Sample Chambers

At the conclusion of the experiment a sample chamber is disconnected from the MFGCS and placed into the anoxic glove box. Once the chamber is in the glove box its end cap is removed and the brine containers with the coupon hangers are taken out of the sample test chamber. The coupon replicate set is then removed from the brine and given a light rinse with DI water to remove any residual brine on the coupons. The hanger with the replicate coupons is then set aside and allowed to air dry inside the glove box for several hours. Once the coupons are removed from the brine container the pH of the brine is measured. The brine is then poured in a glass serum bottle and the bottle is sealed and crimped. All brine bottles are stored in the glove box for later chemical analysis.

After the replicate coupon sets have dried the three coupons are removed from the hangers. Two of the three replicates will be used to determine the weight loss during the experiments. The process used to determine weight loss is discussed below in Section 4.4. The third replicate coupon is used for characterizing the corrosion products that formed. Each coupon is photographed prior to being cleaned for the weight loss measurements or material characterization activities. Coupons are stored inside the glove box until needed for analysis.

4 EXPERIMENTAL RESULTS

4.1 Steel Coupon Post-Experimental Appearance

After six months of exposure in the various brines and atmospheres most of the coupons show clear signs of corrosion. The following figures illustrate the general trends observed among the different experimental conditions. Regardless of the CO_2 concentration, none of the coupons that were exposed only to the humid environment show any clear sign of corrosion. Figure 4-1 shows that there is no obvious change in appearance over the six month exposure period.

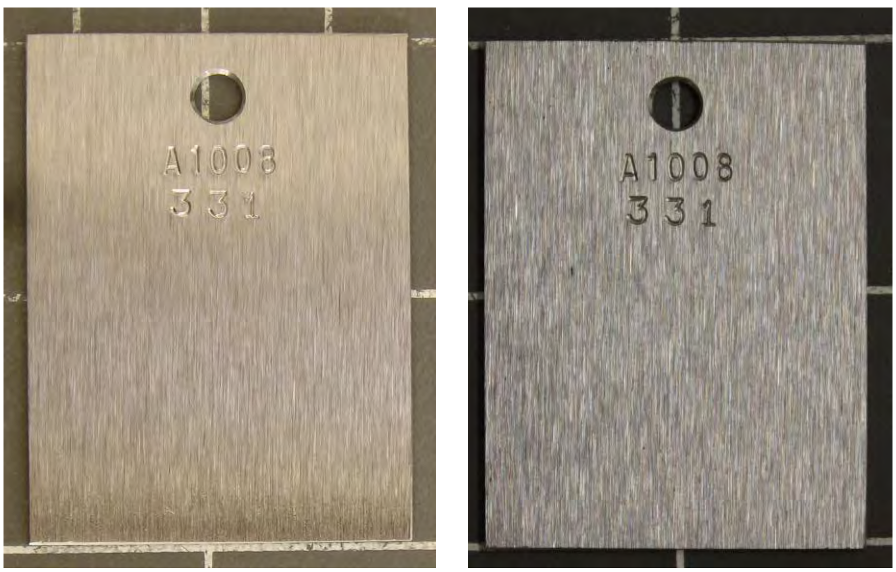

Figure 4-1 Images of steel coupon exposed to humid 1500 ppm CO_2 atmosphere. Left image shows coupon prior to experiments, right image shows coupon after six months exposure.

Figure 4-2 shows a series of coupons that were fully immersed in different brine types at 350 ppm CO_2 for six months. The trends seen in this series of coupons are broadly similar to all four of the different atmospheres used. Although there is no visible corrosion product forming on either of the coupons immersed in GWB brines (upper left and right of Figure 4-2), the coupons do have a "hazy" appearance. The hazy appearance and apparent lack of corrosion products is also characteristic of the coupon that was immersed in ERDA-6 containing organic ligands (lower right of Figure 4-2). Coupon 126 shown on the lower left of Figure 4-2 was immersed in ERDA-6 without organic ligands. The appearance of this coupon is different from the other in that dark green patches of corrosion products can be seen in addition to the hazy appearance of the bulk of the coupon surface. The white blotches also visible on coupon 126 are salt crystals that formed on the coupon either during the experiment or after rinsing. Although no visible corrosion products formed on most of the fully immersed coupons, there was a film of light green corrosion products on every acrylic hanger used to suspend the coupons in the brines (Figure 4-3). The formation of corrosion products on the hangers was seen in all brines and at all CO_2 concentrations. The corrosion products were removed from the hangers using a razor blade and are stored for later analysis.

In contrast to the fully immersed coupons, the partially submerged coupons show more pronounced formation of corrosion products. Figure 4-4 shows a series of coupons that were partially submerged in the different brine types at 350 ppm CO_2 for six months. As with the fully immersed coupons the trends seen in this series of partially submerged coupons are broadly similar in all four of the different atmospheres used. In all cases shown in Figure 4-4 the most significant corrosion product formation occurred at the brine/atmosphere interface. This is consistent with observations made by Telander and Westerman (1993, 1997). From Figure 4-4 it is apparent that those coupons exposed to GWB brines exhibit far less corrosion product formation at the brine/atmosphere interface than those exposed to the ERDA-6 brines. The coupons placed in GWB show only a thin band of greenish corrosion products forming at the interface, whereas coupons in ERDA-6 show a heavy band of dark green corrosion products.

For those portions of the coupons that were below the brine/atmosphere interface the formation of corrosion products appears to be similar to that observed in the fully immersed coupons. Again, there is no visible corrosion product forming on either of the coupons immersed in GWB brines (upper left and right of Figure 4-4) and the coupons have a "hazy" appearance. The same observation can be made for the coupon that was immersed in ERDA-6 containing organic ligands (lower right of Figure 4-4). The portion of the coupon immersed in ERDA-6 without organic ligands likewise shows the appearance of dark green patches of corrosion products in addition to the hazy appearance on the bulk of the coupon surface. No corrosion products formed on the acrylic hangers used in these experiments because the hangers did not extend into the brine. However, corrosion product formation was observed on the sides of the brine containers. Unfortunately, the amount of corrosion product formation on these containers is likely not enough for further analysis.

Figure 4-2 Photographs of fully immersed steel coupons after 6 months exposure in a 350 ppm CO_2 atmosphere. Coupon 115 (top left) submerged in GWB without organics. Coupon 121 (top right) submerged in GWB with organic ligands. Coupon 126 (bottom left) submerged in ERDA-6 without organics. Coupon 132 (bottom right) submerged in ERDA-6 with organic ligands.

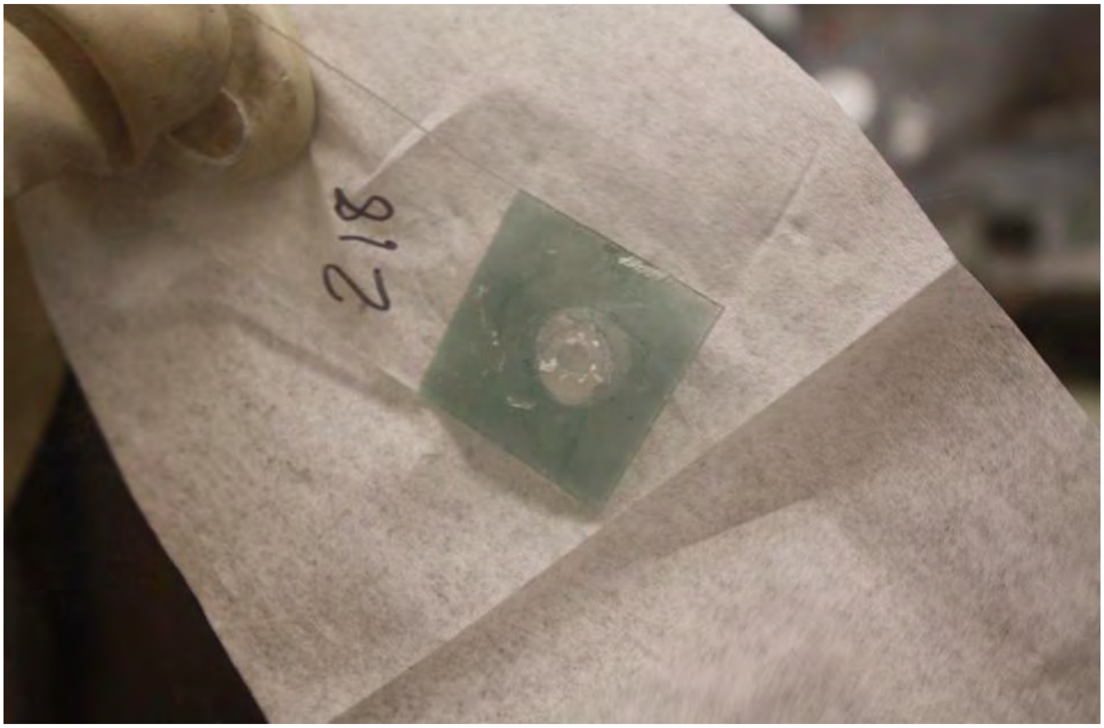

Figure 4-3 Corrosion products covering acrylic hanger used to suspend steel coupon in brine. The formation of corrosion products on the hangers is seen in all brines types and CO_2 concentrations.

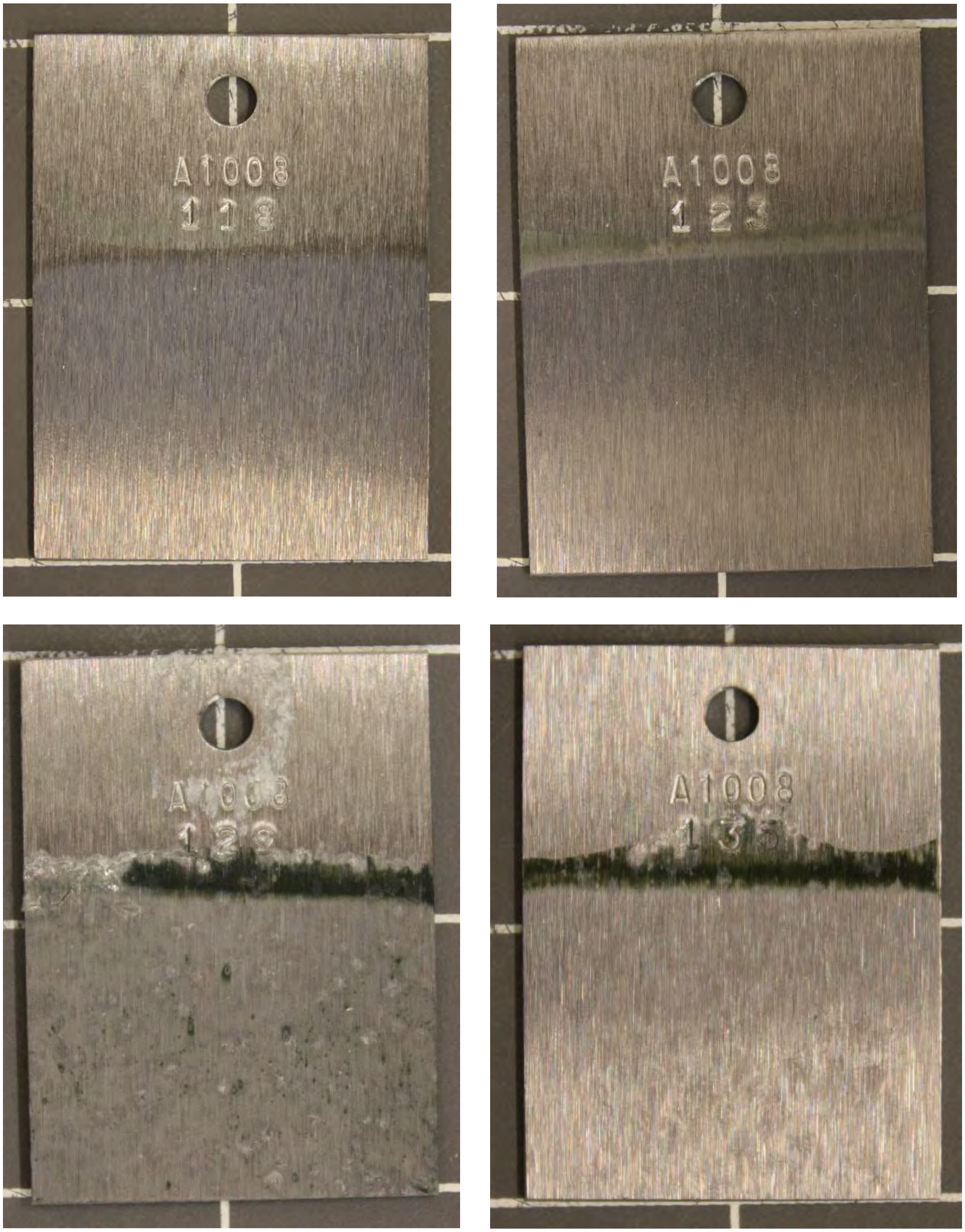

Figure 4-4 Photographs of partially submerged steel coupons after 6 months exposure in a 350 ppm CO_2 atmosphere. Coupon 118 (top left) submerged in GWB without organics. Coupon 123 (top right) submerged in GWB with organic ligands. Coupon 129 (bottom left) submerged in

ERDA-6 without organics. Coupon 135 (bottom right) submerged in ERDA-6 with organic ligands.

4.2 Lead Coupon Post-Experimental Appearance

Lead coupons show little macroscopic evidence of corrosion in any of the experiments. In general, the only visible change in many of the coupons is a discoloration in those parts of the coupons exposed to the humid atmosphere. This is clearly evident in Figure 4-5, which shows before and after pictures of a coupon exposed to the 3500 ppm CO_2 humid atmosphere. The discoloration forms in all of the experimental atmospheres used. This same discoloration is also observed on the upper portion of coupons that were partially submerged. Figure 4-6 shows a series of lead coupons that were partially submerged in the different brine types at 350 ppm CO_2 for six months. Unlike the steel coupons, there seems to be no corrosion product formation occurring at the brine/atmosphere interface. There also appears to have been little corrosion product formation on coupon surfaces exposed to the brine beneath the brine/atmosphere interface. From Figure 4-6 it can be seen that those portions of the coupons within the brine appear much the same as they did before the experiments (compare with Figure 4-5). The dark splotches observed on some of the coupons in Figure 4-6 are salt crystals and not corrosion products.

Coupons that were fully immersed in the brines show similar traits to those observed in the partially submerged coupons (Figure 4-7). Again, there is no visible corrosion product formation on the coupons regardless of the brine type in which they were immersed. As with the partially submerged coupons some of the fully immersed coupons show growth of salt crystals on the coupon surface. It appears that the presence of CO_2 may affect the growth of salt on the coupons. Both Figure 4-6 and Figure 4-7 show no visible salt formation on the coupons in the 0 ppm CO_2 atmosphere, whereas all of the coupons in atmospheres that contained CO_2 have salt growth.

Figure 4-5 Images of lead coupon exposed to humid 3500 ppm CO_2 atmosphere. Left image shows coupon prior to experiments, right image shows coupon after six months exposure.

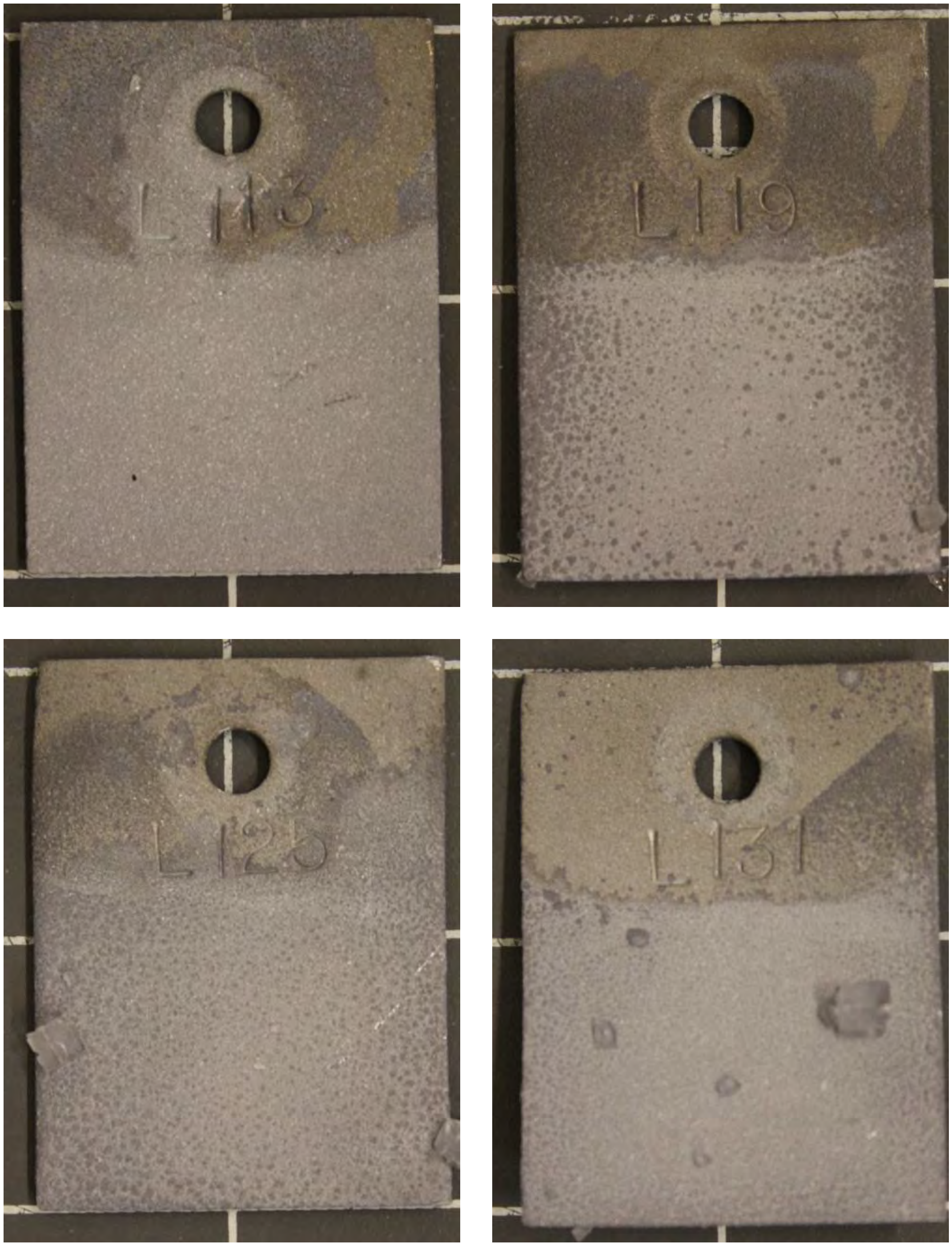

Figure 4-6 Photographs of partially submerged lead coupons after 6 months exposure in a 350 ppm CO_2 atmosphere. Coupon L113 (top left) submerged in GWB without organics. Coupon L119 (top right) submerged in GWB with organic ligands. Coupon L125 (bottom left) submerged in ERDA-6 without organics. Coupon L131 (bottom right) submerged in ERDA-6 with organic ligands.

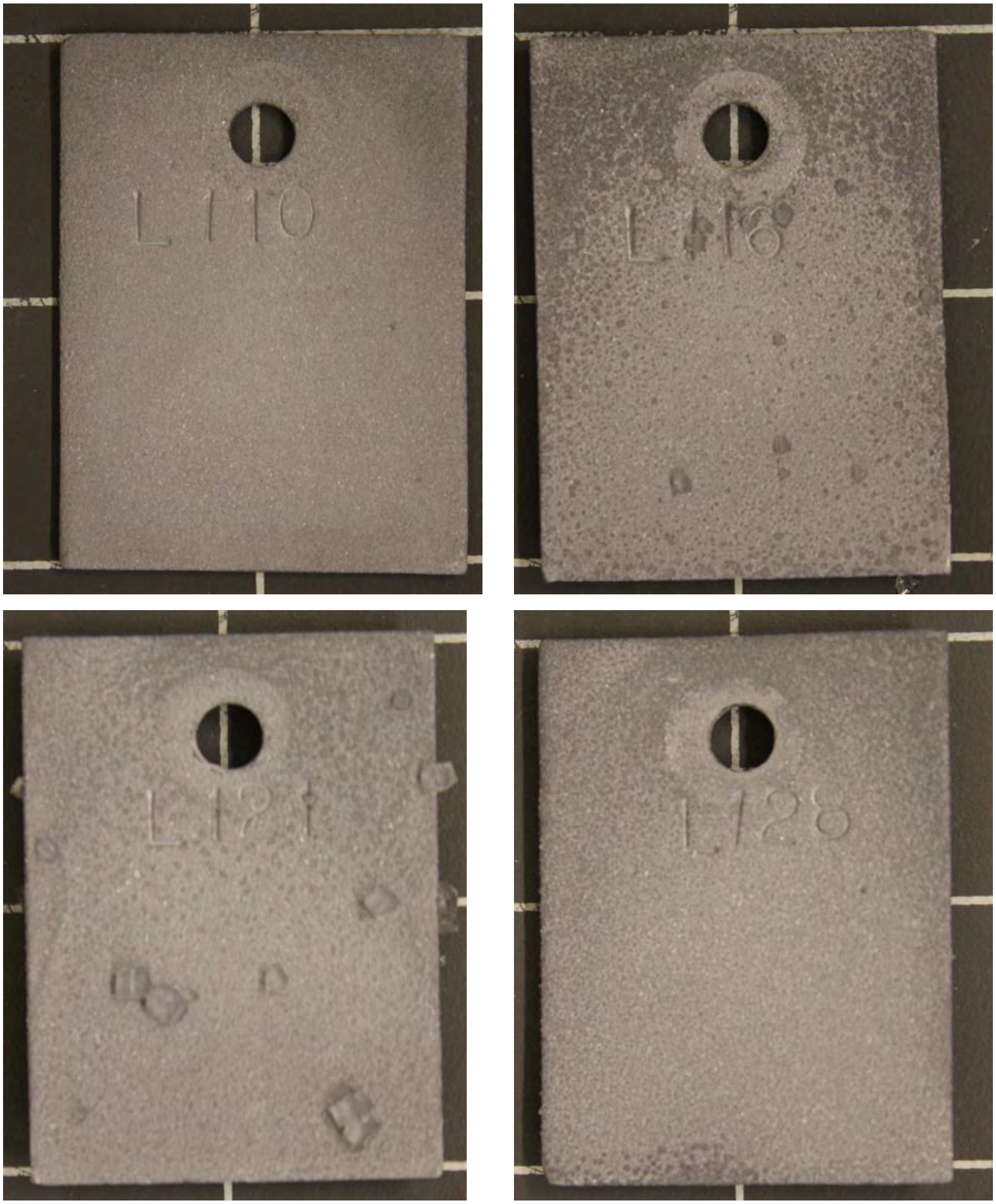

Figure 4-7 Photographs of fully immersed lead coupons after 6 months exposure in a 350 ppm CO_2 atmosphere. Coupon L110 (top left) submerged in GWB without organics. Coupon L116 (top right) submerged in GWB with organic ligands. Coupon L121 (bottom left) submerged in ERDA-6 without organics. Coupon L128 (bottom right) submerged in ERDA-6 with organic ligands.

4.3 Scanning Electron Microscopy

Scanning electron microscopy (SEM) combined with energy dispersive spectroscopy (EDS) was used to characterize the corrosion products on the coupons. Although many of the coupons showed little or no macroscopic evidence of corrosion product formation at the conclusion of the six month experiments, SEM analysis shows that in many cases there are minute quantities of corrosion products. Due to the limited amount of products formed many characterization techniques such as X-ray diffraction (XRD) and electron backscatter diffraction (EBSD) have not yet yielded a positive identification of the different phases. Thus, the SEM imaging and EDS analysis provide an important tool with which to classify, at least qualitatively, the different types of corrosion products.

For each of the test conditions one of the three replicate coupons was used for corrosion product characterization. Each of these coupons was removed from the anoxic glovebox and quickly photographed and then placed into the SEM in order to minimize exposure to air. Coupons were mounted in a large sample holder without any coating. SEM images and EDS spectra were taken using a JEOL JSM-5900LV with a ThermoNORAN Energy Dispersive Spectroscopy system. At the conclusion of the SEM analysis the coupons were quickly placed back into the anoxic glovebox.

4.3.1 Steel Coupons

The appearance of an unreacted steel coupon is shown in Figure 4-8. The surface of the coupon is smooth showing only linear striations due to the surface finishing at the supplier. The EDS spectrum of this coupon is not shown but indicates only the presence of iron. The minor constituents of the steel (Table 2-1) are not present in high enough concentration to be detected. This image serves as a baseline for comparison with other coupons. Although SEM imaging and EDS analysis was completed for one replicate coupon from every test condition, this section will only present a few examples that illustrate the general trends seen in corrosion product formation.

The SEM imaging of coupons exposed only to the humid environments yields results that are consistent with the macroscopic observations in that almost no corrosion product formation is observed. Figure 4-9 shows a SEM image and EDS spectra for one of the coupons exposed to the humid 350 ppm CO_2 atmosphere. The appearance of the coupon shows little change from an unreacted coupon (compare with Figure 4-8) and the EDS spectra shows only an iron peak. Some of the humid condition coupons, however, do show incipient signs of very limited corrosion product formation. These corrosion products tend to form at the interface between the coupon and the nylon spacer used for hanging. It is likely that condensation in this space promoted the formation of some corrosion products. The observed corrosion products in this case are similar to those observed at the brine/atmosphere interface in the partially submerged coupons (discussed below).

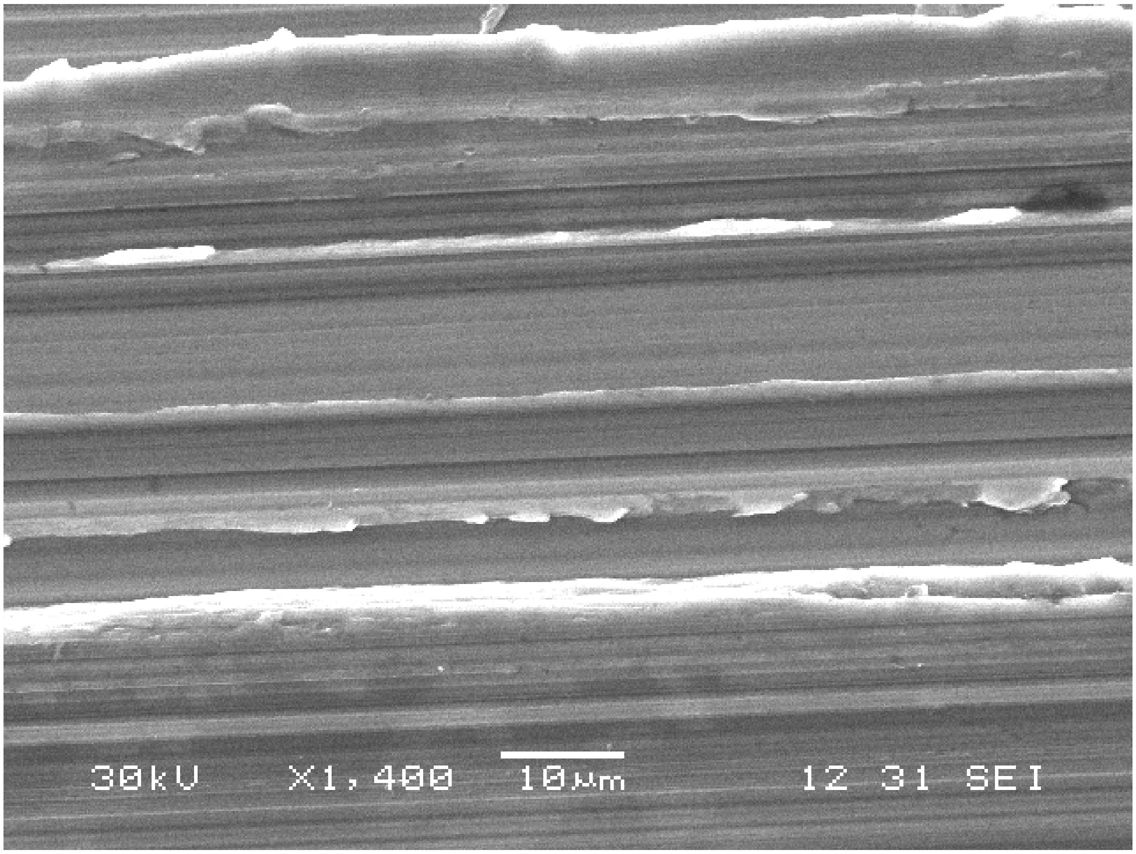

Figure 4-8 SEM image of unreacted portion of steel coupon 110. Image source: *110E_1.BMP* located on disk in “WIPP-FePb-3 Supplemental Binder D”.

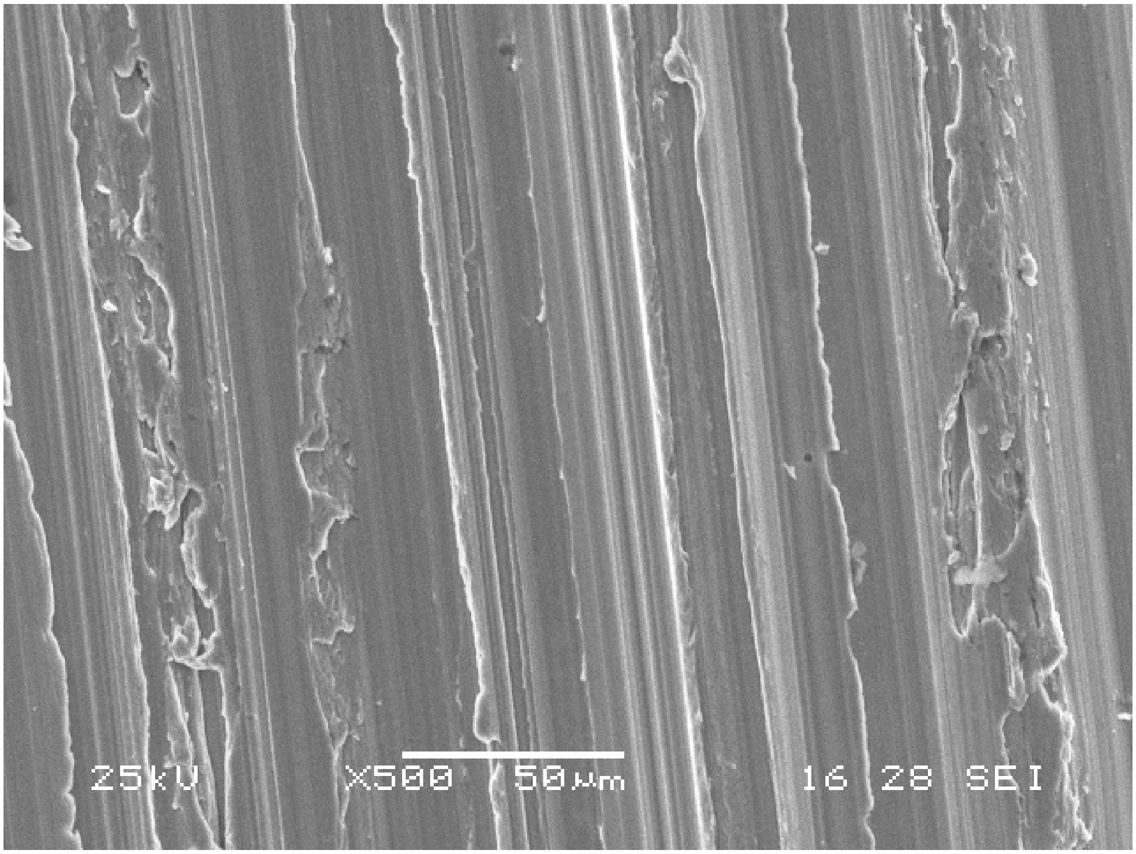

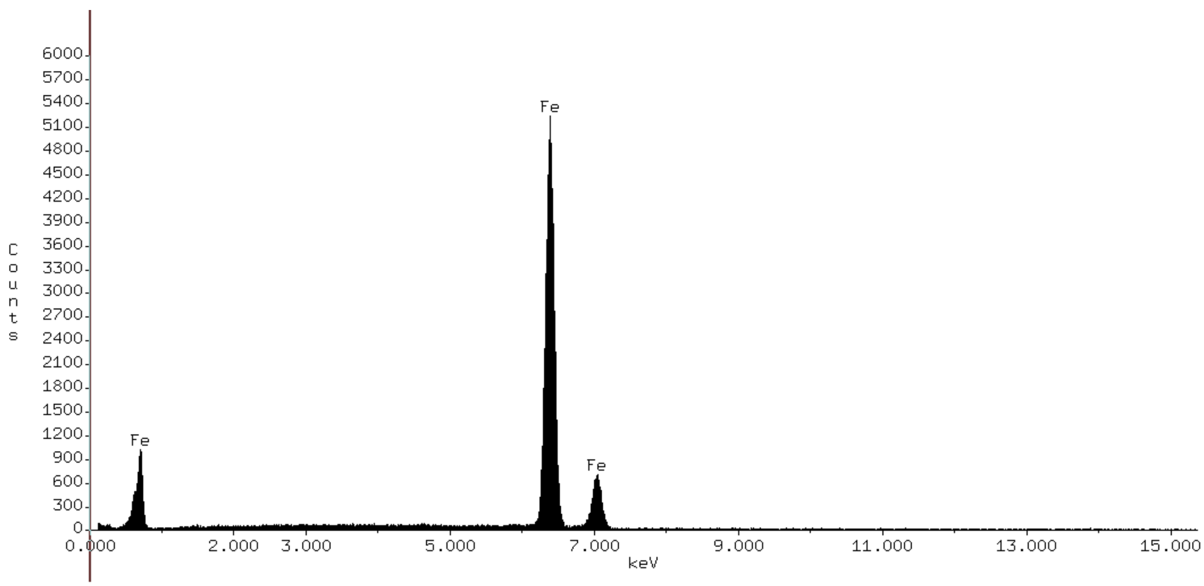

Figure 4-9 SEM image (top) and EDS spectra (bottom) of steel coupon 140 reacted in a humid 350 ppm CO2 atmosphere for six months. EDS spectra indicates the presence of only iron. Sources: image file *140E_3.BMP* and EDS spectra file *140_3.doc* located on disk in “WIPP-FePb-3 Supplemental Binder D”.

Steel coupons that were immersed in brines exhibit several different types of corrosion products. Although the mineralogical identification of the phases has not yet been possible, they can be distinguished by their habit and EDS spectra. Table 4-1 lists each of the major phases with its identifying habit and qualitative composition. The occurrence of each of these phases in the different test conditions is summarized in Table 4-2. Iron chloride 1 is the phase that forms the green bands at the brine/ atmosphere interface in the partially submerged experiments (see Figure 4-4). It is observed in all of the partially submerged coupons regardless of the brine type or exposure atmosphere. This phase is also found on several of the fully immersed coupons in ERDA-6 brines and one GWB brine, although these occurrences are only at 0 or 350 ppm CO_2 concentrations. A SEM image of the typical appearance of the iron chloride 1 phase is shown in Figure 4-10. This phase always exhibits this characteristic angular or blocky habit and often forms columns with a triangular symmetry. Figure 4-11 shows a detailed image of the interface between the iron chloride 1 phase and the unreacted steel coupon from the same coupon shown in Figure 4-10. Energy dispersive spectroscopy (EDS) of this corrosion product shows that it is likely an iron/magnesium-chlori-hydroxide. The EDS spectrum of this phase is shown in Figure 4-12 for this same coupon. The pattern seen here is typical of all occurrences of this phase in the experiments.

The corrosion product phase, iron chloride 2, is found on only a few samples. There is not a consistent pattern for its occurrence as it is observed on both partially and fully submerged samples in all brine types. It is also present on some of the humid atmosphere samples. It often occurs comingled with the iron chloride 1 phase as can be seen in Figure 4-13. This phase consistently appears as aggregates of spherical rosettes of plate-like crystals. Iron chloride 2 often forms along linear features of the steel coupon that are likely sites of high surface energy. It also tends to form on the coupon surface beneath the brine/atmosphere interface in partially submerged coupons. The chemistry of iron chloride 2 as determined by EDS analysis (Figure 4-14) shows that it is also an iron-chlori-hydroxide. It differs from iron chloride 1 in that it has little or no magnesium and the chlorine peak tends to be larger than the oxygen peak.

Table 4-1 Corrosion Product Phases Observed on Steel Coupons

Phase	Habit	Chemistry
Iron chloride 1	angular, blocky columns	Fe-Cl-Mg-O (O peak > Cl peak)
Iron chloride 2	fuzzy aggregates of plates	Fe-Cl-O±Mg (Cl peak > O peak)
Carbonate 1	large ovoid rosettes	Ca-C-O
Carbonate 2	smaller spherical rosettes	Ca-Fe-Mg-C-O

Table 4-2 Occurrence of Steel Coupon Corrosion Product Phases in Different Test Conditions

Test ID	Coupon	Iron chloride 1	Iron chloride 2	Carbonate 1	Carbonate 2	Other
Humid Samples						
Fe-Atm-0000-6-3	113	X	X	--	--	--
Fe-Atm-0350-6-3	140	--	X	--	--	--
Fe-Atm-1500-6-1	330	--	--	--	--	--
Fe-Atm-3500-6-1	443	--	--	--	--	--
GWB Brines						
Fe-G-0000-6-2f	088	--	--	--	--	--
Fe-Go-0000-6-1f	093	--	--	--	--	--
Fe-G-0350-6-3f	116	X	?	--	--	X
Fe-Go-0350-6-3f	122	--	--	--	--	X
Fe-G-1500-6-1f	306	--	X	--	--	--
Fe-Go-1500-6-1f	312	--	--	--	--	--
Fe-G-3500-6-1f	415	--	--	--	X	--
Fe-Go-3500-6-1f	422	--	--	--	X	--
Fe-G-0000-6-3p	092	?	?	--	--	--
Fe-Go-0000-6-1p	096	X	--	--	--	--
Fe-G-0350-6-3p	119	X	--	--	--	--
Fe-Go-0350-6-3p	125	X	--	--	--	--
Fe-G-1500-6-1p	309	X	--	--	X	--
Fe-Go-1500-6-1p	315	X	--	--	--	--
Fe-G-3500-6-1p	421	?	--	--	X	--
Fe-Go-3500-6-1p	428	X	--	--	X	--
ERDA-6 Brines						
Fe-E-0000-6-3f	101	X	--	--	--	--
Fe-Eo-0000-6-1f	105	X	--	--	--	--
Fe-E-0350-6-3f	128	X	--	--	X	--
Fe-Eo-0350-6-3f	134	--	--	--	--	--
Fe-E-1500-6-1f	318	--	--	X	X	X
Fe-Eo-1500-6-1f	324	--	--	X	X	--
Fe-E-3500-6-1f	429	--	--	X	X	X
Fe-Eo-3500-6-1f	437	--	--	X	X	--
Fe-E-0000-6-3p	104	X	X	--	--	--
Fe-Eo-0000-6-3p	110	X	X	--	--	--
Fe-E-0350-6-3p	131	X	--	--	X	--
Fe-Eo-0350-6-3p	137	X	--	--	--	--
Fe-E-1500-6-1p	321	X	--	X	X	X
Fe-Eo-1500-6-1p	327	X	--	X	X	--
Fe-E-3500-6-1p	432	?	--	X	X	--
Fe-Eo-3500-6-1p	440	X	--	X	X	--

Note: ? indicates that the phase is likely present but the results are ambiguous.

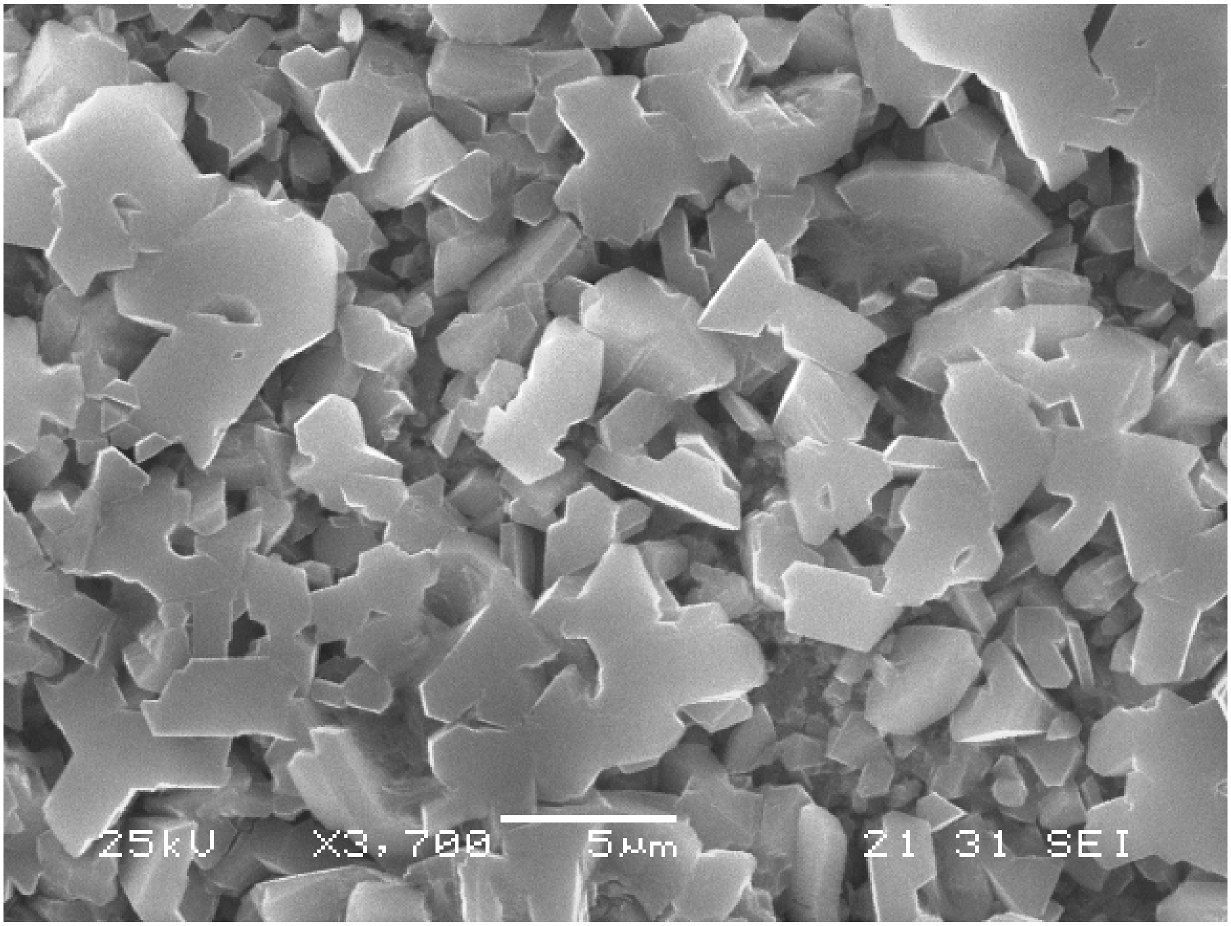

Figure 4-10 SEM image of corrosion product "iron chloride 1" formed on partially submerged coupon 104. This phase forms the green band on partially submerged samples at the brine/atmosphere interface in all brine types and CO_2 concentrations. Image source: *104E_2.BMP* located on disk in "WIPP-FePb-3 Supplemental Binder D".

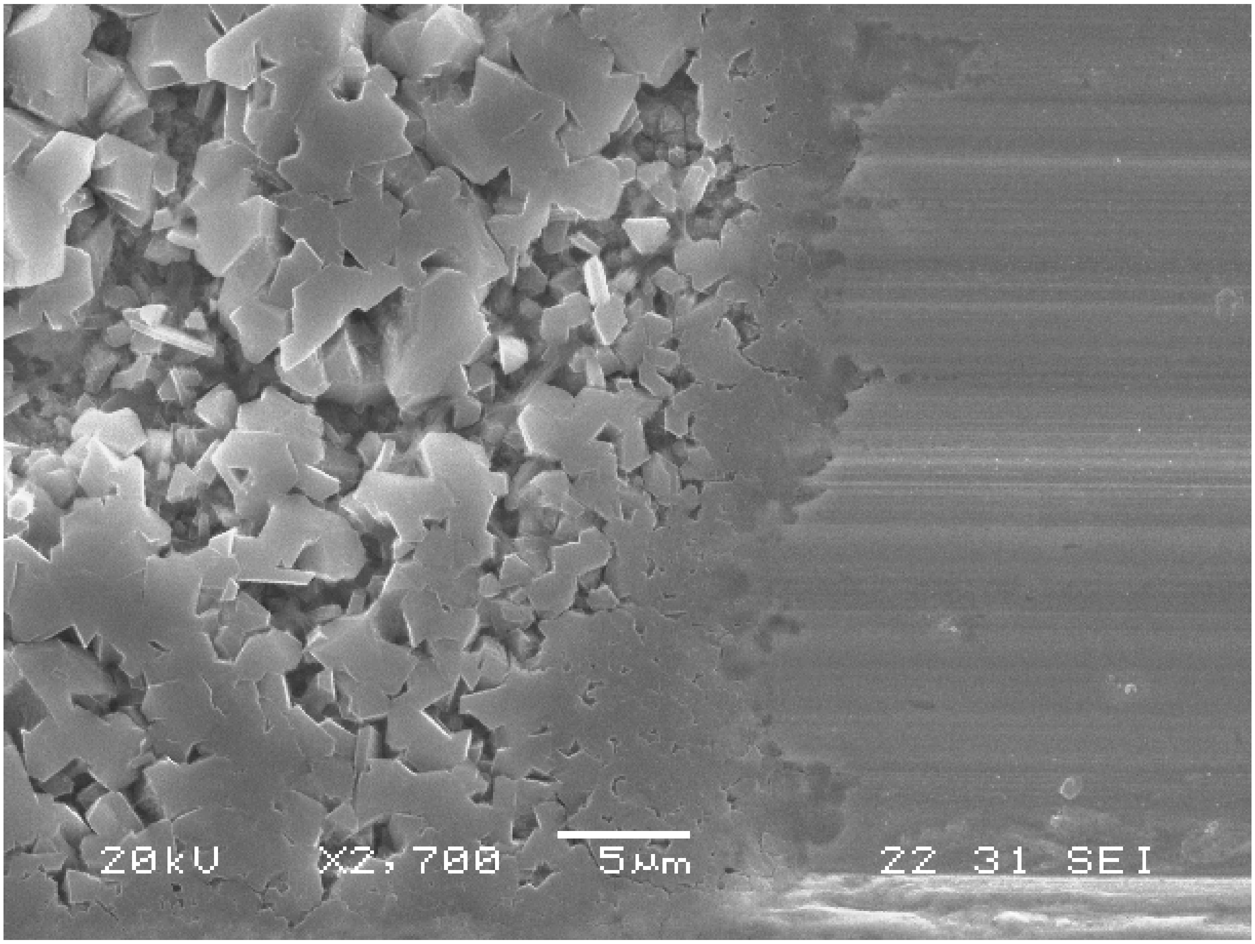

Figure 4-11 SEM image of partially submerged coupon 104 showing the interface between the corrosion products (left) and the unreacted steel (right). Image source: *104E_3B.BMP* located on disk in "WIPP-FePb-3 Supplemental Binder D".

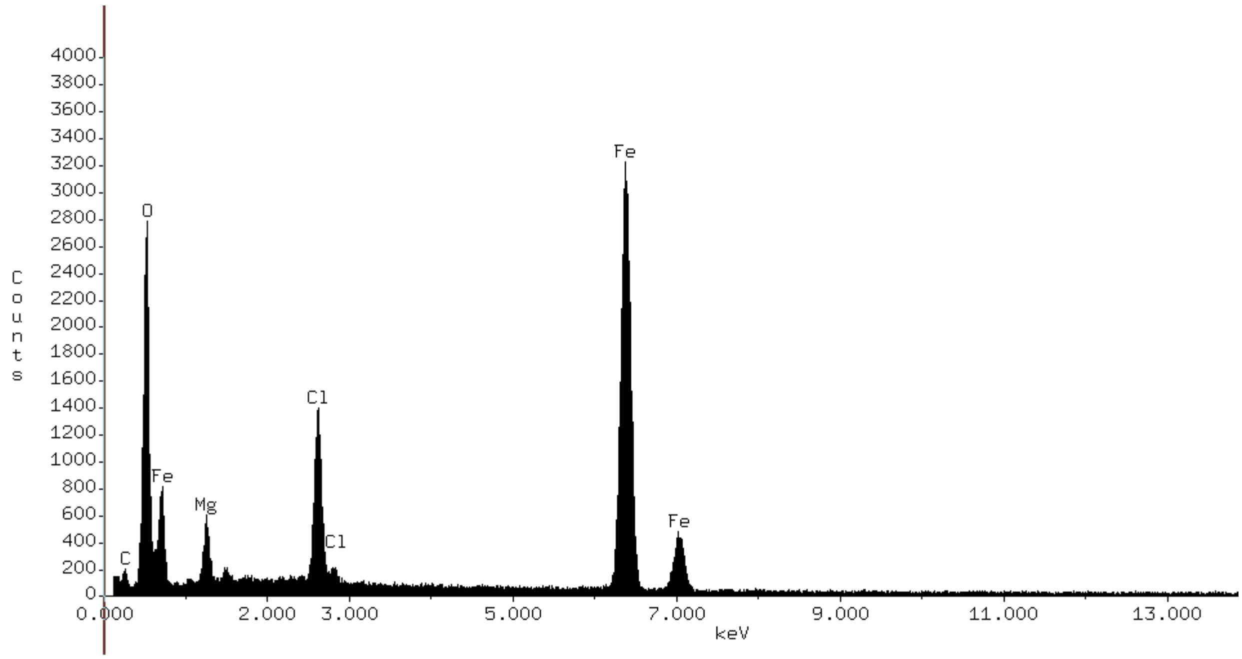

Figure 4-12 EDS spectra of corrosion product phase iron chloride 1 as found on coupon 104. EDS spectra source: file *104_2.doc* located on disk in “WIPP-FePb-3 Supplemental Binder D”.

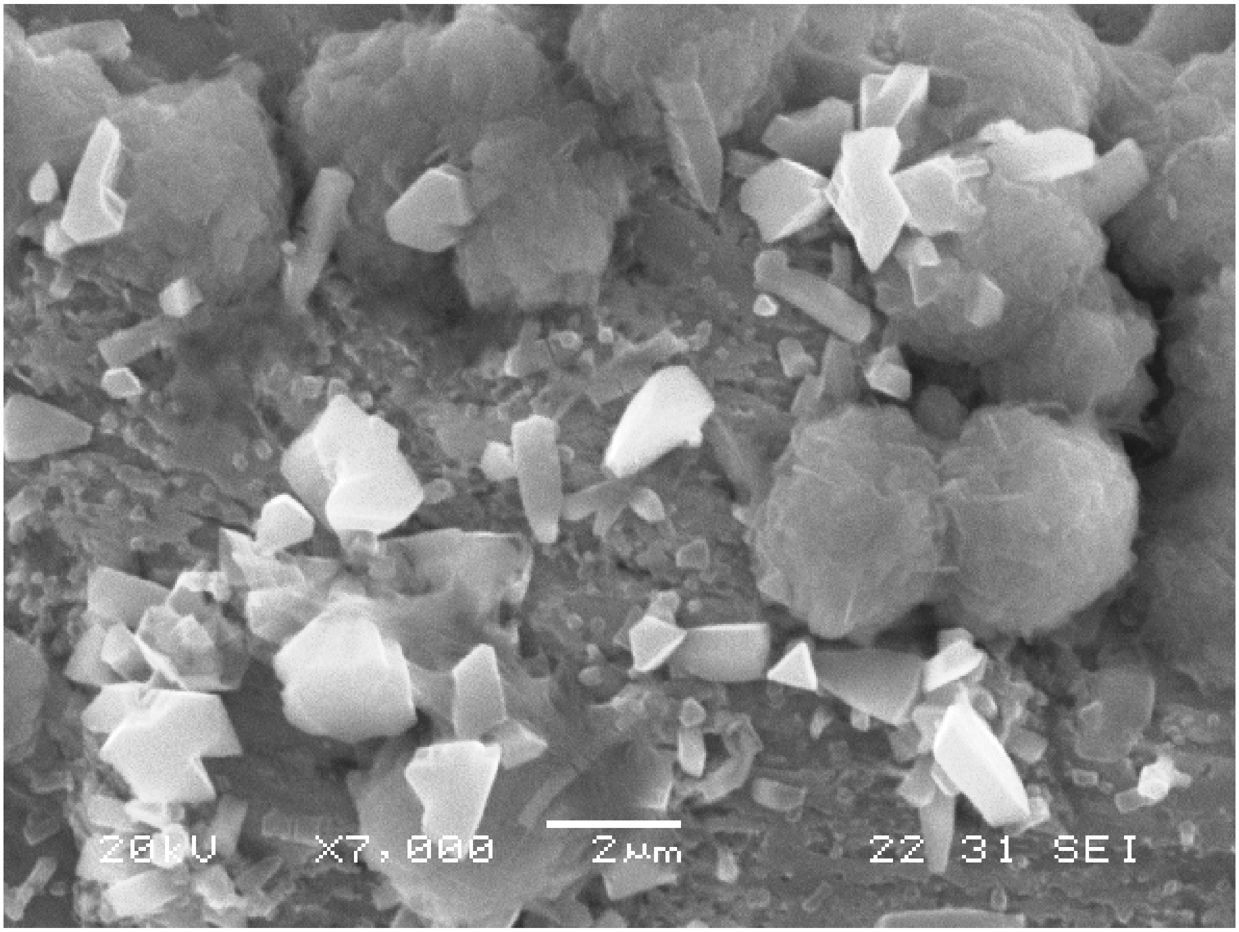

Figure 4-13 SEM image of both iron chloride phases on coupon 104. The angular blocks are iron chloride 1, whereas the spherical rosettes are iron chloride 2. Heavy pitting of the underlying steel surface can also be observed. Image source: *104E_4B.BMP* located on disk in "WIPP-FePb-3 Supplemental Binder D"

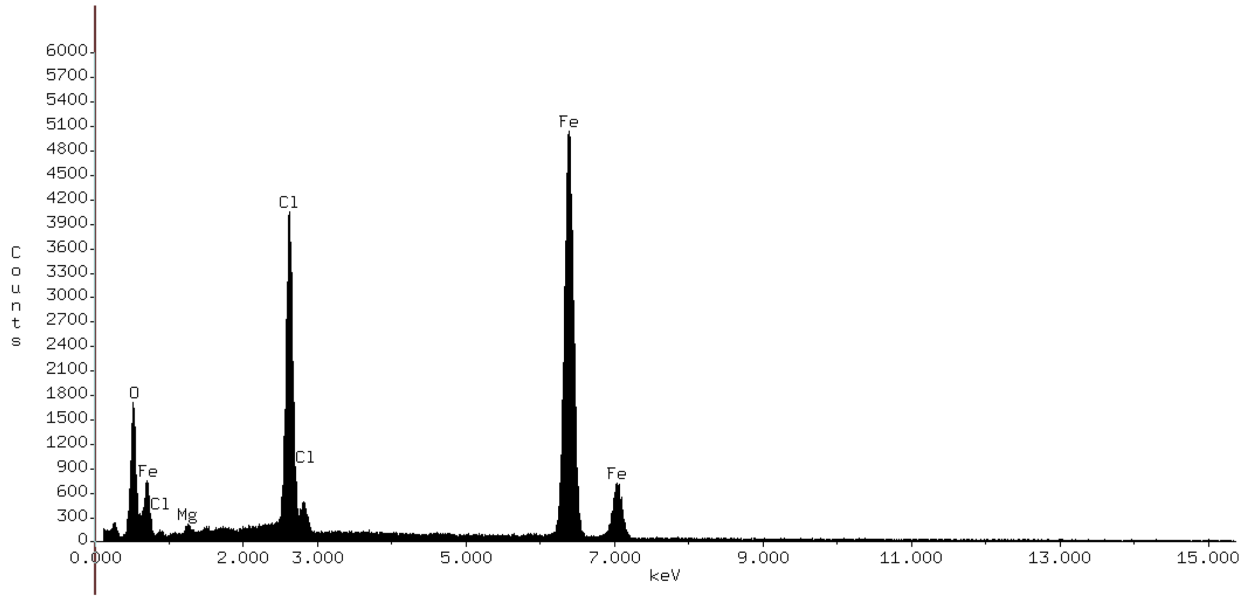

Figure 4-14 EDS spectra of corrosion product phase iron chloride 2 as found on coupon 140. EDS spectra source: file *140_1b.doc* located on disk in “WIPP-FePb-3 Supplemental Binder D”.

In experiments conducted in atmospheres that contained CO_2 two different phases are observed on the coupons. The phases have been labeled as carbonate 1 and carbonate 2 based on their morphology and EDS spectra. The phase carbonate 1 forms large spheres that have a blocky or stepped appearance. Often these spheres occur in pairs making them look ovoid in shape. Figure 4-15 shows an SEM image of coupon 437 that was fully immersed in ERDA-6 with organic ligands in a 3500 ppm CO_2 atmosphere. An enlargement of the carbonate 1 phase is shown in Figure 4-16. A typical EDS spectrum for carbonate 1 is shown in Figure 4-17 and indicates that it is most likely a calcium carbonate phase. The phase carbonate 1 forms only in ERDA-6 brines (both with and without organic ligands) at CO_2 concentrations greater than 1500 ppm (see Table 4-2). The phase carbonate 1 is likely a precipitate from brine that has equilibrated with the higher CO_2 concentrations in these experiments. Therefore, it should not be considered a corrosion product in the strictest sense.

The phase labeled carbonate 2 occurs in most experiments conducted in ERDA-6 brines that contain CO_2 atmospheres (Table 4-2). It is also present in some GWB experiments at the higher CO_2 concentrations. This phase also appears as spherical aggregates of blocky or stepped crystals. The spheres of carbonate 2 are consistently smaller and more abundant than carbonate 1 when they occur together (Figure 4-15). Although in detail (Figure 4-18) they appear to have much the same habit as carbonate 1, the EDS spectra for carbonate 2 is markedly different. The EDS spectrum of carbonate 2 in Figure 4-19 shows that this phase is likely an iron-calcium-magnesium carbonate. Based on its chemistry carbonate 2 can be considered the actual corrosion product in these experiments.

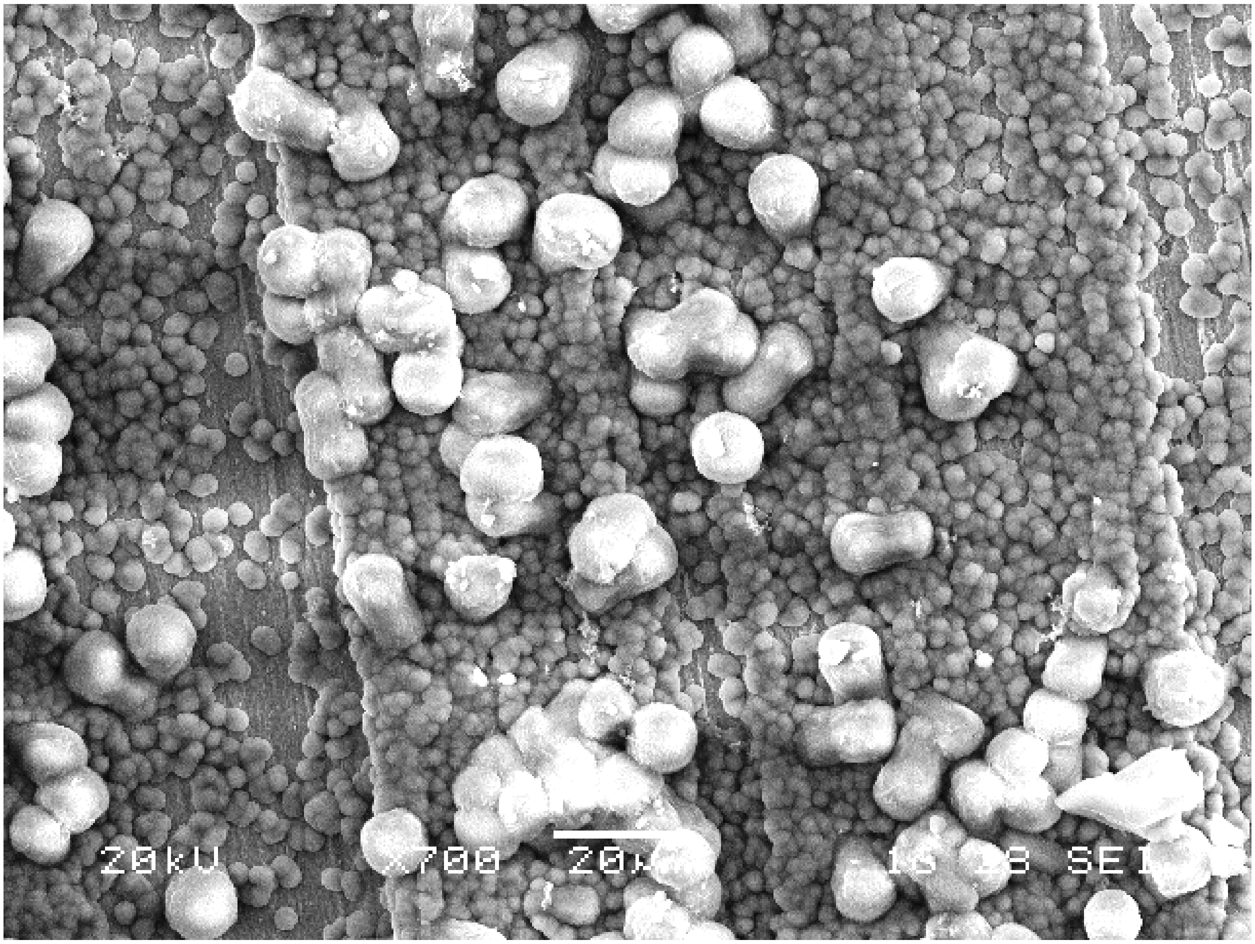

Figure 4-15 SEM image of carbonate corrosion products formed on fully immersed coupon 437. The larger ovoid phases are carbonate 1. The smaller spherical aggregates are carbonate 2. Image source: *437_1.BMP* located on disk in “WIPP-FePb-3 Supplemental Binder D”.

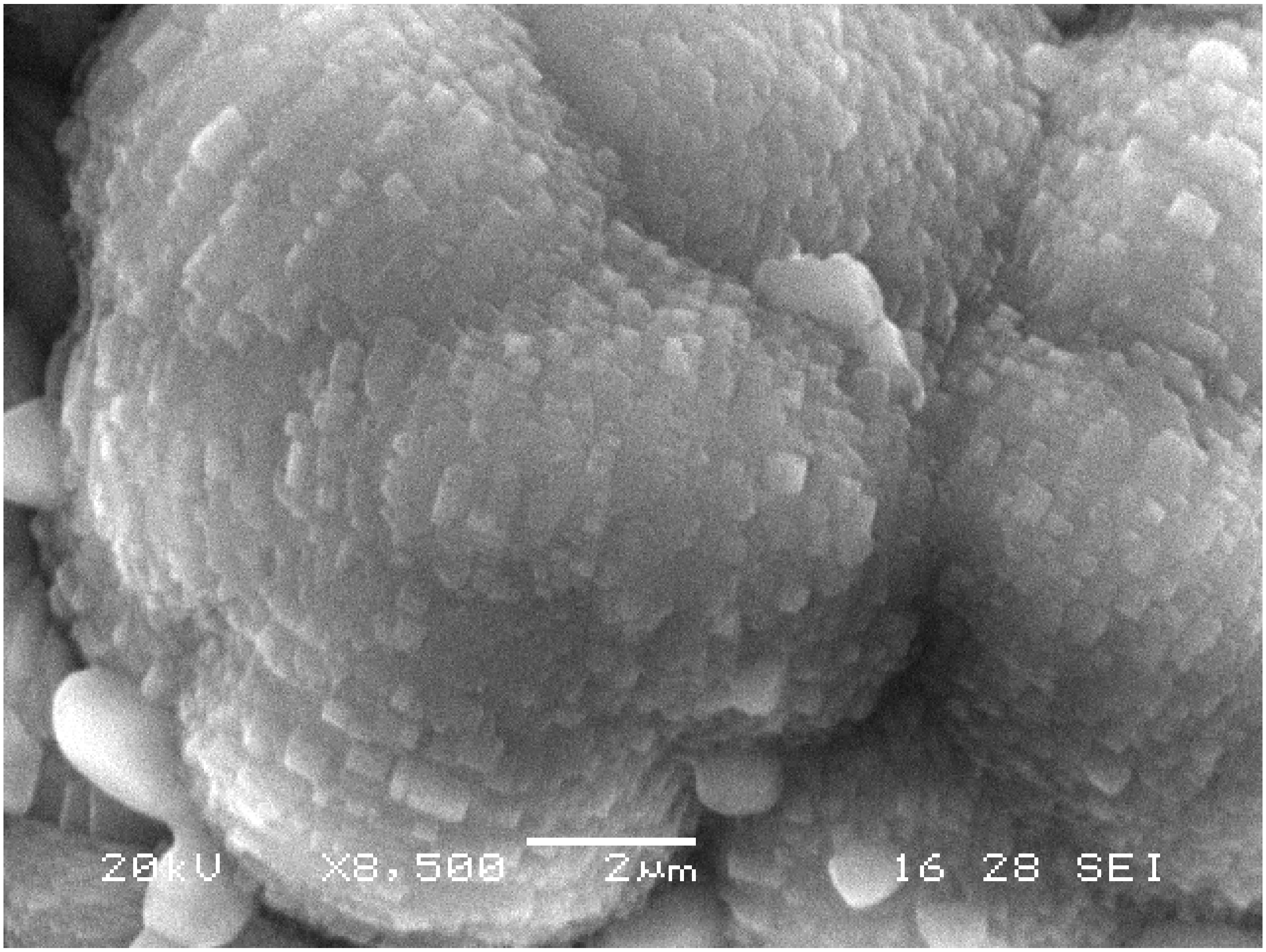

Figure 4-16 Enlargement of carbonate 1 sphere showing blocky nature of the phase. Image source: *429_1C.BMP* located on disk in “WIPP-FePb-3 Supplemental Binder D”.

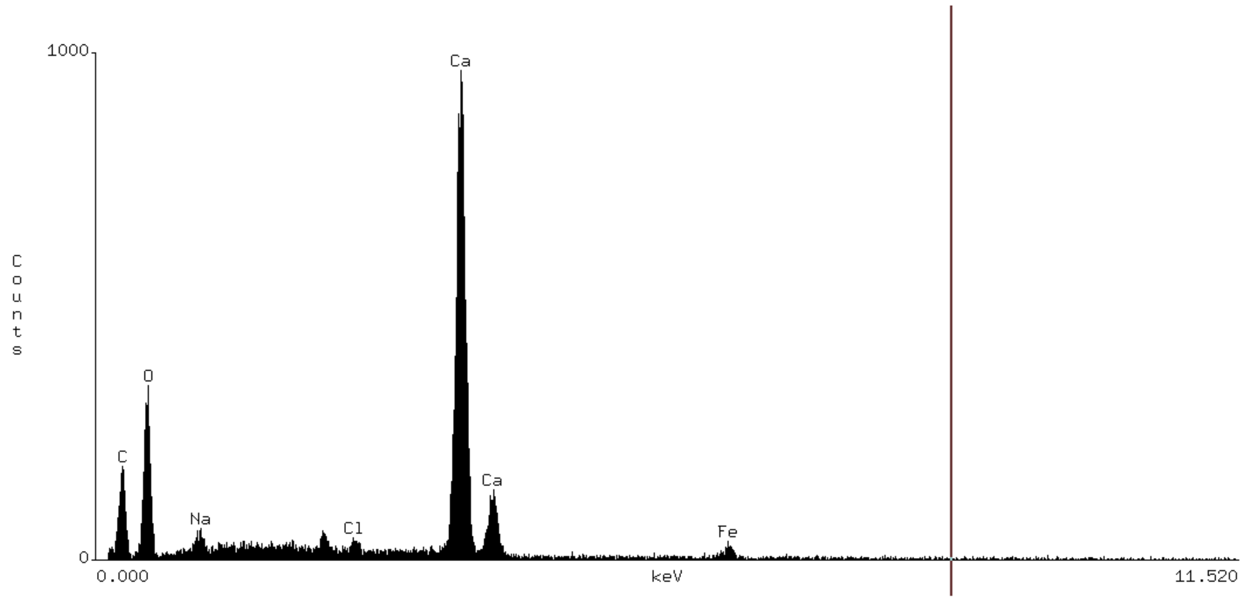

Figure 4-17 EDS spectra carbonate 1 phase as found on coupon 429. EDS spectra source: file *429_1c.doc* located on disk in “WIPP-FePb-3 Supplemental Binder D”.

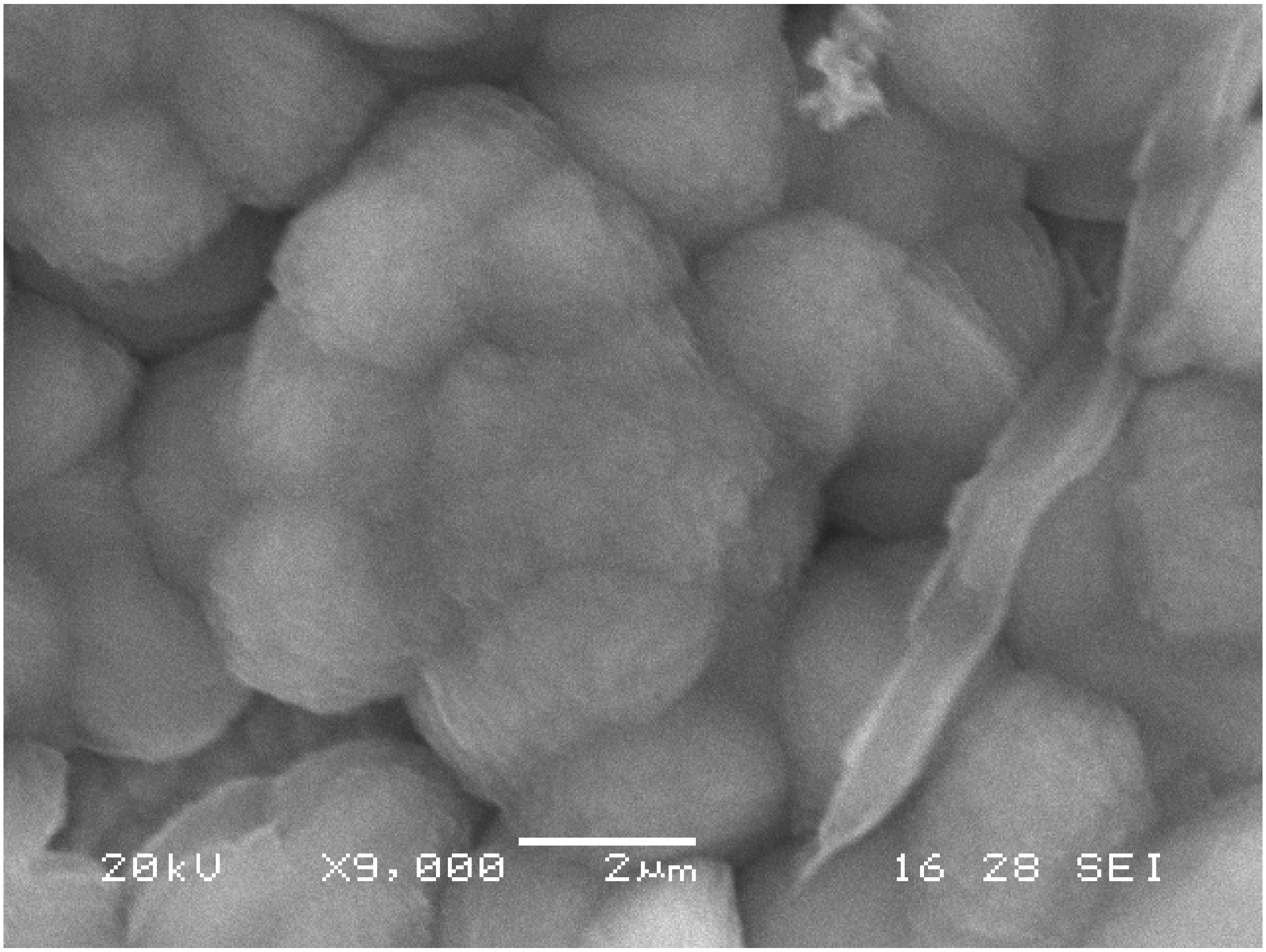

Figure 4-18 Enlargement of carbonate 2 sphere showing blocky nature of the phase. Image source: *437_1B.BMP* located on disk in “WIPP-FePb-3 Supplemental Binder D”.

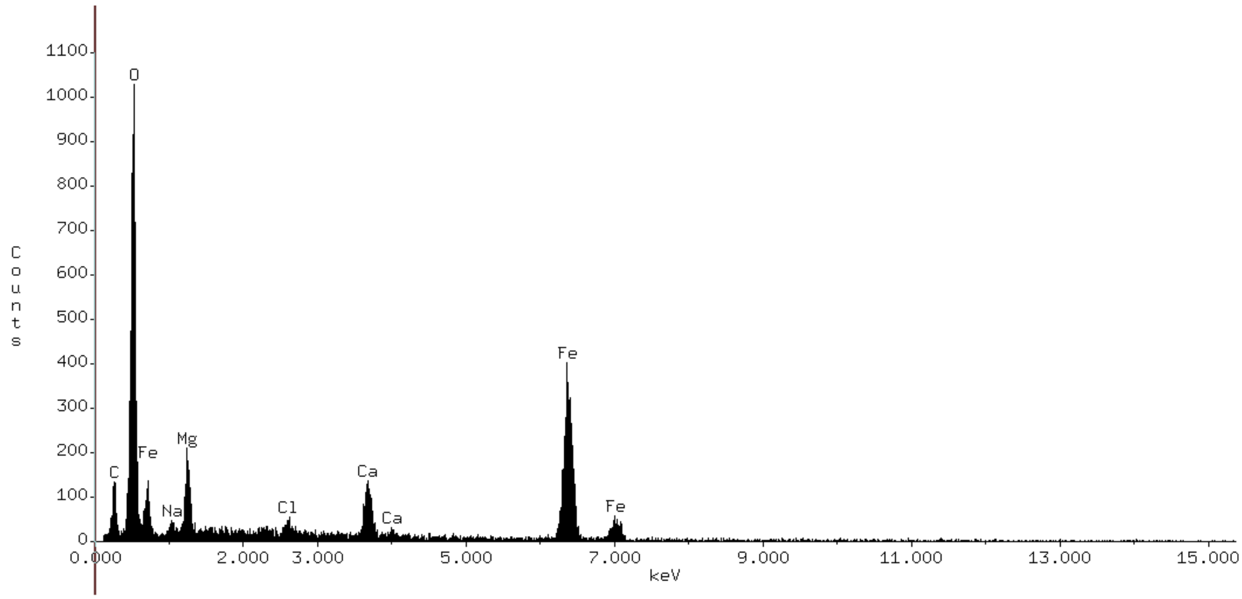

Figure 4-19 EDS spectra carbonate 2 phase as found on coupon 437. EDS spectra source: file *437_1b.doc* located on disk in "WIPP-FePb-3 Supplemental Binder D".

4.3.2 Lead Coupons

The appearance of an unreacted lead coupon is shown in Figure 4-20. The surface of the lead coupons is rough and pitted. The EDS spectrum of this coupon shown in Figure 4-21 indicates only the presence of lead. The minor constituents of the lead (Table 2-2) are not present in high enough concentration to be detected. The image in Figure 4-20, however, shows that the lead coupons contain inclusions of an unknown mineral phase (see Figure 4-22 for detail). An EDS analysis of these inclusions shows that they are a calcium-sodium silicate phase (Figure 4-23). These inclusions are likely a contaminant from the process used to produce the lead coupons, either in their casting or the surface finishing. They are only a minor inclusion but have been observed in all coupons.

The SEM imaging of lead coupons shows a very limited amount of corrosion product formation. In fact, only one corrosion product phase has been identified. It is similar in crystal habit to the carbonate 2 phase identified in the steel coupons. However, in this case it is a lead-calcium carbonate. Table 4-3 shows that the formation of this phase is primarily limited to experiments conducted at CO_2 concentrations of 1500 ppm or greater and only on coupons fully immersed in ERDA-6 brines both with and without organic ligands. An example of the lead carbonate phase is shown in Figure 4-24. This image shows that the phase appears as aggregates of spherical rosettes, much the same as the carbonate 2 phase identified on the steel coupons. An enlargement of the spheres is shown in Figure 4-25. The EDS spectrum for this phase is shown in Figure 4-26.

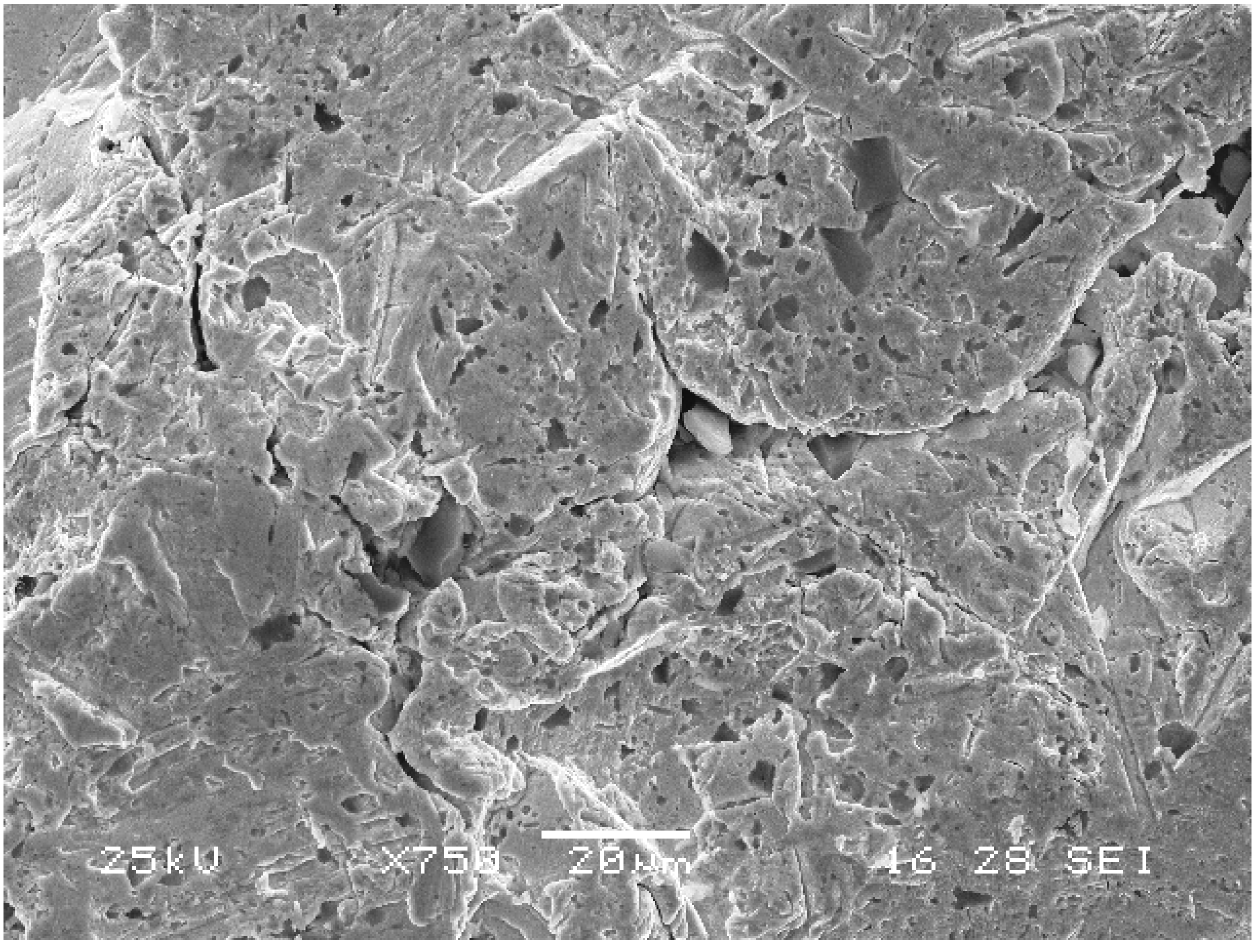

Figure 4-20 SEM image of lead coupon L456 showing the appearance of the coupons prior to placement in the experiments. This particular coupon was cleaned but never used in an experiment. Image source: L*456E_1.BMP* located on disk in “WIPP-FePb-3 Supplemental Binder D”.

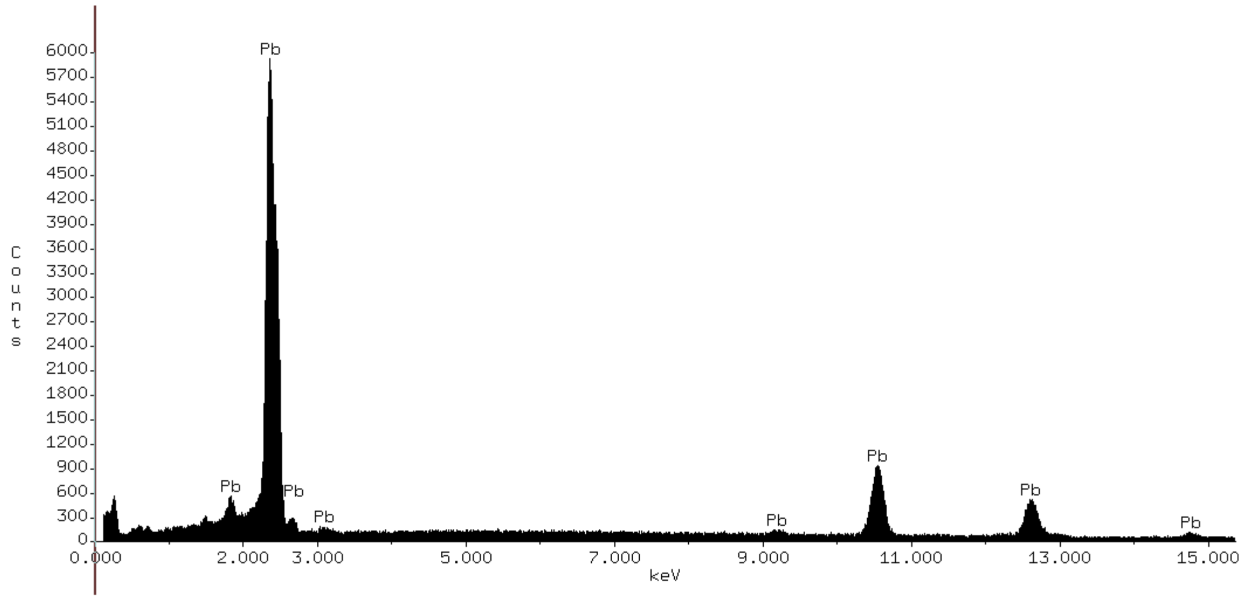

Figure 4-21 EDS spectra of unreacted lead coupon L456. EDS spectra source: file *L456_1b.doc* located on disk in “WIPP-FePb-3 Supplemental Binder D”.

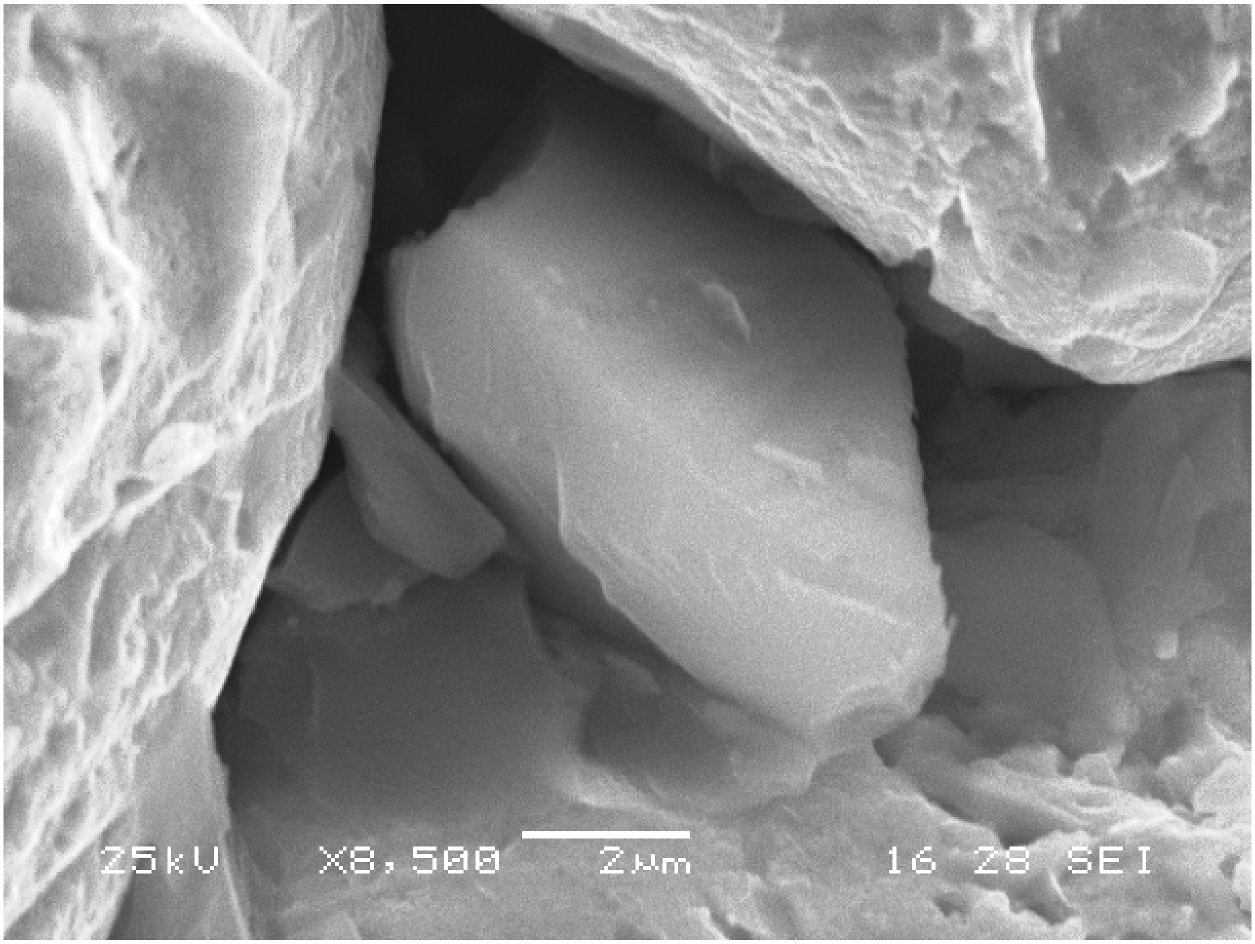

Figure 4-22 Enlarged view of the mineral inclusion seen at the center of the image in Figure 4-20. These calcium-sodium silicate inclusions are only a minor phase but are found in all coupons. They likely represent a contaminant from the production process of the coupons. Image source: L*456E_1A.BMP* located on disk in “WIPP-FePb-3 Supplemental Binder D”.

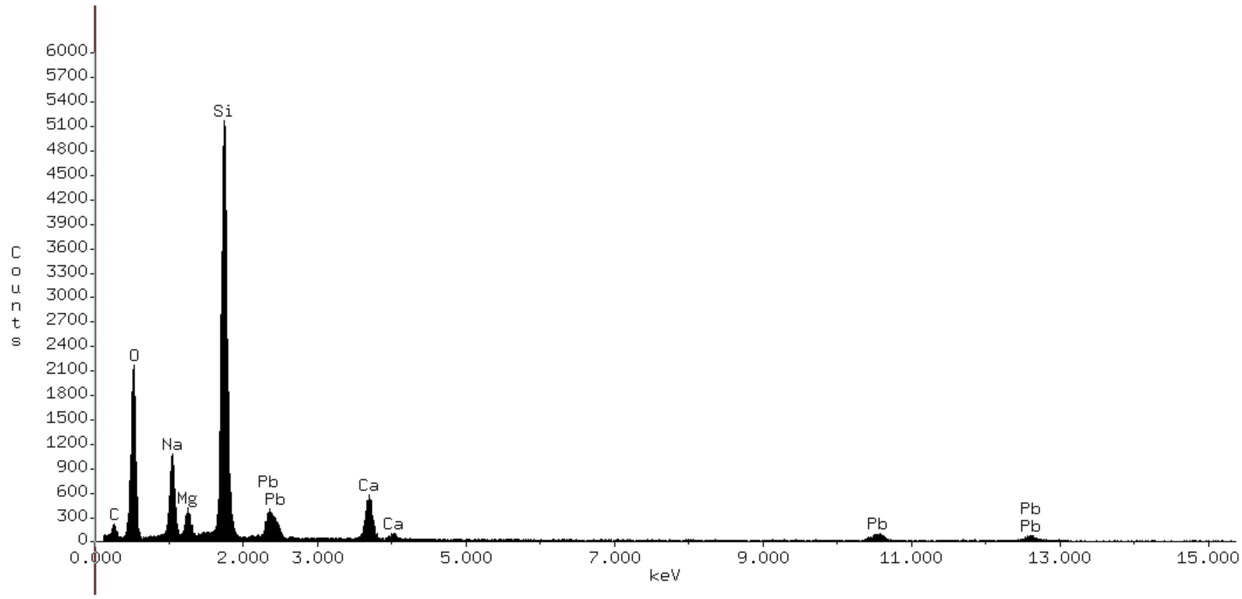

Figure 4-23 EDS spectra of mineral inclusion found in coupon L456. EDS spectra source: file *L456_1a.doc* located on disk in “WIPP-FePb-3 Supplemental Binder D”.

Table 4-3 Occurrence of Lead Coupon Corrosion Product Phases in Different Test Conditions

Test ID	Coupon	Pb Carbonate
Pb-Atm-0000-6-3	L108	--
Pb-Atm-0350-6-3	L135	--
Pb-Atm-1500-6-3	L325	--
Pb-Atm-3500-6-1	L452	--
Pb-G-0000-6-1f	L082	--
Pb-Go-0000-6-1f	L088	--
Pb-G-0350-6-3f	L111	--
Pb-Go-0350-6-3f	L117	--
Pb-G-1500-6-3f	L301	--
Pb-Go-1500-6-3f	L307	--
Pb-G-3500-6-3f	L415	--
Pb-Go-3500-6-3f	L421	--
Pb-G-0000-6-1p	L085	--
Pb-Go-0000-6-2p	L092	--
Pb-G-0350-6-3p	L114	--
Pb-Go-0350-6-3p	L120	--
Pb-G-1500-6-3p	L304	--
Pb-Go-1500-6-3p	L310	--
Pb-G-3500-6-1p	L416	X
Pb-Go-3500-6-3p	L424	--
Pb-E-0000-6-3f	L096	--
Pb-Eo-0000-6-3f	L102	--
Pb-E-0350-6-3f	L123	X
Pb-Eo-0350-6-3f	L129	--
Pb-E-1500-6-3f	L313	X
Pb-Eo-1500-6-3f	L319	X
Pb-E-3500-6-3f	L427	X
Pb-Eo-3500-6-3f	L433	X
Pb-E-0000-6-3p	L099	--
Pb-Eo-0000-6-3p	L105	--
Pb-E-0350-6-3p	L126	--
Pb-Eo-0350-6-3p	L132	--
Pb-E-1500-6-3p	L316	X
Pb-Eo-1500-6-3p	L322	X
Pb-E-3500-6-3p	L430	X
Pb-Eo-3500-6-3p	L451	X

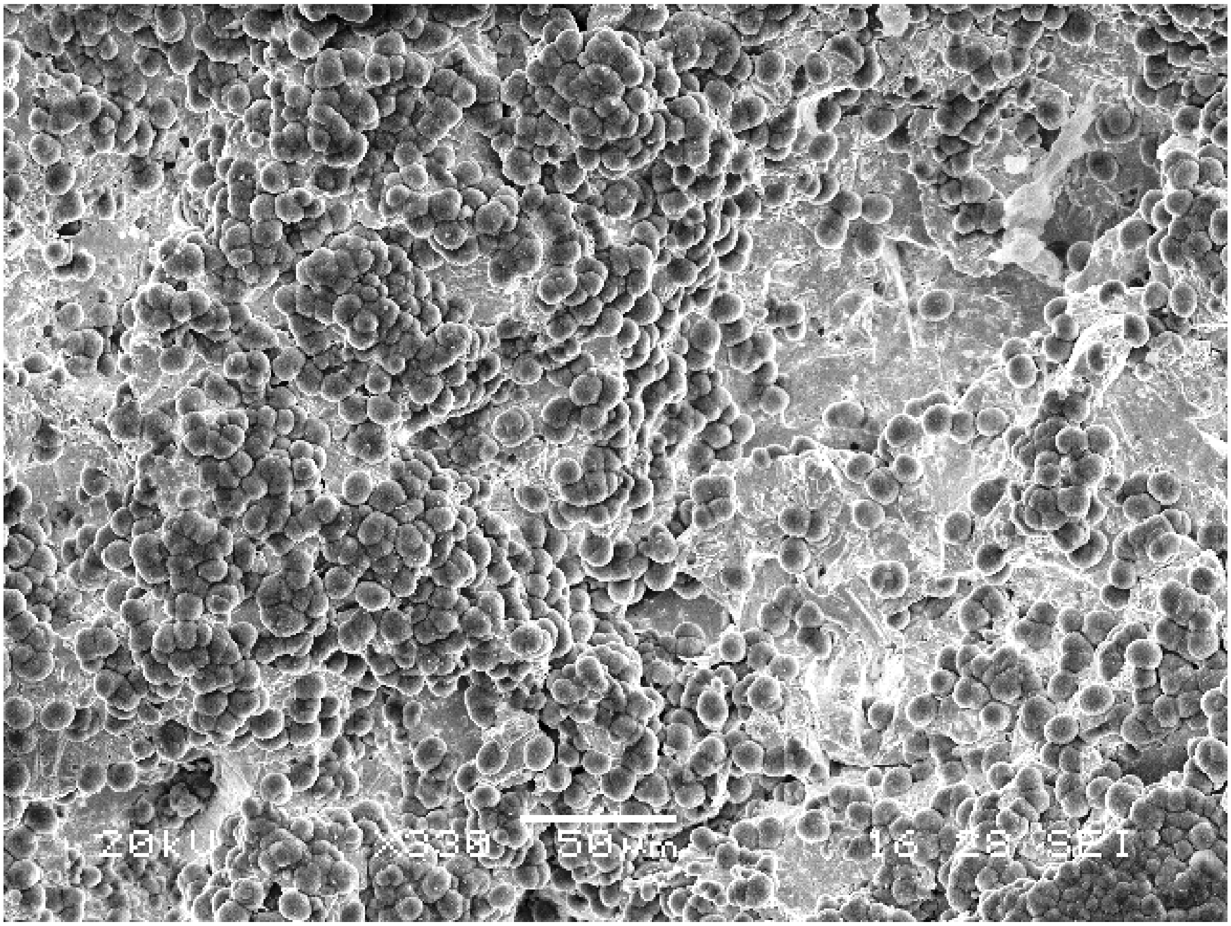

Figure 4-24 SEM image of Pb-carbonate corrosion products formed on partially submerged coupon L430. Image source: *L430_2.BMP* located on disk in “WIPP-FePb-3 Supplemental Binder D”.

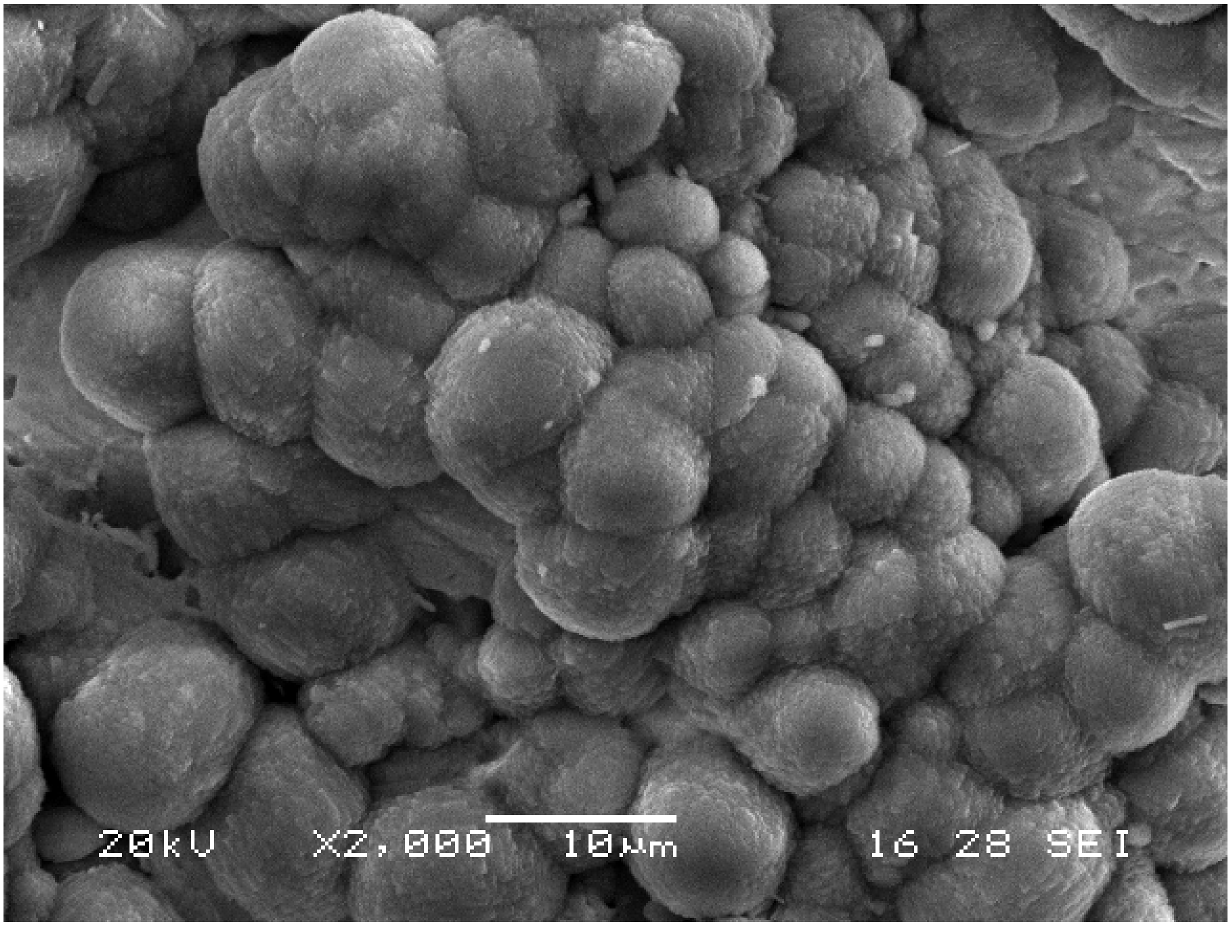

Figure 4-25 Enlarged view of Pb-carbonate corrosion products formed on coupon L430. Image source: *L430_2A.BMP* located on disk in “WIPP-FePb-3 Supplemental Binder D”.

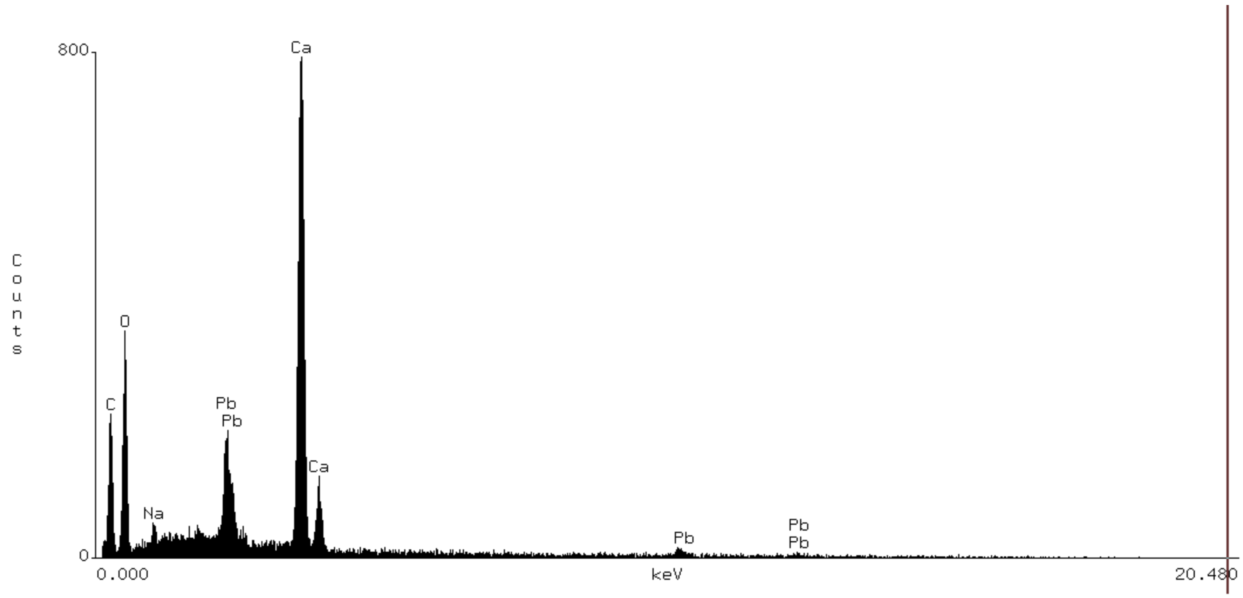

Figure 4-26 EDS spectra of Pb-carbonate corrosion product found in coupon L430. EDS spectra source: file *L430_2a.doc* located on disk in “WIPP-FePb-3 Supplemental Binder D”.

4.4 Determination of Mass-Loss and Corrosion Rates

After the corrosion tests have been completed, two of the three replicate coupons for each test condition were chemically cleaned in order to remove all of the corrosion products. The mass of the coupons after cleaning is compared to the initial mass and the difference represents the loss of material to corrosion. The mass loss can then be used to calculate a corrosion rate.

Table 4-4 Chemical Cleaning Procedures by Metal Type

Material	Chemical	Time	Temperature	Source[1]
Iron (Fe)	concentrated HCl + 50 g/L $SnCl_2$ + 20 g/L $SbCl_3$	25 min max.	Cold	A
	500 mL conc. hydrochloric acid (HCl) 3.5 g hexamethylene tetramine Reagent water to make 1000 mL	10 min	20 to 25 ºC	B
Lead (Pb)	250 g ammonium acetate (CH_3COONH_4) Reagent water to make 1000 mL	5 min	60 to 70 ºC	B
[1]Source: A, NACE Standard TM0169-2000; B, ASTM G 1 – 03.				

There are numerous standard procedures that outline requirements for the cleaning of corrosion samples: ISO 8407:1991, NACE Standard TM0169-2000 and ASTM G 1 – 03. For the most part, each of these standard procedures outlines nearly identical requirements and all coupons were cleaned per the requirements outlined in these standards. Where there are differences between the standards, the source for a particular requirement that was used will be noted. The cleaning process included multiple cycles of chemical etching, brushing with a nonmetallic soft bristle brush followed by rinsing with deionized water. Following each cleaning cycle the coupons were dried and weighed with the weight for each cycle being recorded in the scientific notebook. A minimum of five cleaning cycles was performed for each coupon. The details of the chemical cleaning solutions used for each material type are shown in Table 4-4.

Because the above cleaning procedures remove some amount of base metal in addition to the corrosion products a procedure needs to be employed that corrects the weight loss measurements for the base metal loss. This study uses a procedure of graphical analysis based on multiple cleaning cycles in order to extrapolate the actual weight loss due to corrosion from the total measured weight loss. The graphical analysis method is outlined in ISO 8407:1991 and is shown schematically in Figure 4-27. The mass of a coupon should have a linear relationship with respect to the cleaning cycles as long as the duration of each cycle is the same. A plot of the mass versus cleaning cycles ideally results in two lines (AB and BC in Figure 4-27). Line AB characterizes the removal of corrosion products and possibly base metal, whereas line BC is the result of removal of the base metal substrate after all corrosion products have been removed. Extrapolation of line BC to the 0^{th} cleaning cycle (point D) provides the mass of the coupon at zero cleaning cycles. The true mass of the coupon (minus corrosion products) will be between points B and D. For the purposes of determining mass loss in this study, point D is taken as the final weight.

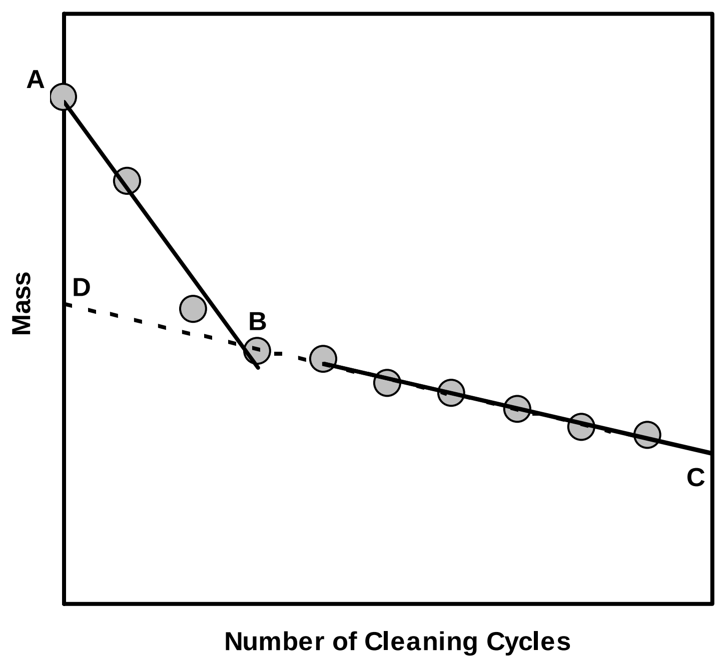

Figure 4-27 Graphical method used to determine coupon mass loss. True mass of the specimen after removal of the corrosion products will be between points B and D.

The raw cleaning cycle data and graphical analysis results for each coupon are given in Appendix B. Corrosion rates are calculated from the mass loss data in Appendix B according to the following formula (NACE, 2007):

$$rate = \frac{W \times 87.6}{SA \times t \times \rho} \times 1000 \tag{3}$$

where *rate* is the corrosion rate in μm/yr, *W* the mass loss (mg), *SA* the exposed surface area of the coupon (cm^2), *t* the exposure duration (hours), ρ the metal density (g/cm^3) and 1,000 converts the rate from mm/yr to μm/yr. The details of the surface area determination for each coupon are described in Appendix A. Metal densities of 7.872 g/cm^3 and 11.340 g/cm^3 were used for steel and lead, respectively (MatWeb, 2009).

Table 4-5 gives the steel coupon average corrosion rates calculated from the weight-loss and surface area measurements for each brine type and the humid samples. The average corrosion rates for the different brine types are calculated using the results for both the fully immersed and partially submerged coupons for each brine type. This was done because the calculated corrosion rates do not seem to be dependent on the coupon placement. The average steel corrosion rates are plotted as a function of CO_2 concentration in Figure 4-28. From this plot it can be seen that for both brine types the corrosion rate appears to be a function of the CO_2 concentration, regardless of the presence or absence of organic ligands. However, there are differences in the corrosion rates between the different brine types. The ERDA-6 brines appear to be more reactive than the GWB brines by a factor of nearly 3 at the higher CO_2 concentrations. It also appears that the addition of organic ligands to the ERDA-6 brine results in significantly less corrosion than the organic free ERDA-6. This does not appear to be the case for GWB. From Figure 4-28 it can be seen that there is little to no difference in the corrosion rates for the two GWB brine types. The humid samples show no corrosion regardless of the CO_2 concentration.

Table 4-5 Average Corrosion Rate (μm/yr) for Steel Samples

Brine	CO_2 Concentration (ppm)			
	0	350	1500	3500
GWB	0.08 ± 0.07	0.19 ± 0.04	0.24 ± 0.04	0.40 ± 0.03
GWB org	0.14 ± 0.09	0.20 ± 0.01	0.26 ± 0.06	0.39 ± 0.07
ERDA-6	0.08 ± 0.04	0.02 ± 0.02	0.53 ± 0.03	1.20 ± 0.25
ERDA-6 org	0.19 ± 0.11	0.02 ± 0.03	0.26 ± 0.07	0.65 ± 0.07
Humid	0.01 ± 0.00	0.00 ± 0.00	0.00 ± 0.00	0.01 ± 0.01

Source: Averages calculated from data in Appendix B. Note that negative corrosion rates given in Appendix B are considered as 0.0 for calculation of averages.

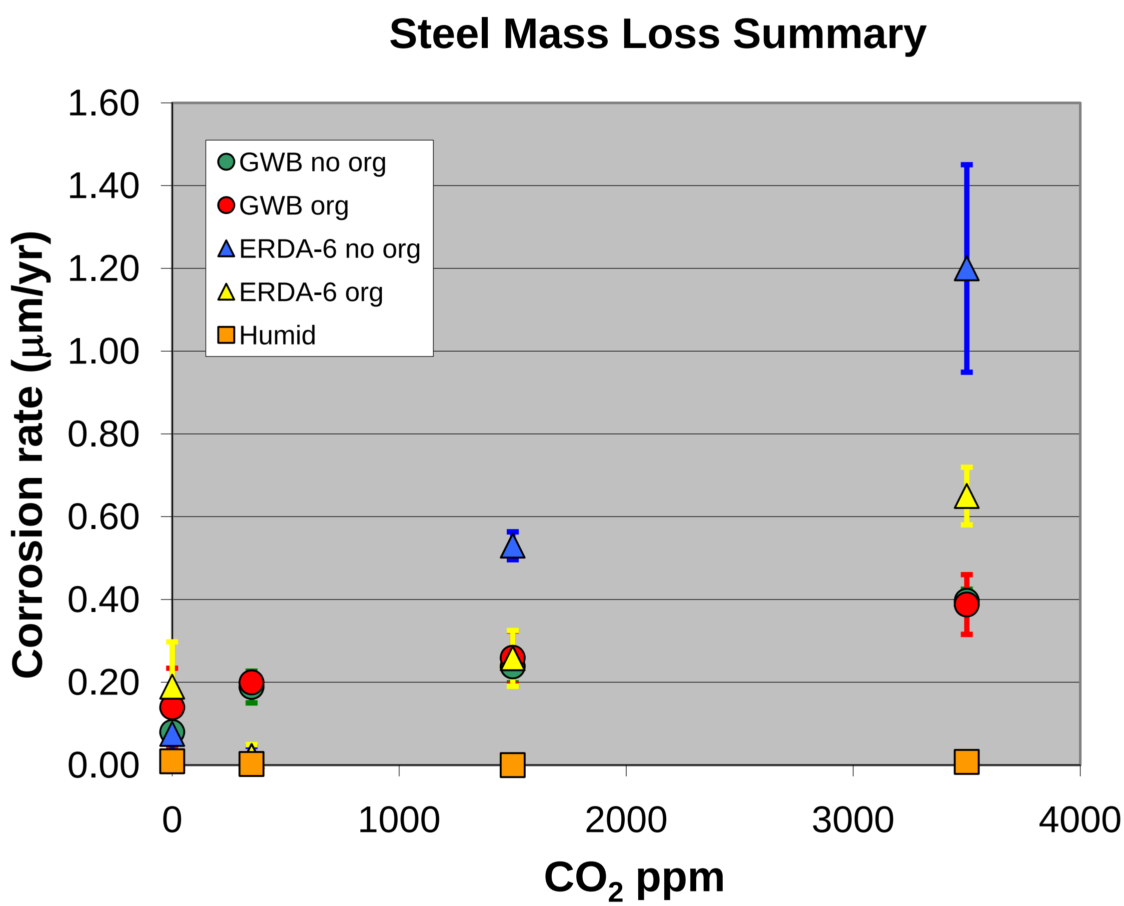

Figure 4-28 Average corrosion rates for steel coupons in the various brines plotted as a function of the atmospheric CO_2 concentration. Bars indicate one standard deviation for the average corrosion rates.

Table 4-6 gives the Pb coupon average corrosion rates calculated from the weight-loss and surface area measurements for each brine type and the humid samples. As with the steel coupons, the average Pb corrosion rates are calculated using the results for both the fully immersed and partially submerged coupons for each brine type. The average lead corrosion rates are plotted as a function of CO_2 concentration in Figure 4-29. From this plot it can be seen that the data for the lead coupons does not present as clear a picture as for the steel coupons. There may be a slight dependence on corrosion rates with the CO_2 concentration. However, given the relatively large standard deviation in the averages it is difficult to determine if there is an actual dependence on CO_2 concentration. Unlike the steel data, there does not appear to be differences in the corrosion rates between the different brine types. From Figure 4-29 it can also be seen that there is little to no difference in the corrosion rates for either brine types with the addition of organic ligands. The humid samples show measureable mass loss regardless of the CO_2

concentration. However, it is not certain if the magnitude of the mass loss is within the measurement uncertainty of the graphical analysis method (Appendix B).

Table 4-6 Average Corrosion Rate (µm/yr) for Lead Samples

Brine	CO_2 Concentration (ppm)			
	0	350	1500	3500
GWB	0.54 ± 0.16	0.31 ± 0.33	0.91 ± 0.82	0.60 ± 0.28
GWB org	0.33 ± 0.12	0.36 ± 0.09	0.95 ± 0.56	0.62 ± 0.34
ERDA-6	0.41 ± 0.22	0.19 ± 0.04	0.47 ± 0.37	0.73 ± 0.51
ERDA-6 org	0.32 ± 0.18	0.33 ± 0.06	0.51 ± 0.31	0.46 ± 0.17
Humid	0.06 ± 0.05	0.00 ± 0.00	0.15 ± 0.05	0.06 ± 0.02

Source: Averages calculated from data in Appendix B. Note that negative corrosion rates given in Appendix B are considered as 0.0 for calculation of averages.

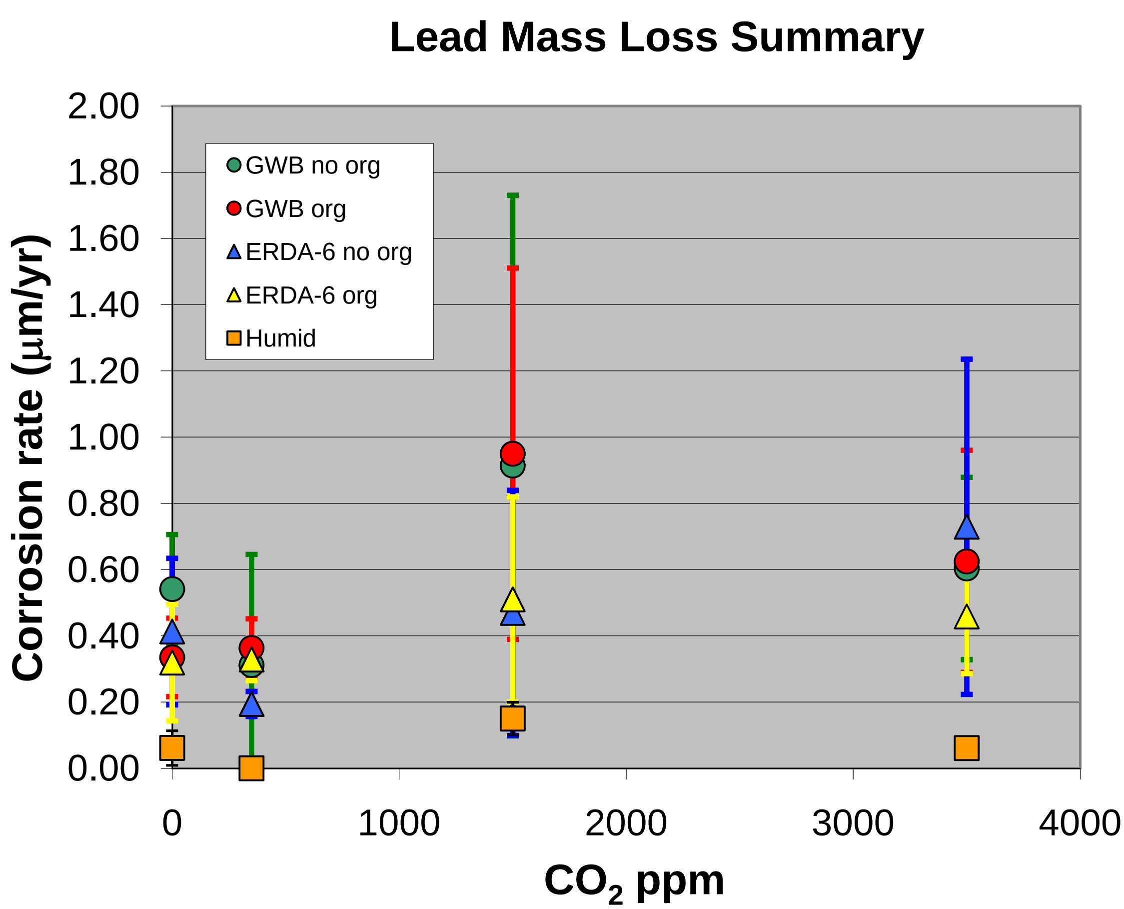

Figure 4-29 Average corrosion rates for lead coupons in the various brines plotted as a function of the atmospheric CO_2 concentration. Bars indicate one standard deviation for the average corrosion rates.

4.5 Brine Chemistry - pH

The initial pH for each of the brines used in the Fe/Pb corrosion experiments was measured at the time the brines were synthesized (Table 4-7). However, the measurement of pH in concentrated solutions using standard pH electrodes is problematic due to variations in the activity coefficients, formation of species such as HSO_4^- or $H_2B_4O_7$ that can consume protons during standardization, and potentially large liquid junction potentials (Rai et al., 1994). As a result, the pH values measured using standard pH electrodes need to be corrected to account for these effects. Several different methods have been proposed for determining the correction needed to convert measured pH values into meaningful hydrogen ion concentrations (Knauss et al., 1990, 1991; Mesmer, 1991; Rai et al., 1994). Each of these methods requires an empirical calibration of the pH electrode with the brines to be measured. At this time, the correction factor for the brines used in these experiments has not been determined. Therefore, the pH values reported here are done so as "measured" values and should not be used to calculate quantitative hydrogen ion concentrations. They are, however, valid measurements for qualitative comparisons of observed pH values among the different experiments.

Table 4-7 Initial Brine pH as Measured

Brine	pH_{meas}
GWB[1]	7.595
GWB[2] with organics	7.605
ERDA-6[1]	7.955
ERDA-6[2] with organics	7.915

[1] WIPP-FePb-3 p. 51
[2] WIPP-FePb-3 p. 52
Source: Average of values given in WIPP FePb-3 p. 65 (ERMS 550783)

At the conclusion of an experiment the brine pH is measured using a combination glass electrode. All pH measurements were conducted inside the anoxic glove box immediately after the coupons were removed from the brine. The final measured pH values for each of the 6 month experiments are given in Table 4-8. The data are shown plotted as a function of experimental duration in Figures 4-30A through 4-30D. From these plots it can be seen that there is almost no difference in the final measured pH values between the Pb and the steel experiments. In addition, there is no significant change in the pH over the duration of the experiments in the 0 ppm and 350 ppm CO_2 atmospheres (Figure 4-30A and 4-30B). In the experiments conducted in the 1500 ppm and 3500 ppm CO_2 atmospheres there is a noticeable trend in the measured pH values (Figure 4-30C and 4-30D). The differences in measured pH values between GWB and ERDA-6 have virtually disappeared. In addition, the measured pH after 6 months is lowered by as much as 0.5 pH units. Both of these trends are due to equilibration of the experimental brines with the relatively high CO_2 concentration of the atmospheres.

Table 4-8 Measured Final Brine pH of 6 month Experiments

0 ppm CO_2		350 ppm CO_2		1500 ppm CO_2		3500 ppm CO_2	
Test Matrix	pH_{meas}	Test Matrix	pH_{meas}	Test Matrix	pH_{meas}	Test Matrix	pH_{meas}
Fe-G-0000-6-f	7.581	Fe-G-0350-6-f	7.670	Fe-G-1500-6-f	7.652	Fe-G-3500-6-f	7.389
Fe-G-0000-6-p	7.577	Fe-G-0350-6-p	7.683	Fe-G-1500-6-p	7.601	Fe-G-3500-6-p	7.432
Fe-Go-0000-6-f	7.569	Fe-Go-0350-6-f	7.661	Fe-Go-1500-6-f	7.644	Fe-Go-3500-6-f	7.397
Fe-Go-0000-6-p	7.578	Fe-Go-0350-6-p	7.670	Fe-Go-1500-6-p	7.646	Fe-Go-3500-6-p	7.435
Fe-E-0000-6-f	7.941	Fe-E-0350-6-f	7.939	Fe-E-1500-6-f	7.642	Fe-E-3500-6-f	7.262
Fe-E-0000-6-p	7.912	Fe-E-0350-6-p	7.917	Fe-E-1500-6-p	7.619	Fe-E-3500-6-p	7.253
Fe-Eo-0000-6-f	7.858	Fe-Eo-0350-6-f	7.950	Fe-Eo-1500-6-f	7.775	Fe-Eo-3500-6-f	7.419
Fe-Eo-0000-6-p	7.890	Fe-Eo-0350-6-p	7.952	Fe-Eo-1500-6-p	7.723	Fe-Eo-3500-6-p	7.377
Pb-G-0000-6-f	7.683	Pb-G-0350-6-f	7.680	Pb-G-1500-6-f	7.658	Pb-G-3500-6-f	7.482
Pb-G-0000-6-p	7.711	Pb-G-0350-6-p	7.720	Pb-G-1500-6-p	7.684	Pb-G-3500-6-p	7.491
Pb-Go-0000-6-f	7.666	Pb-Go-0350-6-f	7.662	Pb-Go-1500-6-f	7.681	Pb-Go-3500-6-f	7.494
Pb-Go-0000-6-p	7.666	Pb-Go-0350-6-p	7.673	Pb-Go-1500-6-p	7.702	Pb-Go-3500-6-p	7.505
Pb-E-0000-6-f	8.023	Pb-E-0350-6-f	7.931	Pb-E-1500-6-f	7.703	Pb-E-3500-6-f	7.428
Pb-E-0000-6-p	8.033	Pb-E-0350-6-p	7.917	Pb-E-1500-6-p	7.682	Pb-E-3500-6-p	7.453
Pb-Eo-0000-6-f	7.970	Pb-Eo-0350-6-f	8.001	Pb-Eo-1500-6-f	7.781	Pb-Eo-3500-6-f	7.479
Pb-Eo-0000-6-p	7.948	Pb-Eo-0350-6-p	7.986	Pb-Eo-1500-6-p	7.772	Pb-Eo-3500-6-p	7.467
Sources: WIPP-FePb-3 p. 94-95 (ERMS: 550783); WIPP-FePb-4 p. 6, 11, 15, 18, 20, 21, 24 (ERMS 546084)							

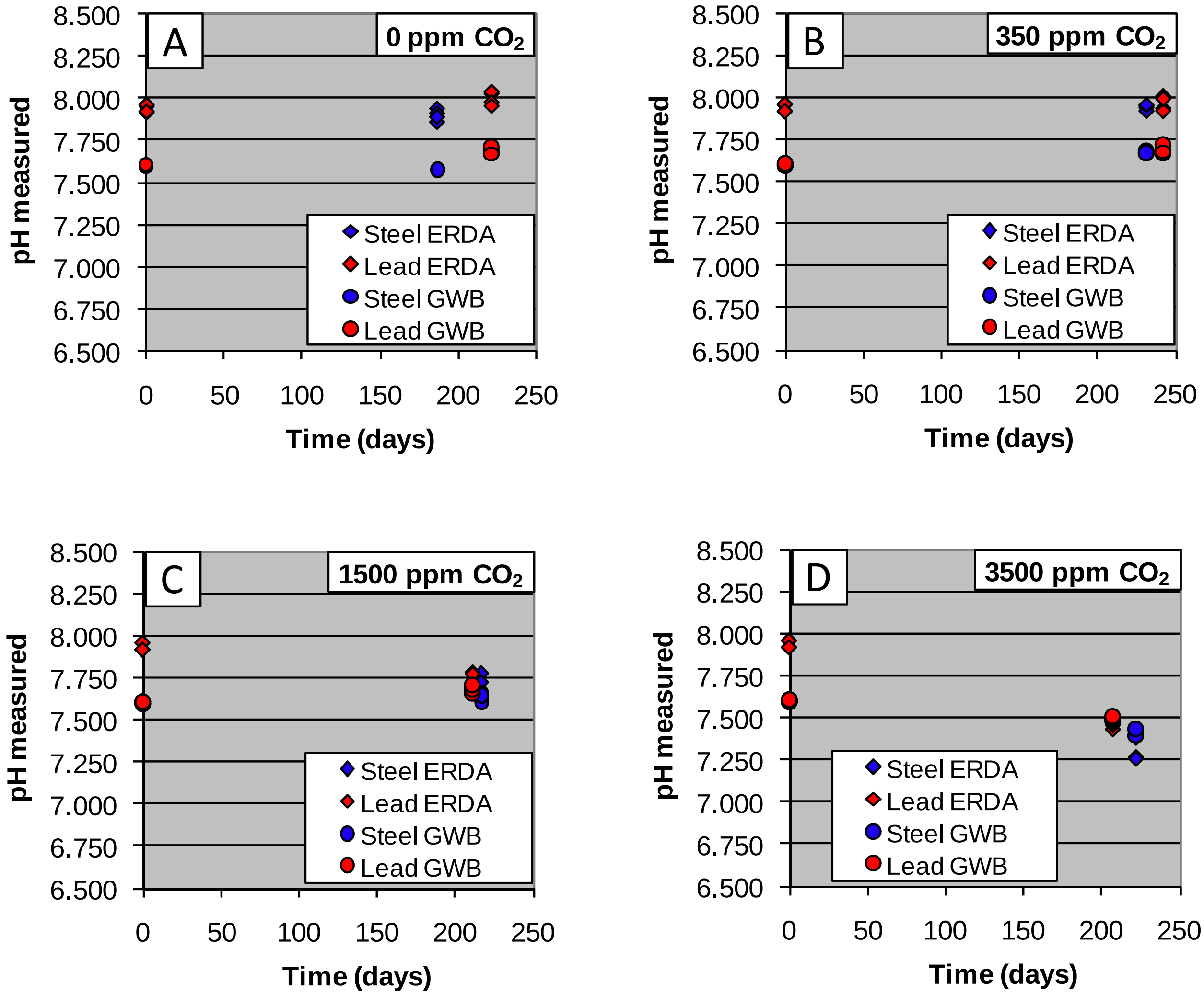

Figure 4-30 Measured pH plotted as a function of experiment duration for different carbon dioxide concentrations: (A) 0 ppm CO_2; (B) 350 ppm CO_2; (C) 1500 ppm CO_2; (D) 3500 ppm CO_2

5 CONCLUSIONS

This report describes the 6 month results of a multi-year study on the corrosion of steel and lead under WIPP-relevant conditions. Analysis of the results from this set of experiments allows the following conclusions to be drawn. It should be noted, however, that the results of future experiments conducted for longer times may require modification to these conclusions.

- ASTM A1008 low-carbon steel coupons show clear evidence of corrosion after 6 months immersion in brines. Partially submerged coupons develop a band of green corrosion product at the brine atmosphere interface. Fully immersed coupons exhibit a hazy luster with isolated spots of green corrosion products. Humid samples show no visible evidence of corrosion.

- SEM and EDS analysis of the steel coupons from the lower CO_2 atmospheres (<1500 ppm) show that the green corrosion product is likely an iron/magnesium-chlori-hydroxide. A second minor phase can be identified by its different habit and appears also to be an iron-chlori-hydroxide (with little or no Mg). At higher CO_2 concentrations the predominant corrosion product is an iron/calcium carbonate. Although the green corrosion product is seen as well. Carbonate formation seems to be favored by the ERDA-6 brines.

- The corrosion rate of ASTM A1008 low-carbon steel immersed in brine appears to be a function of the CO_2 concentration for all brine types. ERDA-6 brines (with and without organics) appear to be more reactive than the GWB brines by a factor of nearly 3 at higher CO_2 concentrations. The addition of organic ligands to the ERDA-6 brine results in significantly less corrosion than the organic free ERDA-6. Corrosion rates for GWB appear to be independent of the presence or absence of organic ligands.

- Chemical Pb coupons show little visible evidence of corrosion after 6 months immersion in brines. Partially submerged and humid coupons develop discoloration on the surfaces exposed to the atmosphere. Those portions of fully immersed and partially submerged coupons exposed to brine exhibit no macroscopic evidence of corrosion. In addition, no evidence of corrosion is visible at the brine/atmosphere interface in partially submerged experiments.

- SEM and EDS analysis of the Pb coupons shows a very limited amount of corrosion product formation. In atmospheres of 350 ppm CO_2 and above the formation of a calcium/lead carbonate phase is seen on coupons immersed in ERDA-6 brines. No carbonate phases are observed in coupons exposed to GWB with the exception of one experiment conducted at 3500 ppm CO_2. No corrosion product formation is seen in any of the discolored areas of coupons exposed to humid conditions.

- The corrosion rate of chemical Pb may show a slight dependence of corrosion rates on the CO_2 concentration. However, given the relatively large standard deviation in the averages it is difficult to determine if there is an actual dependence on CO_2 concentration. There does not appear to be any difference in the corrosion rates between the different brine types.

- Steel samples subjected only to humid conditions show no corrosion regardless of the CO_2 concentration. Whereas, humid Pb samples show measureable mass loss regardless of the CO_2 concentration. However, the magnitude of the mass loss may be within the measurement uncertainty of the graphical analysis method.

6 ACKNOWLEDGEMENTS

These experiments are the result of the dedicated work from numerous people whose assistance is greatly appreciated. The initial conceptual design for this work was developed by Nathalie Wall and David Enos. Michael Schuhen was responsible for most of the design, building, testing and maintenance of the MFGCS; without his insight the system would never have come to fruition. Raul Rascon and Panit Howard provided additional invaluable assistance in the creation of the MFGCS. A large part of the sample preparation and laboratory analysis work was conducted under the direction of Shelly Johnsen with the assistance of student interns: Caitlin Allen, Rachael Roselle, and Tana Saul.

7 REFERENCES

ASTM. 2003. *Standard Practice for Preparing, Cleaning and Evaluation Corrosion Test Specimens*. ASTM G 1 - 03. West Conshohocken, PA: American Society for Testing and Materials (ASTM) International.

Brush, L.H. 1990. *Test Plan for Laboratory and Modeling Studies of repository and Radionuclide Chemistry for the Waste Isolation Pilot Plant*. SAND90-0266. Albuquerque, NM: Sandia National Laboratories.

Brush, L.H. 2005. *Results of Calculations of Actinide Solubilities for the WIPP Performance Assessment Baseline Calculations*. Analysis report, May 18, 2005. Carlsbad, NM: Sandia National Laboratories. ERMS 539800.

Brush, L.H. and Y. Xiong. 2005. *Calculation of Organic-Ligand Concentrations for the WIPP Performance-Assessment Baseline Calculations*. Analysis report, May 4, 2005. Carlsbad, NM: Sandia National Laboratories. ERMS 539635.

Crawford, B.A. 2005. *Waste Material Densities in TRU Waste Streams from TWBID Revision 2.1 Version 3.13, Data Version D.4.15*. Analysis Report, April 13, 2005. Carlsbad, NM: Los Alamos National Laboratory. ERMS 539323.

Dunagan, S.C., G.T. Roselle, E.D. Vugrin, and J.L. Long. 2007. *Analysis Report for the Shielded Container Performance Assessment. Revision 1*. Analysis Report, November 7, 2007. Carlsbad, NM: Sandia National Laboratories. ERMS 547358.

Hertelendy, N.A. 1984. *Rockwell Hanford Operation User's Manual for Remote Handled Transuranic Waste Container*. Rockwell International document no. RHO-RE-MA-7, September, 1984.

ISO. 1991. *Corrosion of Metals and Alloys – Removal of Corrosion Products from Corrosion Test Specimens*. ISO 8407:1991. Geneva, Switzerland: International Organization for Standardization.

Knauss, K.G., T.J. Wolery and K.J. Jackson. 1990. "A new approach to measuring pH in brines and other concentrated electrolytes", *Geochimica et Cosmochimica Acta*, v. 54, 1519-1523.

Knauss, K.G., T.J. Wolery and K.J. Jackson. 1991. "Reply to Comment by R.E. Mesmer on "A new approach to measuring pH in brines and other concentrated electrolytes"", *Geochimica et Cosmochimica Acta*, v. 55, 1177-1179.

Kubal, M. and F. Panacek. 1995. "Potential-pH Diagram for Fe-H_2O-Citric Acid System", *British Corrosion Journal*, v. 30, no. 4, 309-311.

MatWeb. 2009. *Material Properties for AISI 1008 Steel and Chemical Lead (Pb).* http://www.matweb.com. ERMS 551896.

Mesmer, R.E.. 1991. "Comments on "A new approach to measuring pH in brines and other concentrated electrolytes" by K.G. Knauss, T.J. Wolery, and K.J. Jackson", *Geochimica et Cosmochimica Acta*, v. 55, 1175-1176.

Munson, D.E., R.L. Jones, D.L. Hoag, and J.R. Ball. 1987. *Heated Axisymmetric Pillar Test (Room H): In Situ Data Report (February 1985 – April 1987), Waste Isolation Pilot Plant (WIPP) Thermal/Structural Interactions Program*. SAND87-2488. Albuquerque, NM: Sandia National Laboratories.

NACE. 2000. *Standard Test Method - Laboratory Corrosion Testing of Metals*. TM0169-2000. Houston, TX: National Association of Corrosion Engineers (NACE) International.

Pletcher, D., D. Sidorin, and B. Hedges. 2005. "A Comparison of the Corrosion of Carbon and 13% Chromium Steels in Oilfield Brines Containing Acetate." *CO_2 corrosion in Oil and Gas Production Symposium, Proceedings of the NACE Corrosion 2005 Conference held in Houston, TX, April 3-7, 2005*, National Association of Corrosion Engineers (NACE) International, Houston, TX, paper no. 05301.

Rai, D., A.R. Felmy, S.P. Juracich, and F. Rao. 1994. *Estimating the Hydrogen Ion Concentration in Concentrated NaCl and Na_2SO_4 Electrolytes*. SAND94-1949. Albuquerque, NM: Sandia National Laboratories.

Saltykov, S.N., G.V. Makarov, E.L. Toroptseva, and Y.B. Filatova. 1989. "Anodic Behavior of White Iron Phases in Oxalic Media". *Protection of Metals*, v. 40, no. 1, 56-61.

Sankarapapavinasam, S., F. Pushpanaden, and M.F. Ahmed. 1989a. "Dicarboxalic Acids as Corrosion Inhibitors for Lead in $HClO_4$." *Bulletin of Electrochemistry*, v. 5, no. 5, 319-323.

Sankarapapavinasam, S., F. Pushpanaden, and M.F. Ahmed. 1989a. "Hydrazine and Substituted Hydrazines as Corrosion Inhibitors for Lead in Acetic Acid." *British Corrosion Journal*, v. 24, no. 1, 39-42.

Schuhen, M. 2007. Pressure Safety Pressure Package: Mixed Flow Gas Control System for Corrosion Experiments, Rev. 00. Sandia National Laboratories. Carlsbad, NM.

Sellmer, T. 2007. Final Container Design, Shielded Container. Washington TRU Solutions, Carlsbad, NM. ERMS 547052.

Telander, M.R., and R.E. Westerman. 1993. *Hydrogen Generation by Metal Corrosion in Simulated Waste Isolation Pilot Plant Environments*. SAND92-7347. Albuquerque, NM: Sandia National Laboratories.

Telander, M.R., and R.E. Westerman. 1997. *Hydrogen Generation by Metal Corrosion in Simulated Waste Isolation Pilot Plant Environments*. SAND96-2538. Albuquerque, NM: Sandia National Laboratories.

U.S. DOE. 2009. *Title 40 CFR Part 191 Compliance Recertification Application for the Waste Isolation Pilot*, *Vol. 1-8*. DOE/WIPP 2009-3424. Carlsbad, NM: U.S. Department of Energy Carlsbad Field Office.

Wall, N.A. and D. Enos. 2006. Iron and Lead Corrosion in WIPP-Relevant Conditions, TP 06-02, Rev. 1. Sandia National Laboratories, Carlsbad, NM. ERMS 543238.

APPENDIX A

Table A-1 lists the length, width and thickness measurements for each steel coupon, as well as, the average value of these measurements used to calculate the surface area. The equivalent data for the lead coupons is given in Table A-2. Additionally, for each of the coupons that were partially submerged the length of the portion of the coupon that was submerged is also given. In this case two measurements are made because the coupon may not have been submerged exactly parallel to the water surface.

For coupons that were fully submerged or exposed only to the atmosphere the following formula is used to calculate surface area:

$$SA = 2(L_{avg}\times W_{avg}) + 2(L_{avg}\times T_{avg}) + 2(W_{avg}\times T_{avg}) - 2\pi R^2 + 2\pi R\times T_{avg} \qquad \text{(A1)}$$

where L_{avg} is the average measured length, W_{avg} the average width, T_{avg} the average thickness and R the radius of the hole, which is assumed constant for each coupon at 0.235 cm for steel coupons and 0.296 cm for lead coupons. The surface area for coupons that were partially submerged is calculated as follows:

$$SA = 2(L_1\times W_{avg}) + (L_1\times T_{avg}) + (L_2\times T_{avg}) + (W_{avg}\times T_{avg}) + (W_{avg}\times (L_2\text{-}L_1)) \qquad \text{(A2)}$$

where L_1 is the smallest measured partial submersion length, L_2 the largest measured length and all other symbols are the same as for equation A1.

Table A-1 Measured Steel Coupon Dimensions and Calculated Surface Areas

Coupon		1 (mm)	2 (mm)	3 (mm)	Average (mm)	Average (cm)	L_1 (cm)	L_2 (cm)	SA (cm^2)
087	Length	51.24	51.02	51.21	51.16	5.116	N/A	N/A	41.629
	Width	38.44	38.48	38.37	38.43	3.843			
	Thickness	1.35	1.38	1.38	1.37	0.137			
089	Length	51.26	51.29	51.11	51.22	5.122	N/A	N/A	41.663
	Width	38.35	38.47	38.24	38.35	3.835			
	Thickness	1.40	1.40	1.41	1.40	0.140			
090	Length	51.24	51.16	51.04	51.15	5.115	2.838	2.999	23.751
	Width	38.31	38.54	38.36	38.40	3.840			
	Thickness	1.38	1.38	1.38	1.38	0.138			
091	Length	51.11	51.23	51.33	51.22	5.122	2.893	2.999	23.918
	Width	38.55	38.39	38.35	38.43	3.843			
	Thickness	1.30	1.31	1.32	1.31	0.131			
094	Length	51.10	51.24	51.18	51.17	5.117	N/A	N/A	41.625
	Width	38.57	38.53	38.27	38.46	3.846			
	Thickness	1.36	1.36	1.32	1.35	0.135			
095	Length	51.13	51.20	51.07	51.13	5.113	N/A	N/A	41.505
	Width	38.37	38.48	38.36	38.40	3.840			
	Thickness	1.32	1.34	1.33	1.33	0.133			
097	Length	51.13	51.40	51.24	51.26	5.126	2.923	3.111	24.389
	Width	38.36	38.51	38.30	38.39	3.839			
	Thickness	1.29	1.23	1.20	1.24	0.124			
098	Length	51.00	51.16	51.18	51.11	5.111	2.720	3.192	24.033
	Width	38.65	38.65	38.47	38.59	3.859			
	Thickness	1.21	1.26	1.27	1.25	0.125			
099	Length	50.97	51.53	51.18	51.23	5.123	N/A	N/A	41.709
	Width	38.55	38.60	38.67	38.61	3.861			
	Thickness	1.27	1.29	1.30	1.29	0.129			
100	Length	51.17	51.38	51.31	51.29	5.129	N/A	N/A	41.641
	Width	38.40	38.45	38.42	38.42	3.842			
	Thickness	1.30	1.35	1.33	1.33	0.133			
102	Length	51.09	51.18	51.04	51.10	5.110	3.077	3.223	25.583
	Width	38.33	38.54	38.37	38.41	3.841			
	Thickness	1.36	1.36	1.37	1.36	0.136			
103	Length	50.83	51.23	51.23	51.10	5.110	2.947	3.160	24.773
	Width	38.23	38.45	38.34	38.34	3.834			
	Thickness	1.35	1.38	1.37	1.37	0.137			
106	Length	51.00	51.17	51.21	51.13	5.113	N/A	N/A	41.446
	Width	38.24	38.40	38.27	38.30	3.830			
	Thickness	1.35	1.35	1.37	1.36	0.136			
107	Length	51.20	51.22	50.84	51.09	5.109	N/A	N/A	41.464
	Width	38.30	38.49	38.26	38.35	3.835			
	Thickness	1.35	1.37	1.35	1.36	0.136			

Table A-1 continued.

Coupon		1 (mm)	2 (mm)	3 (mm)	Average (mm)	Average (cm)	L_1 (cm)	L_2 (cm)	SA (cm^2)
108	Length	50.98	51.23	51.19	51.13	5.113	2.997	3.075	24.634
	Width	38.24	38.46	38.32	38.34	3.834			
	Thickness	1.36	1.36	1.38	1.37	0.137			
109	Length	51.17	51.27	51.15	51.20	5.120	2.953	3.077	24.473
	Width	38.31	38.47	38.35	38.38	3.838			
	Thickness	1.34	1.34	1.37	1.35	0.135			
111	Length	51.24	51.25	51.07	51.19	5.119	N/A	N/A	41.457
	Width	38.25	38.48	38.35	38.36	3.836			
	Thickness	1.32	1.31	1.29	1.31	0.131			
112	Length	51.01	51.25	51.28	51.18	5.118	N/A	N/A	41.534
	Width	38.25	38.45	38.34	38.35	3.835			
	Thickness	1.34	1.36	1.37	1.36	0.136			
114	Length	51.14	51.29	51.27	51.23	5.123	N/A	N/A	41.594
	Width	38.43	38.50	38.29	38.41	3.841			
	Thickness	1.37	1.32	1.31	1.33	0.133			
115	Length	51.23	51.21	51.06	51.17	5.117	N/A	N/A	41.617
	Width	38.39	38.50	38.49	38.46	3.846			
	Thickness	1.33	1.34	1.36	1.34	0.134			
117	Length	51.08	51.36	51.15	51.20	5.120	2.936	2.987	23.976
	Width	38.36	38.53	38.30	38.40	3.840			
	Thickness	1.24	1.26	1.29	1.26	0.126			
118	Length	50.90	51.23	51.27	51.13	5.113	2.969	3.019	24.272
	Width	38.36	38.55	38.42	38.44	3.844			
	Thickness	1.28	1.28	1.26	1.27	0.127			
120	Length	51.04	51.17	51.23	51.15	5.115	N/A	N/A	41.405
	Width	38.38	38.51	38.30	38.40	3.840			
	Thickness	1.21	1.29	1.33	1.28	0.128			
121	Length	51.27	51.22	51.10	51.20	5.120	N/A	N/A	41.634
	Width	38.37	38.53	38.37	38.42	3.842			
	Thickness	1.37	1.36	1.35	1.36	0.136			
123	Length	51.24	51.17	51.04	51.15	5.115	2.942	3.003	24.181
	Width	38.33	38.51	38.45	38.43	3.843			
	Thickness	1.37	1.36	1.36	1.36	0.136			
124	Length	50.97	51.22	51.25	51.15	5.115	2.981	3.035	24.496
	Width	38.39	38.69	38.37	38.48	3.848			
	Thickness	1.36	1.36	1.37	1.36	0.136			
126	Length	51.44	51.21	51.04	51.23	5.123	N/A	N/A	41.561
	Width	38.32	38.47	38.36	38.38	3.838			
	Thickness	1.35	1.32	1.32	1.33	0.133			
127	Length	51.02	51.32	51.20	51.18	5.118	N/A	N/A	41.526
	Width	38.37	38.51	38.34	38.41	3.841			
	Thickness	1.30	1.31	1.35	1.32	0.132			
129	Length	51.12	51.27	51.29	51.23	5.123	2.799	3.068	23.843
	Width	38.41	38.61	38.31	38.44	3.844			
	Thickness	1.32	1.31	1.35	1.33	0.133			

Table A-1 continued.

Coupon		1 (mm)	2 (mm)	3 (mm)	Average (mm)	Average (cm)	L_1 (cm)	L_2 (cm)	SA (cm^2)
130	Length	51.23	51.21	51.04	51.16	5.116	2.915	3.049	24.270
	Width	38.38	38.74	38.33	38.48	3.848			
	Thickness	1.37	1.32	1.34	1.34	0.134			
132	Length	51.25	51.20	51.03	51.16	5.116	N/A	N/A	41.502
	Width	38.37	38.51	38.39	38.42	3.842			
	Thickness	1.32	1.30	1.30	1.31	0.131			
133	Length	51.33	51.25	51.10	51.23	5.123	N/A	N/A	41.613
	Width	38.41	38.59	38.40	38.47	3.847			
	Thickness	1.33	1.29	1.32	1.31	0.131			
135	Length	51.07	51.24	51.25	51.19	5.119	2.857	2.857	23.204
	Width	38.37	38.53	38.29	38.40	3.840			
	Thickness	1.34	1.31	1.32	1.32	0.132			
136	Length	51.23	51.16	50.93	51.11	5.111	2.818	2.961	23.356
	Width	38.28	38.36	38.37	38.34	3.834			
	Thickness	1.28	1.24	1.23	1.25	0.125			
138	Length	51.04	51.17	51.17	51.13	5.113	N/A	N/A	41.535
	Width	38.42	38.60	38.66	38.56	3.856			
	Thickness	1.27	1.22	1.30	1.26	0.126			
139	Length	50.98	51.18	51.25	51.14	5.114	N/A	N/A	41.375
	Width	38.33	38.46	38.41	38.40	3.840			
	Thickness	1.31	1.23	1.25	1.26	0.126			
307	Length	51.03	51.37	51.37	51.26	5.126	N/A	N/A	41.756
	Width	38.54	38.29	38.67	38.50	3.850			
	Thickness	1.36	1.37	1.34	1.36	0.136			
308	Length	51.17	51.44	51.45	51.35	5.135	N/A	N/A	41.781
	Width	38.40	38.43	38.54	38.46	3.846			
	Thickness	1.35	1.34	1.37	1.35	0.135			
310	Length	51.06	51.25	51.19	51.17	5.117	3.062	3.062	24.858
	Width	38.41	38.29	38.42	38.37	3.837			
	Thickness	1.36	1.35	1.38	1.36	0.136			
311	Length	51.04	51.34	51.29	51.22	5.122	3.016	3.016	24.512
	Width	38.29	38.49	38.53	38.44	3.844			
	Thickness	1.36	1.35	1.32	1.34	0.134			
313	Length	51.17	51.38	51.39	51.31	5.131	N/A	N/A	41.770
	Width	38.44	38.55	38.53	38.51	3.851			
	Thickness	1.34	1.34	1.33	1.34	0.134			
314	Length	51.67	50.99	51.19	51.28	5.128	N/A	N/A	41.711
	Width	38.46	38.49	38.38	38.44	3.844			
	Thickness	1.36	1.36	1.34	1.35	0.135			
316	Length	51.08	51.19	51.14	51.14	5.114	2.829	2.987	23.589
	Width	38.37	38.55	38.28	38.40	3.840			
	Thickness	1.33	1.29	1.28	1.30	0.130			
317	Length	51.25	51.25	51.20	51.23	5.123	2.663	2.871	22.720
	Width	38.61	38.84	38.93	38.79	3.879			
	Thickness	1.32	1.30	1.37	1.33	0.133			

Table A-1 continued.

Coupon		1 (mm)	2 (mm)	3 (mm)	Average (mm)	Average (cm)	L_1 (cm)	L_2 (cm)	SA (cm^2)
319	Length	51.19	51.29	51.29	51.26	5.126	N/A	N/A	41.838
	Width	38.42	38.67	38.68	38.59	3.859			
	Thickness	1.35	1.35	1.35	1.35	0.135			
320	Length	51.07	51.25	51.20	51.17	5.117	N/A	N/A	41.611
	Width	38.35	38.54	38.44	38.44	3.844			
	Thickness	1.35	1.35	1.34	1.35	0.135			
322	Length	51.04	51.32	51.33	51.23	5.123	2.830	2.830	22.927
	Width	38.30	38.46	38.40	38.39	3.839			
	Thickness	1.24	1.28	1.27	1.26	0.126			
323	Length	51.02	51.23	51.28	51.18	5.118	2.830	2.830	23.024
	Width	38.66	38.44	38.50	38.53	3.853			
	Thickness	1.30	1.28	1.25	1.28	0.128			
325	Length	51.17	51.37	51.00	51.18	5.118	N/A	N/A	41.723
	Width	38.45	38.73	38.64	38.61	3.861			
	Thickness	1.30	1.31	1.33	1.31	0.131			
326	Length	51.16	51.23	51.09	51.16	5.116	N/A	N/A	41.636
	Width	38.36	38.52	38.44	38.44	3.844			
	Thickness	1.35	1.41	1.34	1.37	0.137			
328	Length	51.16	51.14	50.94	51.08	5.108	2.663	2.888	22.565
	Width	38.26	38.44	38.35	38.35	3.835			
	Thickness	1.34	1.36	1.38	1.36	0.136			
329	Length	51.10	51.25	51.19	51.18	5.118	2.717	2.830	22.588
	Width	38.33	38.54	38.39	38.42	3.842			
	Thickness	1.43	1.27	1.38	1.36	0.136			
331	Length	50.95	51.25	51.21	51.14	5.114	N/A	N/A	41.612
	Width	38.35	38.49	38.30	38.38	3.838			
	Thickness	1.42	1.38	1.39	1.40	0.140			
332	Length	51.08	51.22	51.15	51.15	5.115	N/A	N/A	41.606
	Width	38.39	38.50	38.35	38.41	3.841			
	Thickness	1.38	1.36	1.37	1.37	0.137			
416	Length	51.03	51.30	51.14	51.16	5.116	N/A	N/A	41.449
	Width	38.25	38.51	38.33	38.36	3.836			
	Thickness	1.34	1.31	1.29	1.31	0.131			
417	Length	51.01	51.19	51.19	51.13	5.113	N/A	N/A	41.443
	Width	38.26	38.48	38.32	38.35	3.835			
	Thickness	1.36	1.33	1.29	1.33	0.133			
418	Length	51.21	51.23	50.91	51.12	5.112	2.514	2.813	21.659
	Width	38.31	38.56	38.31	38.39	3.839			
	Thickness	1.33	1.32	1.30	1.32	0.132			
419	Length	51.00	51.29	51.23	51.17	5.117	2.574	2.727	21.521
	Width	38.30	38.55	38.34	38.40	3.840			
	Thickness	1.27	1.28	1.28	1.28	0.128			
423	Length	51.08	51.23	51.14	51.15	5.115	N/A	N/A	41.317
	Width	38.28	38.45	38.22	38.32	3.832			
	Thickness	1.27	1.28	1.27	1.27	0.127			

Table A-1 continued.

Coupon		1 (mm)	2 (mm)	3 (mm)	Average (mm)	Average (cm)	L_1 (cm)	L_2 (cm)	SA (cm^2)
424	Length	50.98	51.30	51.11	51.13	5.113	N/A	N/A	41.316
	Width	38.25	38.50	38.39	38.38	3.838			
	Thickness	1.25	1.24	1.25	1.25	0.125			
425	Length	51.03	51.29	51.07	51.13	5.113	2.648	2.668	21.545
	Width	38.29	38.53	38.29	38.37	3.837			
	Thickness	1.24	1.26	1.26	1.25	0.125			
426	Length	50.94	51.18	51.15	51.09	5.109	2.650	2.748	22.001
	Width	38.34	38.48	38.32	38.38	3.838			
	Thickness	1.38	1.39	1.40	1.39	0.139			
430	Length	51.09	51.24	51.15	51.16	5.116	N/A	N/A	41.442
	Width	38.37	38.52	38.30	38.40	3.840			
	Thickness	1.25	1.30	1.32	1.29	0.129			
431	Length	50.95	51.25	51.22	51.14	5.114	N/A	N/A	41.617
	Width	38.34	38.53	38.35	38.41	3.841			
	Thickness	1.39	1.38	1.38	1.38	0.138			
433	Length	50.91	51.20	51.16	51.09	5.109	2.793	2.876	23.045
	Width	38.30	38.50	38.36	38.39	3.839			
	Thickness	1.36	1.35	1.34	1.35	0.135			
434	Length	50.97	51.29	51.26	51.17	5.117	2.657	2.792	22.135
	Width	38.29	38.46	38.30	38.35	3.835			
	Thickness	1.35	1.32	1.33	1.33	0.133			
435	Length	51.04	51.23	51.19	51.15	5.115	N/A	N/A	41.597
	Width	38.32	38.64	38.45	38.47	3.847			
	Thickness	1.33	1.33	1.34	1.33	0.133			
436	Length	50.89	51.17	51.13	51.06	5.106	N/A	N/A	41.420
	Width	38.30	38.50	38.27	38.36	3.836			
	Thickness	1.38	1.33	1.31	1.34	0.134			
438	Length	51.14	51.25	51.05	51.15	5.115	2.870	2.870	23.304
	Width	38.40	38.52	38.22	38.38	3.838			
	Thickness	1.33	1.33	1.33	1.33	0.133			
439	Length	51.15	51.22	51.10	51.16	5.116	2.765	2.765	22.475
	Width	38.27	38.49	38.47	38.41	3.841			
	Thickness	1.35	1.31	1.29	1.32	0.132			
441	Length	50.94	51.21	51.19	51.11	5.111	N/A	N/A	41.368
	Width	38.24	38.46	38.20	38.30	3.830			
	Thickness	1.32	1.32	1.33	1.32	0.132			
442	Length	51.03	51.21	51.20	51.15	5.115	N/A	N/A	41.502
	Width	38.33	38.52	38.34	38.40	3.840			
	Thickness	1.35	1.33	1.30	1.33	0.133			

Source: Individual data sheets for each coupon in *WIPP-FePb-3 Supplemental Binder C (ERMS 546084)*

Table A-2 Measured Lead Coupon Dimensions and Calculated Surface Areas

Coupon		1 (mm)	2 (mm)	3 (mm)	Average (mm)	Average (cm)	L_1 (cm)	L_2 (cm)	SA (cm^2)
L083	Length	51.52	51.57	51.45	51.51	5.151	N/A	N/A	43.101
	Width	38.90	38.99	39.01	38.97	3.897			
	Thickness	1.70	1.73	1.84	1.76	0.176			
L084	Length	51.52	51.37	51.32	51.40	5.140	N/A	N/A	42.560
	Width	38.56	38.59	38.70	38.62	3.862			
	Thickness	1.68	1.74	1.73	1.72	0.172			
L086	Length	51.92	51.63	51.64	51.73	5.173	2.702	3.011	23.784
	Width	38.68	38.53	38.70	38.64	3.864			
	Thickness	1.68	1.88	1.80	1.79	0.179			
L087	Length	51.49	51.54	51.65	51.56	5.156	2.693	2.693	22.407
	Width	38.71	38.61	38.64	38.65	3.865			
	Thickness	1.71	1.70	1.74	1.72	0.172			
L089	Length	51.46	51.59	51.26	51.44	5.144	N/A	N/A	42.720
	Width	38.66	38.78	38.60	38.68	3.868			
	Thickness	1.78	1.74	1.73	1.75	0.175			
L090	Length	51.61	51.41	51.44	51.49	5.149	N/A	N/A	42.920
	Width	38.64	38.88	39.25	38.92	3.892			
	Thickness	1.64	1.73	1.73	1.70	0.170			
L091	Length	51.27	51.41	51.50	51.39	5.139	3.030	3.030	25.151
	Width	38.30	38.76	39.09	38.72	3.872			
	Thickness	1.71	1.70	1.69	1.70	0.170			
L093	Length	51.23	51.17	51.55	51.32	5.132	2.834	2.834	23.720
	Width	38.86	38.93	39.00	38.93	3.893			
	Thickness	1.76	1.69	1.74	1.73	0.173			
L094	Length	51.64	51.64	51.86	51.71	5.171	N/A	N/A	42.969
	Width	38.52	38.72	39.00	38.75	3.875			
	Thickness	1.74	1.72	1.72	1.73	0.173			
L095	Length	51.61	51.53	51.43	51.52	5.152	N/A	N/A	42.895
	Width	38.96	38.60	38.85	38.80	3.880			
	Thickness	1.73	1.72	1.76	1.74	0.174			
L097	Length	51.41	51.40	51.47	51.43	5.143	3.029	3.029	25.225
	Width	38.75	38.76	38.91	38.81	3.881			
	Thickness	1.74	1.79	1.65	1.73	0.173			
L098	Length	51.63	51.59	51.67	51.63	5.163	3.051	3.051	25.287
	Width	38.45	38.70	38.84	38.66	3.866			
	Thickness	1.63	1.75	1.72	1.70	0.170			
L100	Length	51.11	51.49	51.51	51.37	5.137	N/A	N/A	42.574
	Width	38.70	38.37	38.82	38.63	3.863			
	Thickness	1.74	1.76	1.69	1.73	0.173			
L101	Length	51.57	51.26	51.25	51.36	5.136	N/A	N/A	42.586
	Width	38.65	38.58	38.83	38.69	3.869			
	Thickness	1.74	1.68	1.71	1.71	0.171			

Table A-2 continued.

Coupon		1 (mm)	2 (mm)	3 (mm)	Average (mm)	Average (cm)	L_1 (cm)	L_2 (cm)	SA (cm^2)
L103	Length	51.35	51.46	51.74	51.52	5.152	3.044	3.161	25.949
	Width	39.08	38.87	39.12	39.02	3.902			
	Thickness	1.75	1.69	1.71	1.72	0.172			
L104	Length	51.44	51.43	51.42	51.43	5.143	3.039	3.156	25.703
	Width	38.73	38.90	38.41	38.68	3.868			
	Thickness	1.66	1.78	1.75	1.73	0.173			
L106	Length	51.46	51.57	51.67	51.57	5.157	N/A	N/A	42.637
	Width	38.48	38.92	38.37	38.59	3.859			
	Thickness	1.67	1.72	1.72	1.70	0.170			
L107	Length	51.23	51.50	51.60	51.44	5.144	N/A	N/A	43.091
	Width	39.03	39.27	39.07	39.12	3.912			
	Thickness	1.70	1.67	1.72	1.70	0.170			
L109	Length	51.17	51.58	51.42	51.39	5.139	N/A	N/A	42.860
	Width	38.80	39.14	39.05	39.00	3.900			
	Thickness	1.70	1.67	1.64	1.67	0.167			
L110	Length	51.47	51.55	51.40	51.47	5.147	N/A	N/A	42.759
	Width	38.87	38.71	38.86	38.81	3.881			
	Thickness	1.69	1.68	1.68	1.68	0.168			
L112	Length	51.56	51.53	51.70	51.60	5.160	2.881	2.940	24.120
	Width	38.77	38.74	38.48	38.66	3.866			
	Thickness	1.65	1.68	1.67	1.67	0.167			
L113	Length	51.62	51.66	51.79	51.69	5.169	2.760	2.783	23.093
	Width	38.93	38.89	38.78	38.87	3.887			
	Thickness	1.66	1.62	1.65	1.64	0.164			
L115	Length	51.77	51.67	51.58	51.67	5.167	N/A	N/A	42.960
	Width	38.76	38.63	38.71	38.70	3.870			
	Thickness	1.72	1.80	1.77	1.76	0.176			
L116	Length	51.48	51.45	51.58	51.50	5.150	N/A	N/A	42.602
	Width	38.74	38.63	38.82	38.73	3.873			
	Thickness	1.61	1.64	1.66	1.64	0.164			
L118	Length	51.58	51.63	51.58	51.60	5.160	3.167	3.167	26.318
	Width	38.78	38.81	38.74	38.78	3.878			
	Thickness	1.75	1.70	1.71	1.72	0.172			
L119	Length	51.61	51.56	51.66	51.61	5.161	2.890	3.039	24.690
	Width	38.78	38.65	38.88	38.77	3.877			
	Thickness	1.70	1.70	1.81	1.74	0.174			
L121	Length	51.22	51.37	51.30	51.30	5.130	N/A	N/A	42.451
	Width	38.73	38.52	38.74	38.66	3.866			
	Thickness	1.69	1.70	1.65	1.68	0.168			
L122	Length	51.42	51.44	51.29	51.38	5.138	N/A	N/A	42.709
	Width	38.75	38.77	38.91	38.81	3.881			
	Thickness	1.67	1.73	1.69	1.70	0.170			
L124	Length	51.76	51.64	51.45	51.62	5.162	3.209	3.367	27.340
	Width	39.07	38.84	38.78	38.90	3.890			
	Thickness	1.67	1.67	1.71	1.68	0.168			

Table A-2 continued.

Coupon		1 (mm)	2 (mm)	3 (mm)	Average (mm)	Average (cm)	L_1 (cm)	L_2 (cm)	SA (cm^2)
L125	Length	51.62	51.44	51.27	51.44	5.144	3.253	3.253	26.866
	Width	38.82	38.56	38.27	38.55	3.855			
	Thickness	1.73	1.62	1.82	1.72	0.172			
L127	Length	51.54	51.62	51.43	51.53	5.153	N/A	N/A	42.616
	Width	38.64	38.77	38.74	38.72	3.872			
	Thickness	1.64	1.64	1.64	1.64	0.164			
L128	Length	51.80	51.66	51.92	51.79	5.179	N/A	N/A	43.014
	Width	38.85	38.83	38.86	38.85	3.885			
	Thickness	1.63	1.67	1.69	1.66	0.166			
L130	Length	51.68	51.62	51.55	51.62	5.162	3.030	3.030	25.160
	Width	38.67	38.61	38.82	38.70	3.870			
	Thickness	1.72	1.72	1.72	1.72	0.172			
L131	Length	51.61	51.70	51.58	51.63	5.163	2.936	2.936	24.301
	Width	38.56	38.56	38.73	38.62	3.862			
	Thickness	1.69	1.68	1.64	1.67	0.167			
L133	Length	51.48	51.40	51.52	51.47	5.147	N/A	N/A	42.745
	Width	38.72	38.88	38.89	38.83	3.883			
	Thickness	1.66	1.64	1.71	1.67	0.167			
L134	Length	51.81	51.68	51.70	51.73	5.173	N/A	N/A	42.864
	Width	38.60	38.71	38.84	38.72	3.872			
	Thickness	1.67	1.67	1.71	1.68	0.168			
L299	Length	51.04	51.37	50.94	51.12	5.112	N/A	N/A	41.986
	Width	38.49	38.47	38.46	38.47	3.847			
	Thickness	1.56	1.65	1.65	1.62	0.162			
L300	Length	51.20	51.08	51.07	51.12	5.112	N/A	N/A	42.156
	Width	38.66	38.48	38.37	38.50	3.850			
	Thickness	1.72	1.73	1.62	1.69	0.169			
L302	Length	51.27	51.24	51.05	51.19	5.119	2.694	2.694	22.383
	Width	38.62	38.53	38.59	38.58	3.858			
	Thickness	1.74	1.73	1.71	1.73	0.173			
L303	Length	51.36	51.26	51.11	51.24	5.124	2.946	2.946	24.413
	Width	38.66	38.58	38.70	38.65	3.865			
	Thickness	1.68	1.68	1.69	1.68	0.168			
L305	Length	51.25	51.69	51.58	51.51	5.151	N/A	N/A	42.651
	Width	38.76	38.75	38.83	38.78	3.878			
	Thickness	1.64	1.60	1.66	1.63	0.163			
L306	Length	51.34	51.37	51.40	51.37	5.137	N/A	N/A	42.390
	Width	38.61	38.52	38.56	38.56	3.856			
	Thickness	1.73	1.62	1.67	1.67	0.167			
L308	Length	51.34	51.35	51.53	51.41	5.141	2.390	2.699	21.148
	Width	38.85	38.62	38.42	38.63	3.863			
	Thickness	1.66	1.67	1.66	1.66	0.166			
L309	Length	51.39	51.36	51.44	51.40	5.140	2.184	2.647	20.147
	Width	38.70	38.70	38.65	38.68	3.868			
	Thickness	1.63	1.74	1.66	1.68	0.168			

Table A-2 continued.

Coupon		1 (mm)	2 (mm)	3 (mm)	Average (mm)	Average (cm)	L_1 (cm)	L_2 (cm)	SA (cm^2)
L311	Length	51.44	51.44	51.52	51.47	5.147	N/A	N/A	42.671
	Width	38.66	38.60	38.74	38.67	3.867			
	Thickness	1.76	1.71	1.69	1.72	0.172			
L312	Length	51.58	51.41	51.42	51.47	5.147	N/A	N/A	42.462
	Width	38.60	38.68	38.76	38.68	3.868			
	Thickness	1.66	1.61	1.55	1.61	0.161			
L314	Length	52.06	51.98	51.77	51.94	5.194	2.964	2.964	24.654
	Width	38.93	38.83	38.83	38.86	3.886			
	Thickness	1.62	1.67	1.65	1.65	0.165			
L315	Length	51.47	51.58	51.50	51.52	5.152	2.890	2.890	24.013
	Width	38.54	38.65	38.77	38.65	3.865			
	Thickness	1.83	1.70	1.67	1.73	0.173			
L317	Length	51.70	51.53	51.08	51.44	5.144	N/A	N/A	42.653
	Width	38.75	38.74	38.64	38.71	3.871			
	Thickness	1.71	1.68	1.71	1.70	0.170			
L318	Length	51.78	51.95	51.70	51.81	5.181	N/A	N/A	42.866
	Width	38.51	38.77	38.88	38.72	3.872			
	Thickness	1.64	1.58	1.73	1.65	0.165			
L320	Length	51.42	51.71	52.07	51.73	5.173	3.028	3.028	25.154
	Width	38.87	38.81	38.77	38.82	3.882			
	Thickness	1.66	1.64	1.67	1.66	0.166			
L321	Length	51.56	51.77	51.80	51.71	5.171	2.951	2.951	24.534
	Width	38.91	38.79	38.93	38.88	3.888			
	Thickness	1.61	1.65	1.61	1.62	0.162			
L323	Length	51.35	51.35	51.38	51.36	5.136	N/A	N/A	42.222
	Width	38.63	38.67	38.18	38.49	3.849			
	Thickness	1.65	1.61	1.63	1.63	0.163			
L324	Length	51.58	51.82	51.78	51.73	5.173	N/A	N/A	42.888
	Width	38.87	38.76	38.97	38.87	3.887			
	Thickness	1.61	1.63	1.61	1.62	0.162			
L413	Length	51.68	51.55	51.46	51.56	5.156	N/A	N/A	42.507
	Width	38.32	38.75	38.79	38.62	3.862			
	Thickness	1.62	1.64	1.61	1.62	0.162			
L414	Length	51.69	51.63	51.64	51.65	5.165	N/A	N/A	42.671
	Width	38.87	38.75	38.61	38.74	3.874			
	Thickness	1.61	1.60	1.60	1.60	0.160			
L417	Length	51.50	51.38	51.35	51.41	5.141	2.779	2.779	22.987
	Width	38.57	38.64	38.58	38.60	3.860			
	Thickness	1.66	1.63	1.60	1.63	0.163			
L418	Length	51.46	51.40	51.44	51.43	5.143	2.780	2.780	23.048
	Width	38.65	38.67	38.65	38.66	3.866			
	Thickness	1.67	1.65	1.63	1.65	0.165			
L419	Length	51.37	51.44	51.40	51.40	5.140	N/A	N/A	42.575
	Width	38.71	38.80	38.70	38.74	3.874			
	Thickness	1.66	1.65	1.67	1.66	0.166			

Table A-2 continued.

Coupon		1 (mm)	2 (mm)	3 (mm)	Average (mm)	Average (cm)	L_1 (cm)	L_2 (cm)	SA (cm^2)
L420	Length	51.55	51.40	51.10	51.35	5.135	N/A	N/A	42.344
	Width	38.54	38.74	38.68	38.65	3.865			
	Thickness	1.59	1.61	1.63	1.61	0.161			
L422	Length	51.40	51.46	51.47	51.44	5.144	2.920	3.476	26.414
	Width	38.59	38.67	38.69	38.65	3.865			
	Thickness	1.67	1.67	1.61	1.65	0.165			
L423	Length	51.68	51.57	51.68	51.64	5.164	3.070	3.070	25.304
	Width	38.37	38.64	38.65	38.55	3.855			
	Thickness	1.63	1.64	1.63	1.63	0.163			
L425	Length	51.09	51.16	51.10	51.12	5.112	N/A	N/A	41.956
	Width	38.42	38.46	38.38	38.42	3.842			
	Thickness	1.64	1.62	1.64	1.63	0.163			
L426	Length	51.56	51.60	51.58	51.58	5.158	N/A	N/A	42.583
	Width	38.66	38.75	38.72	38.71	3.871			
	Thickness	1.66	1.58	1.58	1.61	0.161			
L428	Length	51.49	51.44	51.34	51.42	5.142	2.446	3.058	22.821
	Width	38.74	38.66	38.63	38.68	3.868			
	Thickness	1.65	1.64	1.62	1.64	0.164			
L429	Length	51.37	51.54	51.41	51.44	5.144	2.502	2.781	21.888
	Width	38.58	38.62	38.61	38.60	3.860			
	Thickness	1.67	1.62	1.61	1.63	0.163			
L431	Length	51.41	51.30	51.34	51.35	5.135	N/A	N/A	42.324
	Width	38.57	38.56	38.66	38.60	3.860			
	Thickness	1.65	1.59	1.65	1.63	0.163			
L432	Length	51.41	51.35	51.43	51.40	5.140	N/A	N/A	42.474
	Width	38.57	38.76	38.63	38.65	3.865			
	Thickness	1.65	1.66	1.66	1.66	0.166			
L434	Length	51.48	51.54	51.46	51.49	5.149	2.783	3.340	25.321
	Width	38.64	38.64	38.74	38.67	3.867			
	Thickness	1.67	1.63	1.63	1.64	0.164			
L435	Length	51.59	51.79	51.87	51.75	5.175	2.797	3.077	24.396
	Width	38.75	38.74	39.00	38.83	3.883			
	Thickness	1.64	1.61	1.63	1.63	0.163			
L453	Length	51.32	51.33	51.33	51.33	5.133	N/A	N/A	42.307
	Width	38.58	38.60	38.56	38.58	3.858			
	Thickness	1.64	1.63	1.65	1.64	0.164			
L454	Length	51.36	51.56	51.47	51.46	5.146	N/A	N/A	42.427
	Width	38.68	38.58	38.62	38.63	3.863			
	Thickness	1.63	1.61	1.62	1.62	0.162			

Source: Individual data sheets for each coupon in *WIPP-FePb-3 Supplemental Binder C (ERMS 546084)*

APPENDIX B

Table B-1 lists the exposure duration, initial weight, final weight, weight loss, surface area and calculated corrosion rate for each steel coupon. The equivalent data for the lead coupons is given in Table B-2. The reported surface areas are taken from Tables A-1 and A-2 for steel and lead, respectively. The final weight is determined from the cleaning cycle data and graphical analysis, which is presented in Appendix C for the steel coupons and Appendix D for the lead coupons (see Section 4.4 for details).

Corrosion rates are calculated according to Equation (3) given in Section 4.4.

Table B-1 Summary of Steel Coupon Corrosion Rate Data

Test ID	Coupon	Duration (hours)	Initial Wt (g)	Final Wt (g) (Calculated)	Weight Loss (mg)	Surface Area (cm^2)	Corrosion Rate (μm/yr)
Fe-G-0000-6-1f	087	4488	20.2056	20.2046	1.0	41.629	0.060
Fe-G-0000-6-3f	089	4488	20.0899	20.0887	1.2	41.663	0.071
Fe-G-0000-6-1p	090	4488	20.3926	20.3909	1.7	23.751	0.177
Fe-G-0000-6-2p	091	4488	19.3842	19.3841	0.1	23.918	0.010
Fe-Go-0000-6-2f	094	4488	19.7502	19.7471	3.1	41.625	0.185
Fe-Go-0000-6-3f	095	4488	19.8811	19.8769	4.2	41.505	0.251
Fe-Go-0000-6-2p	097	4488	18.4242	18.4235	0.7	24.389	0.071
Fe-Go-0000-6-3p	098	4488	18.5963	18.5958	0.5	24.033	0.052
Fe-E-0000-6-1f	099	4488	18.8115	18.8113	0.2	41.709	0.012
Fe-E-0000-6-2f	100	4488	19.2114	19.2097	1.7	41.641	0.101
Fe-E-0000-6-1p	102	4488	20.2687	20.2679	0.8	25.583	0.078
Fe-E-0000-6-2p	103	4488	20.0235	20.0224	1.1	24.773	0.110
Fe-Eo-0000-6-2f	106	4488	20.1808	20.1791	1.7	41.446	0.102
Fe-Eo-0000-6-3f	107	4488	20.2049	20.2034	1.5	41.464	0.090
Fe-Eo-0000-6-1p	108	4488	20.2672	20.2645	2.7	24.634	0.272
Fe-Eo-0000-6-2p	109	4488	20.1048	20.1019	2.9	24.473	0.294
Fe-Atm-0000-6-1	111	4488	19.4744	19.4742	0.2	41.457	0.012
Fe-Atm-0000-6-2	112	4488	19.6178	19.6177	0.1	41.534	0.006
Fe-G-0350-6-1f	114	5544	19.8297	19.8248	4.9	41.594	0.236
Fe-G-0350-6-2f	115	5544	20.0005	19.9970	3.5	41.617	0.169
Fe-G-0350-6-1p	117	5544	18.5283	18.5259	2.4	23.976	0.201
Fe-G-0350-6-2p	118	5544	18.7634	18.7616	1.8	24.272	0.149
Fe-Go-0350-6-1f	120	5544	19.3063	19.3021	4.2	41.405	0.204
Fe-Go-0350-6-2f	121	5544	20.4382	20.4339	4.3	41.634	0.207
Fe-Go-0350-6-1p	123	5544	20.1489	20.1465	2.4	24.181	0.199
Fe-Go-0350-6-2p	124	5544	20.2366	20.2343	2.3	24.496	0.188
Fe-E-0350-6-1f	126	5544	20.1509	20.1499	1.0	41.561	0.048
Fe-E-0350-6-2f	127	5544	20.2231	20.2224	0.7	41.526	0.034
Fe-E-0350-6-1p	129	5544	20.0739	20.0758	-1.9	23.843	-0.160
Fe-E-0350-6-2p	130	5544	20.3403	20.3406	-0.3	24.270	-0.025
Fe-Eo-0350-6-1f	132	5544	19.6018	19.6012	0.6	41.502	0.029
Fe-Eo-0350-6-2f	133	5544	19.7301	19.7289	1.2	41.613	0.058
Fe-Eo-0350-6-1p	135	5544	19.9139	19.9141	-0.2	23.204	-0.017
Fe-Eo-0350-6-2p	136	5544	18.3987	18.3992	-0.5	23.356	-0.043
Fe-Atm-0350-6-1	138	5544	18.7107	18.7113	-0.6	41.535	-0.029
Fe-Atm-0350-6-2	139	5544	18.8829	18.8828	0.1	41.375	0.005
Fe-G-1500-6-2f	307	5208	20.4468	20.4433	3.5	41.756	0.179
Fe-G-1500-6-3f	308	5208	20.4428	20.4378	5.0	41.781	0.256

Table B-1 continued.

Test ID	Coupon	Duration (hours)	Initial Wt (g)	Final Wt (g) (Calculated)	Weight Loss (mg)	Surface Area (cm^2)	Corrosion Rate (μm/yr)
Fe-G-1500-6-2p	310	5208	20.6744	20.6714	3.0	24.858	0.258
Fe-G-1500-6-3p	311	5208	20.0198	20.0168	3.0	24.512	0.262
Fe-Go-1500-6-2f	313	5208	20.2360	20.2303	5.7	41.770	0.292
Fe-Go-1500-6-3f	314	5208	20.4547	20.4492	5.5	41.711	0.282
Fe-Go-1500-6-2p	316	5208	19.3890	19.3872	1.8	23.589	0.163
Fe-Go-1500-6-3p	317	5208	19.6472	19.6440	3.2	22.720	0.301
Fe-E-1500-6-2f	319	5208	20.1540	20.1434	10.6	41.838	0.541
Fe-E-1500-6-3f	320	5208	20.3862	20.3752	11.0	41.611	0.565
Fe-E-1500-6-2p	322	5208	18.8133	18.8081	5.2	22.927	0.485
Fe-E-1500-6-3p	323	5208	19.0999	19.0942	5.7	23.024	0.529
Fe-Eo-1500-6-2f	325	5208	19.9421	19.9369	5.2	41.723	0.266
Fe-Eo-1500-6-3f	326	5208	20.2902	20.2845	5.7	41.636	0.293
Fe-Eo-1500-6-2p	328	5208	19.8855	19.8838	1.7	22.565	0.161
Fe-Eo-1500-6-3p	329	5208	19.8942	19.8909	3.3	22.588	0.312
Fe-Atm-1500-6-2	331	5208	20.4723	20.4723	0.0	41.612	0.000
Fe-Atm-1500-6-3	332	5208	20.4969	20.4971	-0.2	41.606	-0.010
Fe-G-3500-6-2f	416	5328	19.9560	19.9487	7.3	41.449	0.368
Fe-G-3500-6-3f	417	5328	19.9064	19.8989	7.5	41.443	0.378
Fe-G-3500-6-1p	418	5328	19.6738	19.6694	4.4	21.659	0.424
Fe-G-3500-6-2p	419	5328	19.5823	19.5780	4.3	21.521	0.417
Fe-Go-3500-6-2f	423	5328	19.1900	19.1833	6.7	41.317	0.339
Fe-Go-3500-6-3f	424	5328	19.1962	19.1893	6.9	41.316	0.349
Fe-Go-3500-6-1p	425	5328	19.2495	19.2444	5.1	21.545	0.494
Fe-Go-3500-6-2p	426	5328	20.7596	20.7557	3.9	22.001	0.370
Fe-E-3500-6-2f	430	5328	19.5257	19.5020	23.7	41.442	1.194
Fe-E-3500-6-3f	431	5328	21.0621	21.0447	17.4	41.617	0.873
Fe-E-3500-6-2p	433	5328	20.5718	20.5580	13.8	23.045	1.251
Fe-E-3500-6-3p	434	5328	20.3482	20.3325	15.7	22.135	1.481
Fe-Eo-3500-6-1f	435	5328	20.2338	20.2212	12.6	41.597	0.633
Fe-Eo-3500-6-2f	436	5328	20.5356	20.5236	12.0	41.420	0.605
Fe-Eo-3500-6-1p	438	5328	20.2190	20.2122	6.8	23.304	0.609
Fe-Eo-3500-6-2p	439	5328	20.1788	20.1707	8.1	22.475	0.753
Fe-Atm-3500-6-1	441	5328	20.0863	20.0860	0.3	41.368	0.015
Fe-Atm-3500-6-2	442	5328	20.0771	20.0776	-0.5	41.502	-0.025

Source: WIPP-FePb-3 Supplemental Binder C (ERMS 546084)

Table B-2 Summary of Lead Coupon Corrosion Rate Data

Test ID	**Coupon**	**Duration (hours)**	**Initial Wt (g)**	**Final Wt (g) (Calculated)**	**Weight Loss (mg)**	**Surface Area (cm^2)**	**Corrosion Rate (μm/yr)**
Pb-G-0000-6-2f	L083	5304	34.9565	34.9425	14.0	43.101	0.473
Pb-G-0000-6-3f	L084	5304	35.0169	35.0062	10.7	42.560	0.366
Pb-G-0000-6-2p	L086	5304	34.9627	34.9504	12.3	23.784	0.753
Pb-G-0000-6-3p	L087	5304	34.7895	34.7807	8.8	22.407	0.572
Pb-Go-0000-6-1f	L089	5304	35.9965	35.9886	7.9	42.720	0.269
Pb-Go-0000-6-2f	L090	5304	35.2017	35.1957	6.0	42.920	0.204
Pb-Go-0000-6-1p	L091	5304	35.4321	35.4251	7.0	25.151	0.405
Pb-Go-0000-6-3p	L093	5304	35.5347	35.5272	7.5	23.720	0.461
Pb-E-0000-6-1f	L094	5304	35.4331	35.4250	8.1	42.969	0.275
Pb-E-0000-6-2f	L095	5304	36.0654	36.0600	5.4	42.895	0.183
Pb-E-0000-6-1p	L097	5304	35.8988	35.8895	9.3	25.225	0.537
Pb-E-0000-6-2p	L098	5304	34.4660	34.4546	11.4	25.287	0.657
Pb-Eo-0000-6-1f	L100	5304	35.4418	35.4369	4.9	42.574	0.168
Pb-Eo-0000-6-2f	L101	5304	35.3272	35.3223	4.9	42.586	0.168
Pb-Eo-0000-6-1p	L103	5304	35.6308	35.6220	8.8	25.949	0.494
Pb-Eo-0000-6-2p	L104	5304	35.1904	35.1825	7.9	25.703	0.448
Pb-Atm-0000-6-1	L106	5304	35.9058	35.9051	0.7	42.637	0.024
Pb-Atm-0000-6-2	L107	5304	35.4546	35.4517	2.9	43.091	0.098
Pb-G-0350-6-1f	L109	5808	34.8781	34.8744	3.7	42.860	0.115
Pb-G-0350-6-2f	L110	5808	35.4684	35.4633	5.1	42.759	0.159
Pb-G-0350-6-1p	L112	5808	35.1391	35.1362	2.9	24.120	0.160
Pb-G-0350-6-2p	L113	5808	34.6572	34.6431	14.1	23.093	0.812
Pb-Go-0350-6-1f	L115	5808	35.0723	35.0626	9.7	42.960	0.300
Pb-Go-0350-6-2f	L116	5808	35.1860	35.1974	-11.4	42.602	-0.356
Pb-Go-0350-6-1p	L118	5808	35.5343	35.5356	-1.3	26.318	-0.066
Pb-Go-0350-6-2p	L119	5808	35.6150	35.6071	7.9	24.690	0.426
Pb-E-0350-6-1f	L121	5808	34.6720	34.6668	5.2	42.451	0.163
Pb-E-0350-6-2f	L122	5808	35.3743	35.3677	6.6	42.709	0.206
Pb-E-0350-6-1p	L124	5808	35.3672	35.3638	3.4	27.340	0.165
Pb-E-0350-6-2p	L125	5808	35.8618	35.8569	4.9	26.866	0.243
Pb-Eo-0350-6-1f	L127	5808	34.6510	34.6404	10.6	42.616	0.331
Pb-Eo-0350-6-2f	L128	5808	34.8518	34.8429	8.9	43.014	0.275
Pb-Eo-0350-6-1p	L130	5808	35.4064	35.3985	7.9	25.160	0.418
Pb-Eo-0350-6-2p	L131	5808	35.0594	35.0541	5.3	24.301	0.290
Pb-Atm-0350-6-1	L133	5808	35.1639	35.1650	-1.1	42.745	-0.034
Pb-Atm-0350-6-2	L134	5808	35.3418	35.3435	-1.7	42.864	-0.053
Pb-G-1500-6-1f	L299	5064	35.1086	35.1001	8.5	41.986	0.309
Pb-G-1500-6-2f	L300	5064	36.0213	36.0137	7.6	42.156	0.275

Table B-2 continued.

Test ID	Coupon	Duration (hours)	Initial Wt (g)	Final Wt (g) (Calculated)	Weight Loss (mg)	Surface Area (cm^2)	Corrosion Rate (µm/yr)
Pb-G-1500-6-1p	L302	5064	35.9088	35.8793	29.5	22.383	2.010
Pb-G-1500-6-2p	L303	5064	35.5716	35.5546	17.0	24.413	1.062
Pb-Go-1500-6-1f	L305	5064	34.6158	34.6036	12.2	42.651	0.436
Pb-Go-1500-6-2f	L306	5064	34.8760	34.8621	13.9	42.390	0.500
Pb-Go-1500-6-1p	L308	5064	35.0408	35.0221	18.7	21.148	1.349
Pb-Go-1500-6-2p	L309	5064	34.8474	34.8274	20.0	20.147	1.514
Pb-E-1500-6-1f	L311	5064	36.0171	36.0132	3.9	42.671	0.139
Pb-E-1500-6-2f	L312	5064	34.1353	34.1305	4.8	42.462	0.172
Pb-E-1500-6-1p	L314	5064	34.8270	34.8128	14.2	24.654	0.879
Pb-E-1500-6-2p	L315	5064	35.7921	35.7813	10.8	24.013	0.686
Pb-Eo-1500-6-1f	L317	5064	35.8858	35.8788	7.0	42.653	0.250
Pb-Eo-1500-6-2f	L318	5064	34.8114	34.8040	7.4	42.866	0.263
Pb-Eo-1500-6-1p	L320	5064	35.3177	35.3072	10.5	25.154	0.637
Pb-Eo-1500-6-2p	L321	5064	34.6691	34.6548	14.3	24.534	0.889
Pb-Atm-1500-6-1	L323	5064	35.0368	35.0336	3.2	42.222	0.116
Pb-Atm-1500-6-2	L324	5064	35.1052	35.1000	5.2	42.888	0.185
Pb-G-3500-6-1f	L413	4968	34.6030	34.5922	10.8	42.507	0.395
Pb-G-3500-6-2f	L414	4968	34.2356	34.2262	9.4	42.671	0.343
Pb-G-3500-6-2p	L417	4968	35.1097	35.0965	13.2	22.987	0.893
Pb-G-3500-6-3p	L418	4968	34.9317	34.9201	11.6	23.048	0.783
Pb-Go-3500-6-1f	L419	4968	34.9312	34.9194	11.8	42.575	0.431
Pb-Go-3500-6-2f	L420	4968	34.1202	34.1119	8.3	42.344	0.305
Pb-Go-3500-6-1p	L422	4968	34.7956	34.7837	11.9	26.414	0.701
Pb-Go-3500-6-2p	L423	4968	35.1465	35.1292	17.3	25.304	1.063
Pb-E-3500-6-1f	L425	4968	34.3943	34.3891	5.2	41.956	0.193
Pb-E-3500-6-2f	L426	4968	34.1568	34.1452	11.6	42.583	0.424
Pb-E-3500-6-1p	L428	4968	35.1248	35.1098	15.0	22.821	1.022
Pb-E-3500-6-2p	L429	4968	34.6425	34.6245	18.0	21.888	1.279
Pb-Eo-3500-6-1f	L431	4968	34.7844	34.7754	9.0	42.324	0.331
Pb-Eo-3500-6-2f	L432	4968	34.7211	34.7132	7.9	42.474	0.289
Pb-Eo-3500-6-1p	L434	4968	34.8573	34.8476	9.7	25.321	0.596
Pb-Eo-3500-6-2p	L435	4968	35.1251	35.1154	9.7	24.396	0.618
Pb-Atm-3500-6-2	L453	4968	34.9586	34.9565	2.1	42.307	0.077
Pb-Atm-3500-6-3	L454	4968	34.7891	34.7879	1.2	42.427	0.044

Source: WIPP-FePb-3 Supplemental Binder C (ERMS 546084)

APPENDIX C

This appendix contains all of the weight loss cleaning cycle data, as well as the results of the graphical analysis of that data for each of the steel coupons (see individual data sheets for each coupon in WIPP-FePb-3 Supplemental Binder C). Each of the following pages lists the initial coupon weight, removal weight, cleaning cycle weights, calculated final weight and the resulting weight loss. The environmental conditions for each coupon can be read from the test matrix label that is given for each coupon. The meaning of the test matrix labels is discussed in Section 2.4.

For each coupon the graphical analysis is shown (see Section 4.4 for details of the process). The blue symbols indicate those parts of the cleaning cycle data used to determine the calculated final weight, which is the y-intercept of the line fit to the blue symbols. The red symbols show the cleaning cycle data not used in the linear regression. Yellow symbols indicate the initial coupon weight (prior to the experiment) and the final calculated weight. Note that in some samples the final weight is taken either as the 0^{th} cleaning cycle or the 1^{st} cleaning cycle value. This is a judgment call made by the investigator based on the appearance of the weight loss plots.

Coupon:	087			
Test matrix:	Fe-G-0000-6-1f			
Initial wt (g)	20.2056		**Calculated final wt (g)**	20.2046
Removal wt (g)	20.2013		**Total wt loss (g)**	0.0010
			Total wt loss (mg)	1.0

Cleaning Cycle	Wt (g)
0	20.2013
1	20.2020
2	20.2010
3	20.1994
4	20.1976
5	20.1957

Note: The removal weight is suspect likely due to problems with the balance

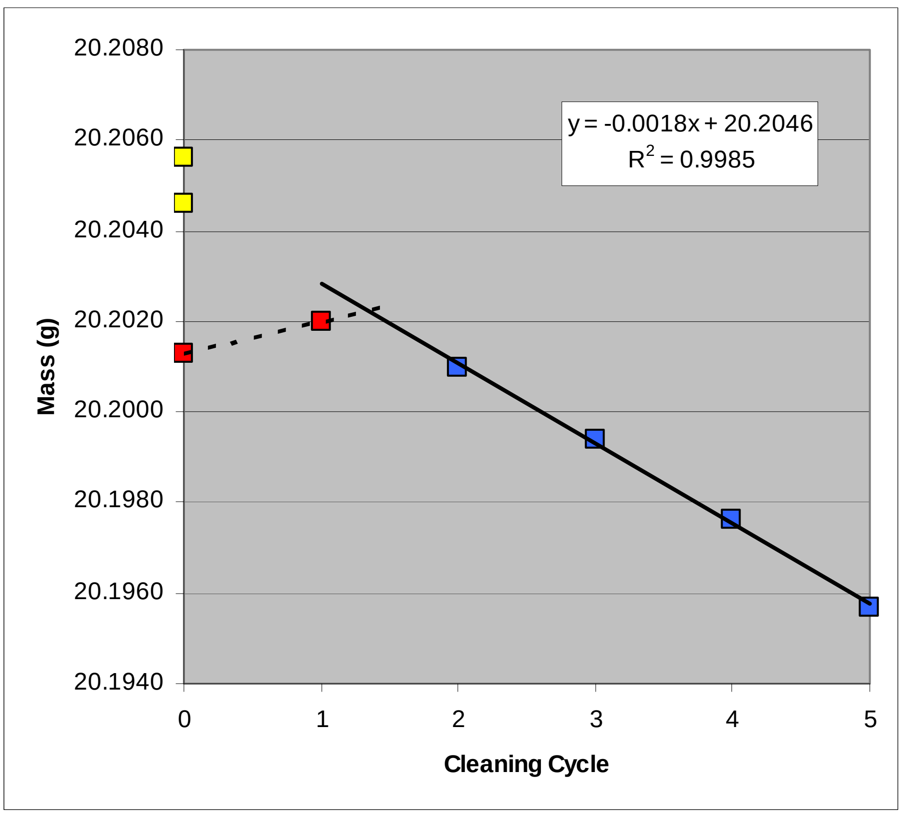

Coupon:	089			
Test matrix:	Fe-G-0000-6-3f			
Initial wt (g)	20.0899		**Calculated final wt (g)**	20.0887
Removal wt (g)	20.0986		**Total wt loss (g)**	0.0012
			Total wt loss (mg)	1.2

Cleaning Cycle	Wt (g)
0	20.0986
1	20.0856
2	20.0844
3	20.0830
4	20.0808
5	20.0784

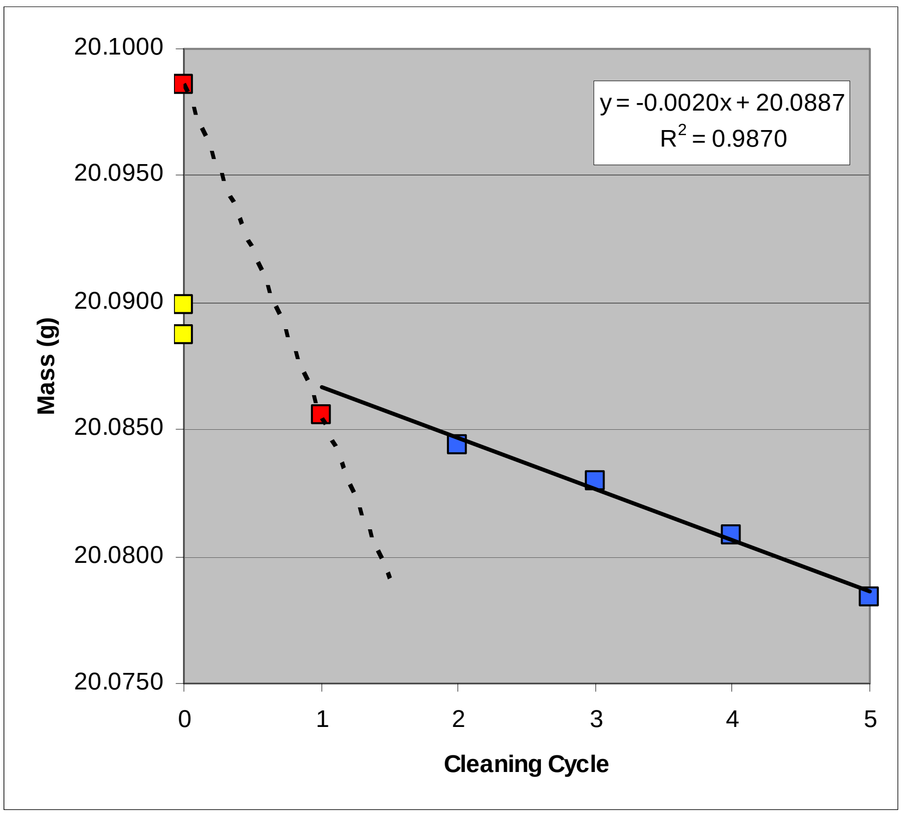

Coupon:	090			
Test matrix:	Fe-G-0000-6-1p			
Initial wt (g)	20.3926		**Calculated final wt (g)**	20.3909
Removal wt (g)	20.3909		**Total wt loss (g)**	0.0017
			Total wt loss (mg)	1.7

Cleaning Cycle	Wt (g)
0	20.3909
1	20.3898
2	20.3885
3	20.3866
4	20.3843
5	20.3810

Note: Based on appearance of graph the 0th cleaning cycle was taken as the final weight.

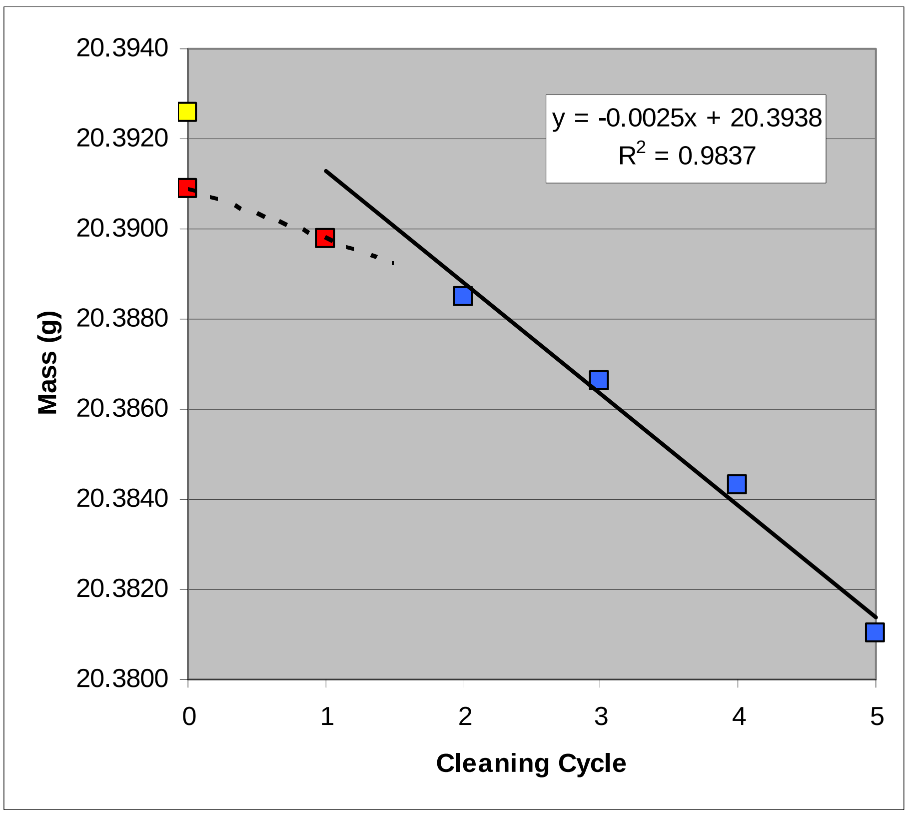

Coupon:	091		
Test matrix:	Fe-G-0000-6-2p		
Initial wt (g)	19.3842	**Calculated final wt (g)**	19.3841
Removal wt (g)	19.3841	**Total wt loss (g)**	0.0001
		Total wt loss (mg)	0.1

Cleaning Cycle	Wt (g)
0	19.3841
1	19.3818
2	19.3809
3	19.3787
4	19.3764
5	19.3729

Note: Based on appearance of graph the 0th cleaning cycle was taken as the final weight.

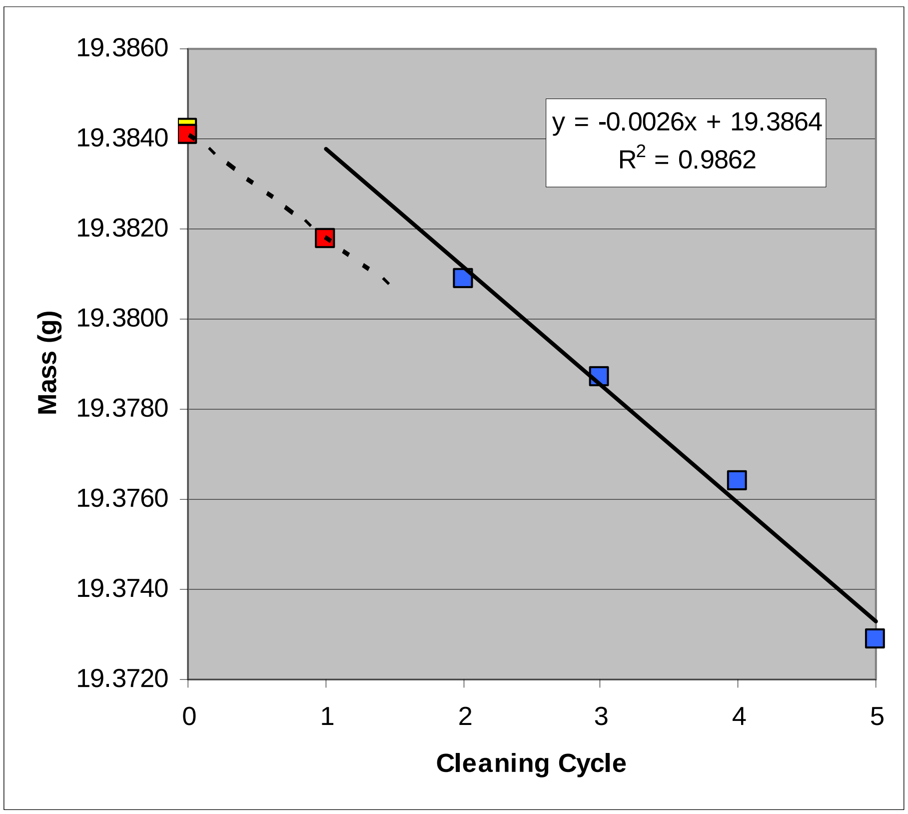

Coupon:	094
Test matrix:	Fe-Go-0000-6-2f
Initial wt (g)	19.7502
Removal wt (g)	19.7492

Calculated final wt (g)	19.7471
Total wt loss (g)	0.0031
Total wt loss (mg)	3.1

Cleaning Cycle	Wt (g)
0	19.7492
1	19.7450
2	19.7433
3	19.7411
4	19.7394
5	19.7374

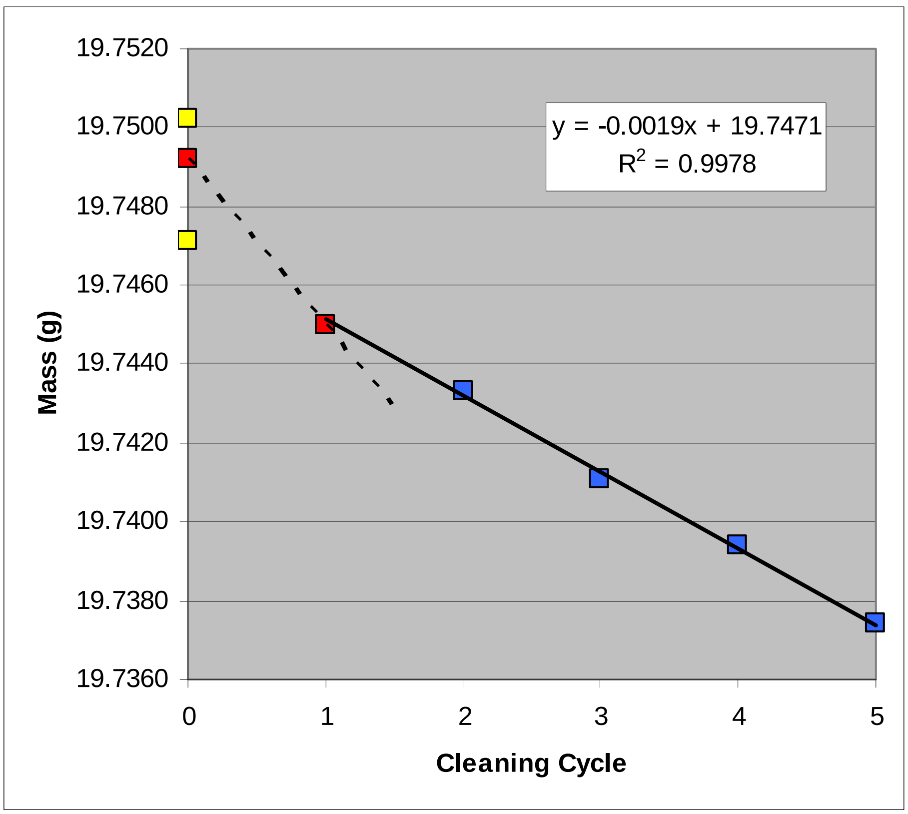

Coupon:	095		
Test matrix:	Fe-Go-0000-6-3f		
Initial wt (g)	19.8811	**Calculated final wt (g)**	19.8769
Removal wt (g)	19.8806	**Total wt loss (g)**	0.0042
		Total wt loss (mg)	4.2

Cleaning Cycle	Wt (g)
0	19.8806
1	19.8756
2	19.8740
3	19.8723
4	19.8710
5	19.8695

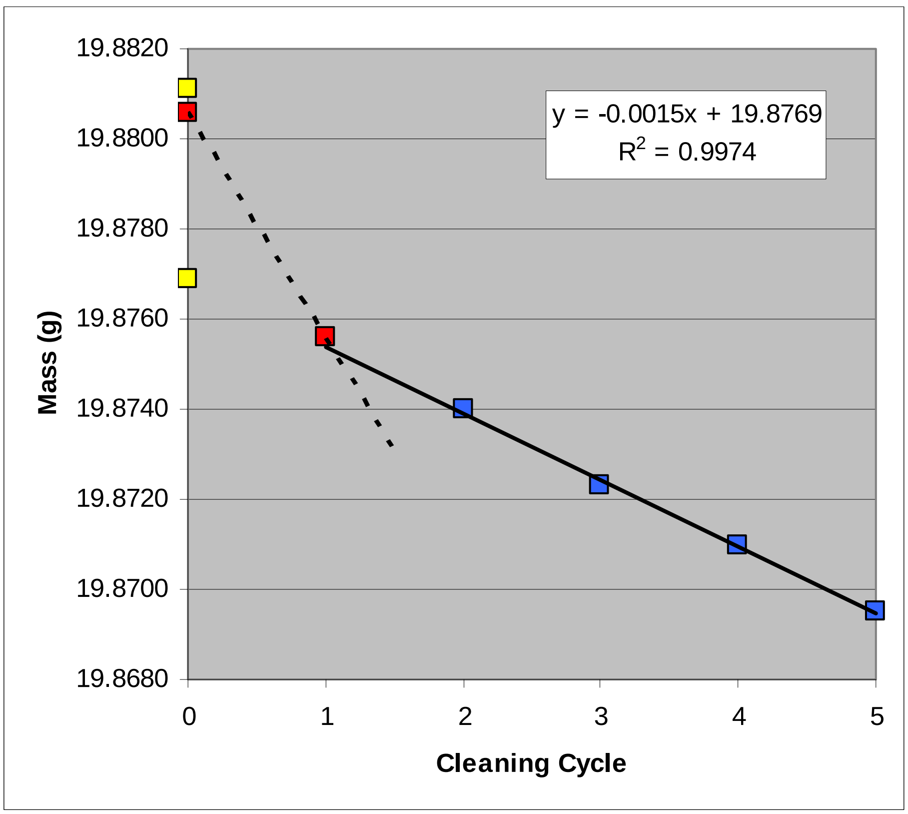

Coupon:	097
Test matrix:	Fe-Go-0000-6-2p
Initial wt (g)	18.4242
Removal wt (g)	18.4235

Calculated final wt (g)	18.4235
Total wt loss (g)	0.0007
Total wt loss (mg)	0.7

Cleaning Cycle	Wt (g)
0	18.4235
1	18.4220
2	18.4205
3	18.4185
4	18.4169
5	18.4150

Note: Based on appearance of graph the 0th cleaning cycle was taken as the final weight.

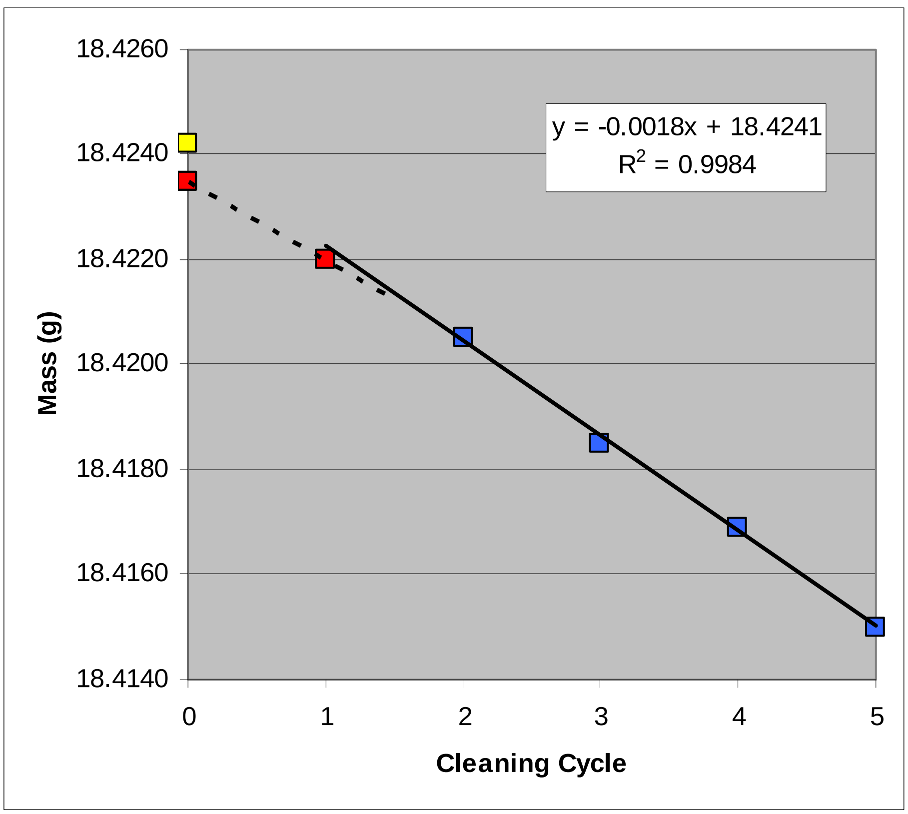

Coupon:	098
Test matrix:	Fe-Go-0000-6-3p
Initial wt (g)	18.5963
Removal wt (g)	18.5952

Calculated final wt (g)	18.5958
Total wt loss (g)	0.0005
Total wt loss (mg)	0.5

Cleaning Cycle	Wt (g)
0	18.5952
1	18.5937
2	18.5924
3	18.5909
4	18.5886
5	18.5868

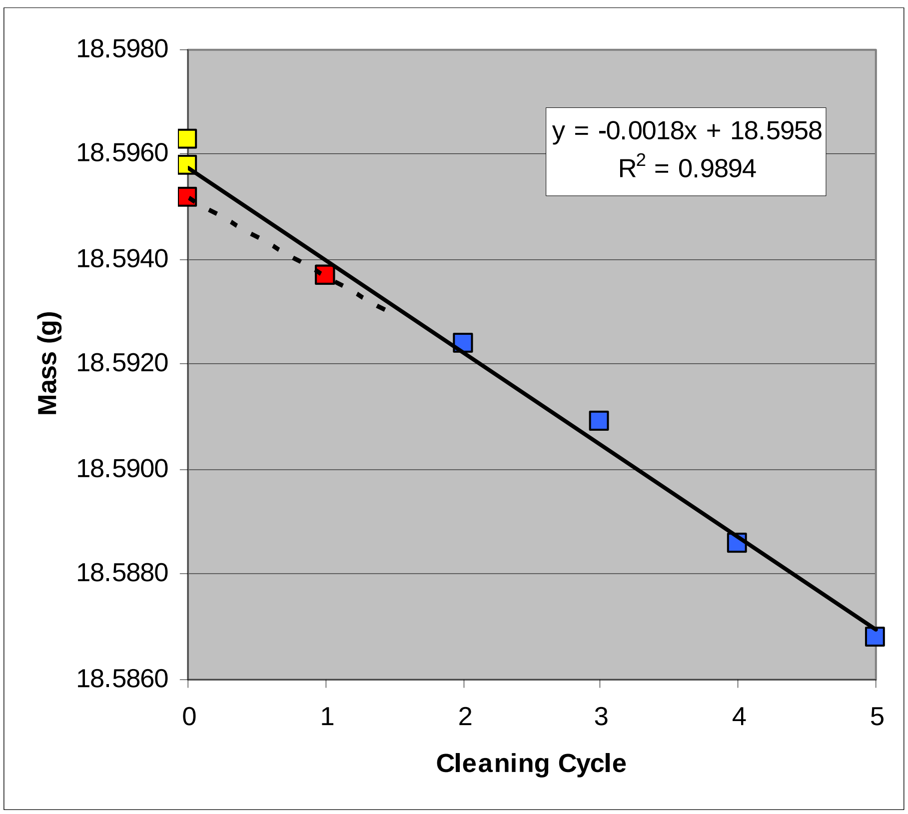

Coupon:	099
Test matrix:	Fe-E-0000-6-1f
Initial wt (g)	18.8115
Removal wt (g)	18.8342

Calculated final wt (g)	18.8113
Total wt loss (g)	0.0002
Total wt loss (mg)	0.2

Cleaning Cycle	Wt (g)
0	18.8342
1	18.8077
2	18.8070
3	18.8051
4	18.8030
5	18.8007

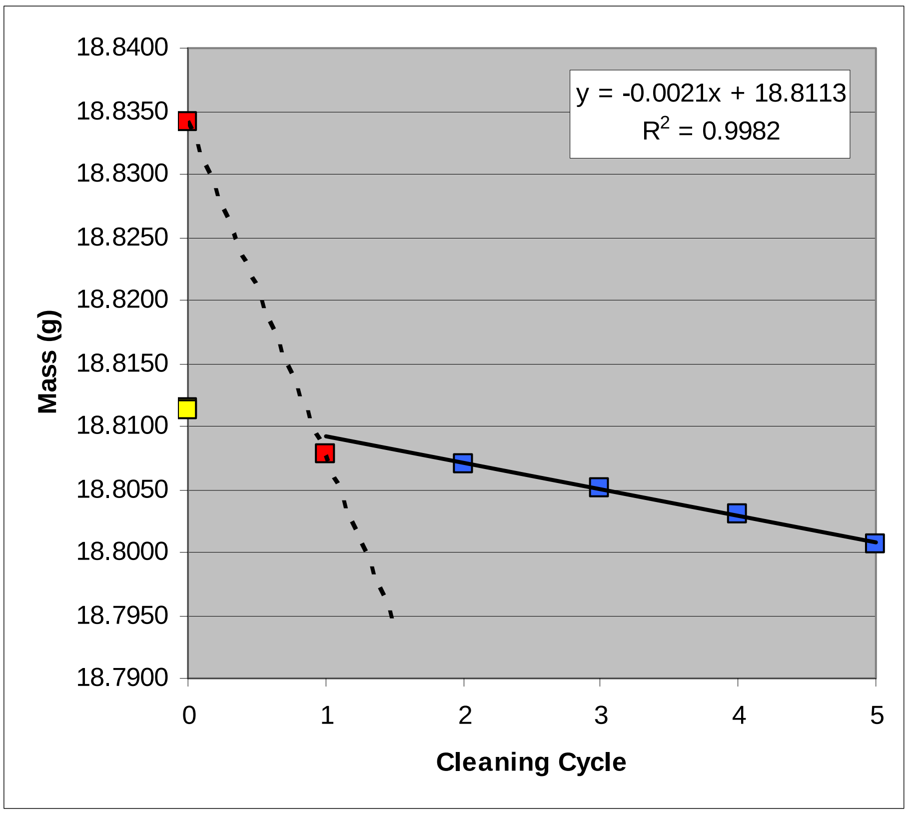

Coupon:	100
Test matrix:	Fe-E-0000-6-2f
Initial wt (g)	19.2114
Removal wt (g)	19.2381

Calculated final wt (g)	19.2097
Total wt loss (g)	0.0017
Total wt loss (mg)	1.7

Cleaning Cycle	Wt (g)
0	19.2381
1	19.2067
2	19.2056
3	19.2043
4	19.2020
5	19.2000

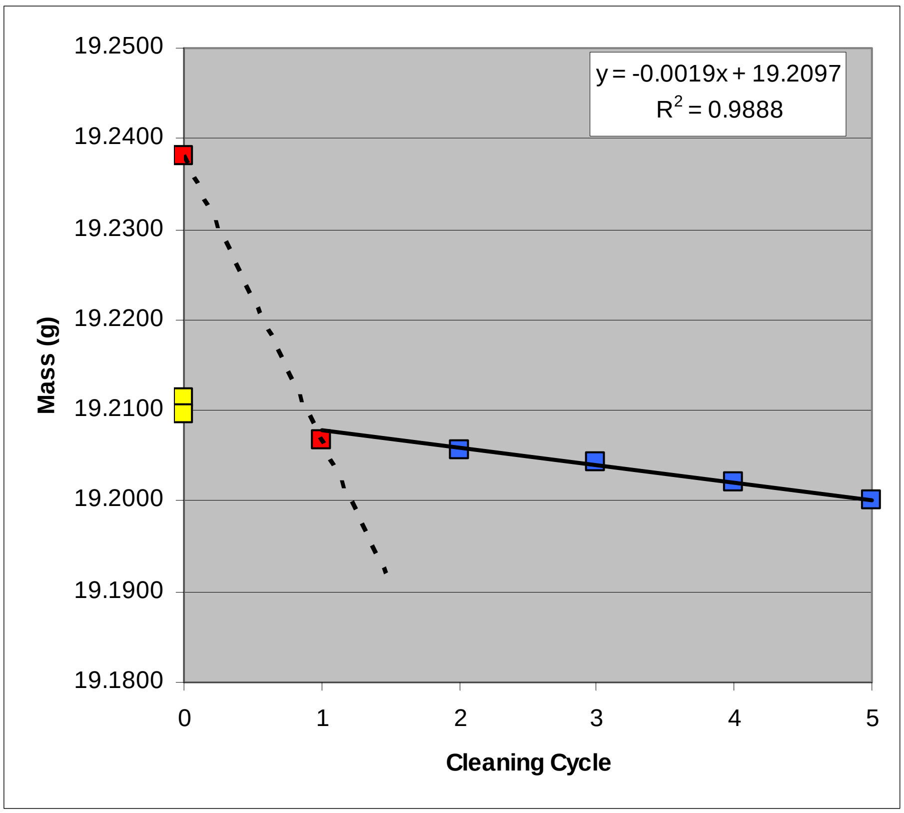

Coupon:	102
Test matrix:	Fe-E-0000-6-1p
Initial wt (g)	20.2687
Removal wt (g)	20.2706

Calculated final wt (g)	20.2679
Total wt loss (g)	0.0008
Total wt loss (mg)	0.8

Cleaning Cycle	Wt (g)
0	20.2706
1	20.2653
2	20.2641
3	20.2628
4	20.2611
5	20.2588

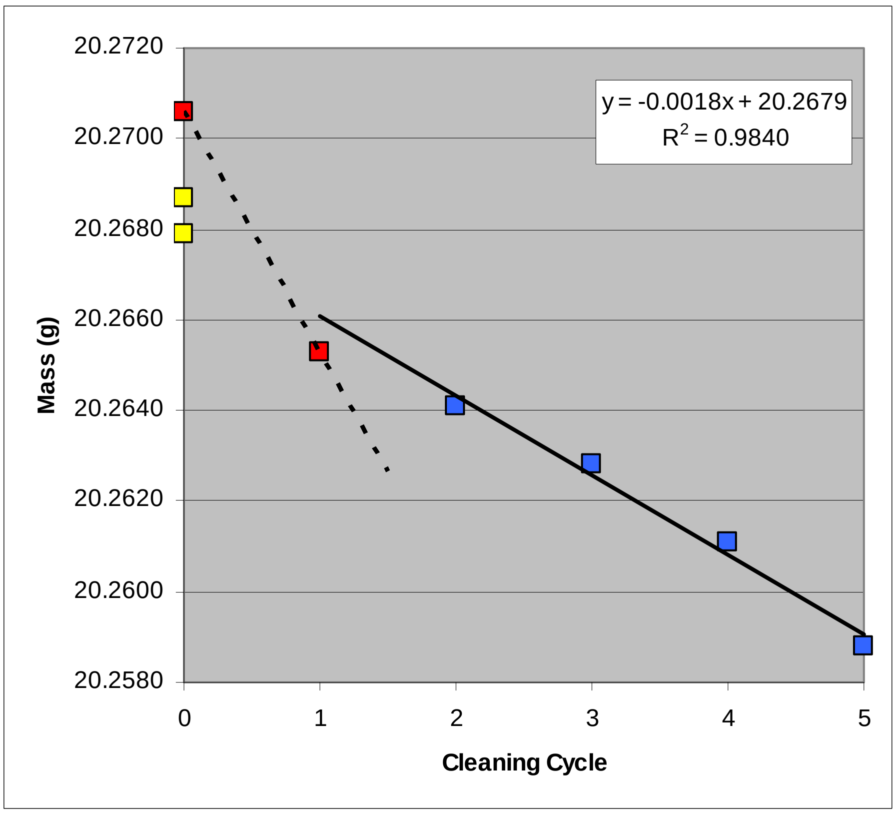

Coupon:	103
Test matrix:	Fe-E-0000-6-2p
Initial wt (g)	20.0235
Removal wt (g)	20.0290

Calculated final wt (g)	20.0224
Total wt loss (g)	0.0011
Total wt loss (mg)	1.1

Cleaning Cycle	Wt (g)
0	20.0290
1	20.0204
2	20.0190
3	20.0179
4	20.0161
5	20.0143

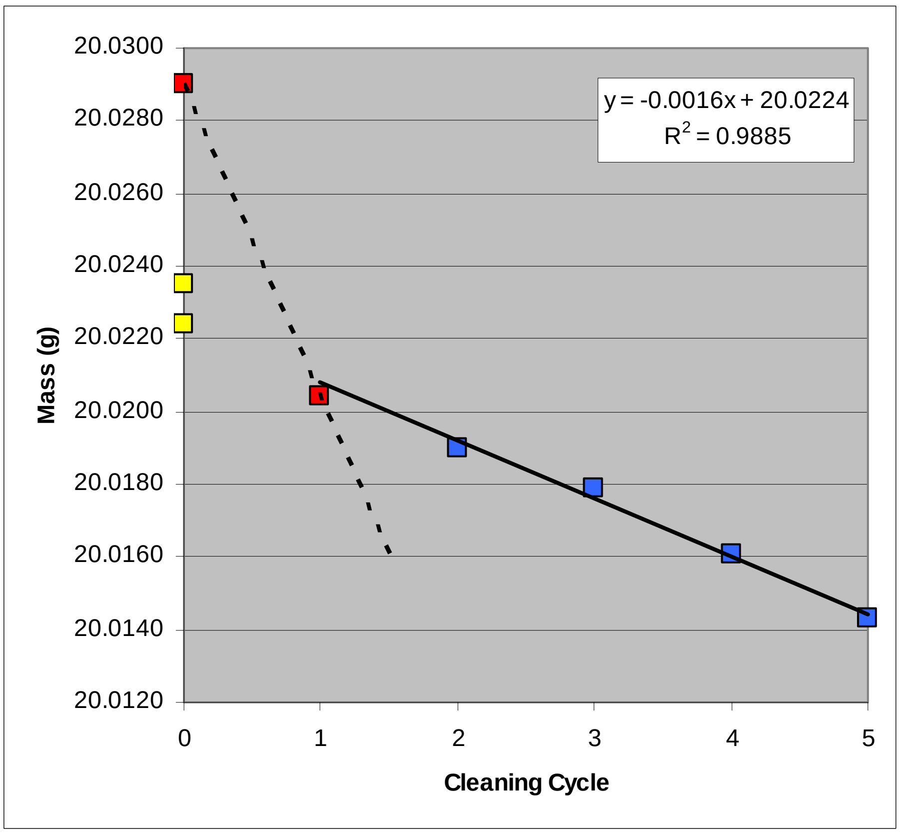

Coupon:	106
Test matrix:	Fe-Eo-0000-6-2f
Initial wt (g)	20.1808
Removal wt (g)	20.1859

Calculated final wt (g)	20.1791
Total wt loss (g)	0.0017
Total wt loss (mg)	1.7

Cleaning Cycle	Wt (g)
0	20.1859
1	20.1767
2	20.1753
3	20.1734
4	20.1716
5	20.1696

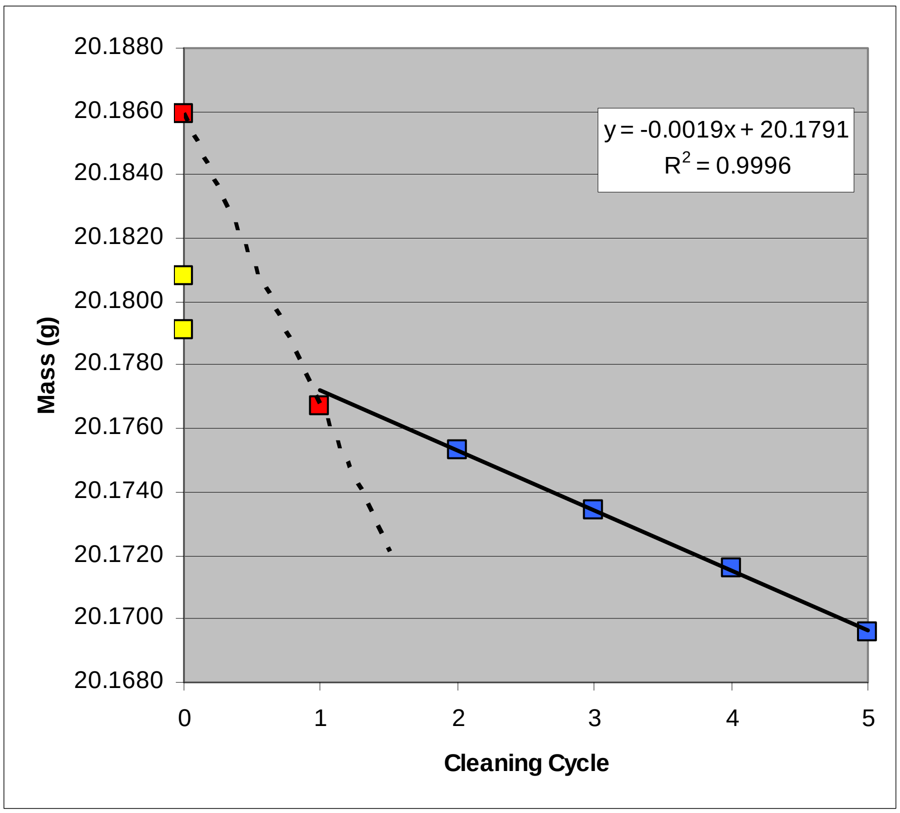

Coupon:	107
Test matrix:	Fe-Eo-0000-6-3f
Initial wt (g)	20.2049
Removal wt (g)	20.2085

Calculated final wt (g)	20.2034
Total wt loss (g)	0.0015
Total wt loss (mg)	1.5

Cleaning Cycle	Wt (g)
0	20.2085
1	20.2005
2	20.1994
3	20.1974
4	20.1955
5	20.1934

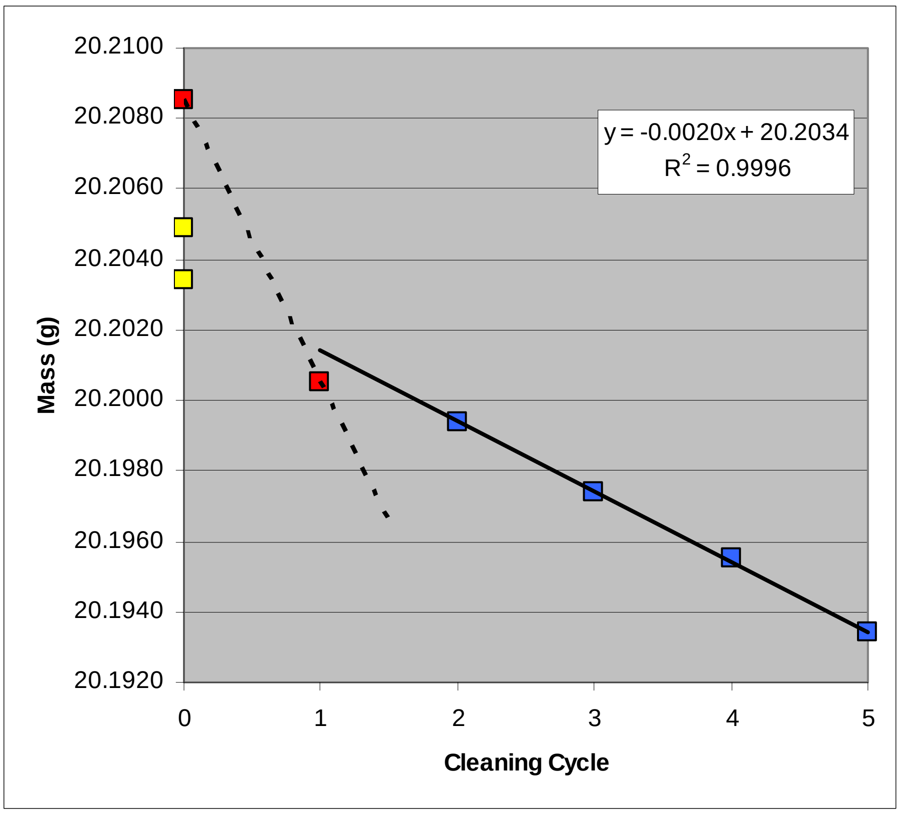

Coupon:	108
Test matrix:	Fe-Eo-0000-6-1p
Initial wt (g)	20.2672
Removal wt (g)	20.2695

Calculated final wt (g)	20.2645
Total wt loss (g)	0.0027
Total wt loss (mg)	2.7

Cleaning Cycle	**Wt (g)**
0	20.2695
1	20.2645
2	20.2630
3	20.2608
4	20.2582
5	20.2552

Note: Based on appearance of graph the 1st cleaning cycle was taken as the final weight.

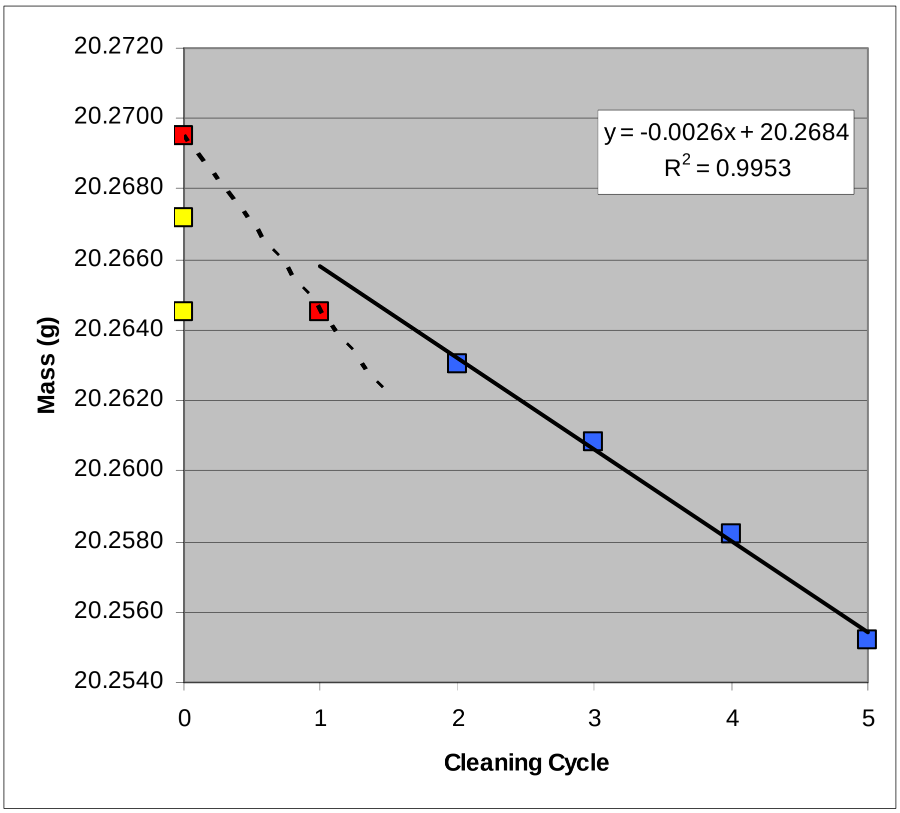

Coupon:	109			
Test matrix:	Fe-Eo-0000-6-2p			
Initial wt (g)	20.1048		**Calculated final wt (g)**	20.1019
Removal wt (g)	20.1072		**Total wt loss (g)**	0.0029
			Total wt loss (mg)	2.9

Cleaning Cycle	Wt (g)
0	20.1072
1	20.1019
2	20.1005
3	20.0979
4	20.0955
5	20.0925

Note: Based on appearance of graph the 1st cleaning cycle was taken as the final weight.

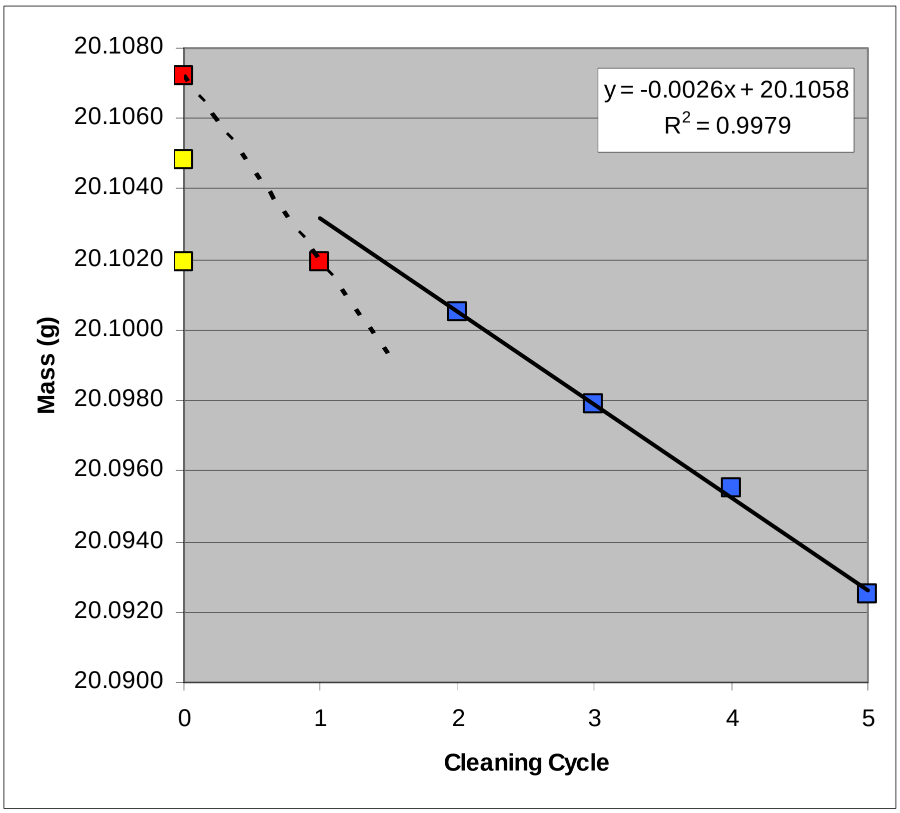

Coupon:	111
Test matrix:	Fe-Atm-0000-6-1
Initial wt (g)	19.4744
Removal wt (g)	19.4740

Calculated final wt (g)	19.4742
Total wt loss (g)	0.0002
Total wt loss (mg)	0.2

Cleaning Cycle	Wt (g)
0	19.4740
1	19.4728
2	19.4709
3	19.4691
4	19.4671
5	19.4659

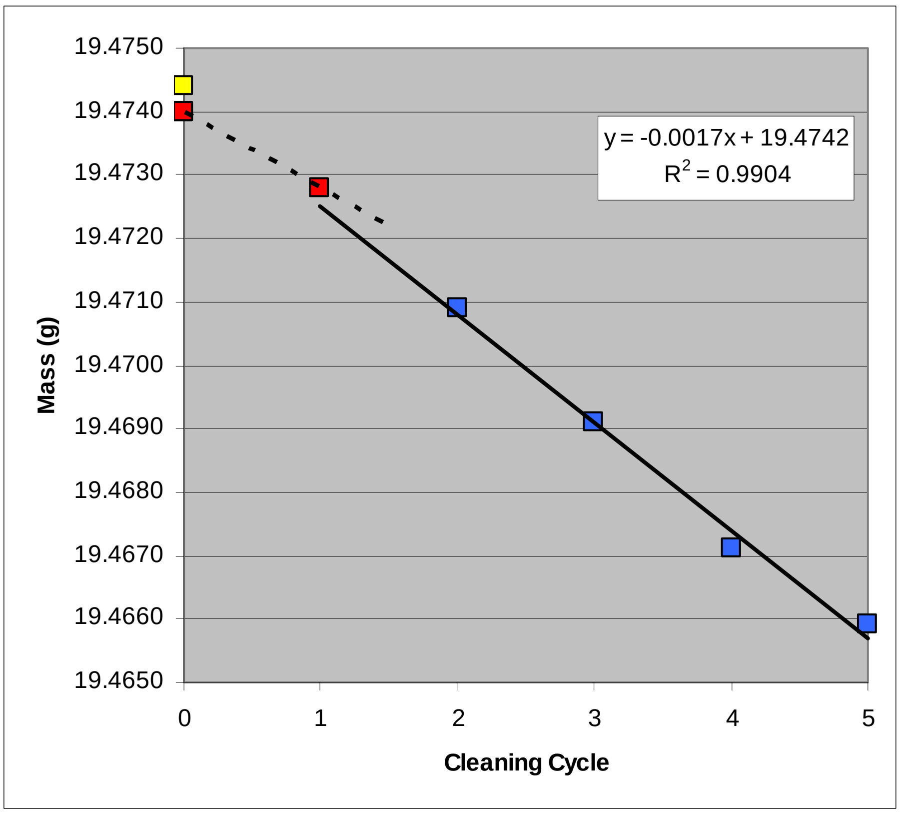

Coupon:	112
Test matrix:	Fe-Atm-0000-6-2
Initial wt (g)	19.6178
Removal wt (g)	19.6177

Calculated final wt (g)	19.6177
Total wt loss (g)	0.0001
Total wt loss (mg)	0.1

Cleaning Cycle	**Wt (g)**
0	19.6177
1	19.6166
2	19.6147
3	19.6125
4	19.6108
5	19.6089

Note: Based on appearance of graph the 0th cleaning cycle was taken as the final weight.

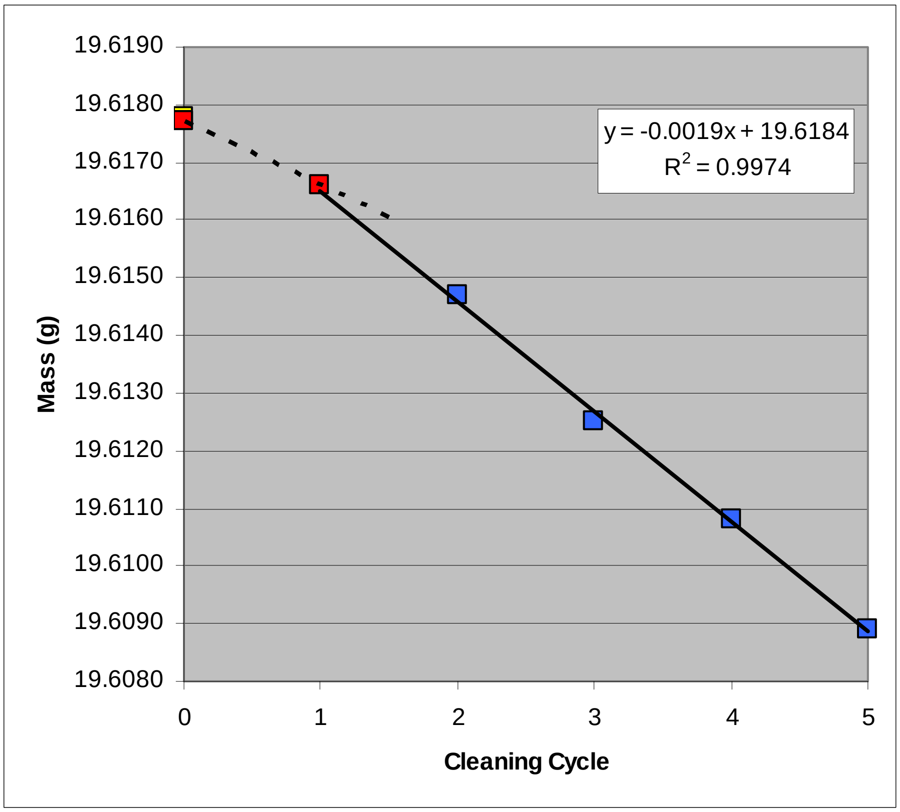

Coupon:	114
Test matrix:	Fe-G-0350-6-1f
Initial wt (g)	19.8297
Removal wt (g)	19.8280

Calculated final wt (g)	19.8248
Total wt loss (g)	0.0049
Total wt loss (mg)	4.9

Cleaning Cycle	Wt (g)
0	19.8280
1	19.8250
2	19.8244
3	19.8244
4	19.8243
5	19.8239

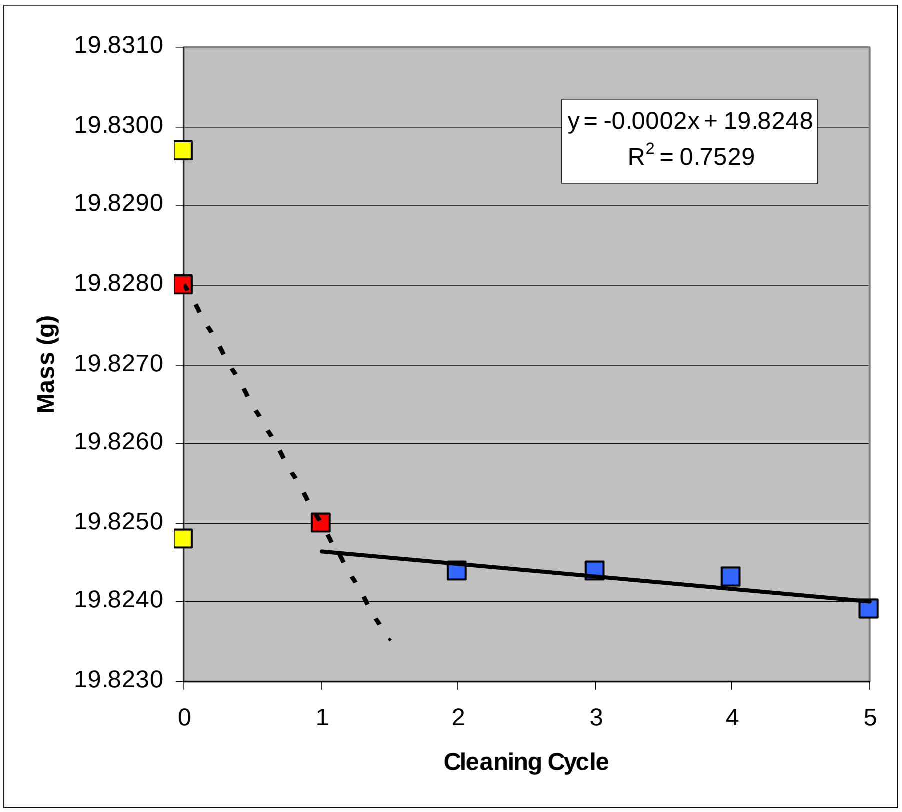

Coupon:	115		
Test matrix:	Fe-G-0350-6-2f		
Initial wt (g)	20.0005	**Calculated final wt (g)**	19.9970
Removal wt (g)	19.9972	**Total wt loss (g)**	0.0035
		Total wt loss (mg)	3.5

Cleaning Cycle	Wt (g)
0	19.9972
1	19.9962
2	19.9957
3	19.9952
4	19.9946
5	19.9939

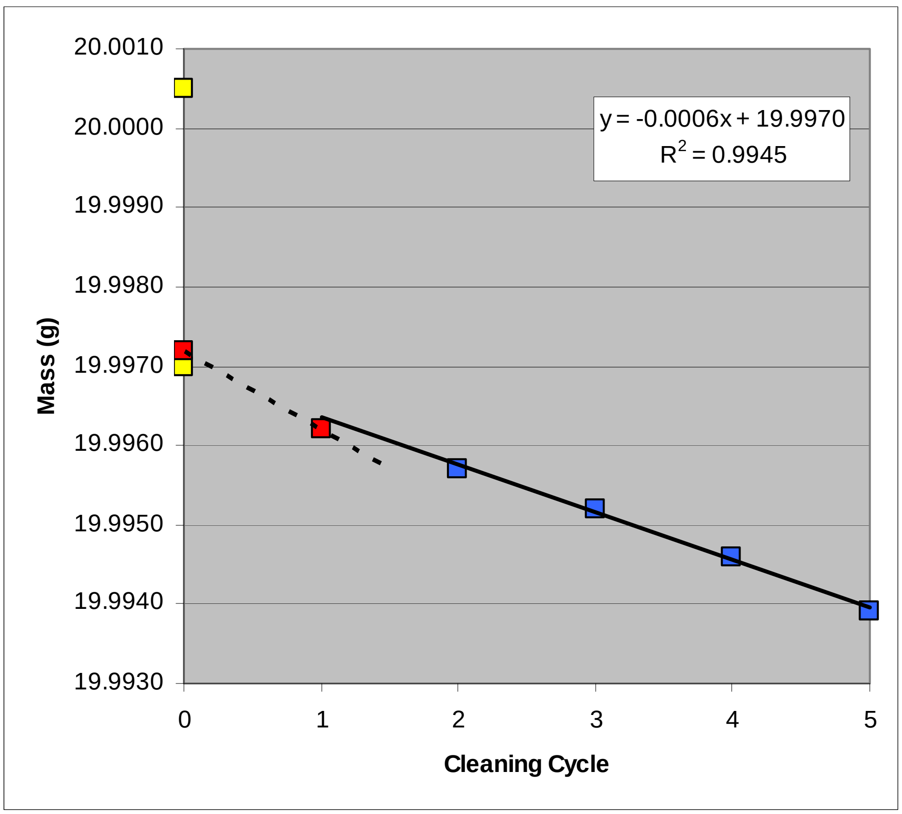

Coupon:	117
Test matrix:	Fe-G-0350-6-1p
Initial wt (g)	18.5283
Removal wt (g)	18.5277

Calculated final wt (g)	18.5259
Total wt loss (g)	0.0024
Total wt loss (mg)	2.4

Cleaning Cycle	Wt (g)
0	18.5277
1	18.5252
2	18.5255
3	18.5249
4	18.5250
5	18.5246

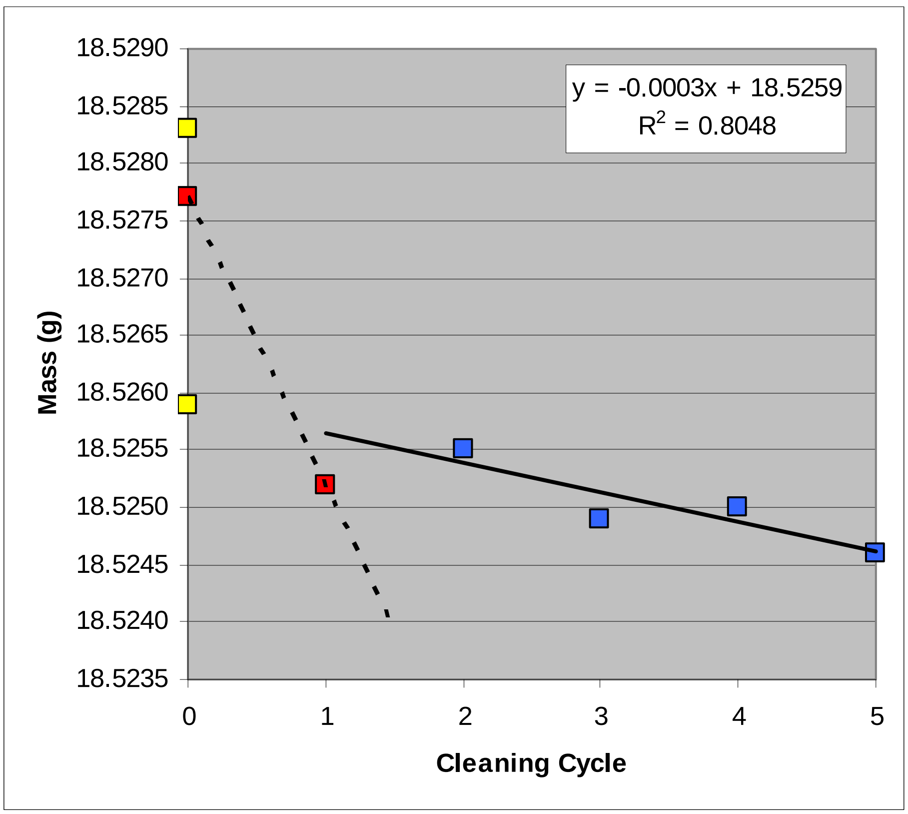

Coupon:	118		
Test matrix:	Fe-G-0350-6-2p		
Initial wt (g)	18.7634	**Calculated final wt (g)**	18.7616
Removal wt (g)	18.7615	**Total wt loss (g)**	0.0018
		Total wt loss (mg)	1.8

Cleaning Cycle	Wt (g)
0	18.7615
1	18.7612
2	18.7610
3	18.7605
4	18.7603
5	18.7600

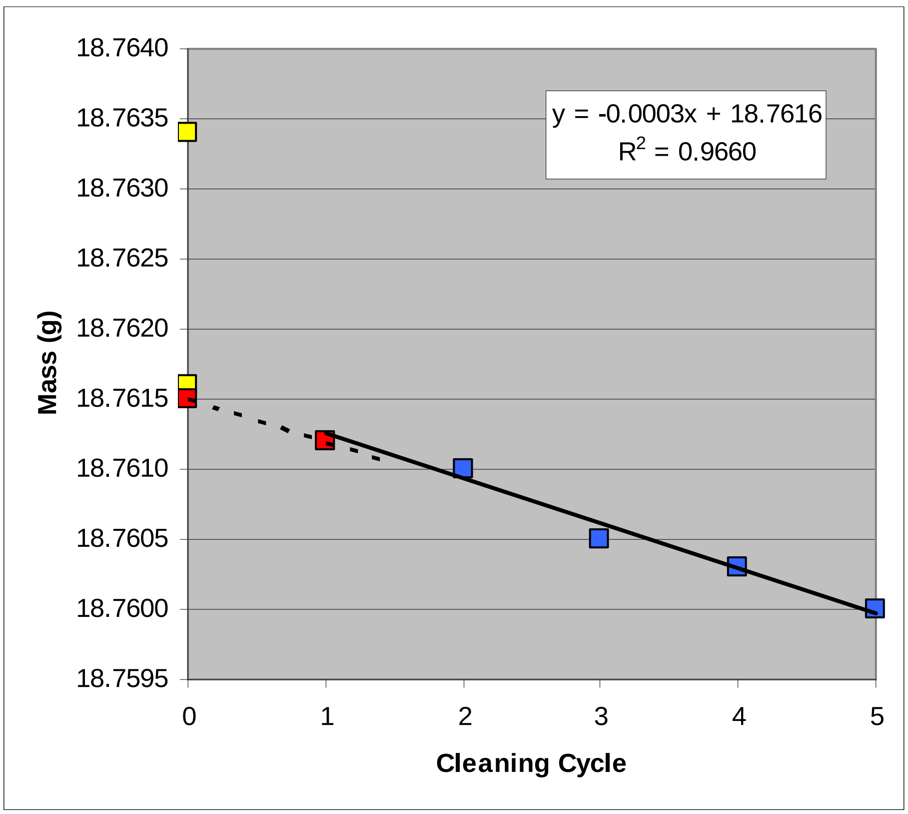

Coupon:	120		
Test matrix:	Fe-Go-0350-6-1f		
Initial wt (g)	19.3063	**Calculated final wt (g)**	19.3021
Removal wt (g)	19.3151	**Total wt loss (g)**	0.0042
		Total wt loss (mg)	4.2

Cleaning Cycle	Wt (g)
0	19.3151
1	19.3016
2	19.3014
3	19.3011
4	19.3007
5	19.3010

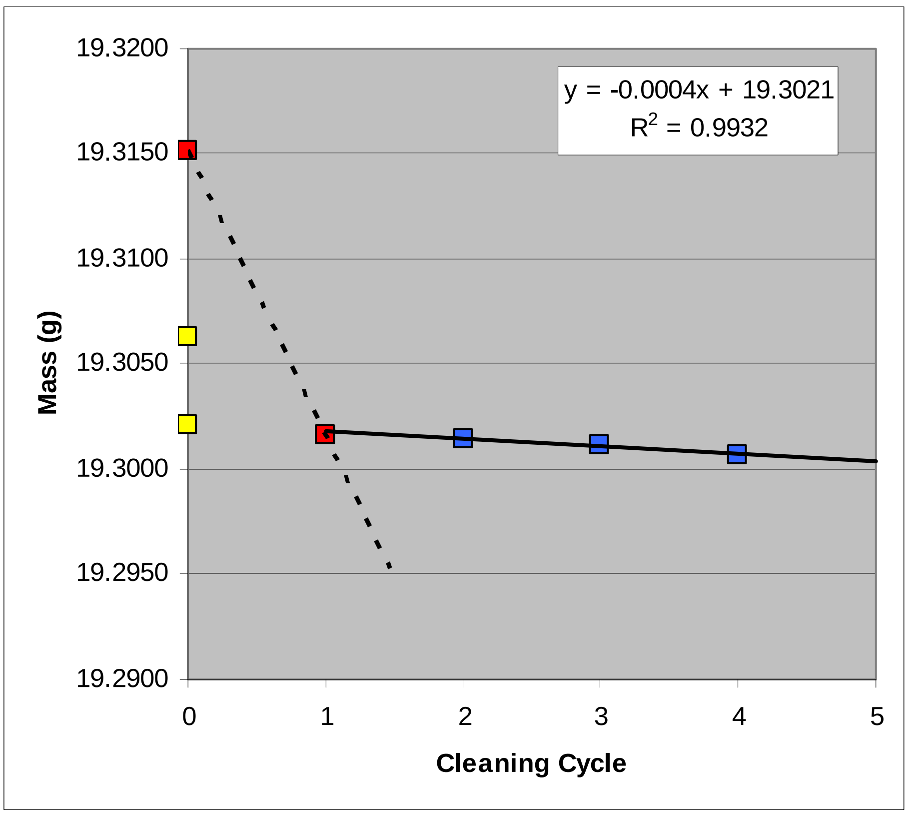

Coupon:	121
Test matrix:	Fe-Go-0350-6-2f
Initial wt (g)	20.4382
Removal wt (g)	20.4430

Calculated final wt (g)	20.4339
Total wt loss (g)	0.0043
Total wt loss (mg)	4.3

Cleaning Cycle	Wt (g)
0	20.4430
1	20.4344
2	20.4336
3	20.4333
4	20.4331
5	20.4331

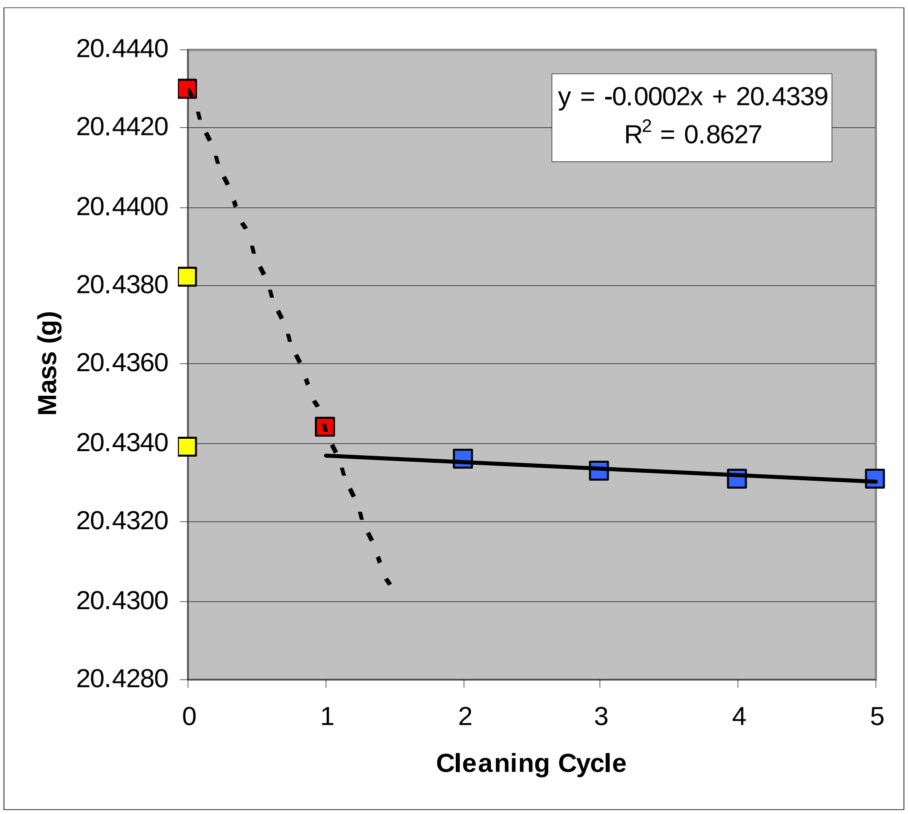

Coupon:	123
Test matrix:	Fe-Go-0350-6-1p
Initial wt (g)	20.1489
Removal wt (g)	20.1470

Calculated final wt (g)	20.1465
Total wt loss (g)	0.0024
Total wt loss (mg)	2.4

Cleaning Cycle	Wt (g)
0	20.1470
1	20.1466
2	20.1461
3	20.1462
4	20.1459
5	20.1457

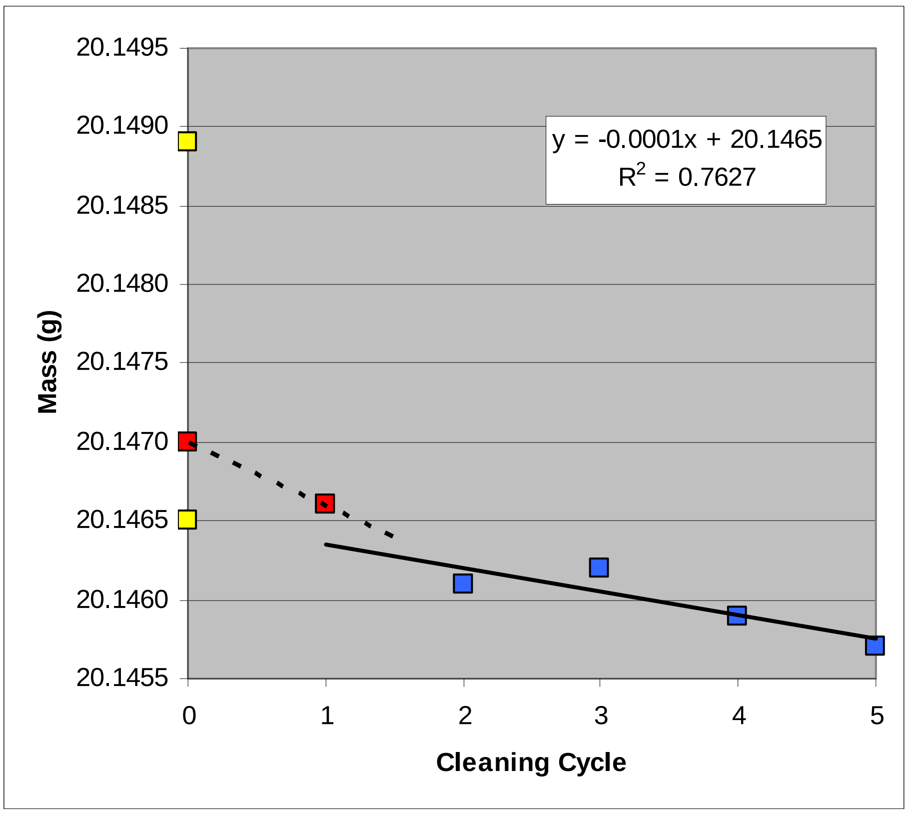

Coupon: 124
Test matrix: Fe-Go-0350-6-2p
Initial wt (g) 20.2366
Removal wt (g) 20.2347

Calculated final wt (g) 20.2343
Total wt loss (g) 0.0023
Total wt loss (mg) 2.3

Cleaning Cycle	Wt (g)
0	20.2347
1	20.2345
2	20.2340
3	20.2338
4	20.2338
5	20.2335

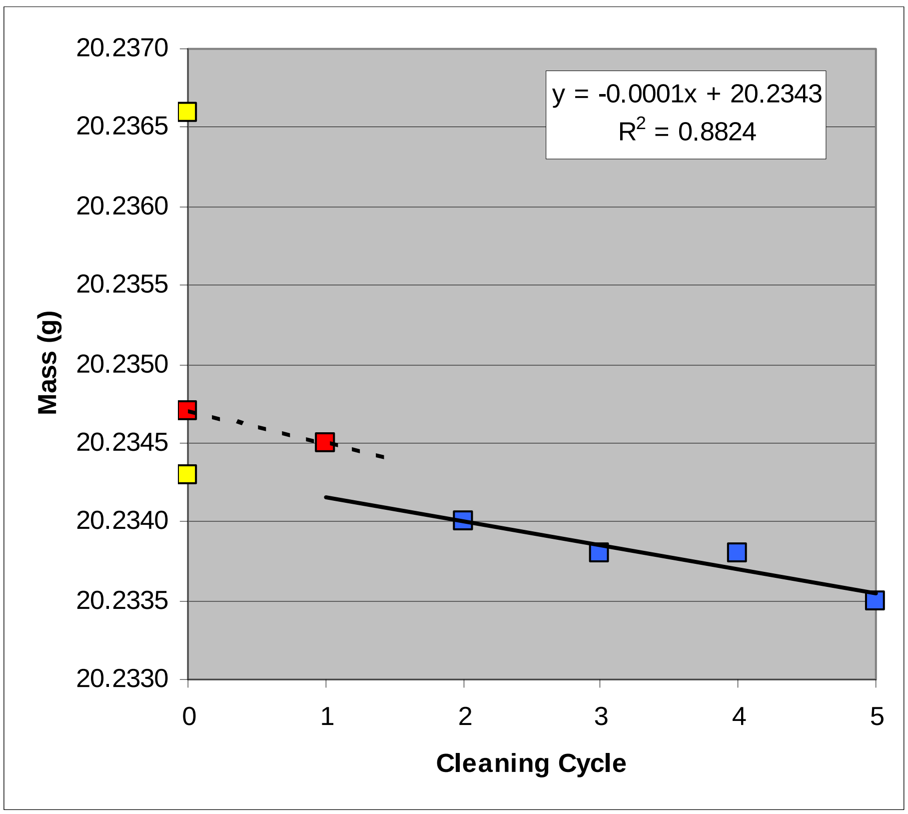

Coupon:	126
Test matrix:	Fe-E-0350-6-1f
Initial wt (g)	20.1509
Removal wt (g)	20.1676

Calculated final wt (g)	20.1499
Total wt loss (g)	0.0010
Total wt loss (mg)	1.0

Cleaning Cycle	Wt (g)
0	20.1676
1	20.1468
2	20.1451
3	20.1429
4	20.1403
5	20.1380

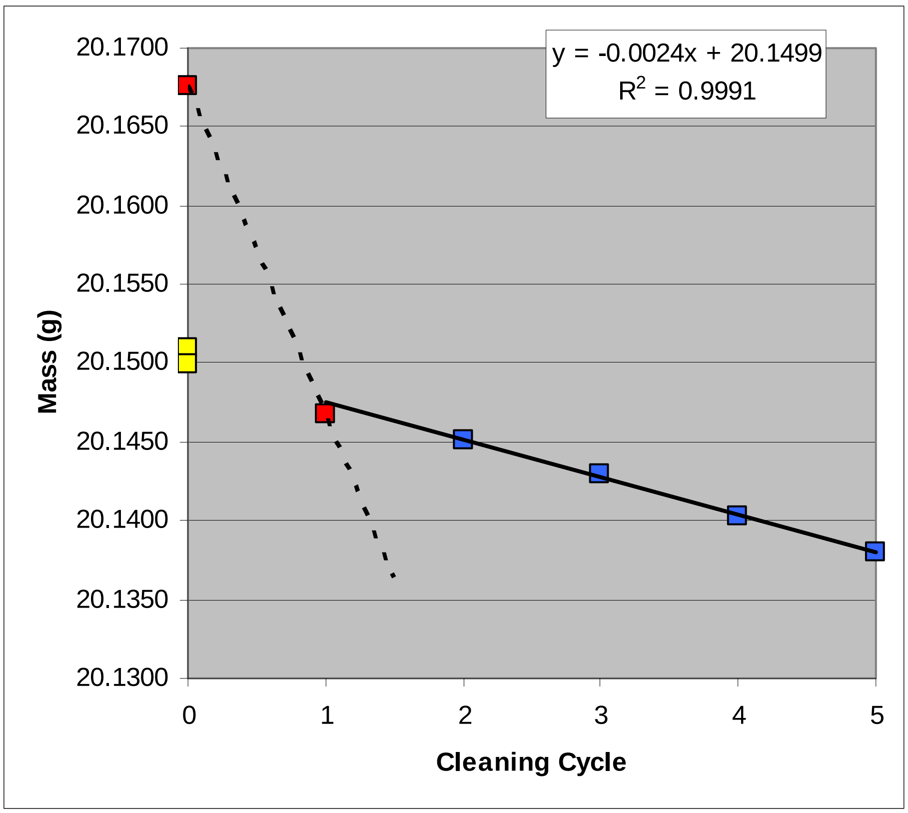

Coupon:	127		
Test matrix:	Fe-E-0350-6-2f		
Initial wt (g)	20.2231	**Calculated final wt (g)**	20.2224
Removal wt (g)	20.3289	**Total wt loss (g)**	0.0007
		Total wt loss (mg)	0.7

Cleaning Cycle	Wt (g)
0	20.3289
1	20.2191
2	20.2171
3	20.2148
4	20.2123
5	20.2094

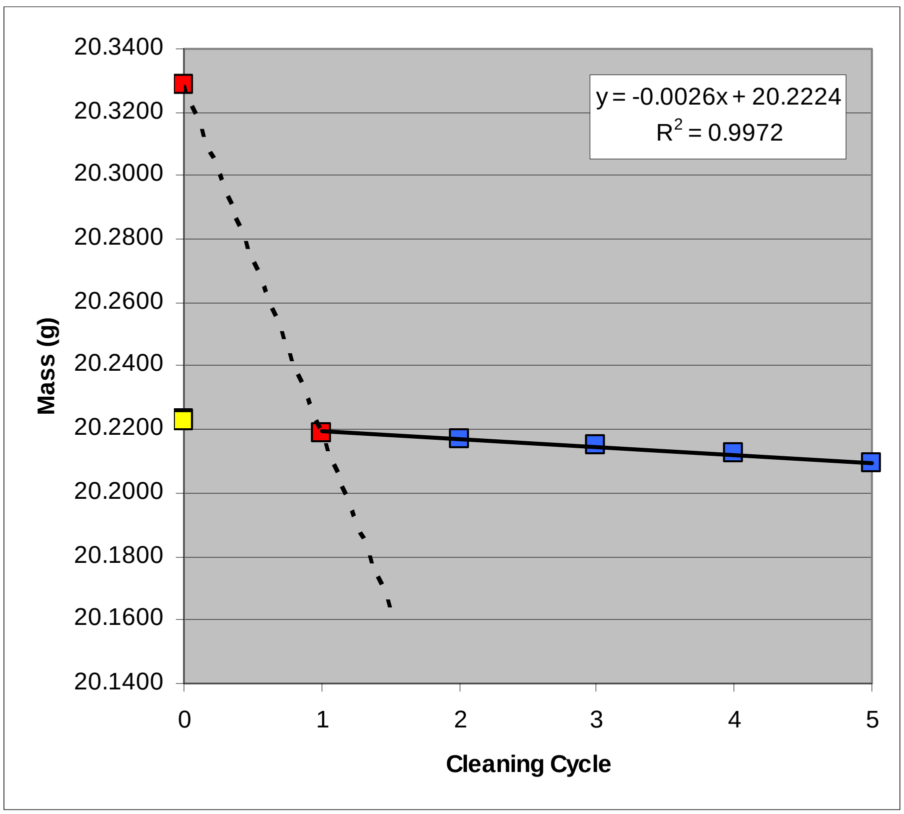

Coupon:	129
Test matrix:	Fe-E-0350-6-1p
Initial wt (g)	20.0739
Removal wt (g)	20.1105

Calculated final wt (g)	20.0758
Total wt loss (g)	-0.0019
Total wt loss (mg)	-1.9

Cleaning Cycle	Wt (g)
0	20.1105
1	20.0807
2	20.0701
3	20.0674
4	20.0655
5	20.0615

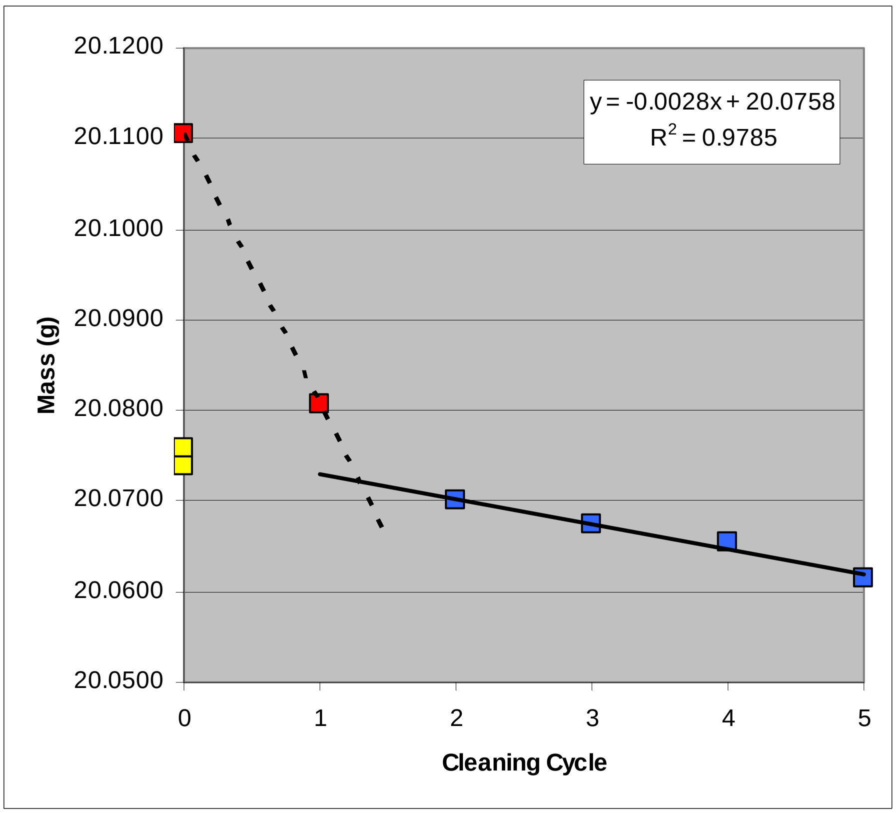

Coupon:	130		
Test matrix:	Fe-E-0350-6-2p		
Initial wt (g)	20.3403	**Calculated final wt (g)**	20.3406
Removal wt (g)	20.3536	**Total wt loss (g)**	-0.0003
		Total wt loss (mg)	-0.3

Cleaning Cycle	Wt (g)
0	20.3536
1	20.3363
2	20.3340
3	20.3310
4	20.3276
5	20.3243

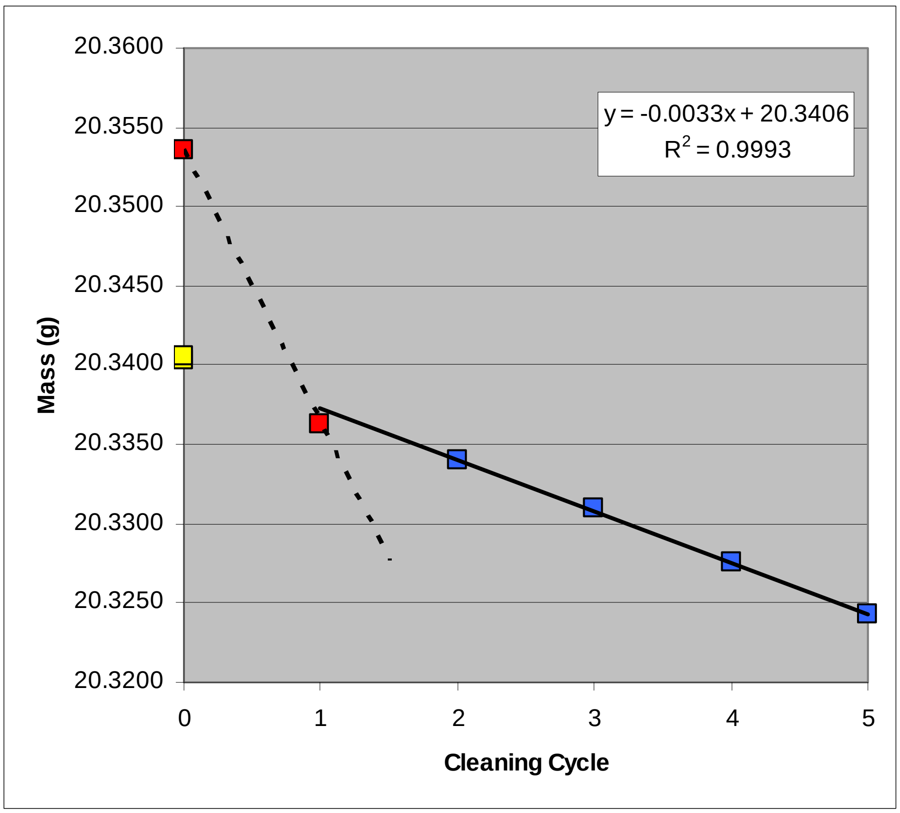

Coupon:	132
Test matrix:	Fe-Eo-0350-6-1f
Initial wt (g)	19.6018
Removal wt (g)	19.6006

Calculated final wt (g)	19.6012
Total wt loss (g)	0.0006
Total wt loss (mg)	0.6

Cleaning Cycle	Wt (g)
0	19.6006
1	19.5978
2	19.5960
3	19.5933
4	19.5908
5	19.5881

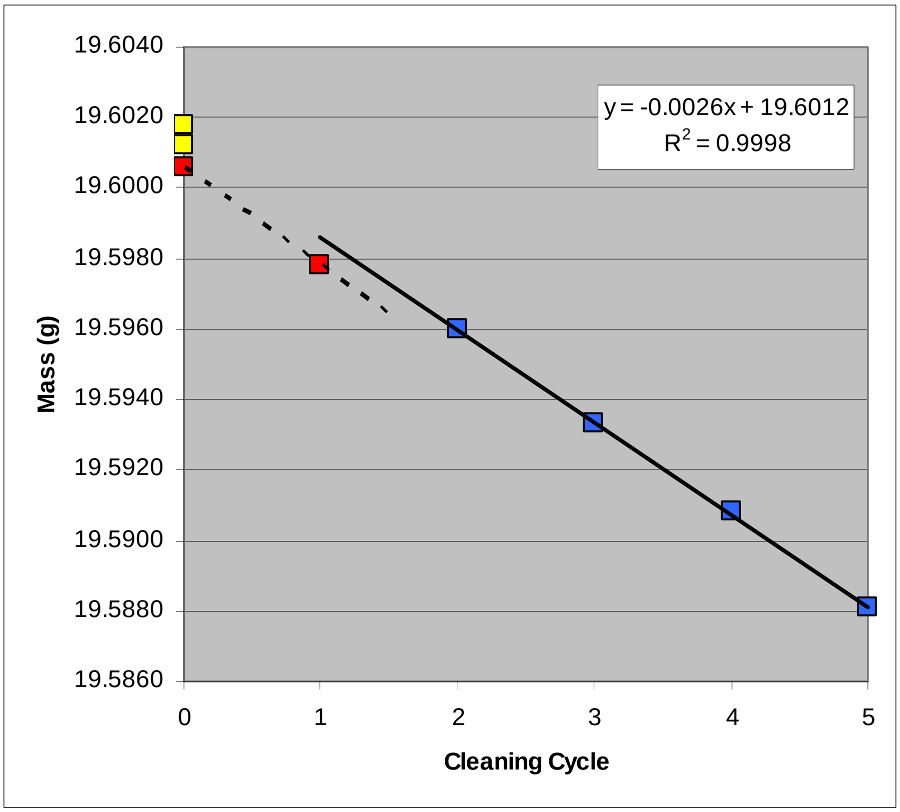

Coupon:	133		
Test matrix:	Fe-Eo-0350-6-2f		
Initial wt (g)	19.7301	**Calculated final wt (g)**	19.7289
Removal wt (g)	19.7312	**Total wt loss (g)**	0.0012
		Total wt loss (mg)	1.2

Cleaning Cycle	Wt (g)
0	19.7312
1	19.7255
2	19.7233
3	19.7205
4	19.7176
5	19.7149

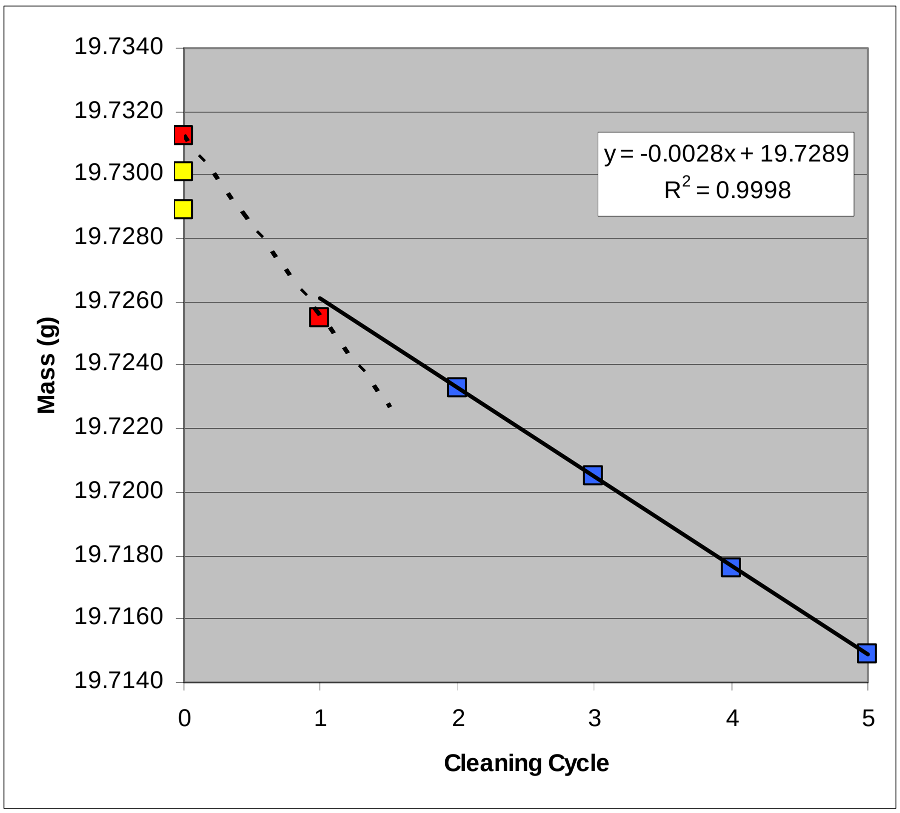

Coupon:	135			
Test matrix:	Fe-Eo-0350-6-1p			
Initial wt (g)	19.9139		**Calculated final wt (g)**	19.9141
Removal wt (g)	19.9174		**Total wt loss (g)**	-0.0002
			Total wt loss (mg)	-0.2

Cleaning Cycle	Wt (g)
0	19.9174
1	19.9112
2	19.9089
3	19.9068
4	19.9042
5	19.9014

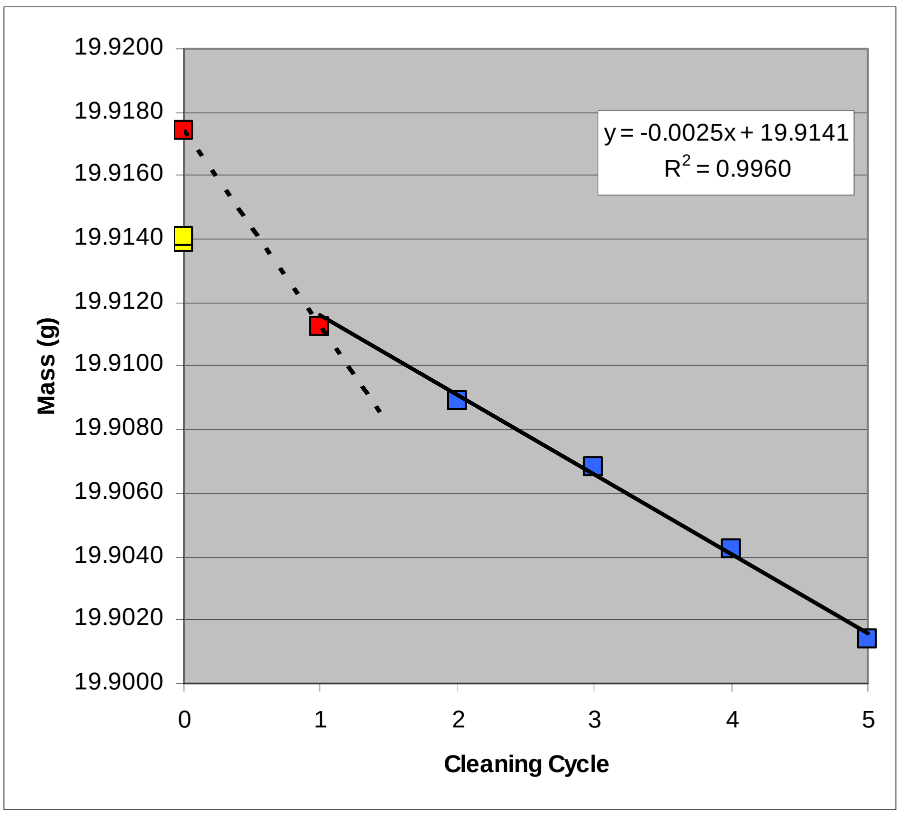

Coupon:	136		
Test matrix:	Fe-Eo-0350-6-2p		
Initial wt (g)	18.3987	**Calculated final wt (g)**	18.3992
Removal wt (g)	18.3990	**Total wt loss (g)**	-0.0005
		Total wt loss (mg)	-0.5

Cleaning Cycle	**Wt (g)**
0	18.3990
1	18.3953
2	18.3934
3	18.3897
4	18.3879
5	18.3841

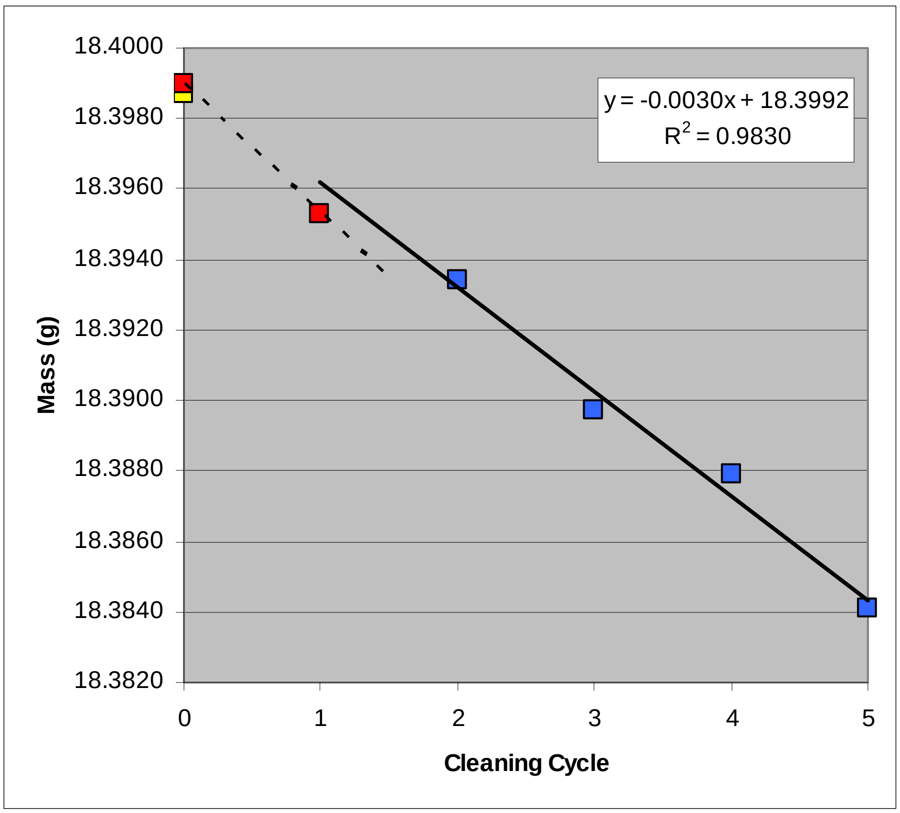

Coupon:	138		
Test matrix:	Fe-Atm-0350-6-1		
Initial wt (g)	18.7107	**Calculated final wt (g)**	18.7113
Removal wt (g)	18.7110	**Total wt loss (g)**	-0.0006
		Total wt loss (mg)	-0.6

Cleaning Cycle	Wt (g)
0	18.7110
1	18.7107
2	18.7102
3	18.7100
4	18.7093
5	18.7088

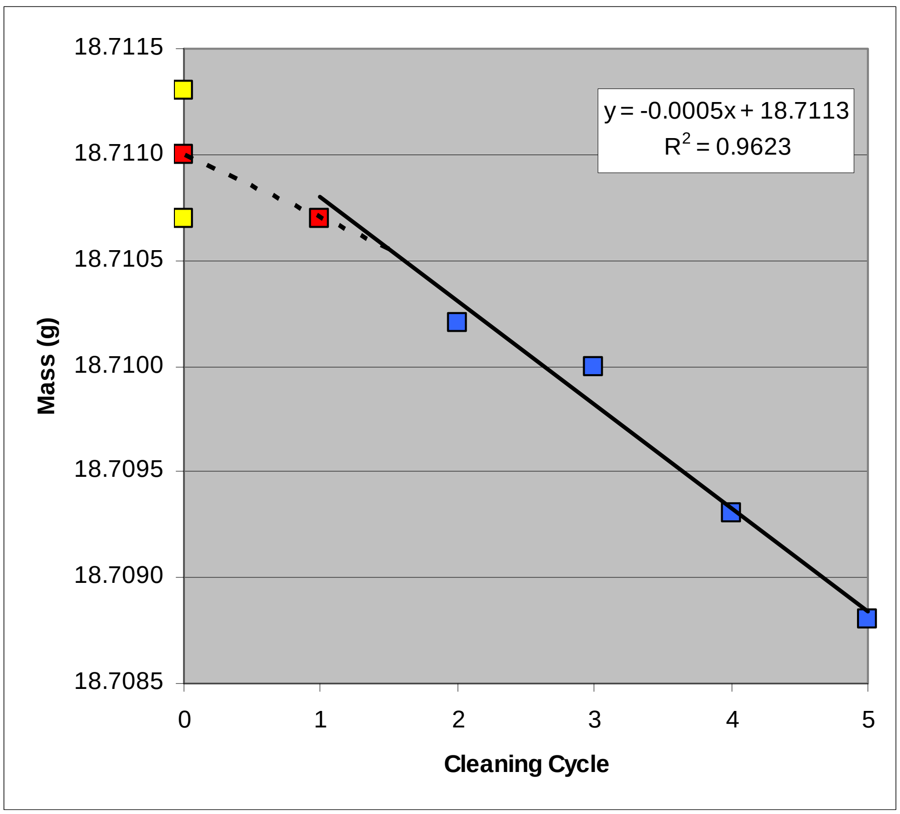

Coupon: 139
Test matrix: Fe-Atm-0350-6-2

Initial wt (g) 18.8829
Removal wt (g) 18.8830

Calculated final wt (g) 18.8828
Total wt loss (g) 0.0001
Total wt loss (mg) 0.1

Cleaning Cycle	Wt (g)
0	18.8830
1	18.8825
2	18.8822
3	18.8818
4	18.8814
5	18.8812

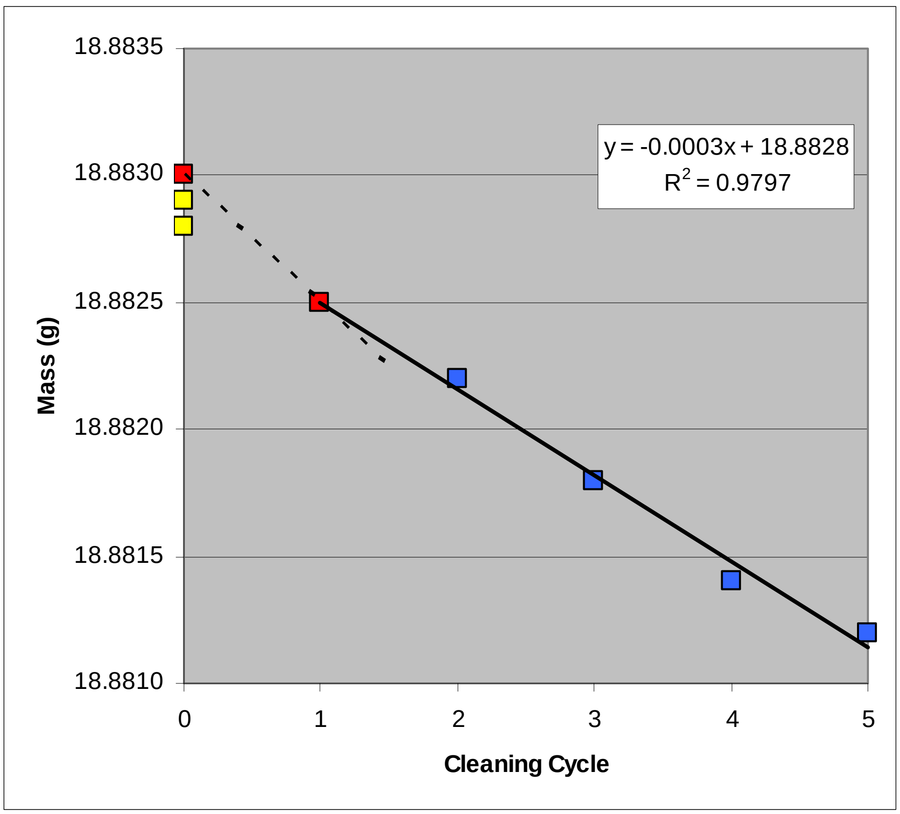

Coupon: 307
Test matrix: Fe-G-1500-6-2f

Initial wt (g) 20.4468
Removal wt (g) 20.4624

Calculated final wt (g) 20.4433
Total wt loss (g) 0.0035
Total wt loss (mg) 3.5

Cleaning Cycle	Wt (g)
0	20.4624
1	20.4415
2	20.4423
3	20.4406
4	20.4403
5	20.4400

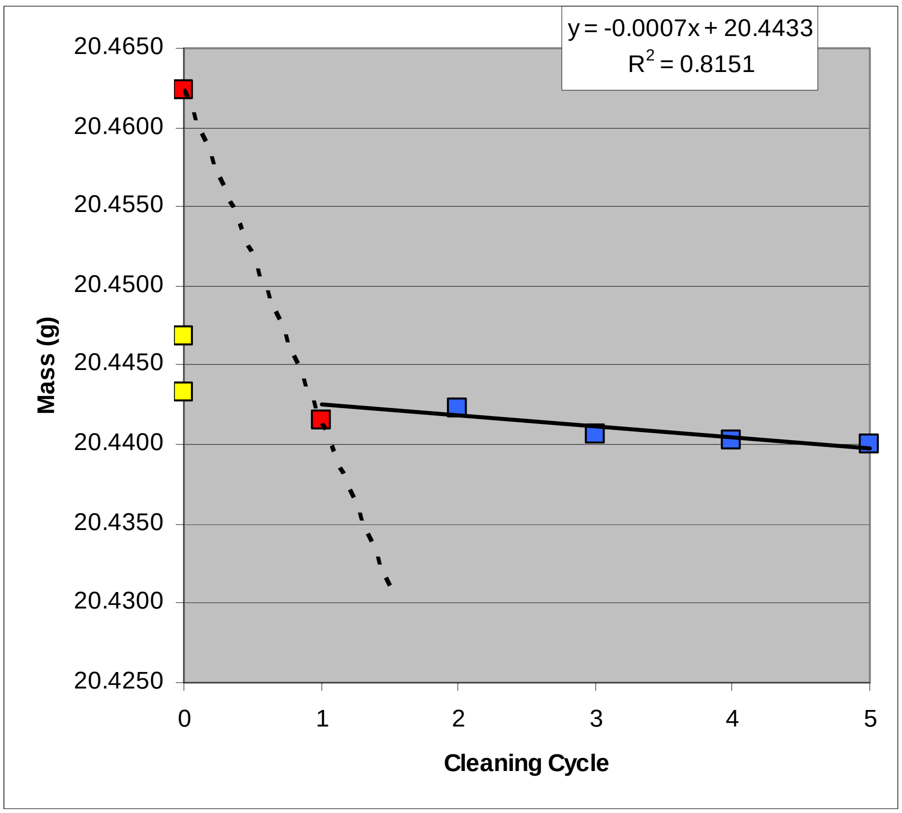

Coupon: 308
Test matrix: Fe-G-1500-6-3f

Initial wt (g)	20.4428	**Calculated final wt (g)**	20.4378
Removal wt (g)	20.4501	**Total wt loss (g)**	0.0050
		Total wt loss (mg)	5.0

Cleaning Cycle	Wt (g)
0	20.4501
1	20.4378
2	20.4373
3	20.4374
4	20.4368
5	20.4368

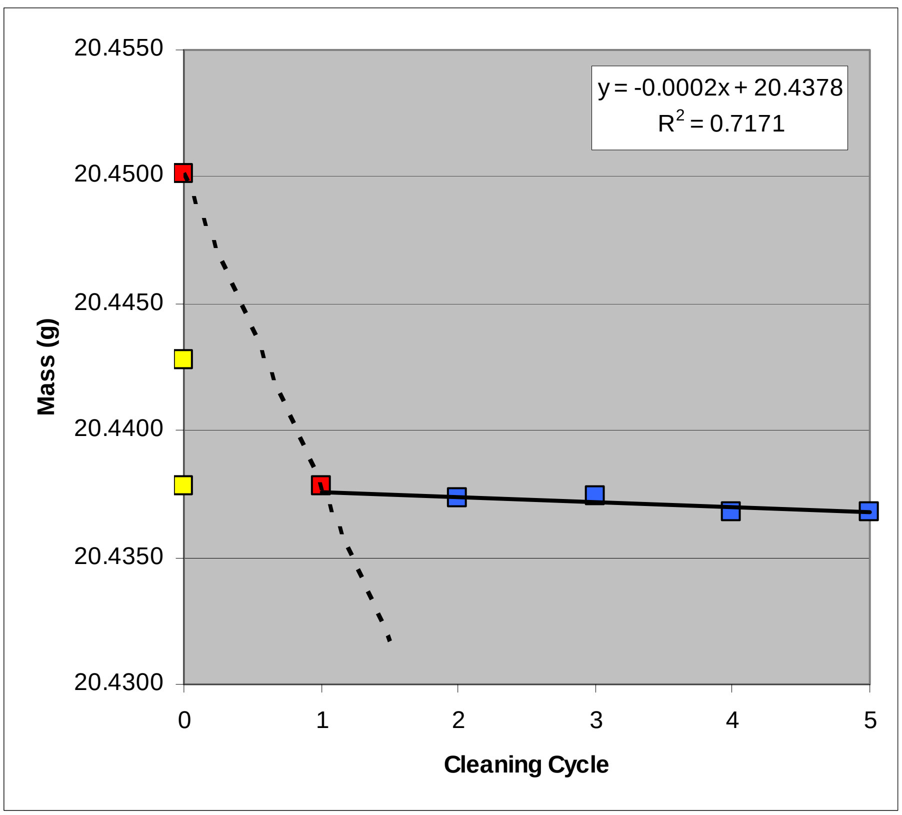

Coupon: 310
Test matrix: Fe-G-1500-6-2p

Initial wt (g) 20.6744
Removal wt (g) 20.6725

Calculated final wt (g) 20.6714
Total wt loss (g) 0.0030
Total wt loss (mg) 3.0

Cleaning Cycle	Wt (g)
0	20.6725
1	20.6710
2	20.6707
3	20.6708
4	20.6703
5	20.6699

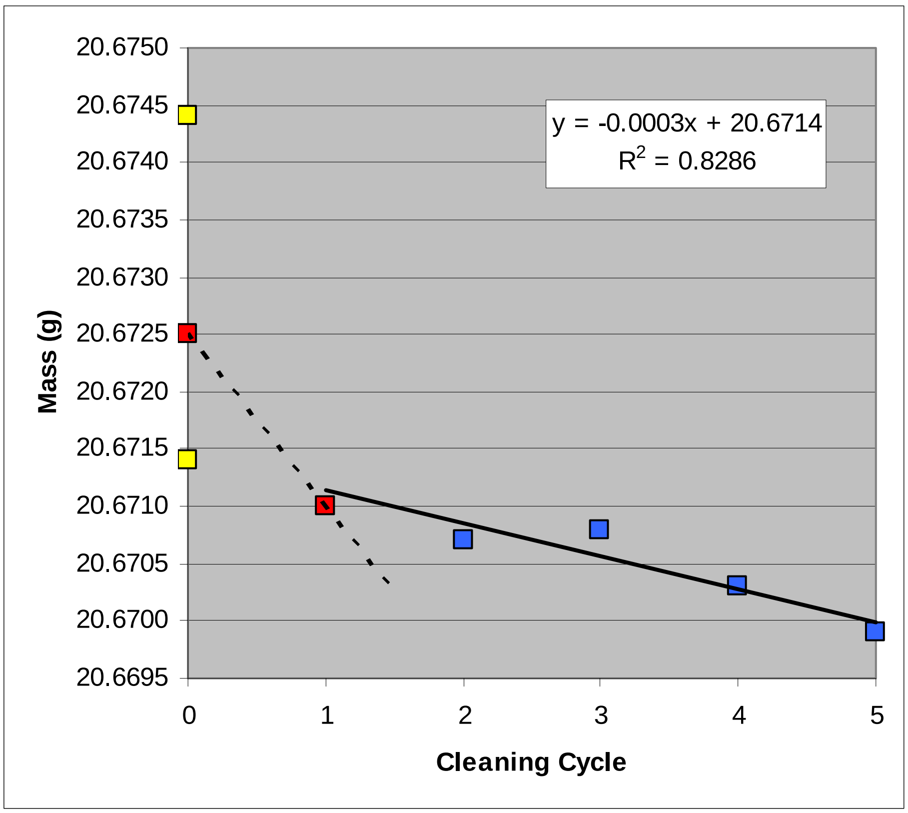

Coupon:	311
Test matrix:	Fe-G-1500-6-3p
Initial wt (g)	20.0198
Removal wt (g)	20.0180

Calculated final wt (g)	20.0168
Total wt loss (g)	0.0030
Total wt loss (mg)	3.0

Cleaning Cycle	**Wt (g)**
0	20.0180
1	20.0177
2	20.0174
3	20.0169
4	20.0170
5	20.0170

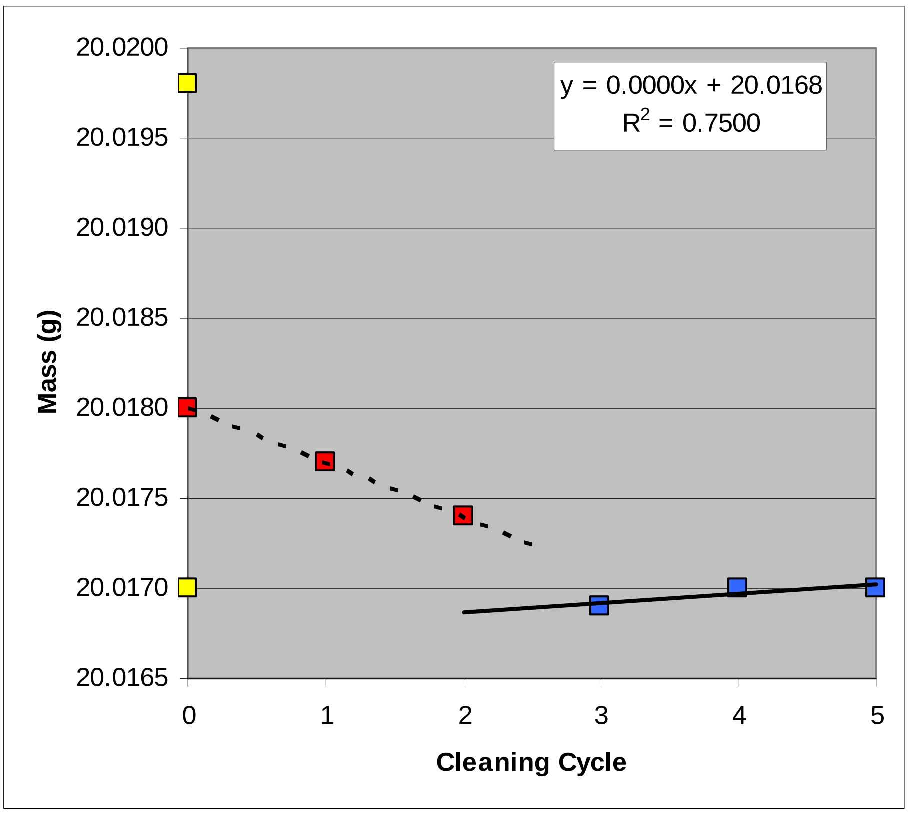

Coupon:	313			
Test matrix:	Fe-Go-1500-6-2f			
Initial wt (g)	20.2360		**Calculated final wt (g)**	20.2303
Removal wt (g)	20.2327		**Total wt loss (g)**	0.0057
			Total wt loss (mg)	5.7

Cleaning Cycle	Wt (g)
0	20.2327
1	20.2305
2	20.2313
3	20.2301
4	20.2301
5	20.2300

Note: Cycle 2 not used in regression

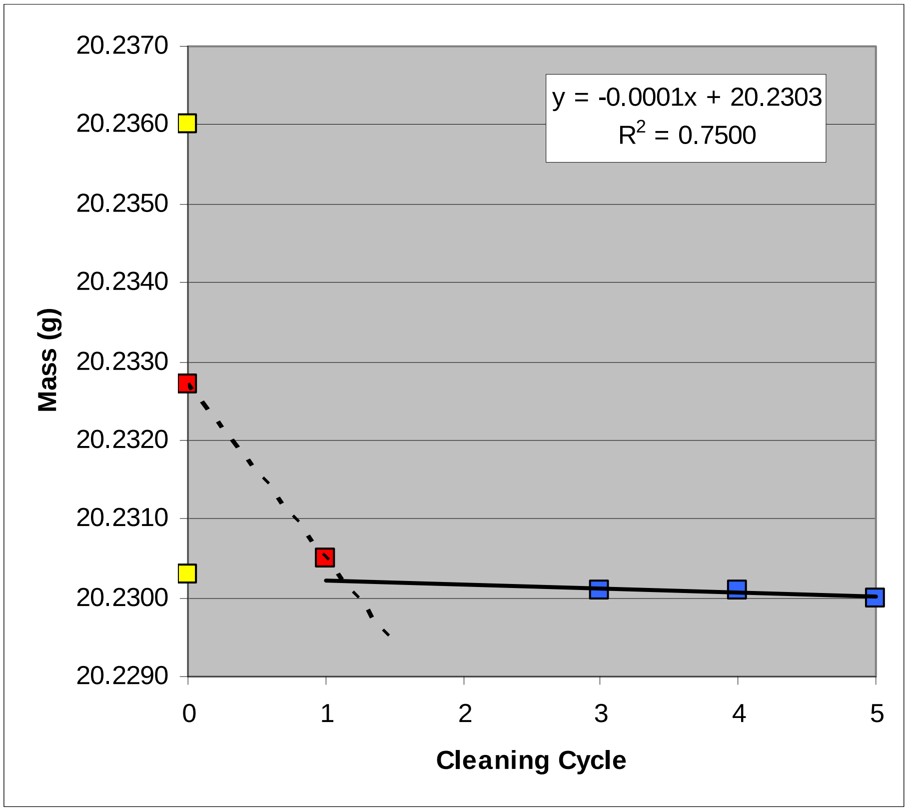

Coupon:	314		
Test matrix:	Fe-Go-1500-6-3f		
Initial wt (g)	20.4547	**Calculated final wt (g)**	20.4492
Removal wt (g)	20.4585	**Total wt loss (g)**	0.0055
		Total wt loss (mg)	5.5

Cleaning Cycle	Wt (g)
0	20.4585
1	20.4490
2	20.4488
3	20.4483
4	20.4483
5	20.4480

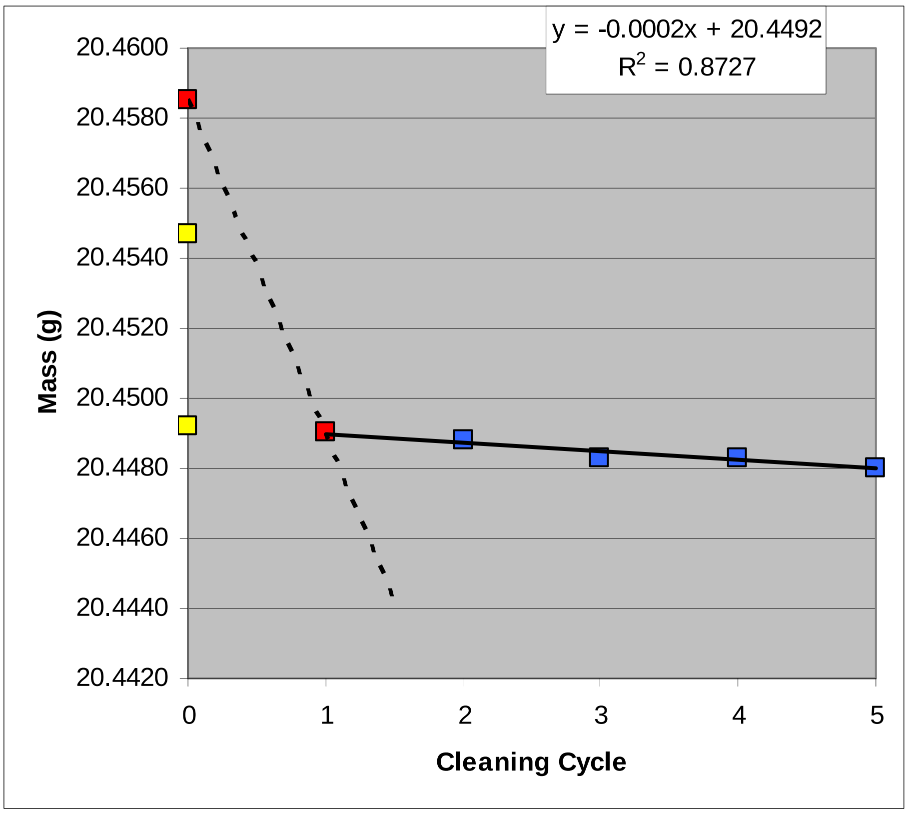

Coupon:	316
Test matrix:	Fe-Go-1500-6-2p
Initial wt (g)	19.3890
Removal wt (g)	19.3870

Calculated final wt (g)	19.3872
Total wt loss (g)	0.0018
Total wt loss (mg)	1.8

Cleaning Cycle	Wt (g)
0	19.3870
1	19.3866
2	19.3862
3	19.3856
4	19.3858
5	19.3861
7	19.3831
9	19.3825
11	19.3818
13	19.3814
15	19.3809

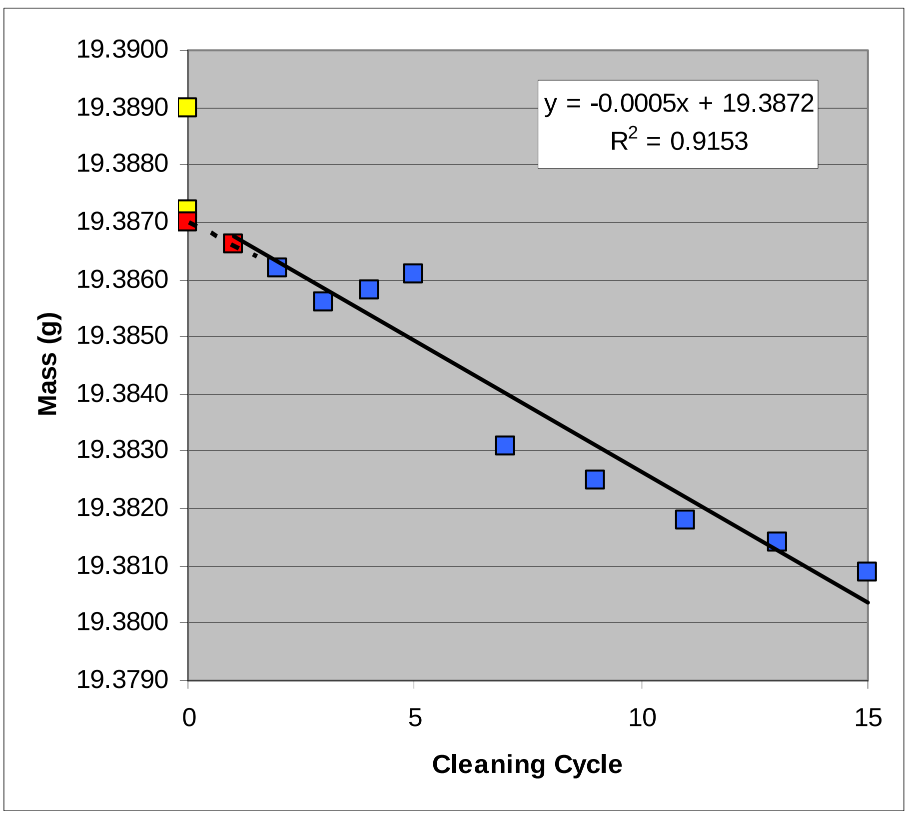

Coupon:	317
Test matrix:	Fe-Go-1500-6-3p
Initial wt (g)	19.6472
Removal wt (g)	19.6450

Calculated final wt (g)	19.6440
Total wt loss (g)	0.0032
Total wt loss (mg)	3.2

Cleaning Cycle	Wt (g)
0	19.6450
1	19.6442
2	19.6435
3	19.6437
4	19.6433
5	19.6431

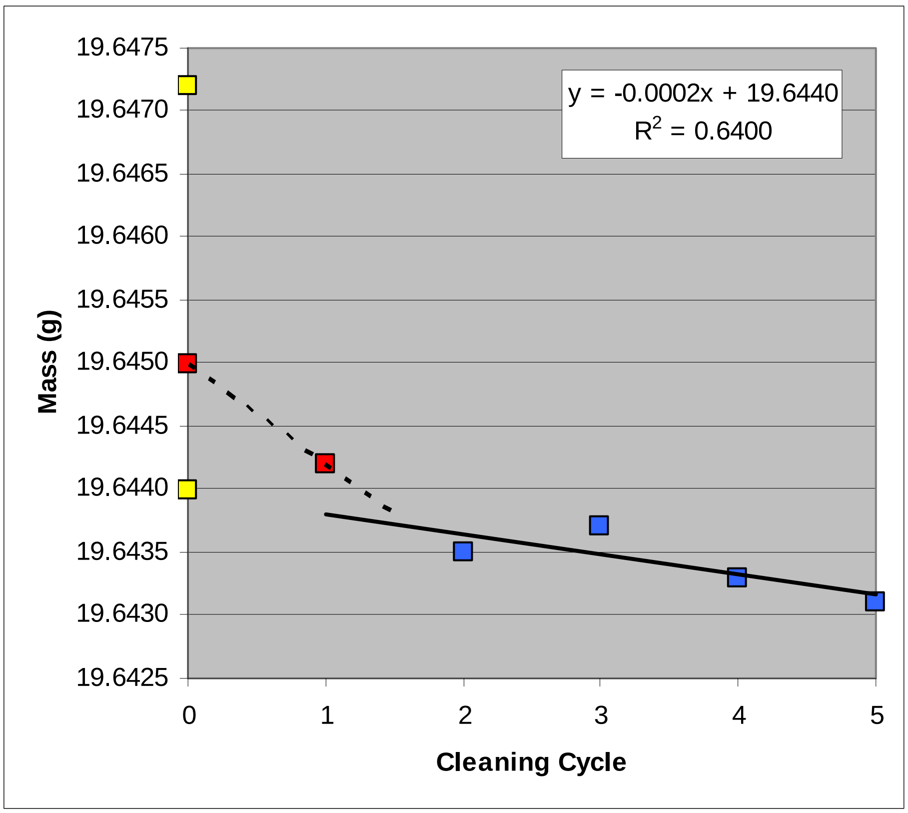

Coupon:	319
Test matrix:	Fe-E-1500-6-2f
Initial wt (g)	20.1540
Removal wt (g)	20.1799

Calculated final wt (g)	20.1434
Total wt loss (g)	0.0106
Total wt loss (mg)	10.6

Cleaning Cycle	Wt (g)
0	20.1799
1	20.1434
2	20.1428
3	20.1421
4	20.1418
5	20.1416

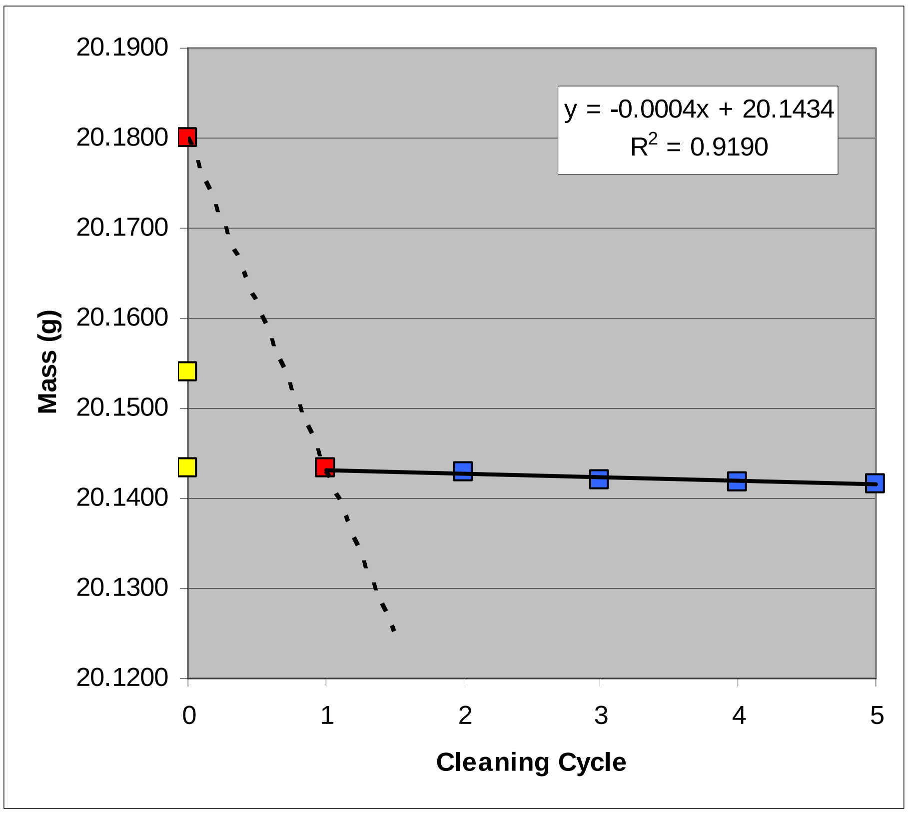

Coupon:	320
Test matrix:	Fe-E-1500-6-3f
Initial wt (g)	20.3862
Removal wt (g)	20.4138

Calculated final wt (g)	20.3752
Total wt loss (g)	0.0110
Total wt loss (mg)	11.0

Cleaning Cycle	Wt (g)
0	20.4138
1	20.3756
2	20.3751
3	20.3750
4	20.3750
5	20.3749

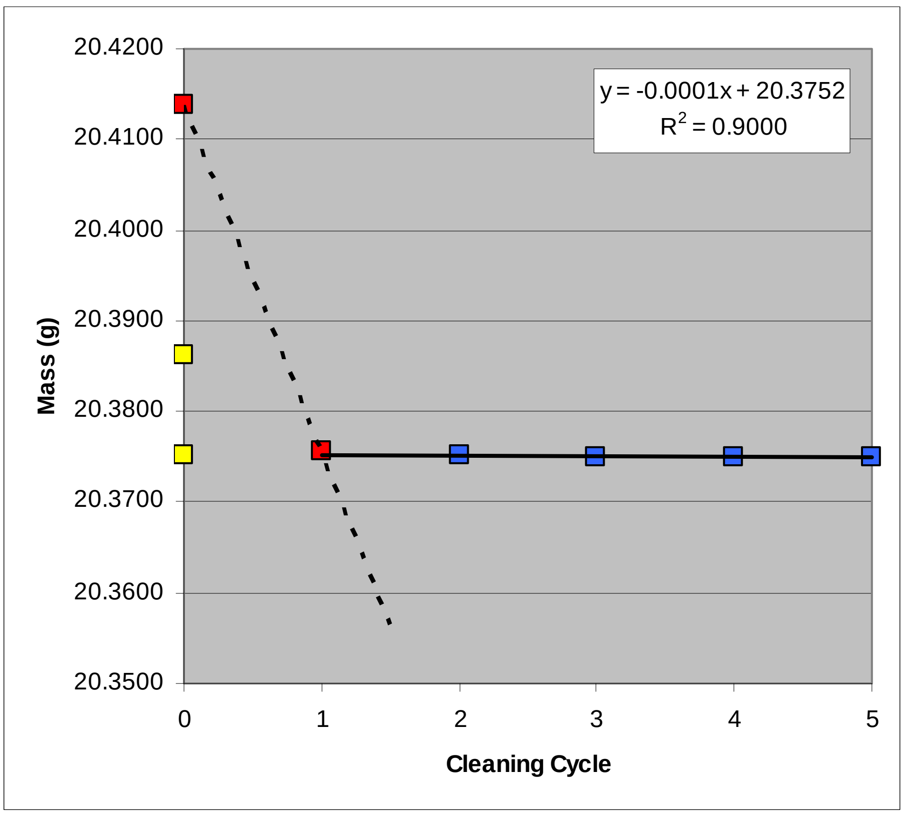

Coupon:	322
Test matrix:	Fe-E-1500-6-2p
Initial wt (g)	18.8133
Removal wt (g)	18.8260

Calculated final wt (g)	18.8081
Total wt loss (g)	0.0052
Total wt loss (mg)	5.2

Cleaning Cycle	Wt (g)
0	18.8260
1	18.807
2	18.8069
3	18.8075
4	18.8060
5	18.8060

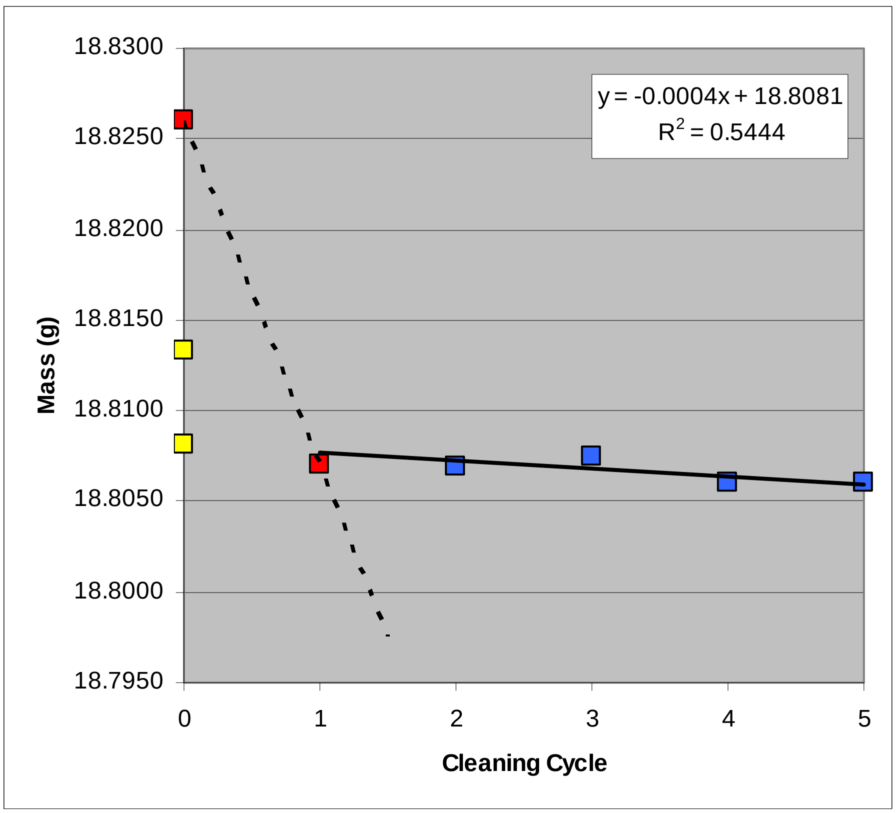

Coupon:	323
Test matrix:	Fe-E-1500-6-3p
Initial wt (g)	19.0999
Removal wt (g)	19.1151

Calculated final wt (g)	19.0942
Total wt loss (g)	0.0057
Total wt loss (mg)	5.7

Cleaning Cycle	Wt (g)
0	19.1151
1	19.0933
2	19.0936
3	19.0933
4	19.0925
5	19.0921
7	19.0903
9	19.0900
11	19.0892
13	19.0888
15	19.0881

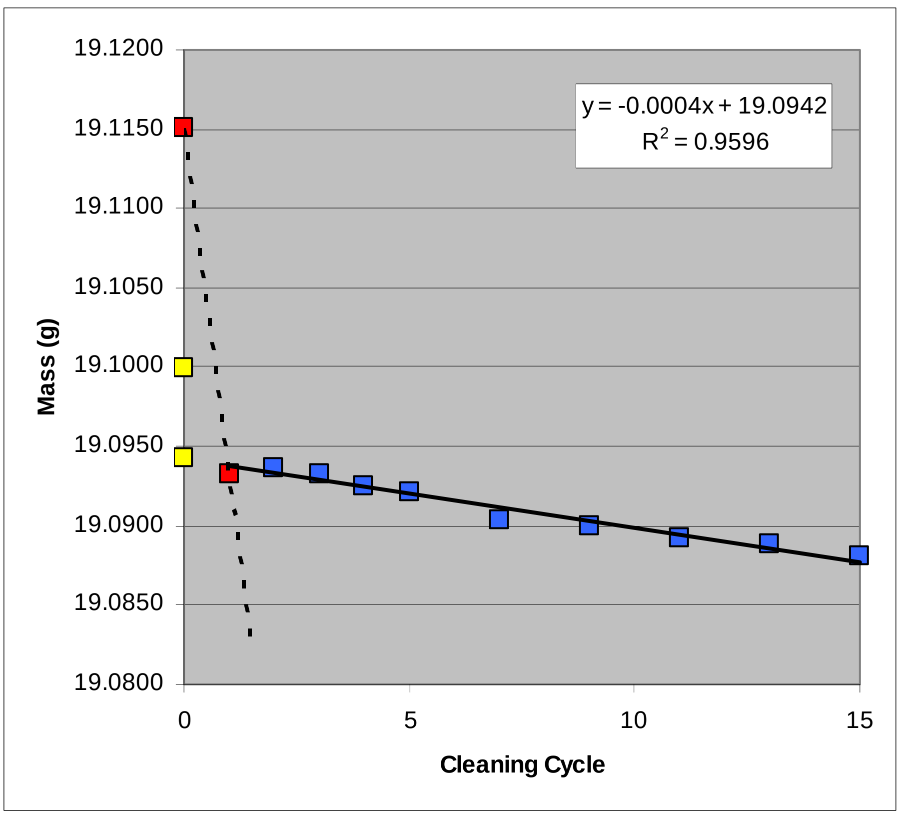

Coupon:	325
Test matrix:	Fe-Eo-1500-6-2f
Initial wt (g)	19.9421
Removal wt (g)	19.9539

Calculated final wt (g)	19.9369
Total wt loss (g)	0.0052
Total wt loss (mg)	5.2

Cleaning Cycle	Wt (g)
0	19.9539
1	19.9366
2	19.9367
3	19.9367
4	19.9363
5	19.9365

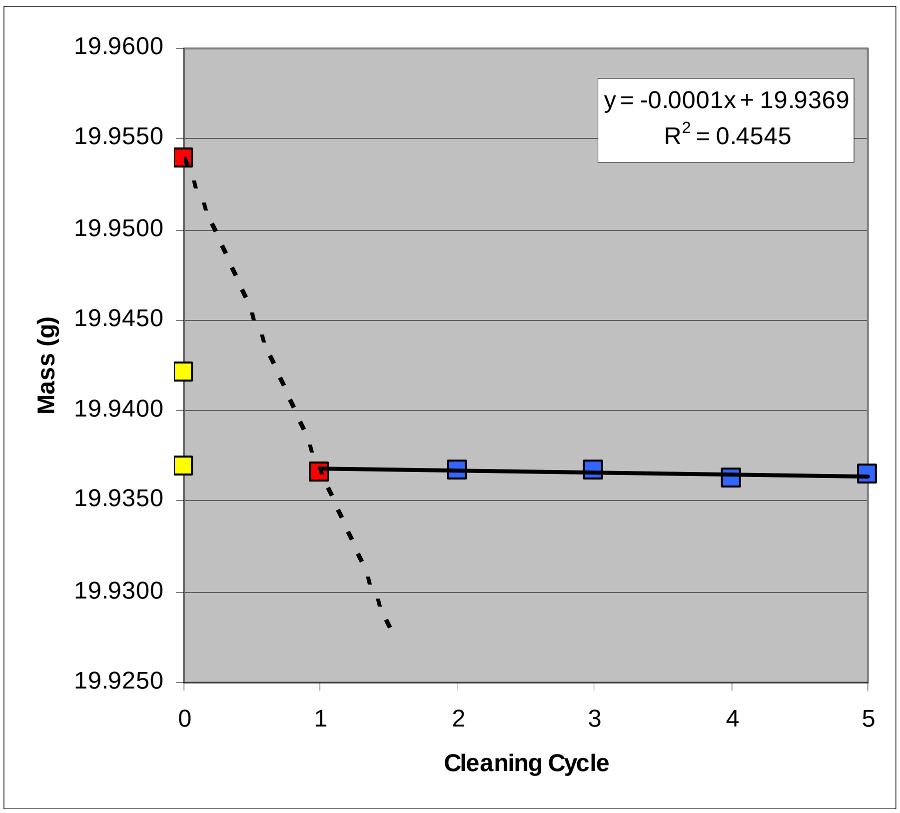

Coupon:	326
Test matrix:	Fe-Eo-1500-6-3f
Initial wt (g)	20.2902
Removal wt (g)	20.3451

Calculated final wt (g)	20.2845
Total wt loss (g)	0.0057
Total wt loss (mg)	5.7

Cleaning Cycle	**Wt (g)**
0	20.3451
1	20.2857
2	20.2836
3	20.2835
4	20.2825
5	20.2826

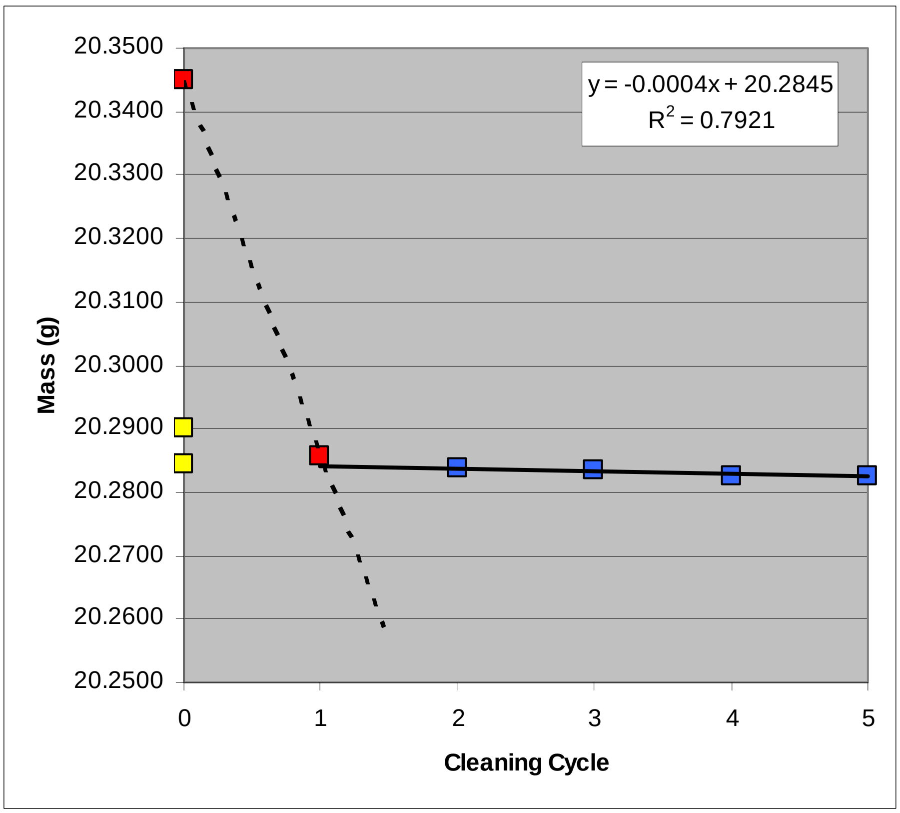

Coupon:	328		
Test matrix:	Fe-Eo-1500-6-2p		
Initial wt (g)	19.8855	**Calculated final wt (g)**	19.8838
Removal wt (g)	19.8961	**Total wt loss (g)**	0.0017
		Total wt loss (mg)	1.7

Cleaning Cycle	Wt (g)
0	19.8961
1	19.8825
2	19.8837
3	19.8837
4	19.8817
5	19.8815

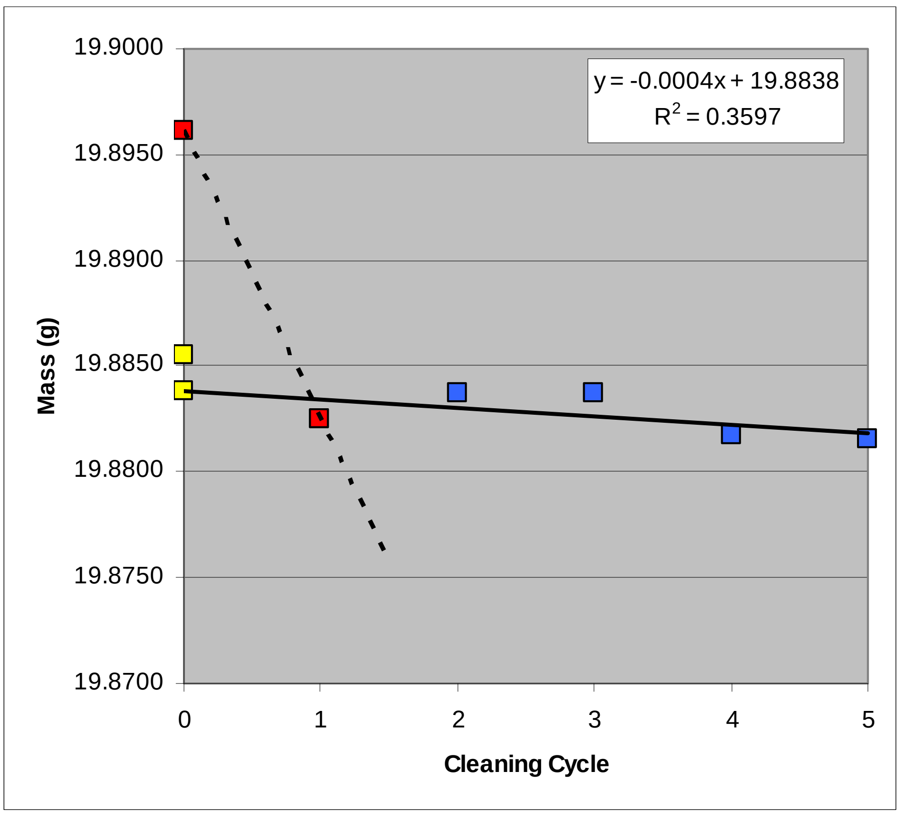

Coupon:	329
Test matrix:	Fe-Eo-1500-6-3p
Initial wt (g)	19.8942
Removal wt (g)	19.9022

Calculated final wt (g)	19.8909
Total wt loss (g)	0.0033
Total wt loss (mg)	3.3

Cleaning Cycle	Wt (g)
0	19.9022
1	19.8898
2	19.8898
3	19.8892
4	19.8893
5	19.8881

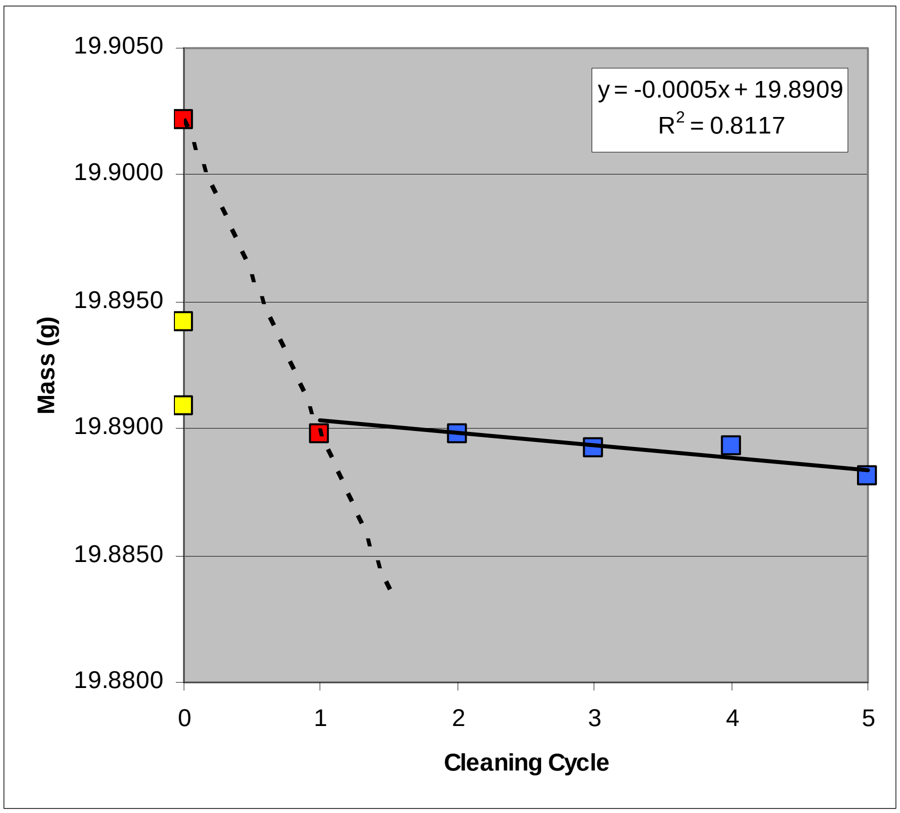

Coupon:	331
Test matrix:	Fe-Atm-1500-6-2
Initial wt (g)	20.4723
Removal wt (g)	20.4724

Calculated final wt (g)	20.4723
Total wt loss (g)	0.0000
Total wt loss (mg)	0.0

Cleaning Cycle	Wt (g)
0	20.4724
1	20.4716
2	20.4714
3	20.4709
4	20.4707
5	20.4700

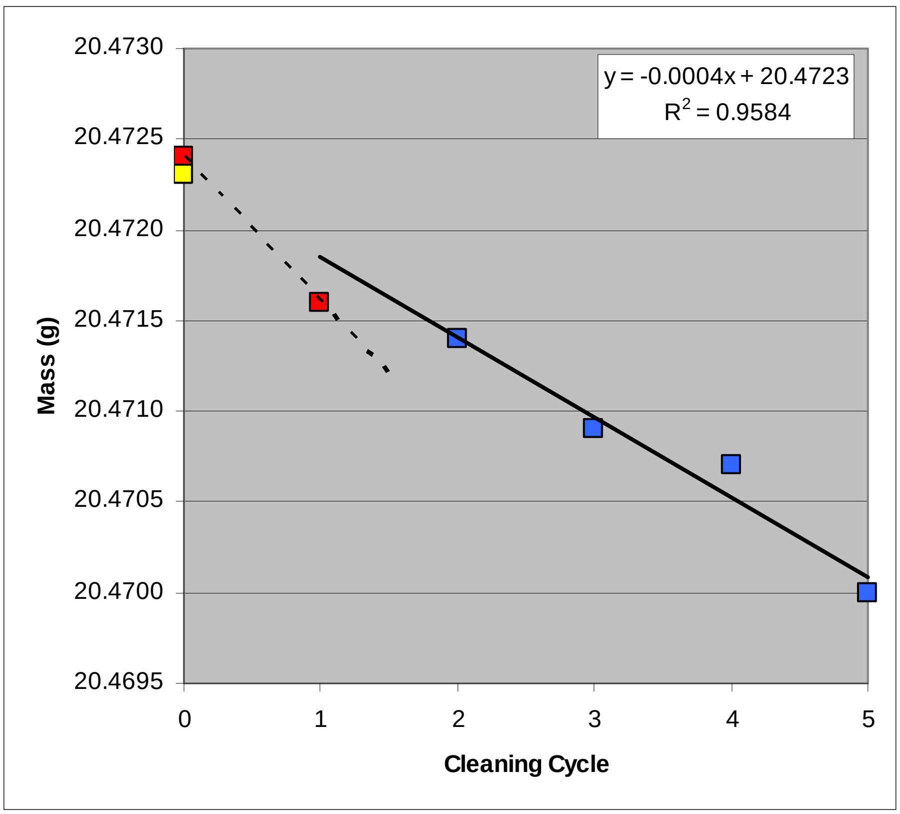

Coupon:	332		
Test matrix:	Fe-Atm-1500-6-3		
Initial wt (g)	20.4969	**Calculated final wt (g)**	20.4971
Removal wt (g)	20.4965	**Total wt loss (g)**	-0.0002
		Total wt loss (mg)	-0.2

Cleaning Cycle	Wt (g)
0	20.4965
1	20.4970
2	20.4995
3	20.4968
4	20.4966
5	20.4965

Note: The point for the 2nd cleaning cycle was not used in the regression analysis as it falls well outside the trend. In general, this analysis seems to have suffered from problems with the balance (i.e. 0th cleaning cycle weight is less than 1st cycle).

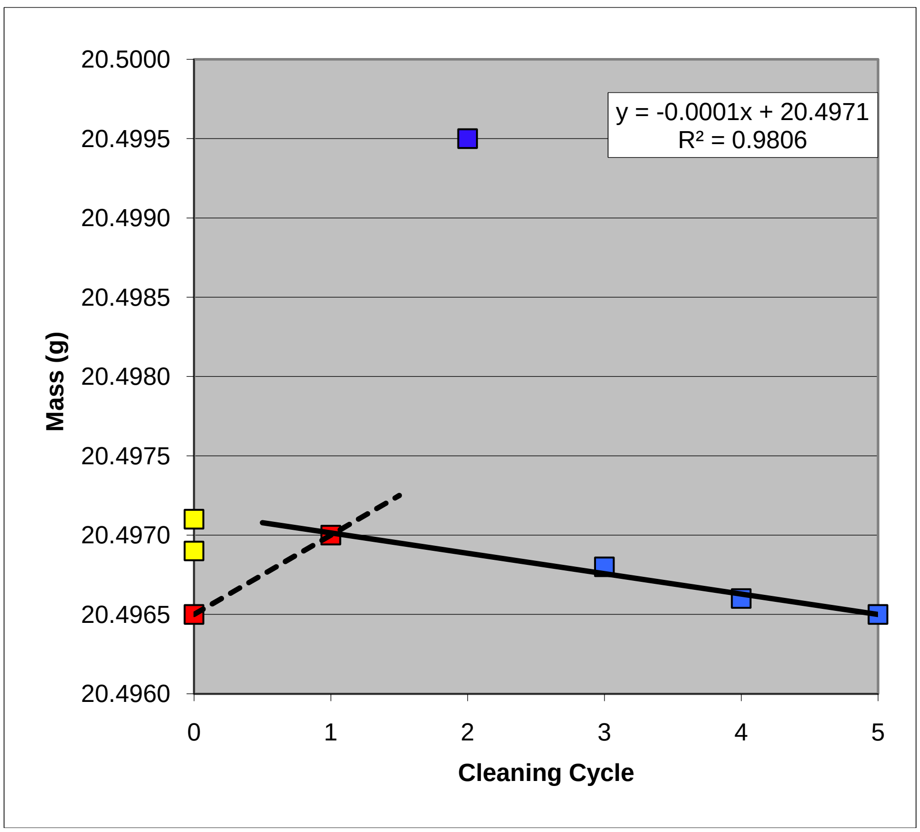

Coupon:	416
Test matrix:	Fe-G-3500-6-2f
Initial wt (g)	19.9560
Removal wt (g)	19.9822

Calculated final wt (g)	19.9487
Total wt loss (g)	0.0073
Total wt loss (mg)	7.3

Cleaning Cycle	Wt (g)
0	19.9822
1	19.9486
2	19.9480
3	19.9475
4	19.9471
5	19.9469

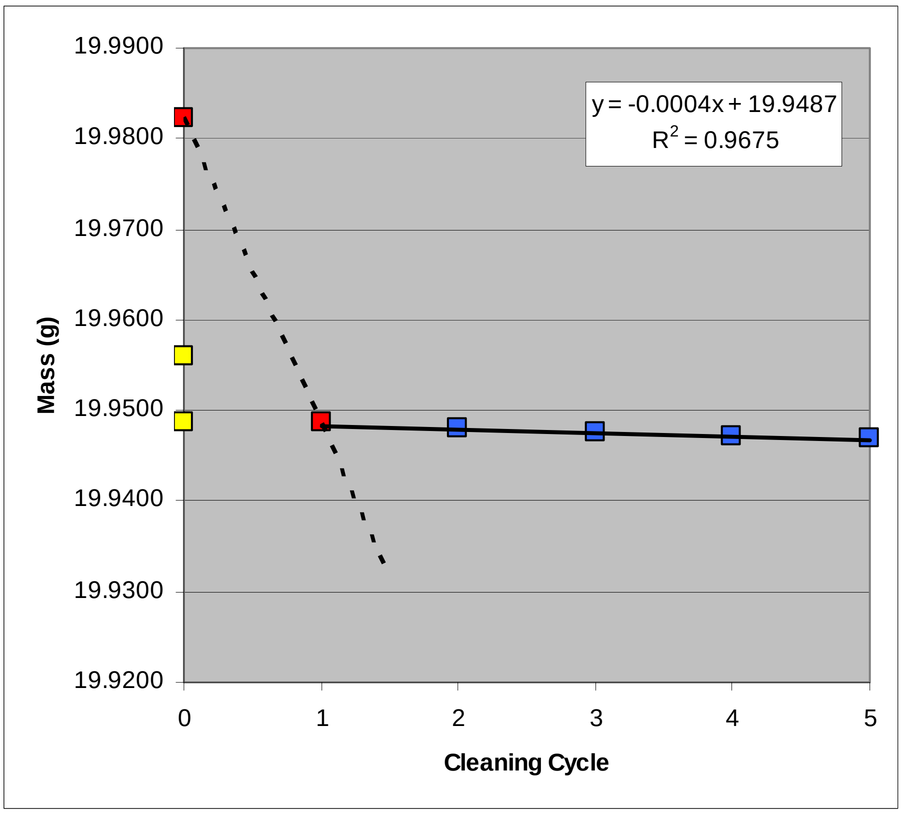

Coupon:	417
Test matrix:	Fe-G-3500-6-3f
Initial wt (g)	19.9064
Removal wt (g)	19.9329

Calculated final wt (g)	19.8989
Total wt loss (g)	0.0075
Total wt loss (mg)	7.5

Cleaning Cycle	Wt (g)
0	19.9329
1	19.8980
2	19.8978
3	19.8974
4	19.8969
5	19.8963

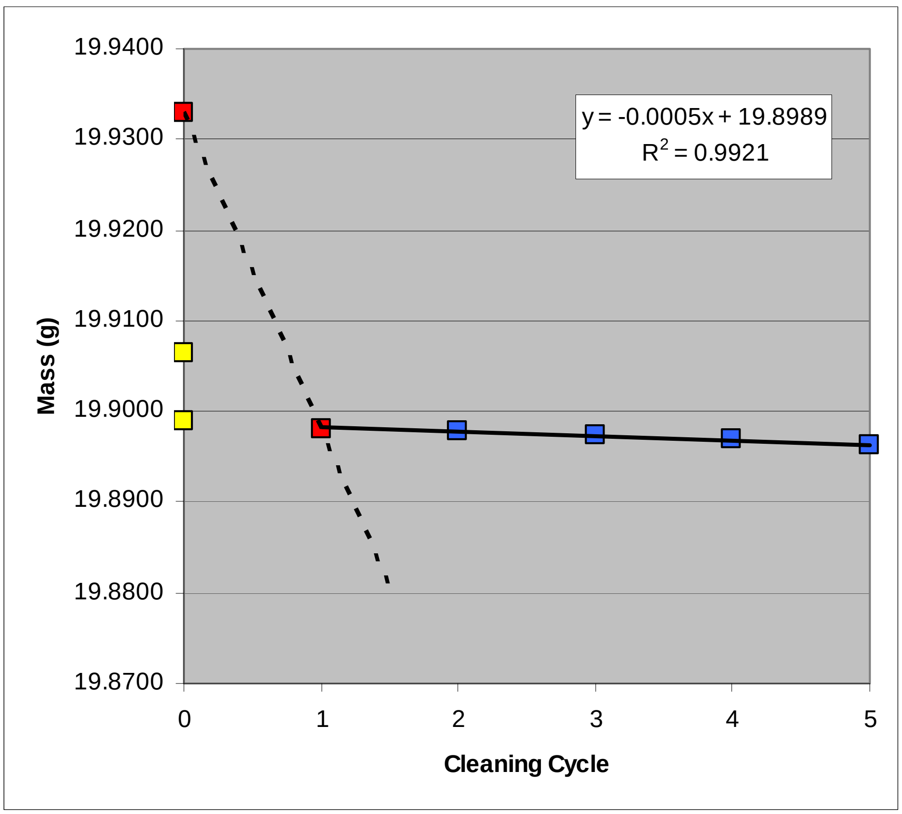

Coupon:	418
Test matrix:	Fe-G-3500-6-1p
Initial wt (g)	19.6738
Removal wt (g)	19.6981

Calculated final wt (g)	19.6694
Total wt loss (g)	0.0044
Total wt loss (mg)	4.4

Cleaning Cycle	Wt (g)
0	19.6981
1	19.6692
2	19.6686
3	19.6678
4	19.6674
5	19.6671

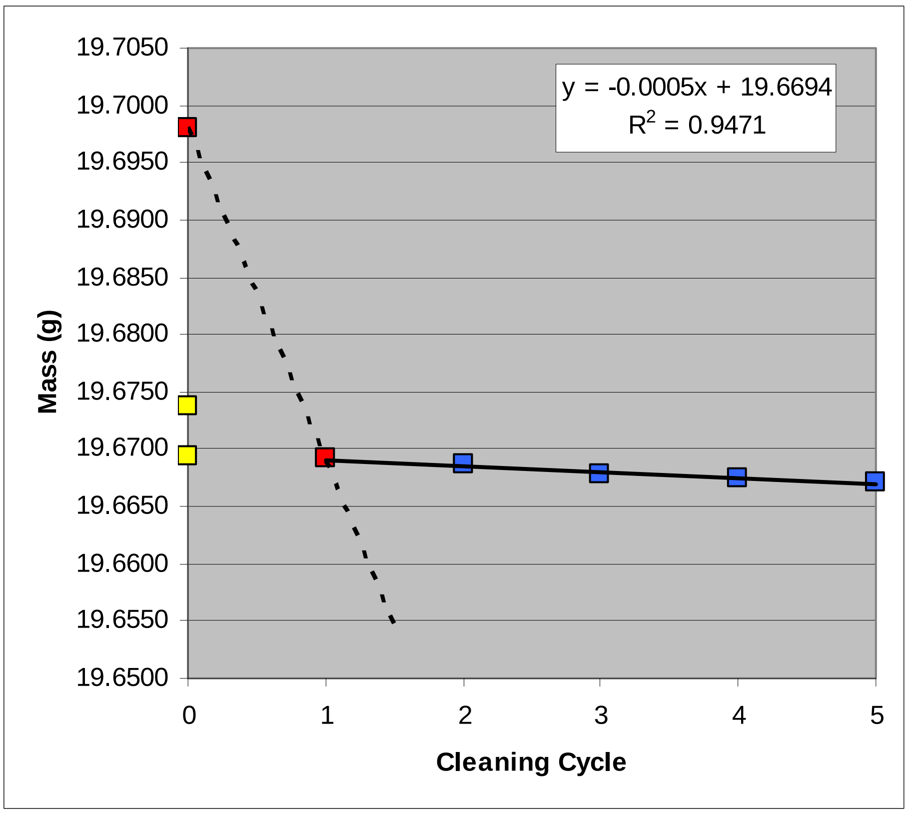

Coupon:	419
Test matrix:	Fe-G-3500-6-2p
Initial wt (g)	19.5823
Removal wt (g)	19.6029

Calculated final wt (g)	19.5780
Total wt loss (g)	0.0043
Total wt loss (mg)	4.3

Cleaning Cycle	Wt (g)
0	19.6029
1	19.5776
2	19.5772
3	19.5766
4	19.5762
5	19.5759

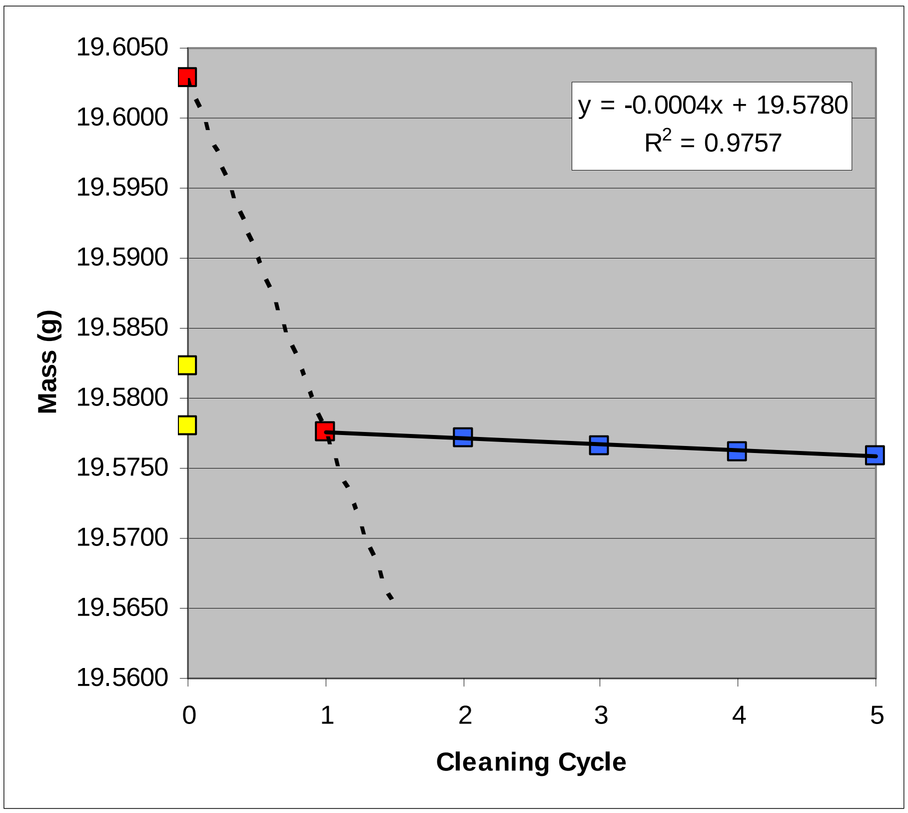

Coupon:	423
Test matrix:	Fe-Go-3500-6-2f
Initial wt (g)	19.1900
Removal wt (g)	19.2031

Calculated final wt (g)	19.1833
Total wt loss (g)	0.0067
Total wt loss (mg)	6.7

Cleaning Cycle	Wt (g)
0	19.2031
1	19.1831
2	19.1826
3	19.1822
4	19.1818
5	19.1815

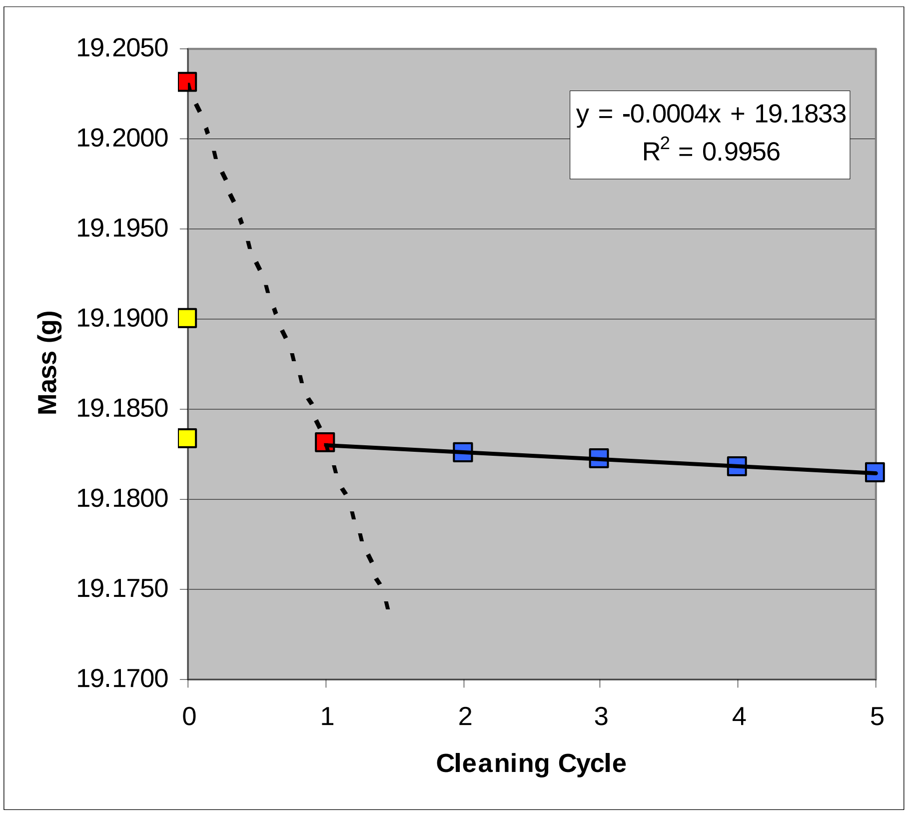

Coupon:	424
Test matrix:	Fe-Go-3500-6-3f
Initial wt (g)	19.1962
Removal wt (g)	19.2295

Calculated final wt (g)	19.1893
Total wt loss (g)	0.0069
Total wt loss (mg)	6.9

Cleaning Cycle	Wt (g)
0	19.2295
1	19.1890
2	19.1885
3	19.1885
4	19.1881
5	19.1875

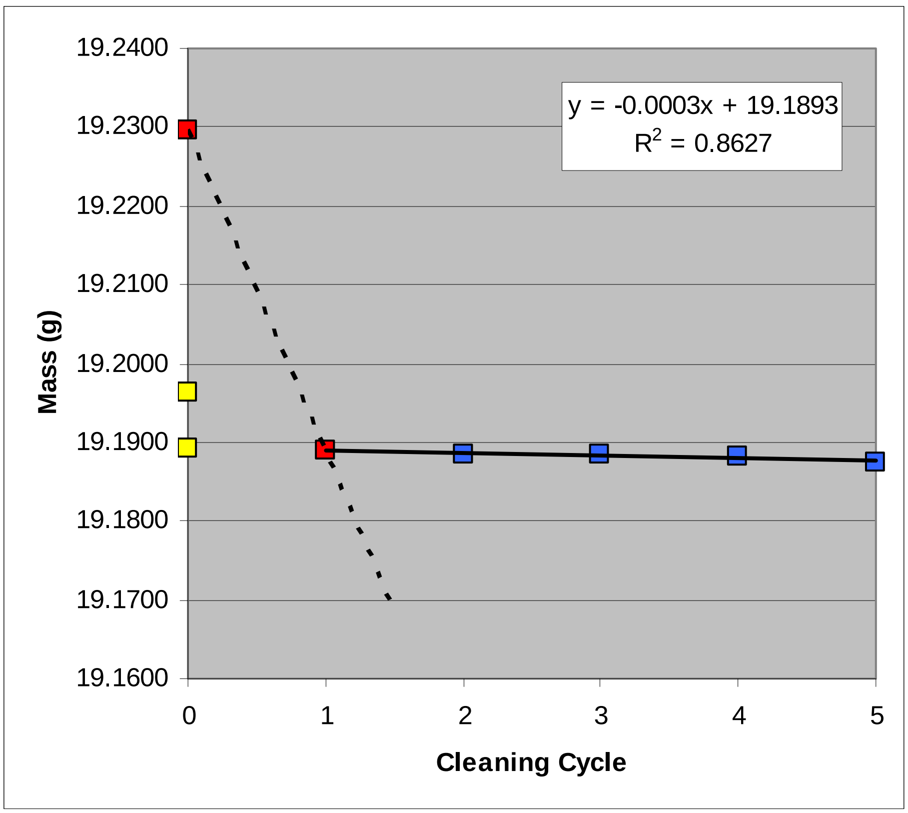

Coupon:	425
Test matrix:	Fe-Go-3500-6-1p
Initial wt (g)	19.2495
Removal wt (g)	19.2546

Calculated final wt (g)	19.2444
Total wt loss (g)	0.0051
Total wt loss (mg)	5.1

Cleaning Cycle	Wt (g)
0	19.2546
1	19.2437
2	19.2434
3	19.2428
4	19.2420
5	19.2419

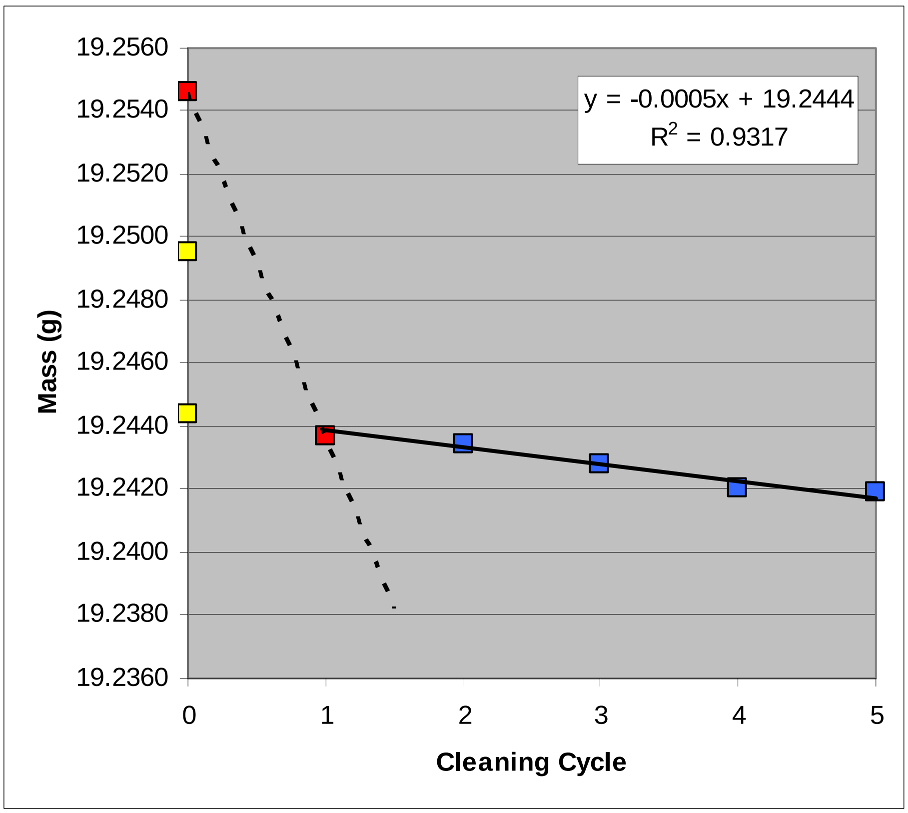

Coupon:	426
Test matrix:	Fe-Go-3500-6-2p
Initial wt (g)	20.7596
Removal wt (g)	20.7741

Calculated final wt (g)	20.7557
Total wt loss (g)	0.0039
Total wt loss (mg)	3.9

Cleaning Cycle	Wt (g)
0	20.7741
1	20.7556
2	20.7547
3	20.7547
4	20.7544
5	20.7535

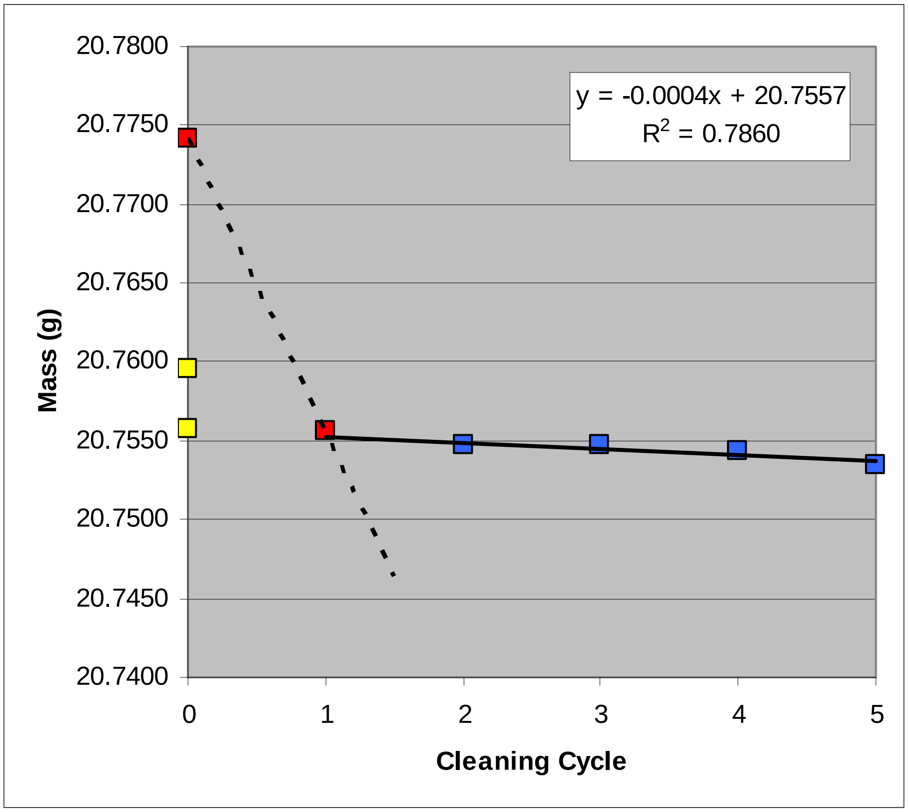

Coupon:	430
Test matrix:	Fe-E-3500-6-2f
Initial wt (g)	19.5257
Removal wt (g)	19.6166

Calculated final wt (g)	19.5020
Total wt loss (g)	0.0237
Total wt loss (mg)	23.7

Cleaning Cycle	Wt (g)
0	19.6166
1	19.5016
2	19.5010
3	19.5008
4	19.5002
5	19.4997

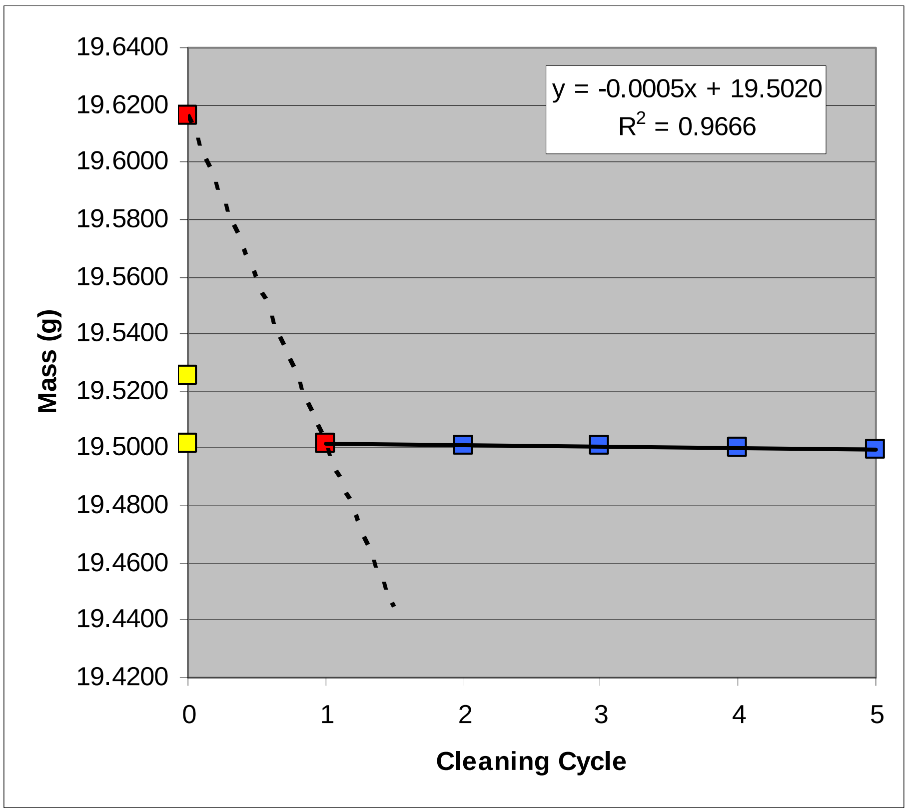

Coupon:	431
Test matrix:	Fe-E-3500-6-3f
Initial wt (g)	21.0621
Removal wt (g)	21.1583

Calculated final wt (g)	21.0447
Total wt loss (g)	0.0174
Total wt loss (mg)	17.4

Cleaning Cycle	Wt (g)
0	21.1583
1	21.0449
2	21.0441
3	21.0439
4	21.0436
5	21.0433

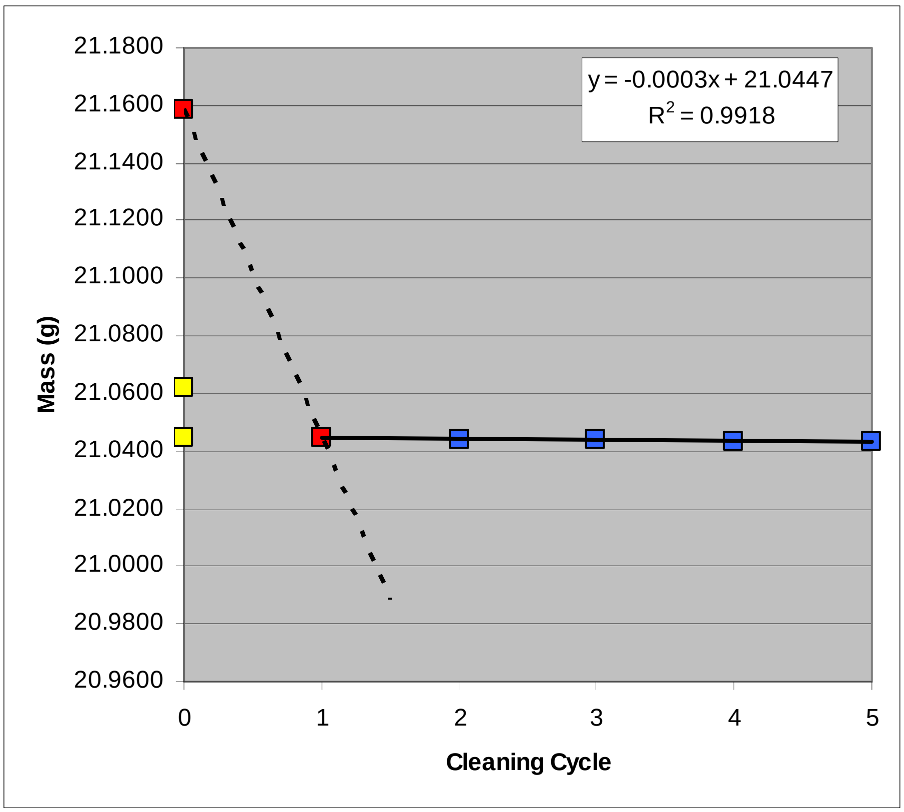

Coupon:	433
Test matrix:	Fe-E-3500-6-2p
Initial wt (g)	20.5718
Removal wt (g)	20.6553

Calculated final wt (g)	20.5580
Total wt loss (g)	0.0138
Total wt loss (mg)	13.8

Cleaning Cycle	Wt (g)
0	20.6553
1	20.5584
2	20.5573
3	20.5566
4	20.5563
5	20.5560

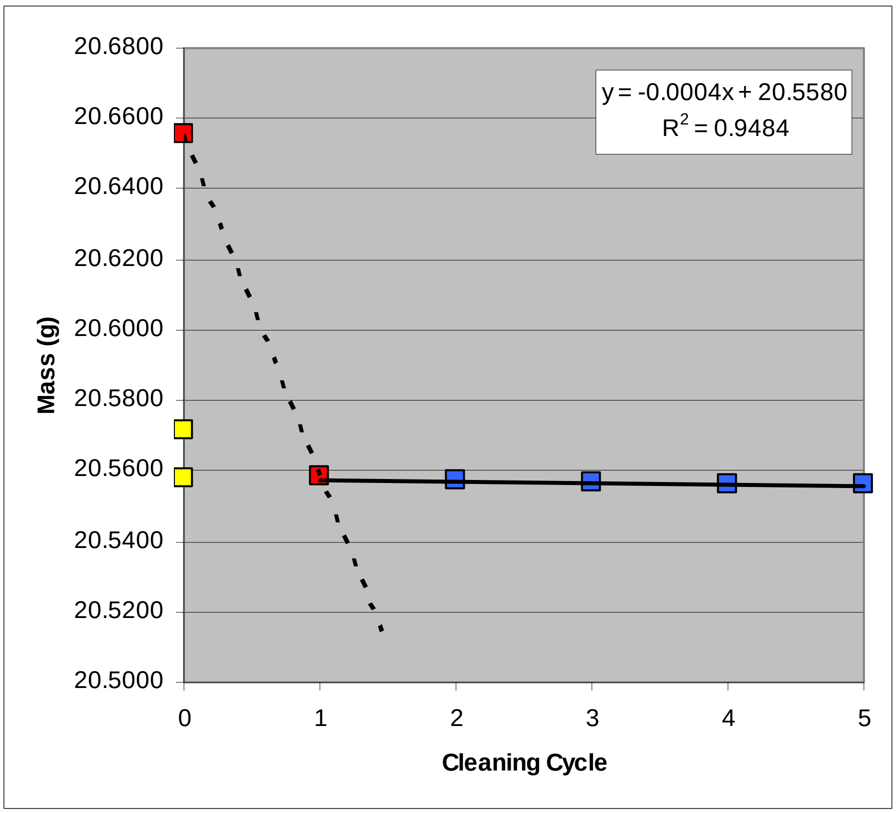

Coupon:	434
Test matrix:	Fe-E-3500-6-3p
Initial wt (g)	20.3482
Removal wt (g)	20.4364

Calculated final wt (g)	20.3325
Total wt loss (g)	0.0157
Total wt loss (mg)	15.7

Cleaning Cycle	Wt (g)
0	20.4364
1	20.3331
2	20.3319
3	20.3314
4	20.3311
5	20.3309

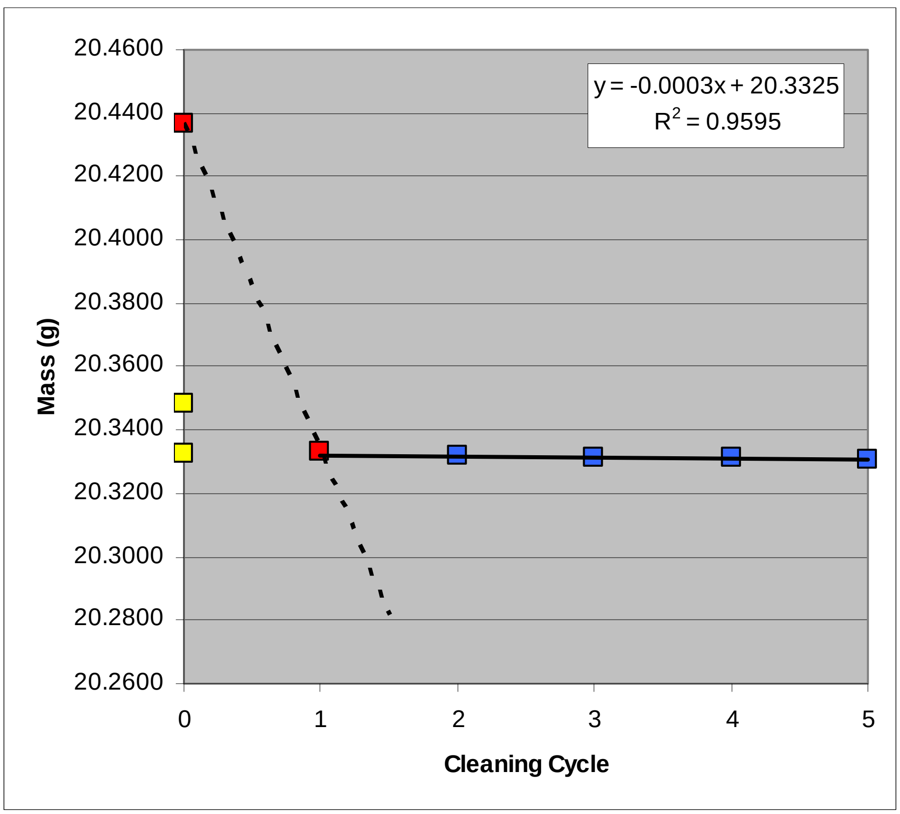

Coupon: 435
Test matrix: Fe-Eo-3500-6-1f
Initial wt (g) 20.2338
Removal wt (g) 20.3110

Calculated final wt (g) 20.2212
Total wt loss (g) 0.0126
Total wt loss (mg) 12.6

Cleaning Cycle	Wt (g)
0	20.3110
1	20.2206
2	20.2205
3	20.2200
4	20.2197
5	20.2194

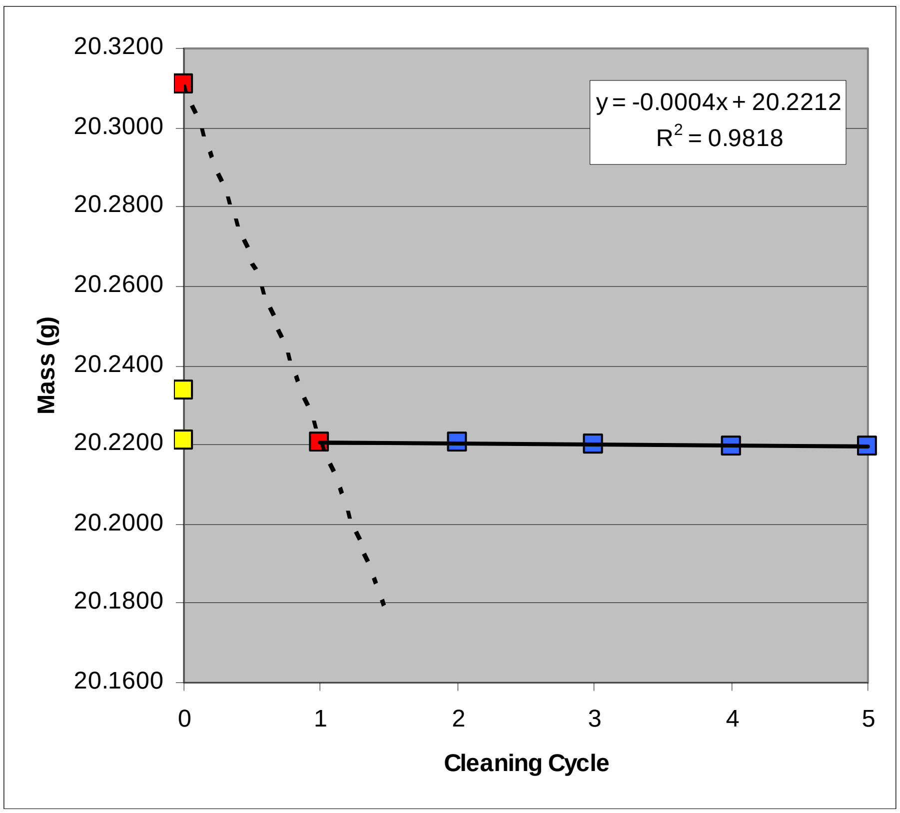

Coupon:	436
Test matrix:	Fe-Eo-3500-6-2f
Initial wt (g)	20.5356
Removal wt (g)	20.5899

Calculated final wt (g)	20.5236
Total wt loss (g)	0.0120
Total wt loss (mg)	12.0

Cleaning Cycle	Wt (g)
0	20.5899
1	20.5239
2	20.5231
3	20.5226
4	20.5224
5	20.5222

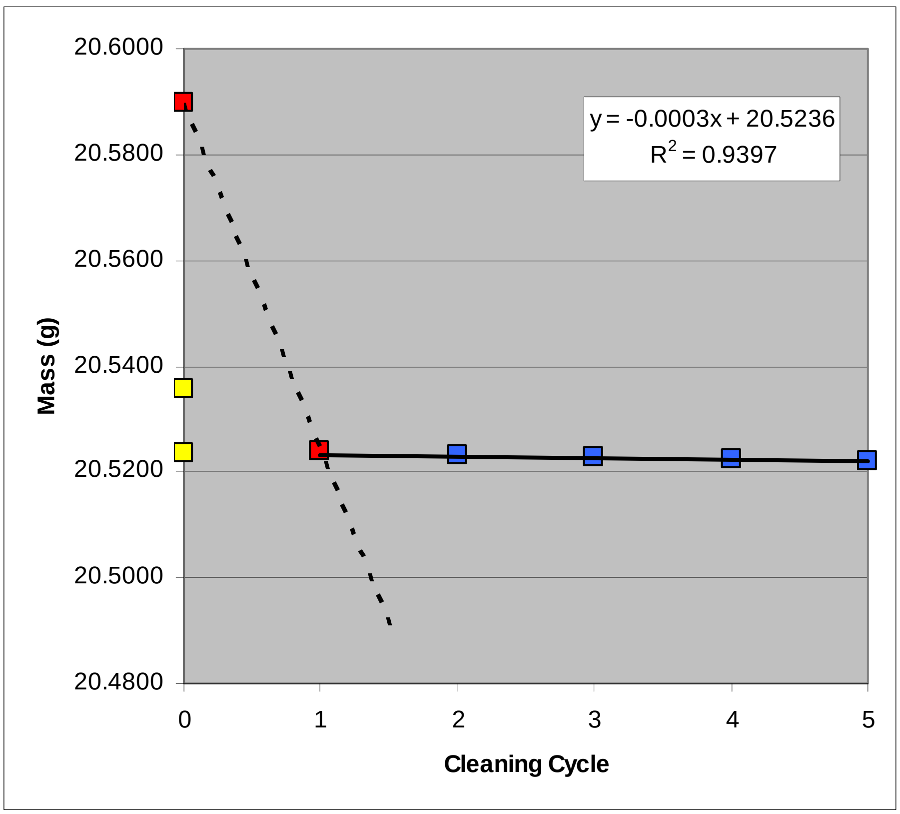

Coupon:	438
Test matrix:	Fe-Eo-3500-6-1p
Initial wt (g)	20.2190
Removal wt (g)	20.4318

Calculated final wt (g)	20.2122
Total wt loss (g)	0.0068
Total wt loss (mg)	6.8

Cleaning Cycle	Wt (g)
0	20.4318
1	20.2121
2	20.2114
3	20.2110
4	20.2108
5	20.2102

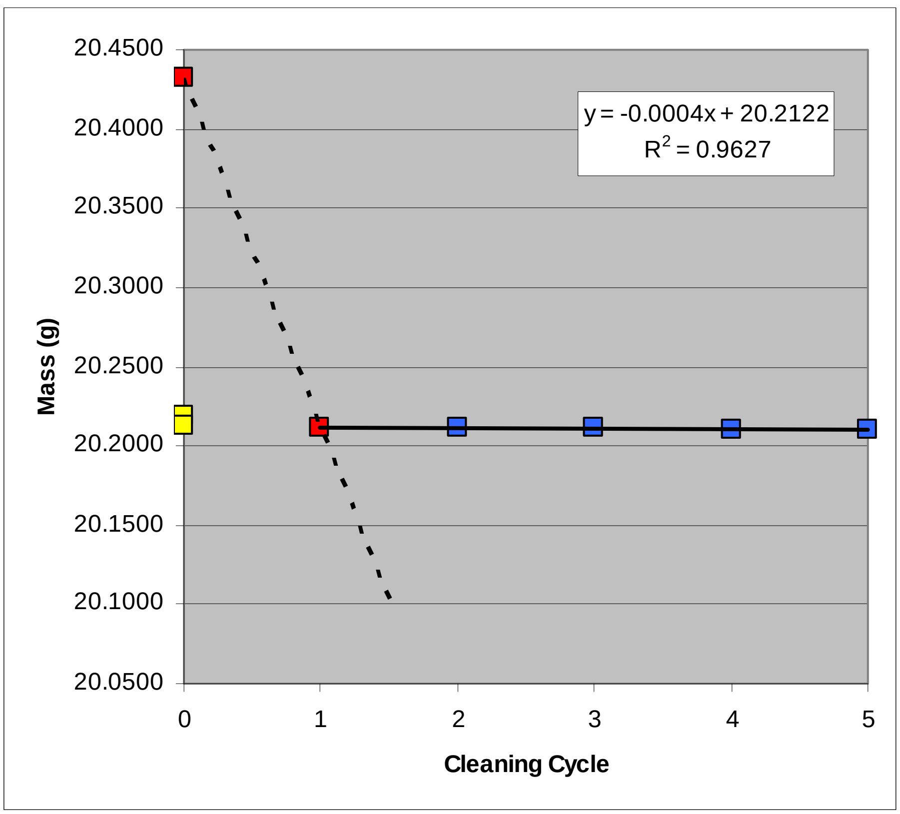

Coupon:	439
Test matrix:	Fe-Eo-3500-6-2p
Initial wt (g)	20.1788
Removal wt (g)	20.2861

Calculated final wt (g)	20.1707
Total wt loss (g)	0.0081
Total wt loss (mg)	8.1

Cleaning Cycle	Wt (g)
0	20.2861
1	20.1706
2	20.1700
3	20.1692
4	20.1687
5	20.1687

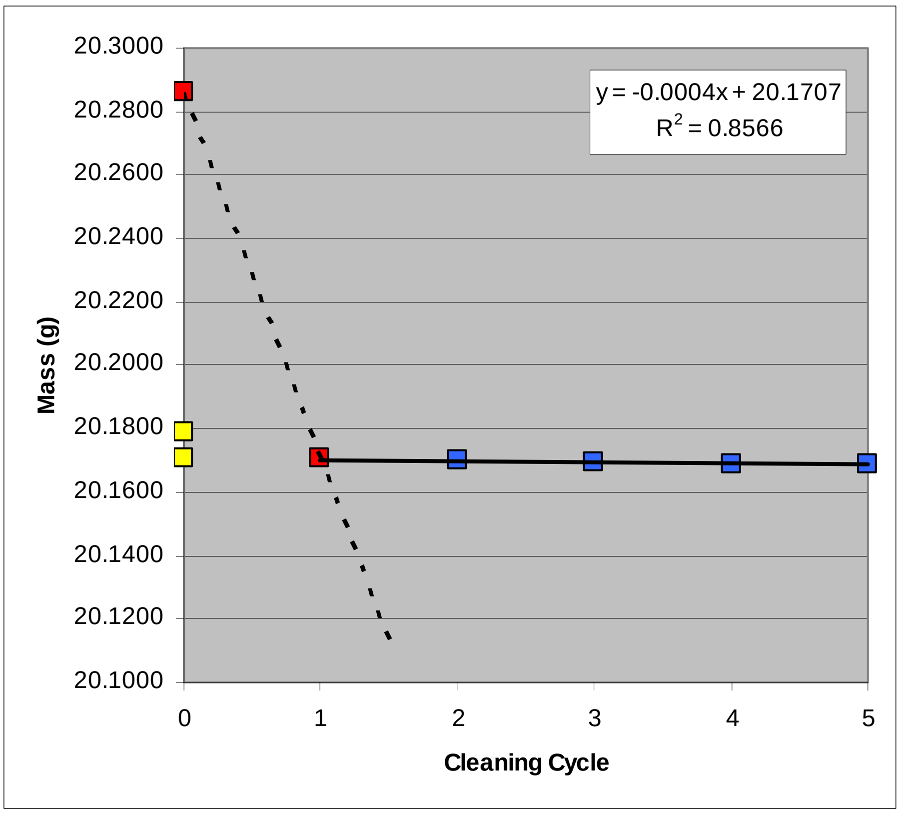

Coupon:	441
Test matrix:	Fe-Atm-3500-6-1
Initial wt (g)	20.0863
Removal wt (g)	20.0866

Calculated final wt (g)	20.0860
Total wt loss (g)	0.0003
Total wt loss (mg)	0.3

Cleaning Cycle	Wt (g)
0	20.0866
1	20.0859
2	20.0854
3	20.0848
4	20.0848
5	20.0843

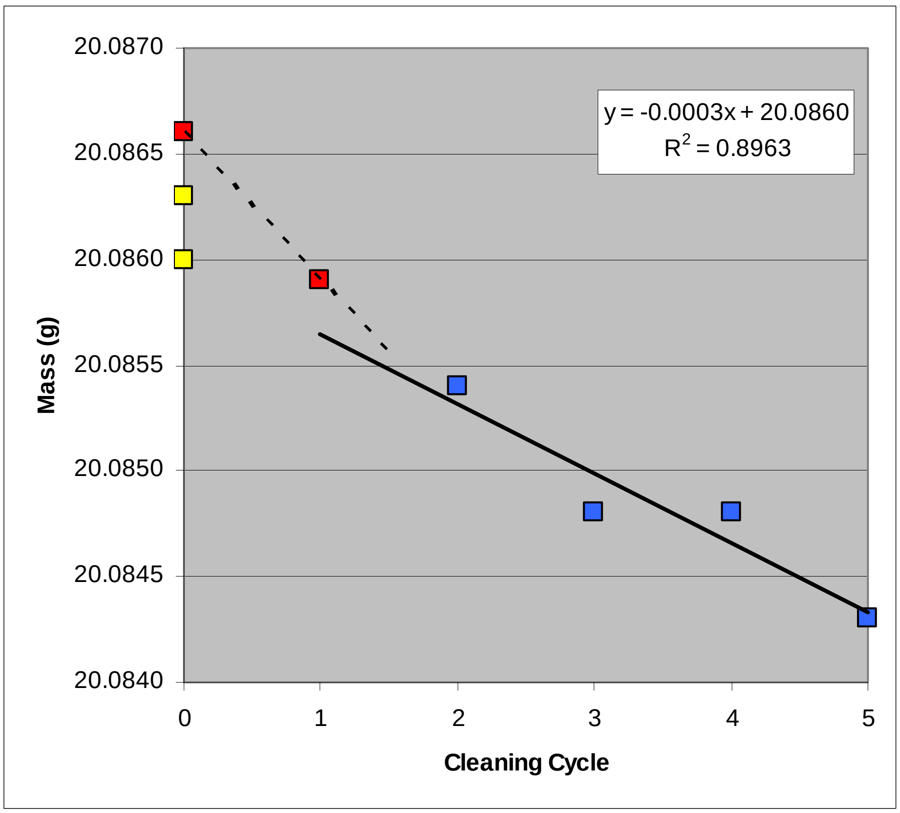

Coupon:	442		
Test matrix:	Fe-Atm-3500-6-2		
Initial wt (g)	20.0771	**Calculated final wt (g)**	20.0776
Removal wt (g)	20.0779	**Total wt loss (g)**	-0.0005
		Total wt loss (mg)	-0.5

Cleaning Cycle	**Wt (g)**
0	20.0779
1	20.0769
2	20.0766
3	20.0759
4	20.0755
5	20.0750

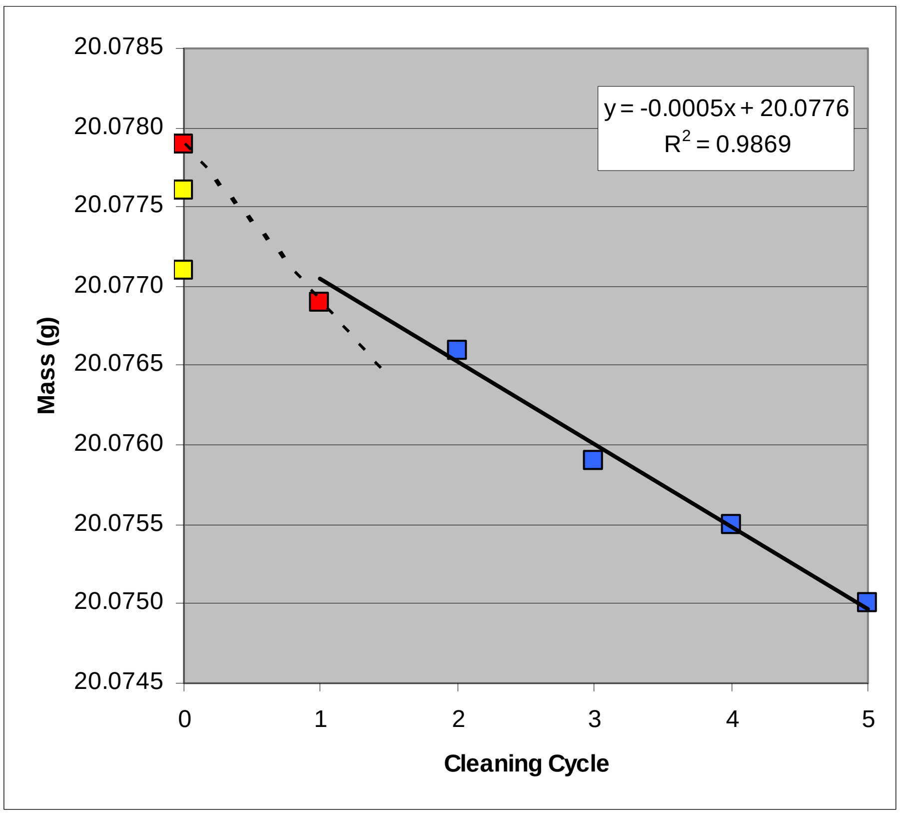

APPENDIX D

This appendix contains all of the weight loss cleaning cycle data, as well as the results of the graphical analysis of that data for each of the lead coupons (see individual data sheets for each coupon in WIPP-FePb-3 Supplemental Binder C). Each of the following pages lists the initial coupon weight, removal weight, cleaning cycle weights, calculated final weight and the resulting weight loss. The environmental conditions for each coupon can be read from the test matrix label that is given for each coupon. The meaning of the test matrix labels is discussed in Section 2.4.

For each coupon the graphical analysis is shown (see Section 4.4 for details of the process). The blue symbols indicate those parts of the cleaning cycle data used to determine the calculated final weight, which is the y-intercept of the line fit to the blue symbols. The red symbols show the cleaning cycle data not used in the linear regression. Yellow symbols indicate the initial coupon weight (prior to the experiment) and the final calculated weight. Note that in some samples the final weight is taken either as the 0^{th} cleaning cycle or the 1^{st} cleaning cycle value. This is a judgment call made by the investigator based on the appearance of the weight loss plots.

Coupon:	L083		
Test Matrix:	Pb-G-0000-6-2f		
Initial wt (g)	34.9565	**Calculated final wt (g)**	34.9425
Removal wt (g)	34.9466	**Total wt loss (g)**	0.0140
		Total wt loss (mg)	14.0

Cleaning Cycle	Wt (g)
0	34.9466
1	34.9389
2	34.9341
3	34.9299
4	34.9258
5	34.9215

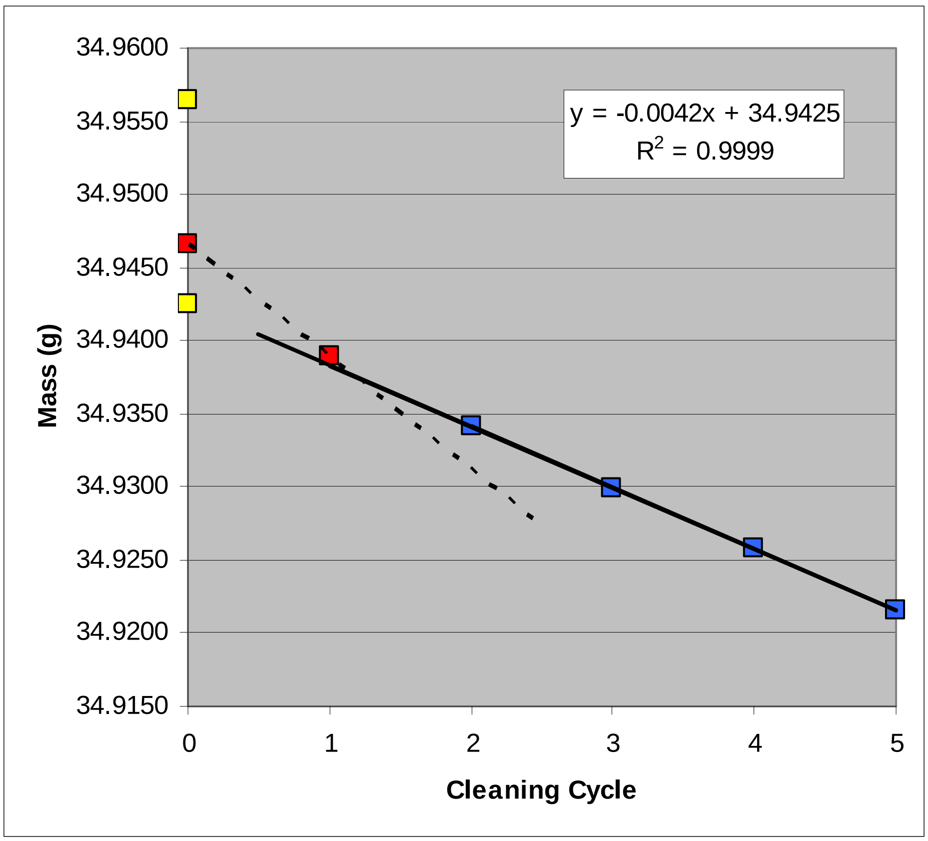

Coupon:	L084
Test Matrix:	Pb-G-0000-6-3f
Initial wt (g)	35.0169
Removal wt (g)	35.0075

Calculated final wt (g)	35.0048
Total wt loss (g)	0.0107
Total wt loss (mg)	10.7

Cleaning Cycle	Wt (g)
0	35.0075
1	34.9996
2	34.9972
3	34.9908
4	34.9863
5	34.9825

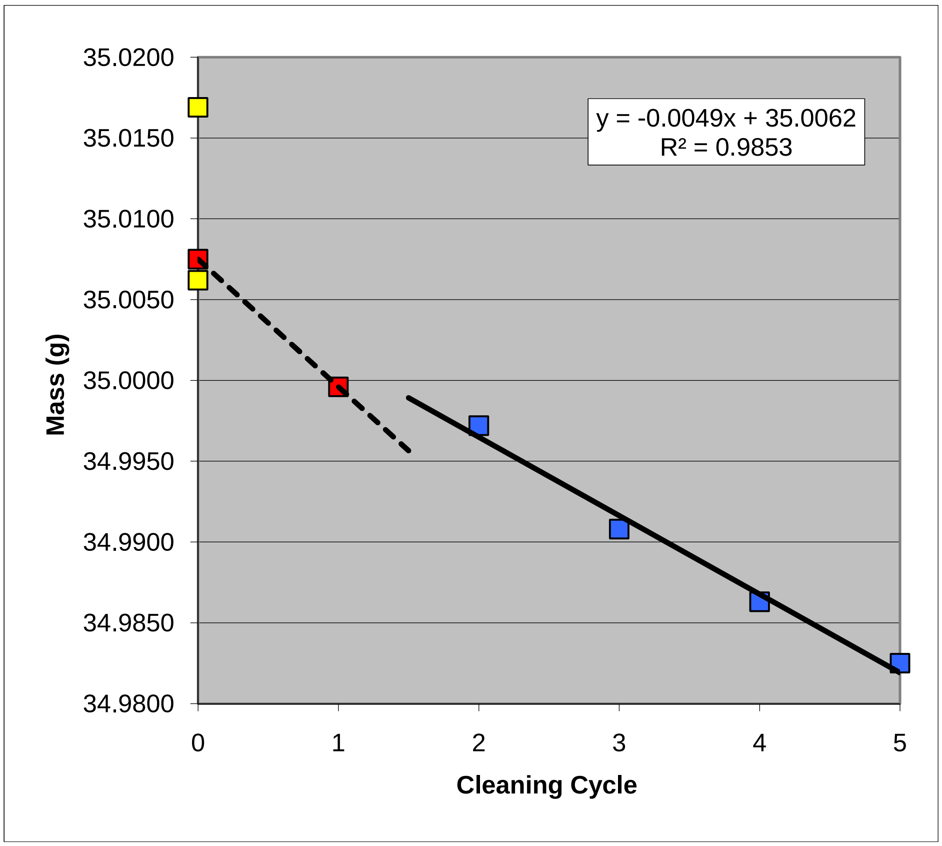

Coupon:	L086
Test Matrix:	Pb-G-0000-6-2p
Initial wt (g)	34.9627
Removal wt (g)	34.9577

Calculated final wt (g)	34.9504
Total wt loss (g)	0.0123
Total wt loss (mg)	12.3

Cleaning Cycle	Wt (g)
0	34.9577
1	34.9456
2	34.9408
3	34.9352
4	34.9300
5	34.9260

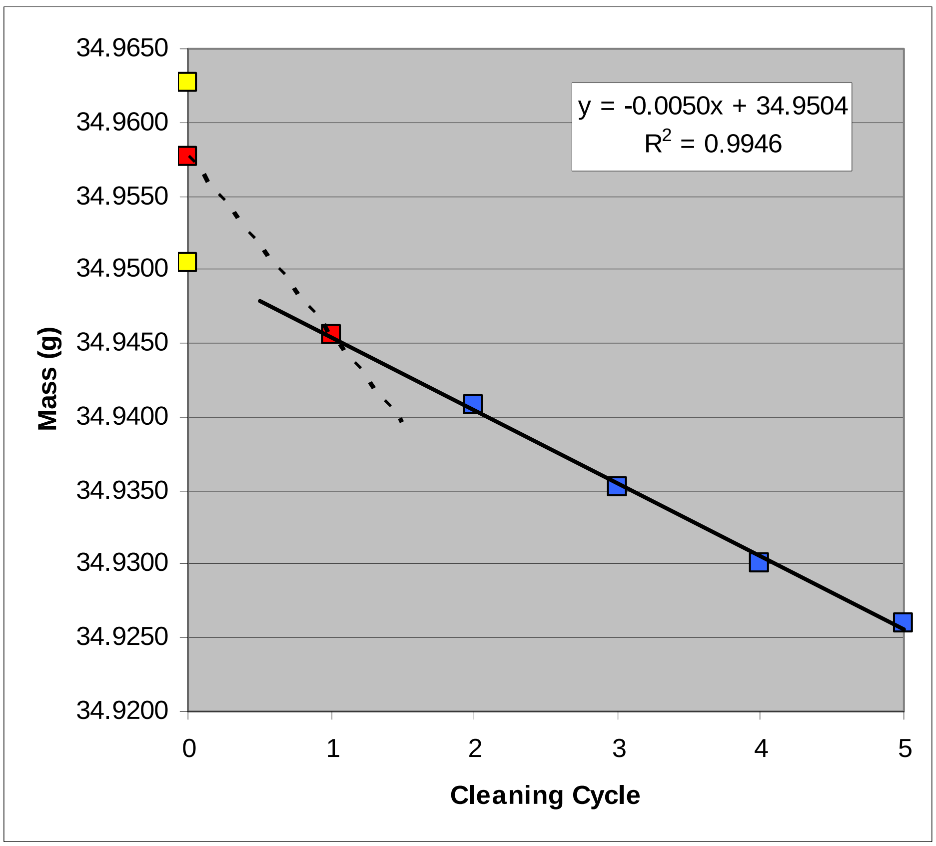

Coupon:	L087
Test Matrix:	Pb-G-0000-6-3p
Initial wt (g)	34.7895
Removal wt (g)	34.7851

Calculated final wt (g)	34.7807
Total wt loss (g)	0.0088
Total wt loss (mg)	8.8

Cleaning Cycle	Wt (g)
0	34.7851
1	34.7744
2	34.7703
3	34.7641
4	34.7590
5	34.7541

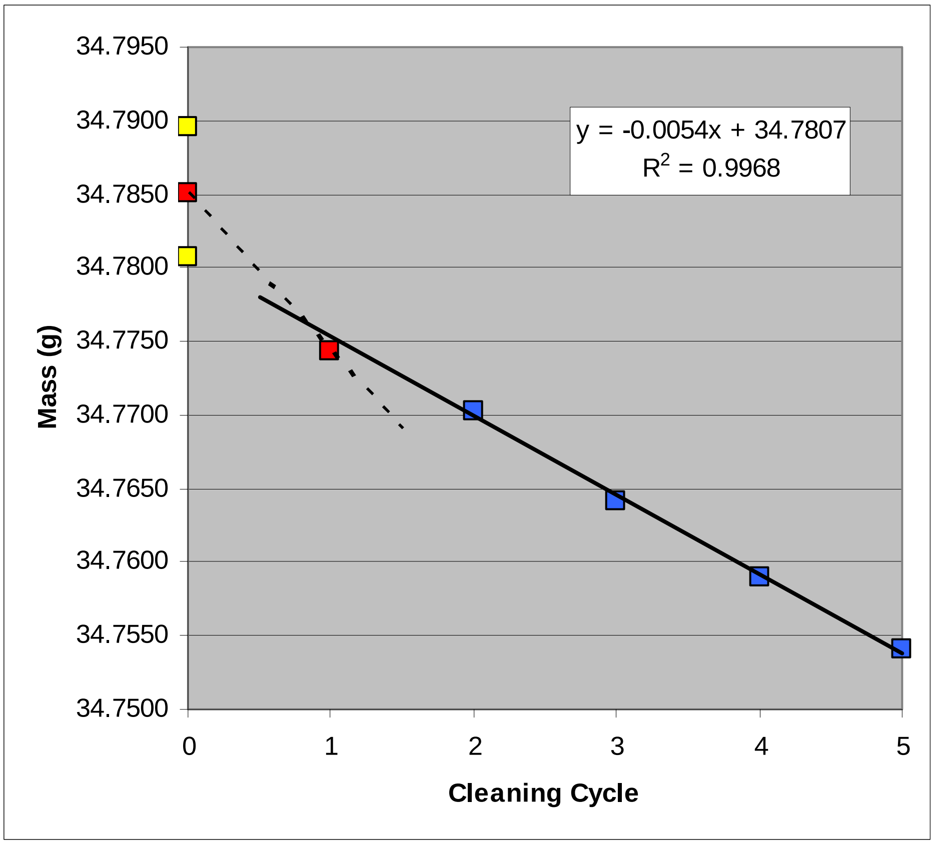

Coupon:	L089			
Test Matrix:	Pb-Go-0000-6-2f			
Initial wt (g)	35.9965		**Calculated final wt (g)**	35.9886
Removal wt (g)	35.9924		**Total wt loss (g)**	0.0079
			Total wt loss (mg)	7.9

Cleaning Cycle	Wt (g)
0	35.9924
1	35.9862
2	35.9822
3	35.9787
4	35.9755
5	35.9724

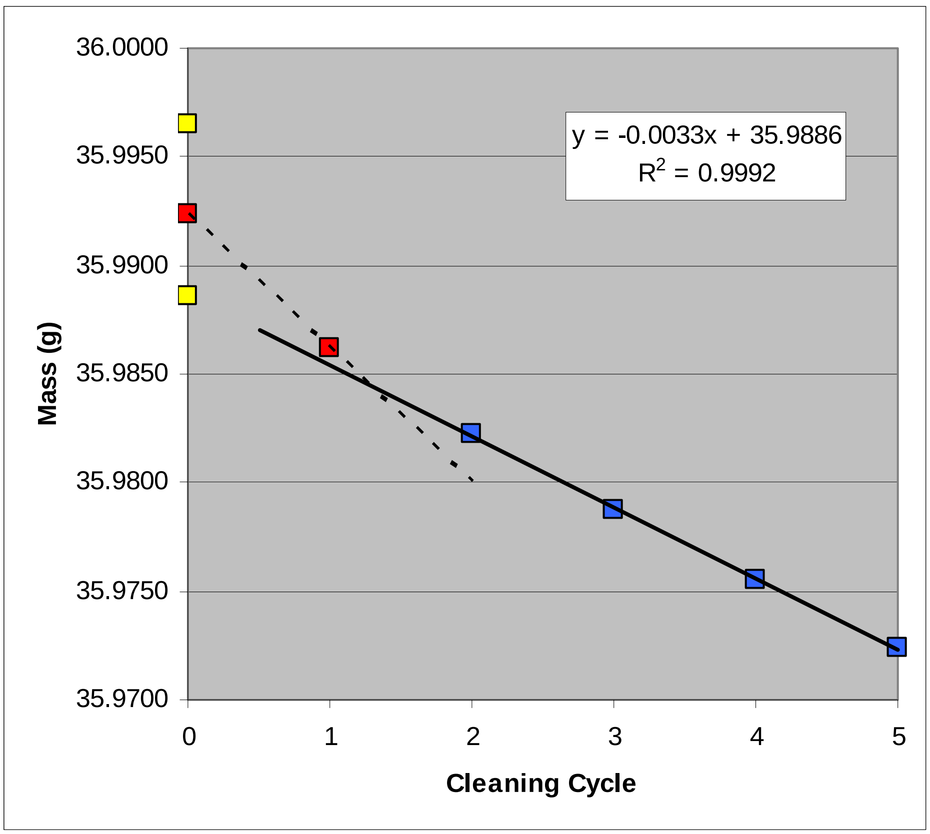

Coupon:	L090
Test Matrix:	Pb-Go-0000-6-3f
Initial wt (g)	35.2017
Removal wt (g)	35.1966

Calculated final wt (g)	35.1957
Total wt loss (g)	0.006
Total wt loss (mg)	6.0

Cleaning Cycle	Wt (g)
0	35.1966
1	35.1920
2	35.1886
3	35.1846
4	35.1812
5	35.1777

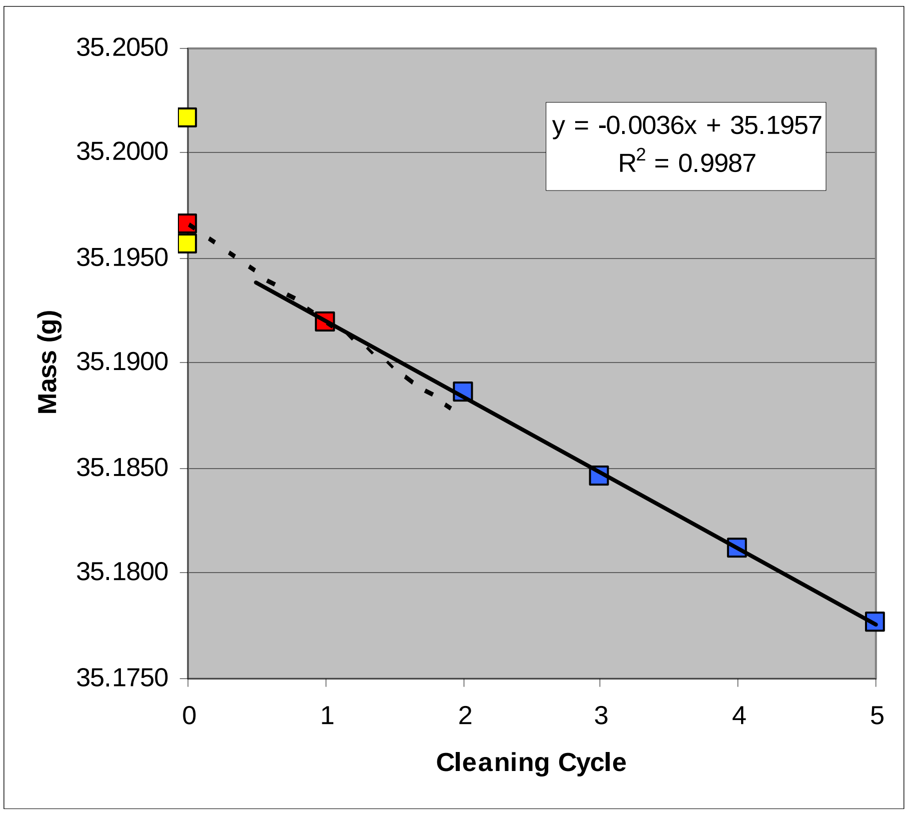

Coupon:	L091
Test Matrix:	Pb-Go-0000-6-1p
Initial wt (g)	35.4321
Removal wt (g)	35.4290

Calculated final wt (g)	35.4251
Total wt loss (g)	0.0070
Total wt loss (mg)	7.0

Cleaning Cycle	Wt (g)
0	35.4290
1	35.4220
2	35.4174
3	35.4134
4	35.4090
5	35.4058

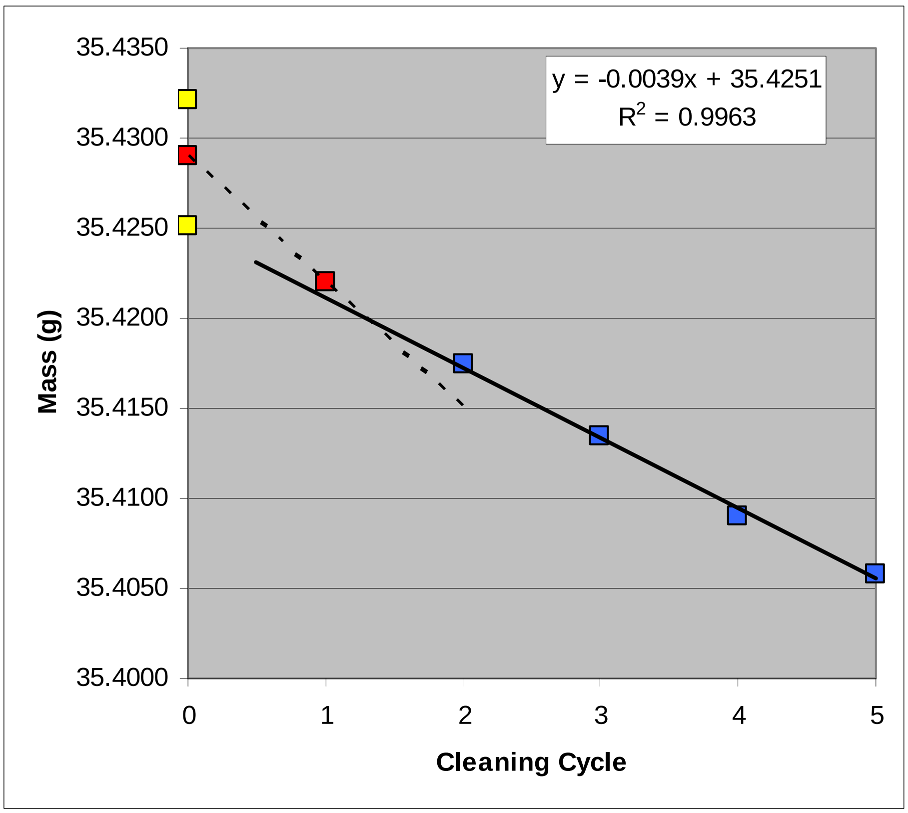

Coupon:	L093
Test Matrix:	Pb-Go-0000-6-3p
Initial wt (g)	35.5347
Removal wt (g)	35.5312

Calculated final wt (g)	35.5272
Total wt loss (g)	0.0075
Total wt loss (mg)	7.5

Cleaning Cycle	Wt (g)
0	35.5312
1	35.5254
2	35.5208
3	35.5170
4	35.5135
5	35.5108

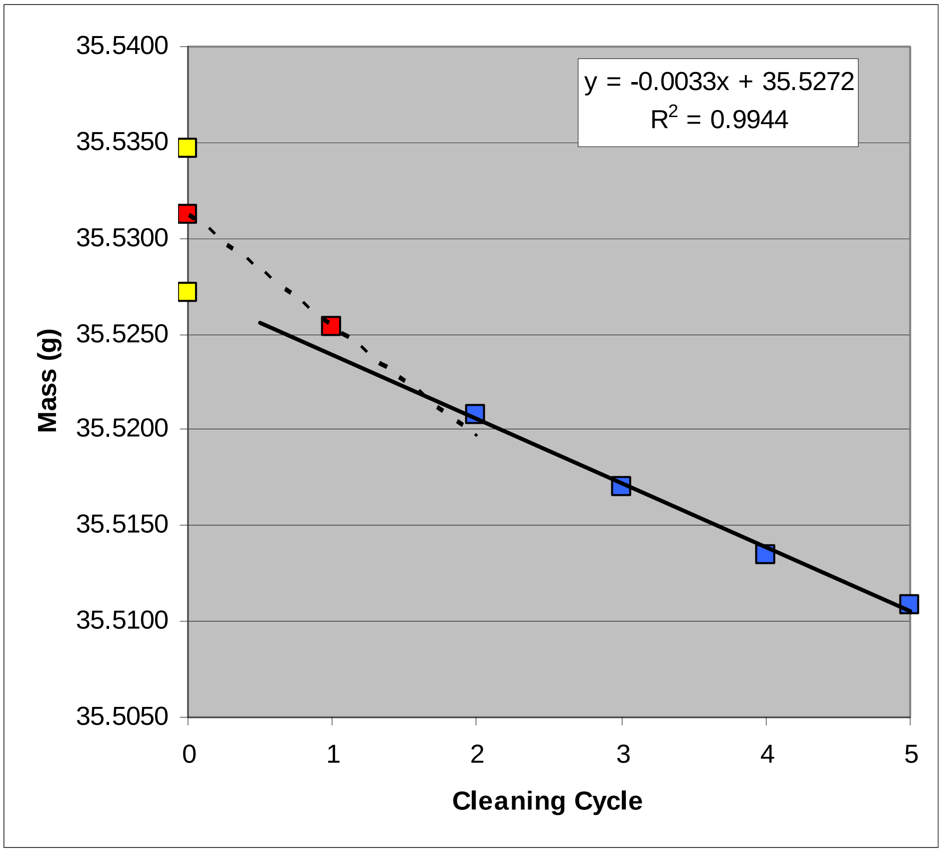

Coupon:	L094
Test Matrix:	Pb-E-0000-6-1f
Initial wt (g)	35.4331
Removal wt (g)	35.4372

Calculated final wt (g)	35.4250
Total wt loss (g)	0.0081
Total wt loss (mg)	8.1

Cleaning Cycle	Wt (g)
0	35.4372
1	35.4214
2	35.4159
3	35.4111
4	35.4068
5	35.4021

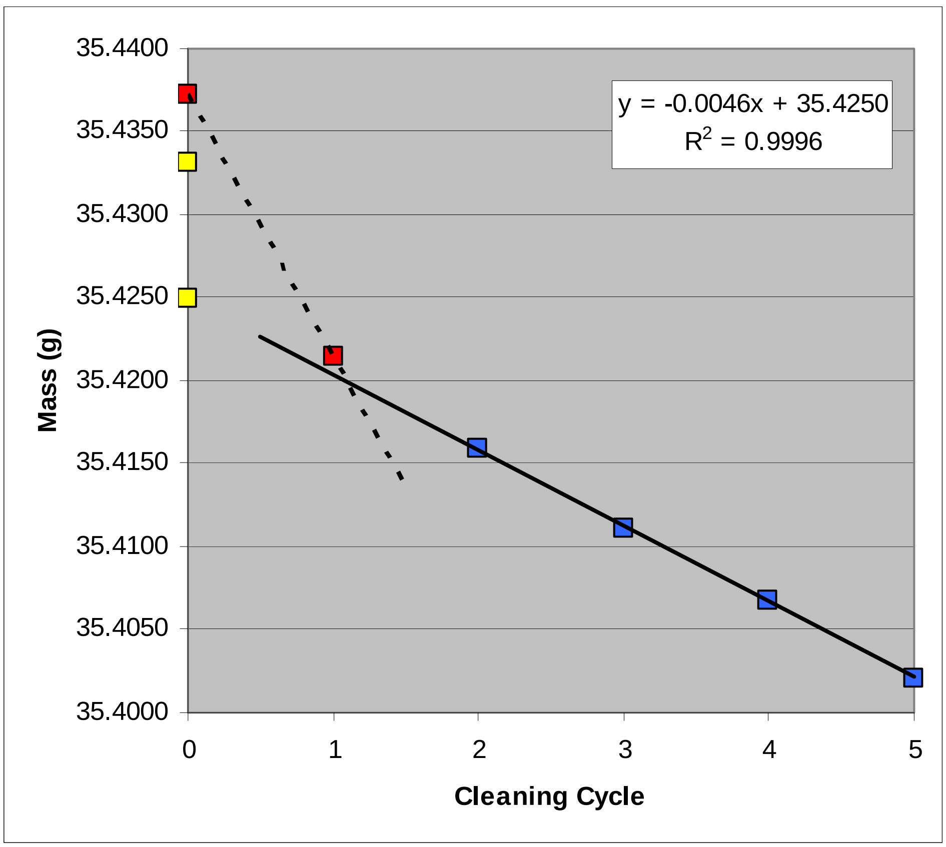

Coupon:	L095
Test Matrix:	Pb-E-0000-6-2f
Initial wt (g)	36.0654
Removal wt (g)	36.0644

Calculated final wt (g)	36.0600
Total wt loss (g)	0.0054
Total wt loss (mg)	5.4

Cleaning Cycle	Wt (g)
0	36.0644
1	36.0555
2	36.0507
3	36.0460
4	36.0411
5	36.0367

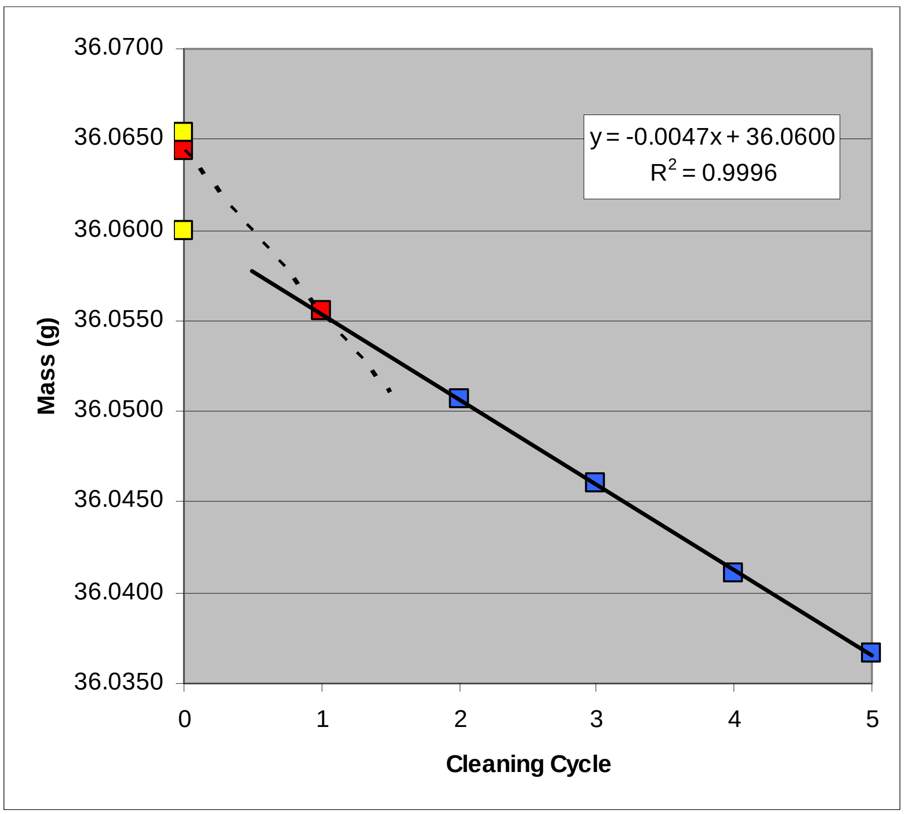

Coupon:	L097
Test Matrix:	Pb-E-0000-6-1p
Initial wt (g)	35.8988
Removal wt (g)	35.9021

Calculated final wt (g)	35.8895
Total wt loss (g)	0.0093
Total wt loss (mg)	9.3

Cleaning Cycle	**Wt (g)**
0	35.9021
1	35.8856
2	35.8813
3	35.8780
4	35.8734
5	35.8696

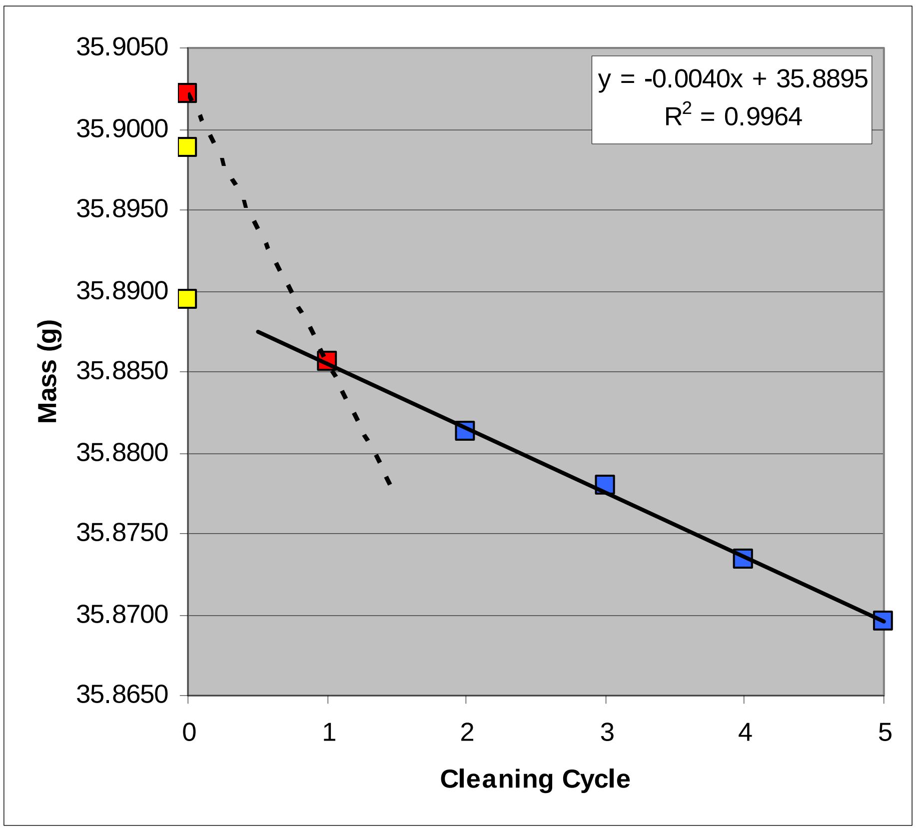

Coupon:	L098
Test Matrix:	Pb-E-0000-6-2p
Initial wt (g)	34.4660
Removal wt (g)	34.4612

Calculated final wt (g)	34.4546
Total wt loss (g)	0.0114
Total wt loss (mg)	11.4

Cleaning Cycle	Wt (g)
0	34.4612
1	34.4505
2	34.4448
3	34.4396
4	34.4345
5	34.4299

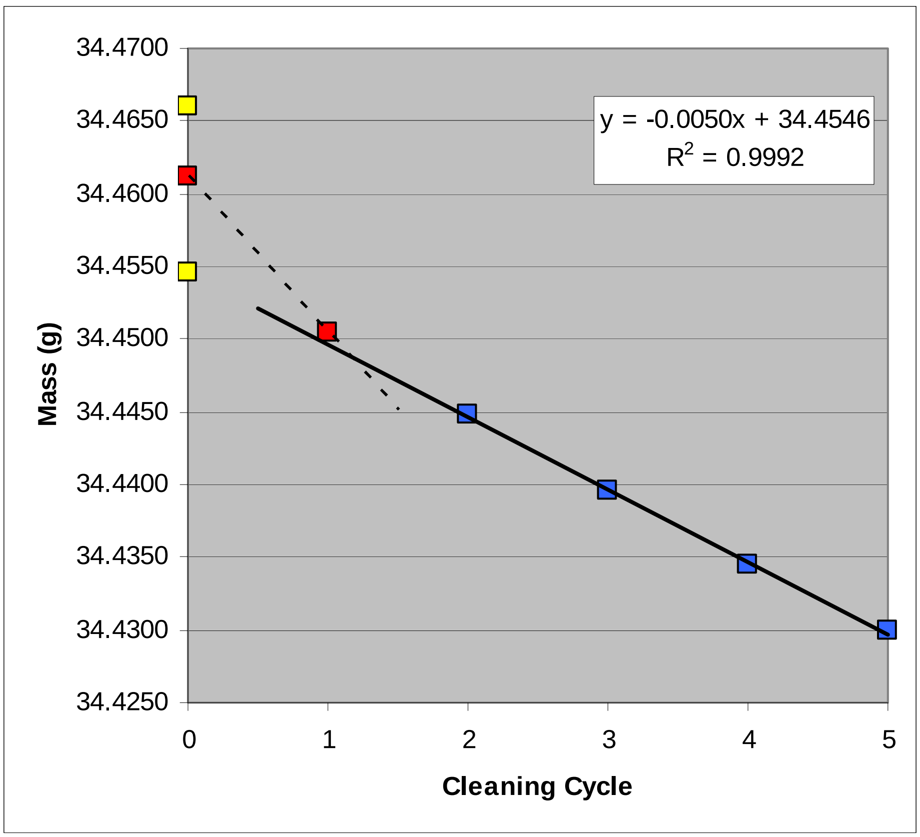

Coupon:	L100
Test Matrix:	Pb-Eo-0000-6-1f
Initial wt (g)	35.4418
Removal wt (g)	35.4415

Calculated final wt (g)	35.4369
Total wt loss (g)	0.0049
Total wt loss (mg)	4.9

Cleaning Cycle	Wt (g)
0	35.4415
1	35.4324
2	35.4272
3	35.4225
4	35.4167
5	35.4129

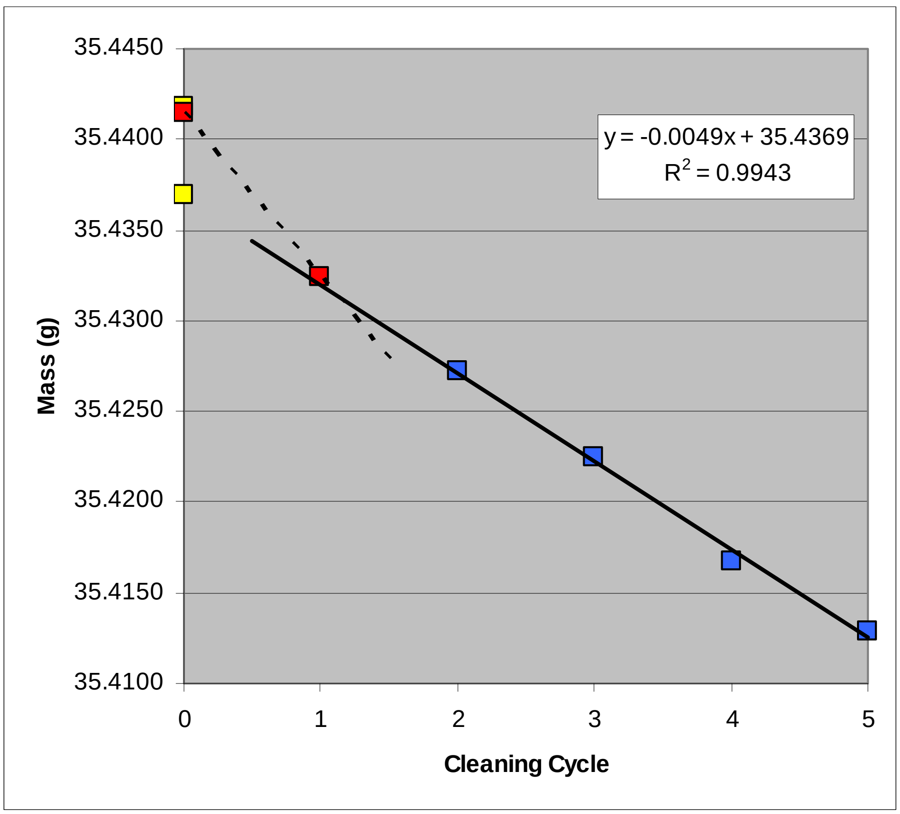

Coupon:	L101
Test Matrix:	Pb-Eo-0000-6-2f
Initial wt (g)	35.3272
Removal wt (g)	35.3431

Calculated final wt (g)	35.3223
Total wt loss (g)	0.0049
Total wt loss (mg)	4.9

Cleaning Cycle	Wt (g)
0	35.3431
1	35.3188
2	35.3136
3	35.3091
4	35.3045
5	35.3005

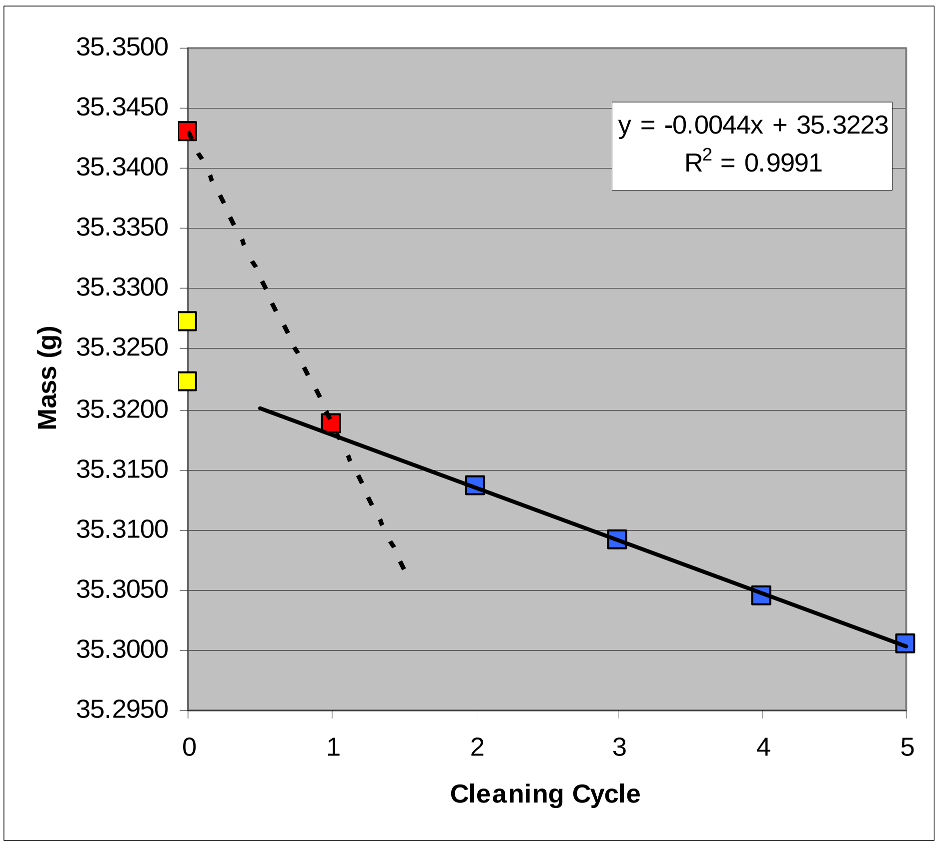

Coupon:	L103
Test Matrix:	Pb-Eo-0000-6-1p
Initial wt (g)	35.6308
Removal wt (g)	35.6329

Calculated final wt (g)	35.6220
Total wt loss (g)	0.0088
Total wt loss (mg)	8.8

Cleaning Cycle	Wt (g)
0	35.6329
1	35.6189
2	35.6137
3	35.6091
4	35.6049
5	35.6010

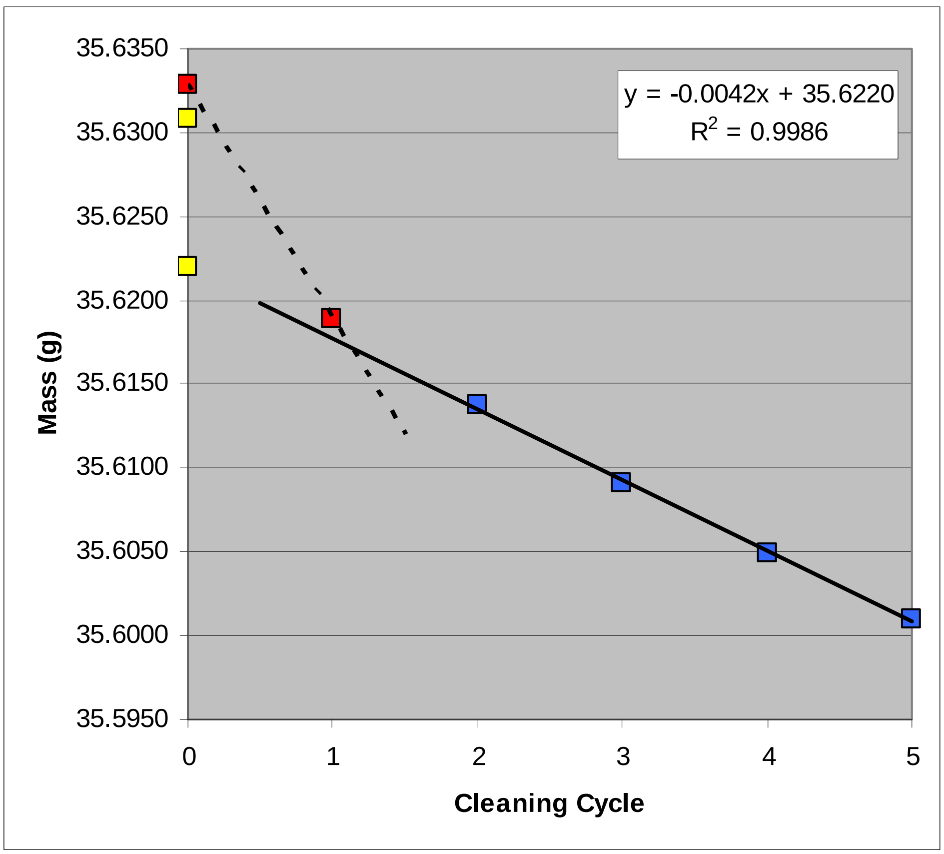

Coupon:	L104
Test Matrix:	Pb-Eo-0000-6-2p
Initial wt (g)	35.1904
Removal wt (g)	35.1900

Calculated final wt (g)	35.1825
Total wt loss (g)	0.0079
Total wt loss (mg)	7.9

Cleaning Cycle	Wt (g)
0	35.1900
1	35.1787
2	35.1748
3	35.1709
4	35.1669
5	35.1632

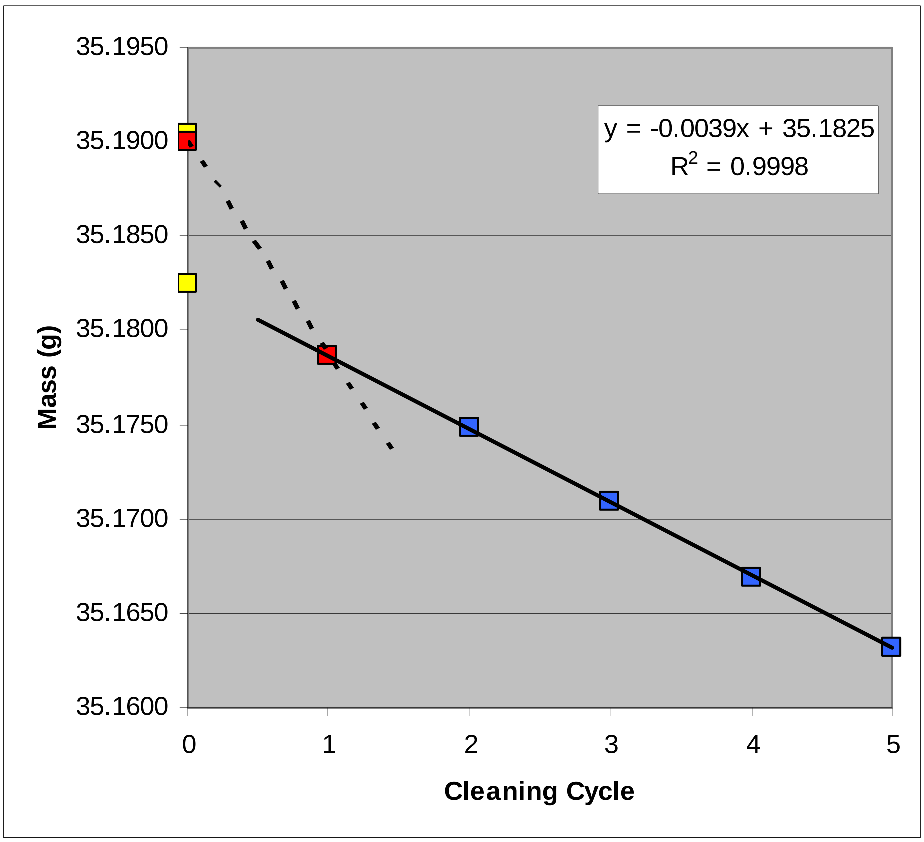

Coupon:	L106
Test Matrix:	Pb-Atm-0000-6-1
Initial wt (g)	35.9058
Removal wt (g)	35.9063

Calculated final wt (g)	35.9051
Total wt loss (g)	0.0007
Total wt loss (mg)	0.7

Cleaning Cycle	Wt (g)
0	35.9063
1	35.9018
2	35.8977
3	35.8943
4	35.8900
5	35.8869

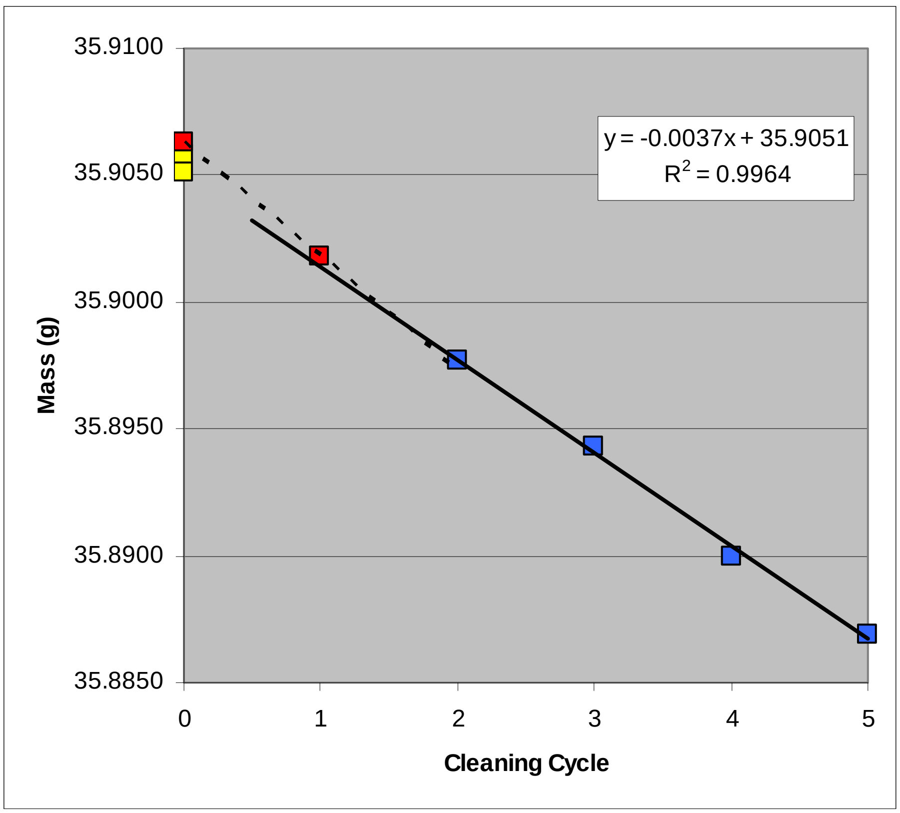

Coupon:	L107
Test Matrix:	Pb-Atm-0000-6-2
Initial wt (g)	35.4546
Removal wt (g)	35.4543

Calculated final wt (g)	35.4517
Total wt loss (g)	0.0029
Total wt loss (mg)	2.9

Cleaning Cycle	Wt (g)
0	35.4543
1	35.4498
2	35.4461
3	35.4421
4	35.4401
5	35.4369

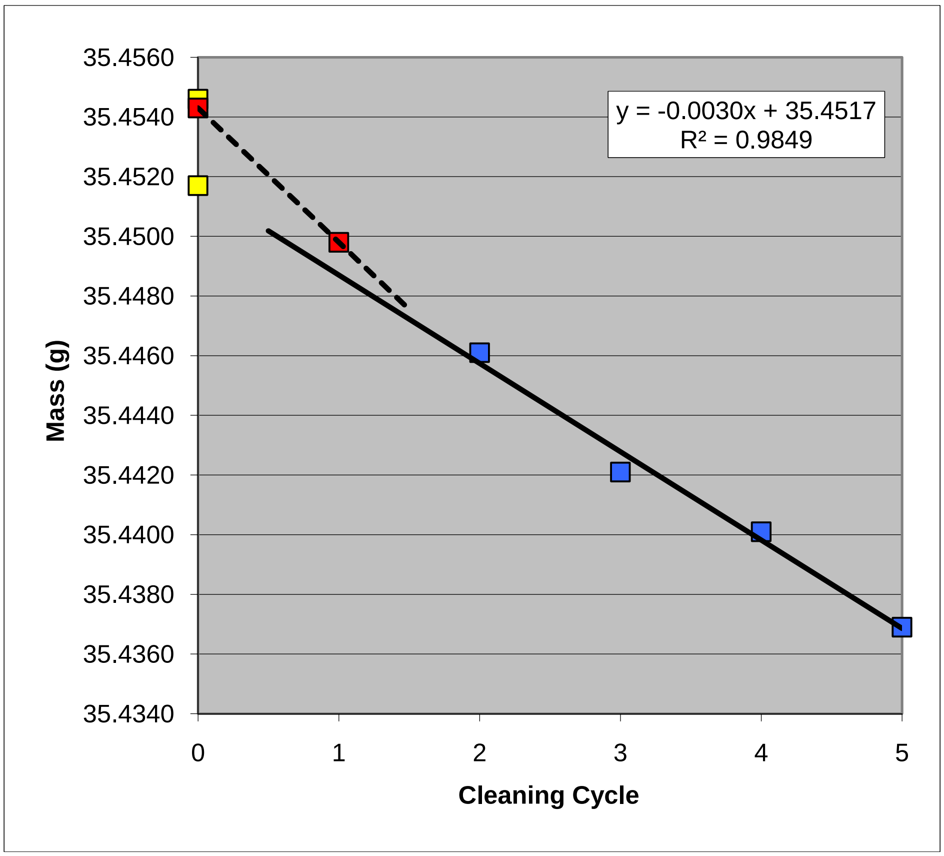

Coupon:	L109
Test Matrix:	Pb-G-0350-6-1f
Initial wt (g)	34.8781
Removal wt (g)	34.8834

Calculated final wt (g)	34.8744
Total wt loss (g)	0.0037
Total wt loss (mg)	3.7

Cleaning Cycle	Wt (g)
0	34.8834
1	34.8682
2	34.8619
3	34.8558
4	34.8501
5	34.8432

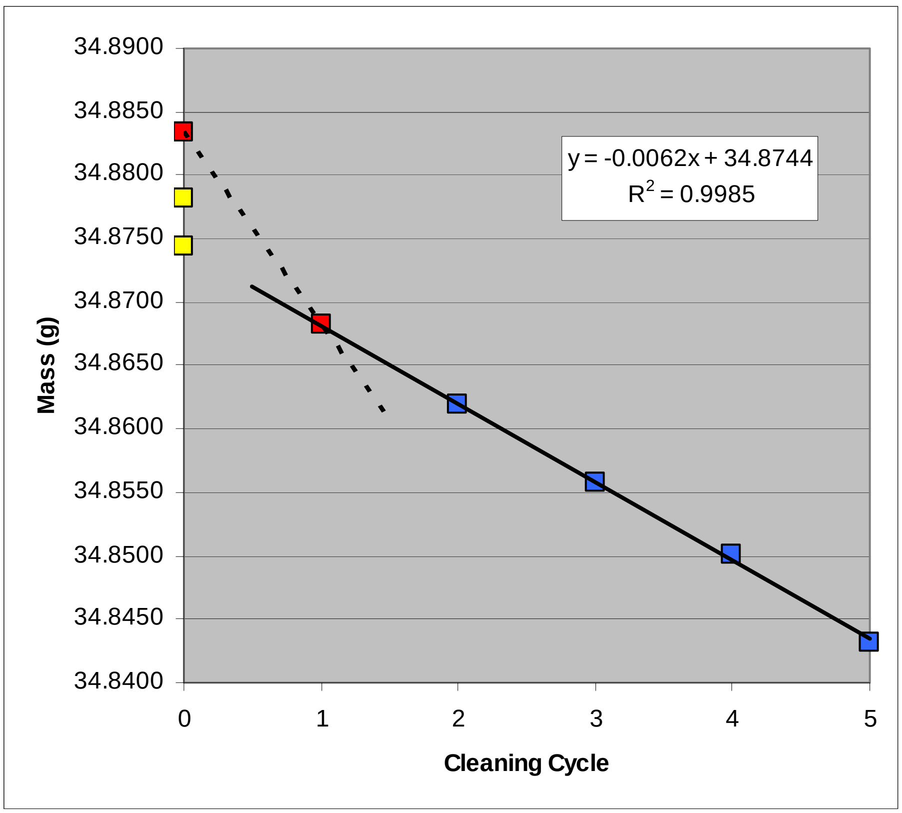

Coupon:	L110
Test Matrix:	Pb-G-0350-6-2f
Initial wt (g)	35.4684
Removal wt (g)	35.4681

Calculated final wt (g)	35.4633
Total wt loss (g)	0.0051
Total wt loss (mg)	5.1

Cleaning Cycle	Wt (g)
0	35.4681
1	35.4596
2	35.4538
3	35.4492
4	35.4442
5	35.4397

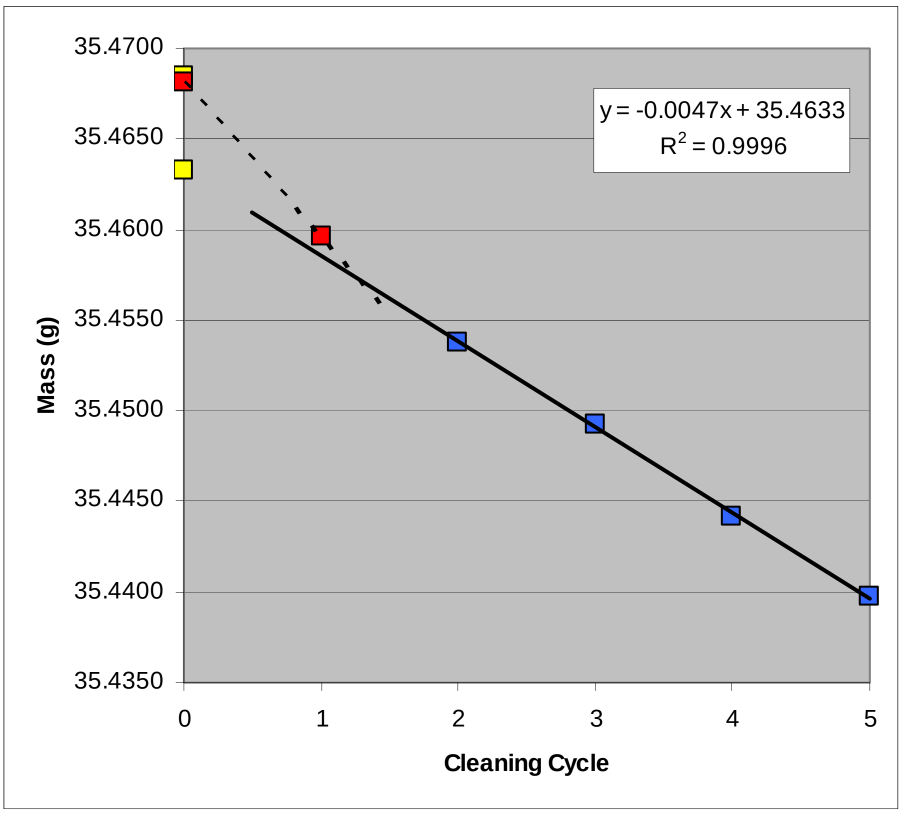

Coupon: L112
Test Matrix: Pb-G-0350-6-1p
Initial wt (g) 35.1391
Removal wt (g) 35.1408

Calculated final wt (g) 35.1362
Total wt loss (g) 0.0029
Total wt loss (mg) 2.9

Cleaning Cycle	Wt (g)
0	35.1408
1	35.1333
2	35.1220
3	35.1143
4	35.1074
5	35.1003

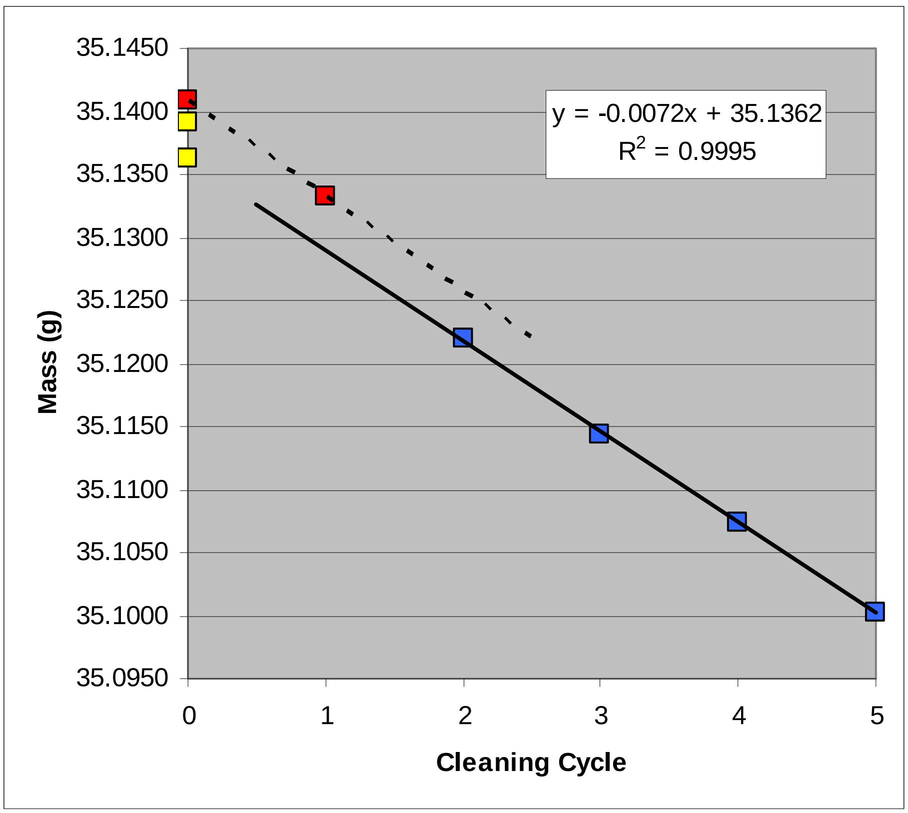

Coupon:	L113
Test Matrix:	Pb-G-0350-6-2p
Initial wt (g)	34.6572
Removal wt (g)	34.6553

Calculated final wt (g)	34.6431
Total wt loss (g)	0.0141
Total wt loss (mg)	14.1

Cleaning Cycle	Wt (g)
0	34.6553
1	34.6391
2	34.6329
3	34.6263
4	34.6216
5	34.6166

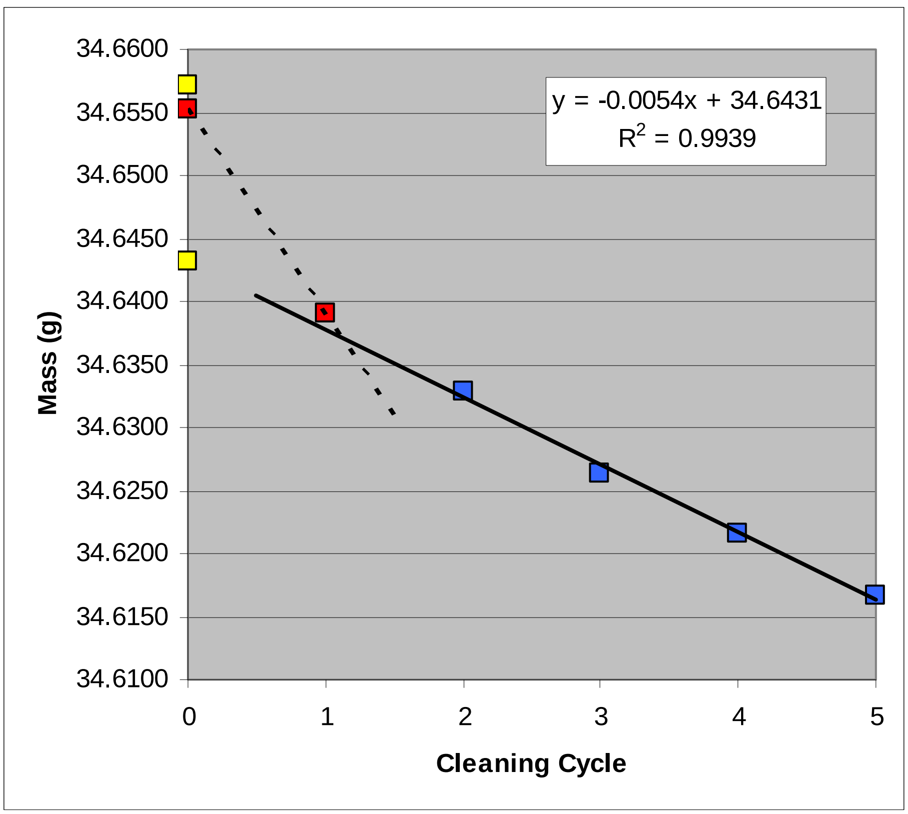

Coupon:	L115
Test Matrix:	Pb-Go-0350-6-1f
Initial wt (g)	35.0723
Removal wt (g)	35.0717

Calculated final wt (g)	35.0626
Total wt loss (g)	0.0097
Total wt loss (mg)	9.7

Cleaning Cycle	Wt (g)
0	35.0717
1	35.0579
2	35.0503
3	35.0456
4	35.0389
5	35.0328

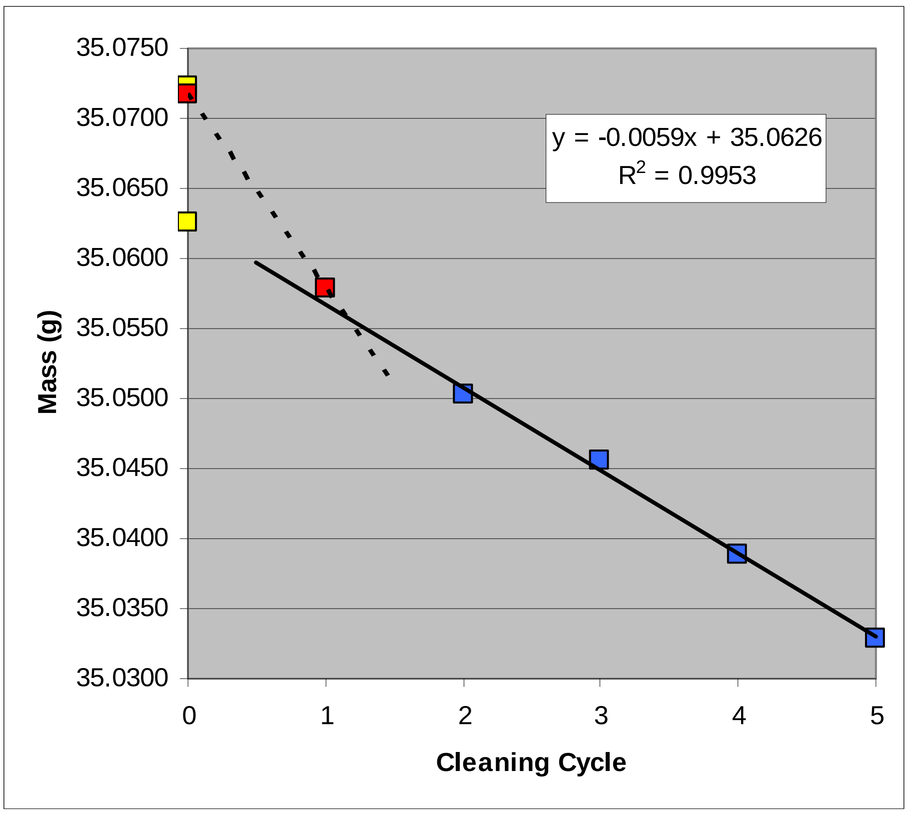

Coupon:	L116
Test Matrix:	Pb-Go-0350-6-2f
Initial wt (g)	35.1860
Removal wt (g)	35.3104

Calculated final wt (g)	35.1974
Total wt loss (g)	-0.0114
Total wt loss (mg)	-11.4

Cleaning Cycle	Wt (g)
0	35.3104
1	35.2050
2	35.1835
3	35.1806
4	35.1758
5	35.1649

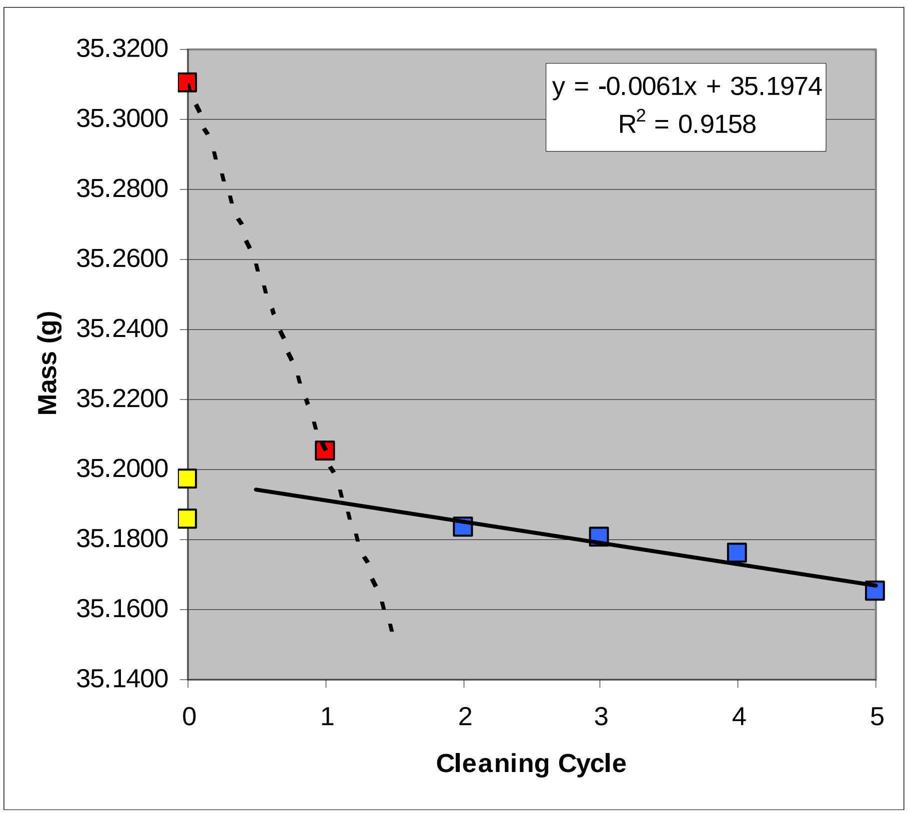

Coupon:	L118		
Test Matrix:	Pb-Go-0350-6-1p		
Initial wt (g)	35.5343	**Calculated final wt (g)**	35.5356
Removal wt (g)	35.6098	**Total wt loss (g)**	-0.0013
		Total wt loss (mg)	-1.3

Cleaning Cycle	Wt (g)
0	35.6098
1	35.5300
2	35.5255
3	35.5240
4	35.5175
5	35.5128

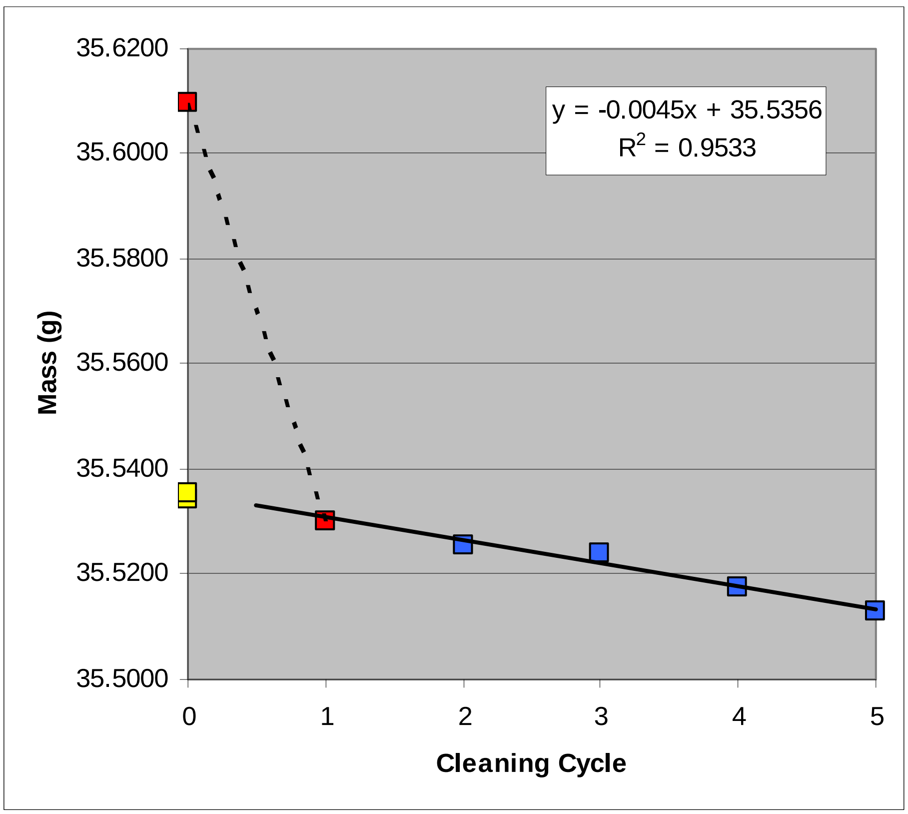

Coupon:	L119
Test Matrix:	Pb-Go-0350-6-2p
Initial wt (g)	35.6150
Removal wt (g)	35.7091

Calculated final wt (g)	35.6071
Total wt loss (g)	0.0079
Total wt loss (mg)	7.9

Cleaning Cycle	Wt (g)
0	35.7091
1	35.6048
2	35.5991
3	35.5949
4	35.5903
5	35.5870

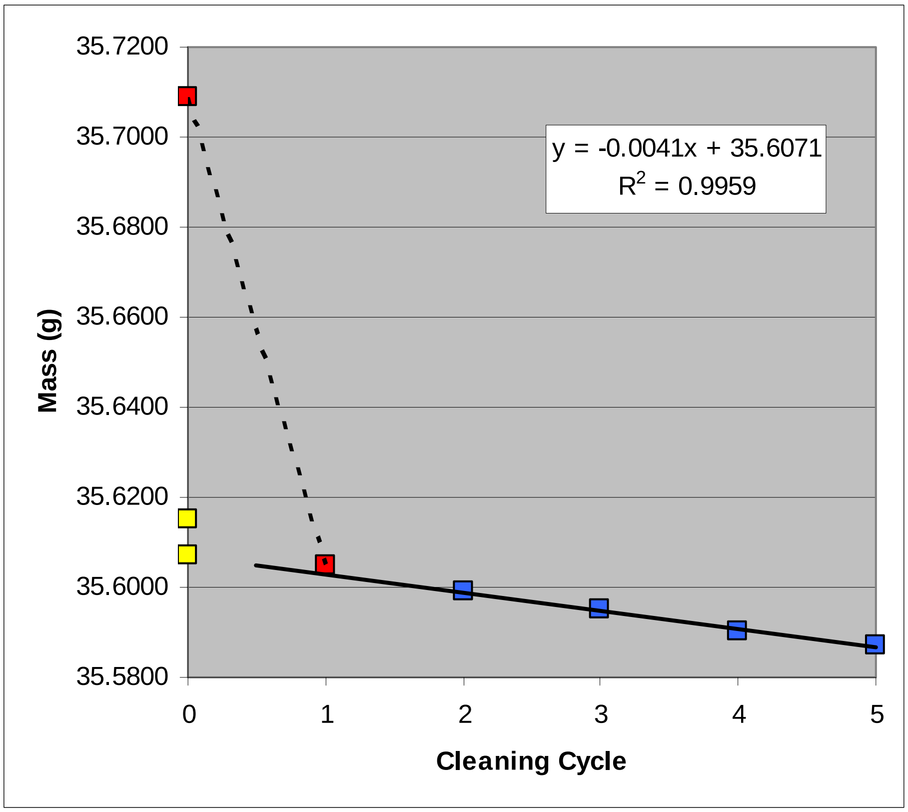

Coupon:	L121
Test Matrix:	Pb-E-0350-6-1f
Initial wt (g)	34.6720
Removal wt (g)	35.5965

Calculated final wt (g)	34.6668
Total wt loss (g)	0.0052
Total wt loss (mg)	5.2

Cleaning Cycle	Wt (g)
0	35.5965
1	34.6666
2	34.6578
3	34.6552
4	34.6475
5	34.6459

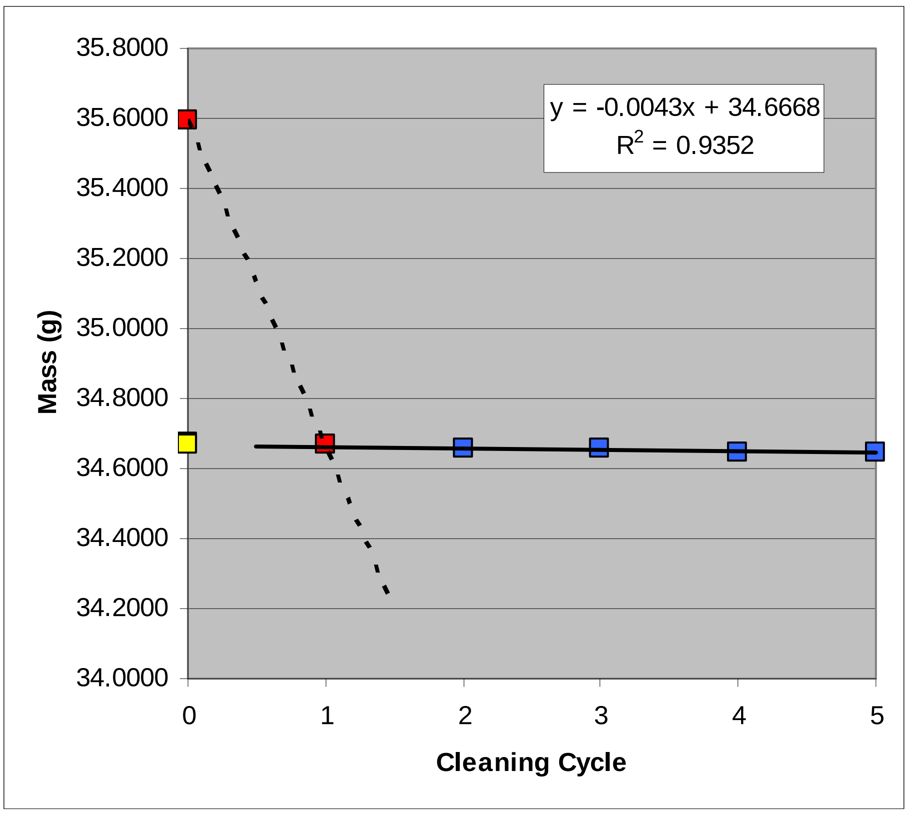

Coupon:	L122
Test Matrix:	Pb-E-0350-6-2f
Initial wt (g)	35.3743
Removal wt (g)	36.4406

Calculated final wt (g)	35.3677
Total wt loss (g)	0.0066
Total wt loss (mg)	6.6

Cleaning Cycle	Wt (g)
0	36.4406
1	35.3739
2	35.3545
3	35.3445
4	35.3388
5	35.3325

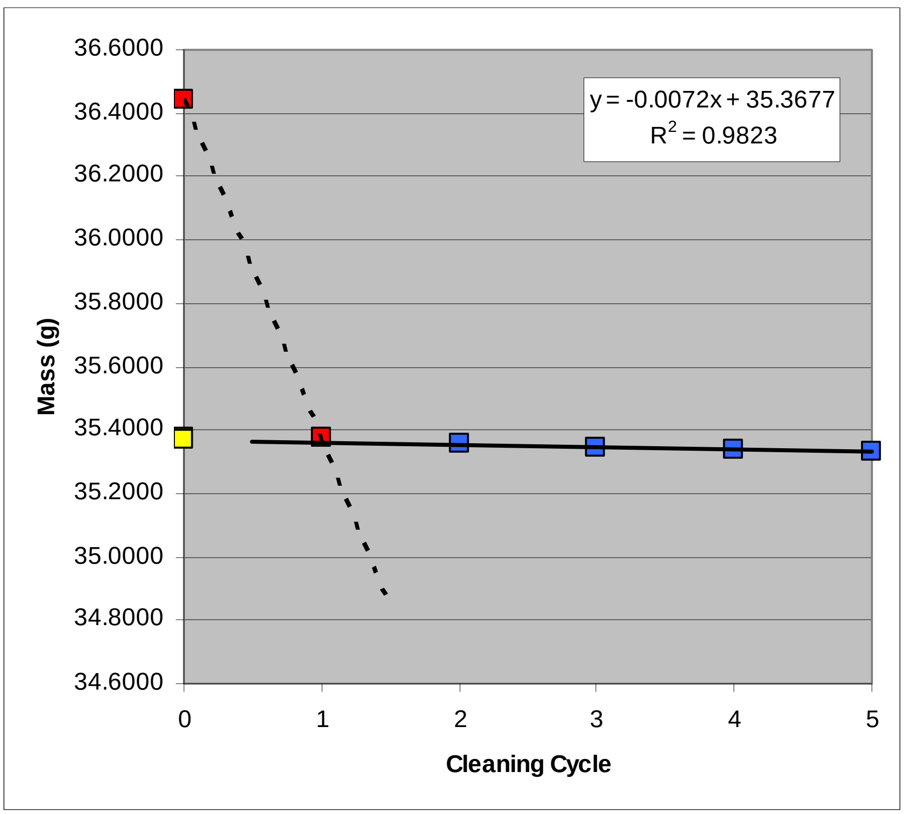

Coupon:	L124
Test Matrix:	Pb-E-0350-6-1p
Initial wt (g)	35.3672
Removal wt (g)	36.3790

Calculated final wt (g)	35.3638
Total wt loss (g)	0.0034
Total wt loss (mg)	3.4

Cleaning Cycle	Wt (g)
0	36.3790
1	35.3580
2	35.3523
3	35.3475
4	35.3418
5	35.3357

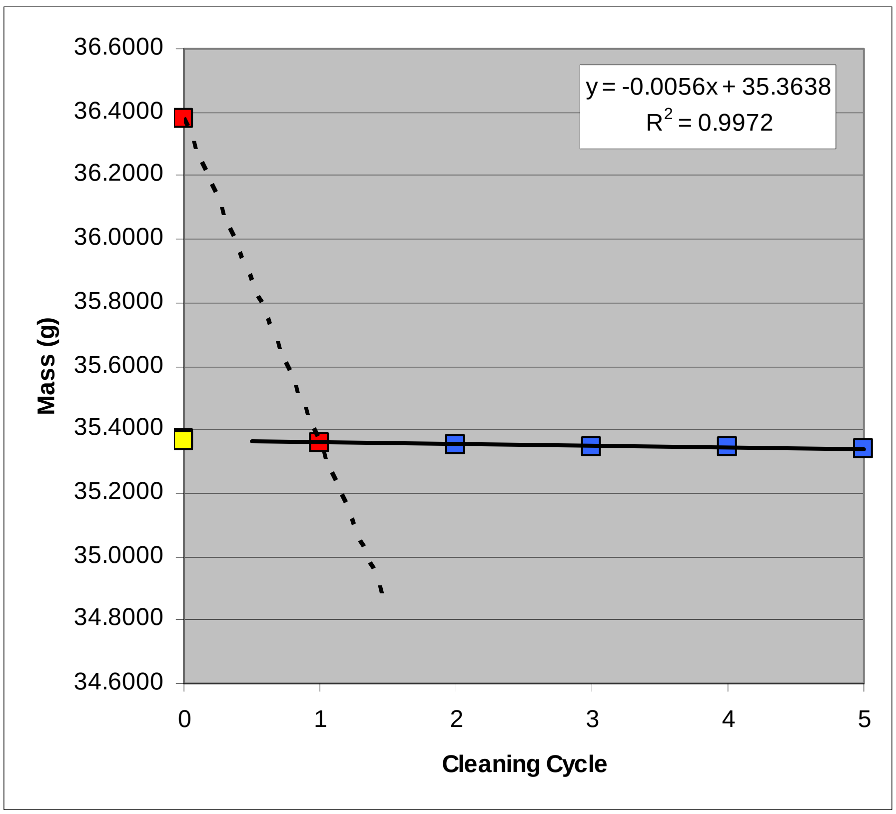

Coupon:	L125			
Test Matrix:	Pb-E-0350-6-2p			
Initial wt (g)	35.8618		**Calculated final wt (g)**	35.8569
Removal wt (g)	36.0169		**Total wt loss (g)**	0.0049
			Total wt loss (mg)	4.9

Cleaning Cycle	**Wt (g)**
0	36.0169
1	35.8538
2	35.8487
3	35.8446
4	35.8409
5	35.8363

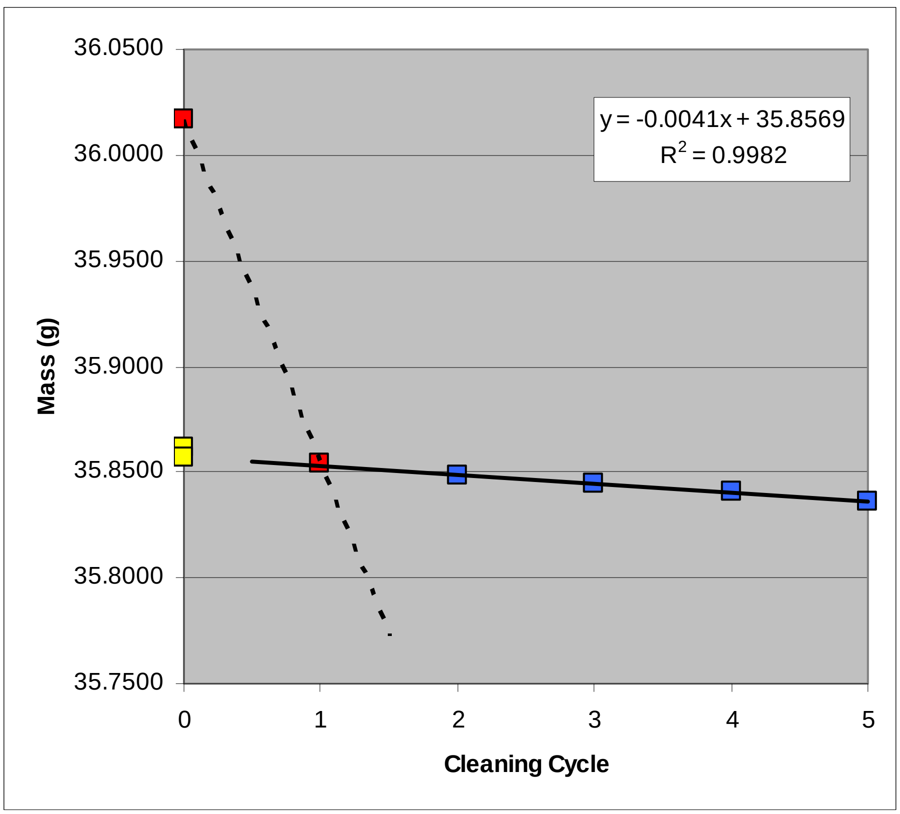

Coupon:	L127			
Test Matrix:	Pb-Eo-0350-6-1f			
Initial wt (g)	34.6510		**Calculated final wt (g)**	34.6404
Removal wt (g)	36.2326		**Total wt loss (g)**	0.0106
			Total wt loss (mg)	10.6

Cleaning Cycle	Wt (g)
0	36.2326
1	34.6391
2	34.6299
3	34.6245
4	34.6187
5	34.6141

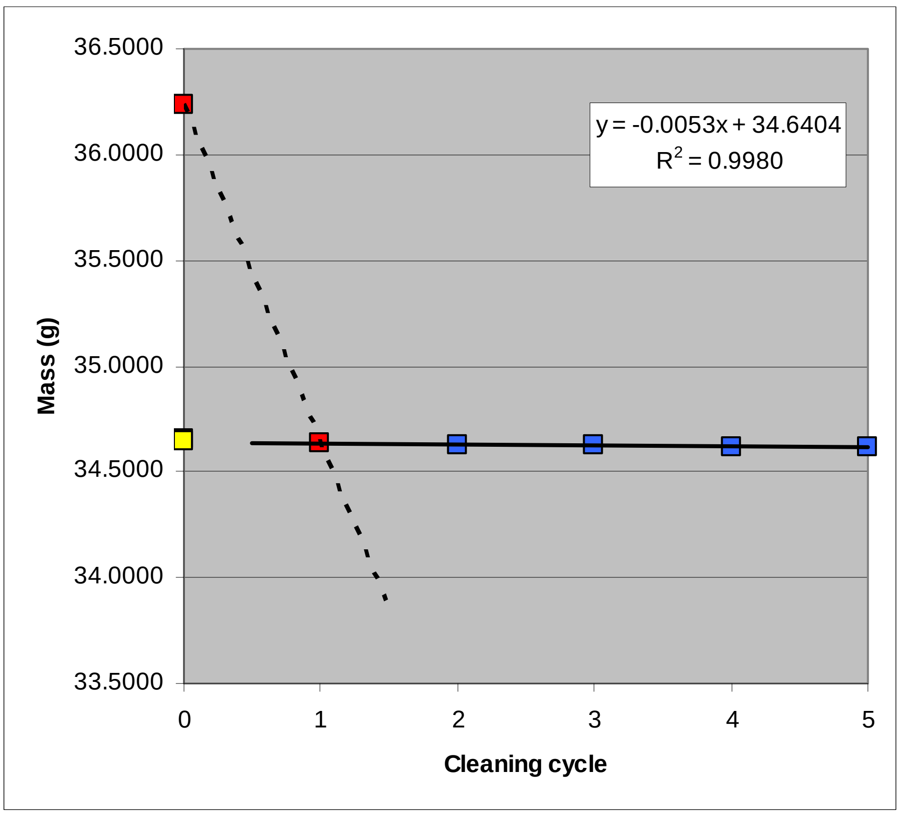

Coupon:	L128
Test Matrix:	Pb-Eo-0350-6-2f
Initial wt (g)	34.8518
Removal wt (g)	35.3104

Calculated final wt (g)	34.8429
Total wt loss (g)	0.0089
Total wt loss (mg)	8.9

Cleaning Cycle	**Wt (g)**
0	35.3104
1	34.8835
2	34.8287
3	34.8204
4	34.8130
5	34.8047
6	34.7999
7	34.7901
8	34.7842

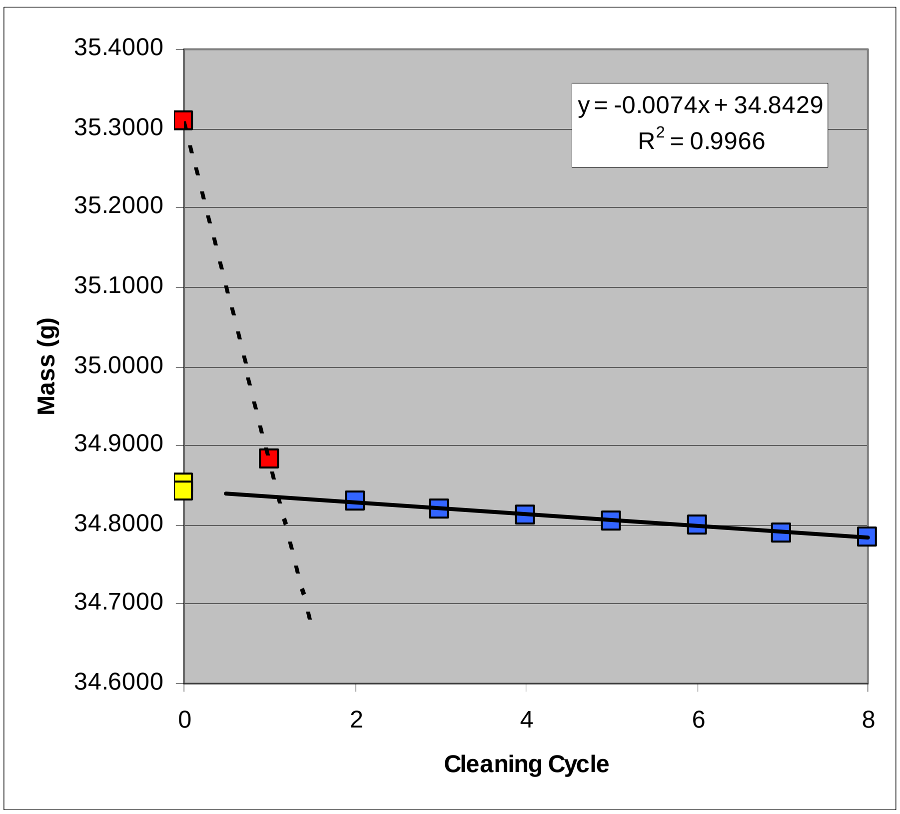

Coupon:	L130
Test Matrix:	Pb-Eo-0350-6-1p
Initial wt (g)	35.4064
Removal wt (g)	36.1061

Calculated final wt (g)	35.3985
Total wt loss (g)	0.0079
Total wt loss (mg)	7.9

Cleaning Cycle	Wt (g)
0	36.1061
1	35.3928
2	35.3885
3	35.3838
4	35.3784
5	35.3738

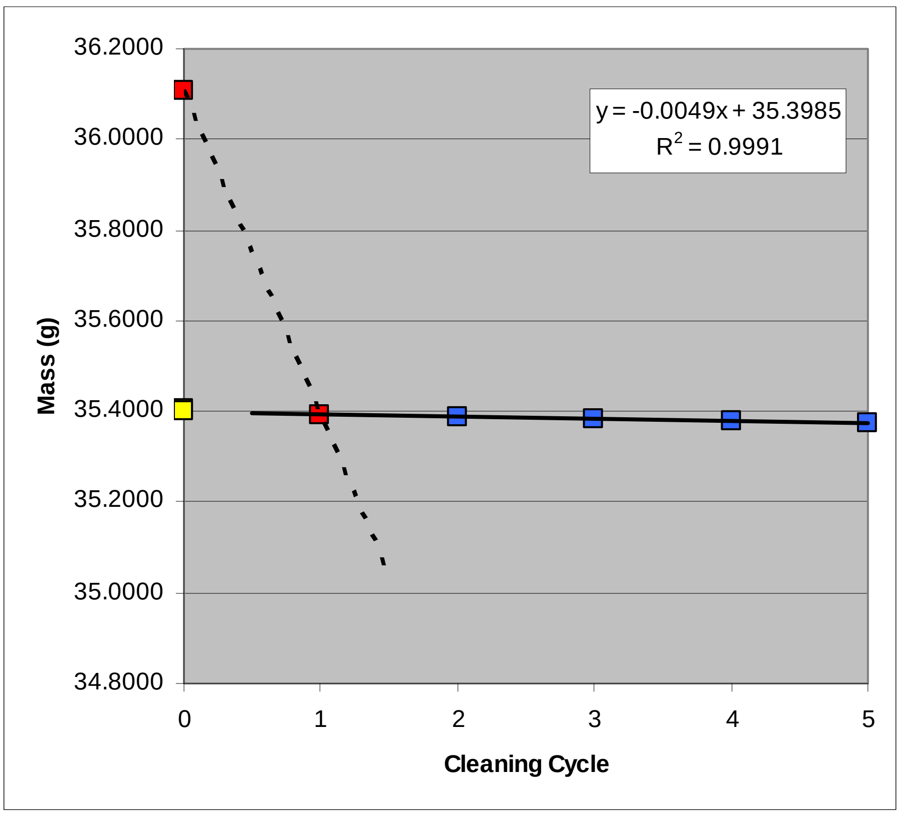

Coupon:	L131
Test Matrix:	Pb-Eo-0350-6-2p
Initial wt (g)	35.0594
Removal wt (g)	35.5319

Calculated final wt (g)	35.0541
Total wt loss (g)	0.0053
Total wt loss (mg)	5.3

Cleaning Cycle	**Wt (g)**
0	35.5319
1	35.0417
2	35.0432
3	35.0307
4	35.0273
5	35.0222

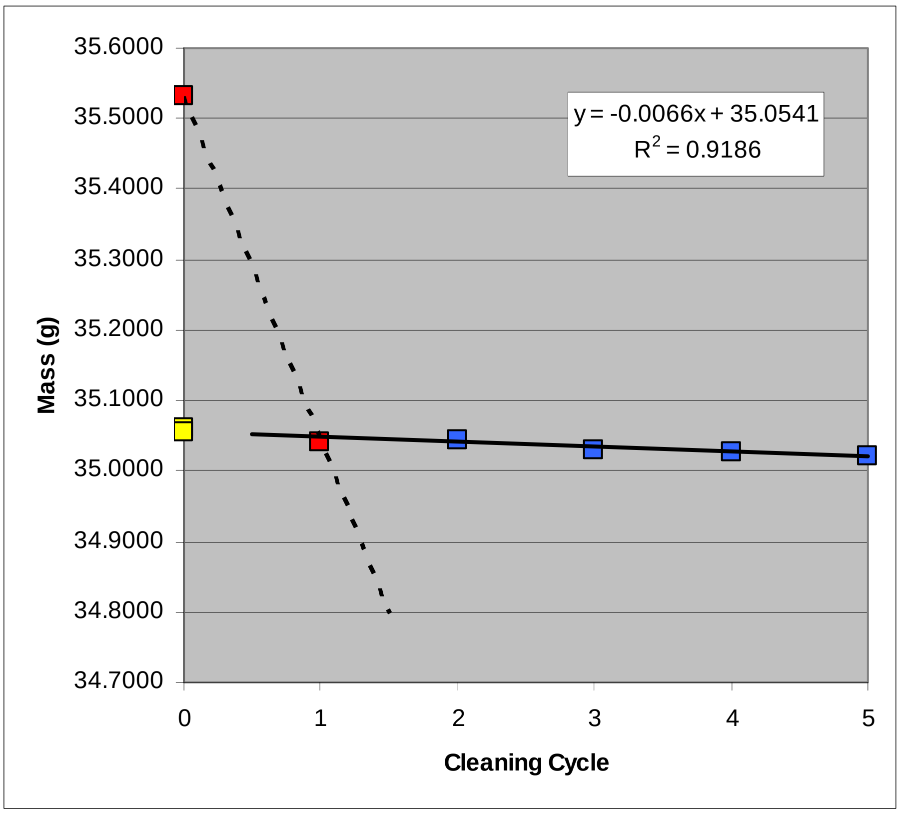

Coupon:	L133			
Test Matrix:	Pb-Atm-0350-6-1			
Initial wt (g)	35.1639		**Calculated final wt (g)**	35.1650
Removal wt (g)	35.1643		**Total wt loss (g)**	-0.0011
			Total wt loss (mg)	-1.1

Cleaning Cycle	Wt (g)
0	35.1643
1	35.1610
2	35.1555
3	35.1515
4	35.1480
5	35.1416

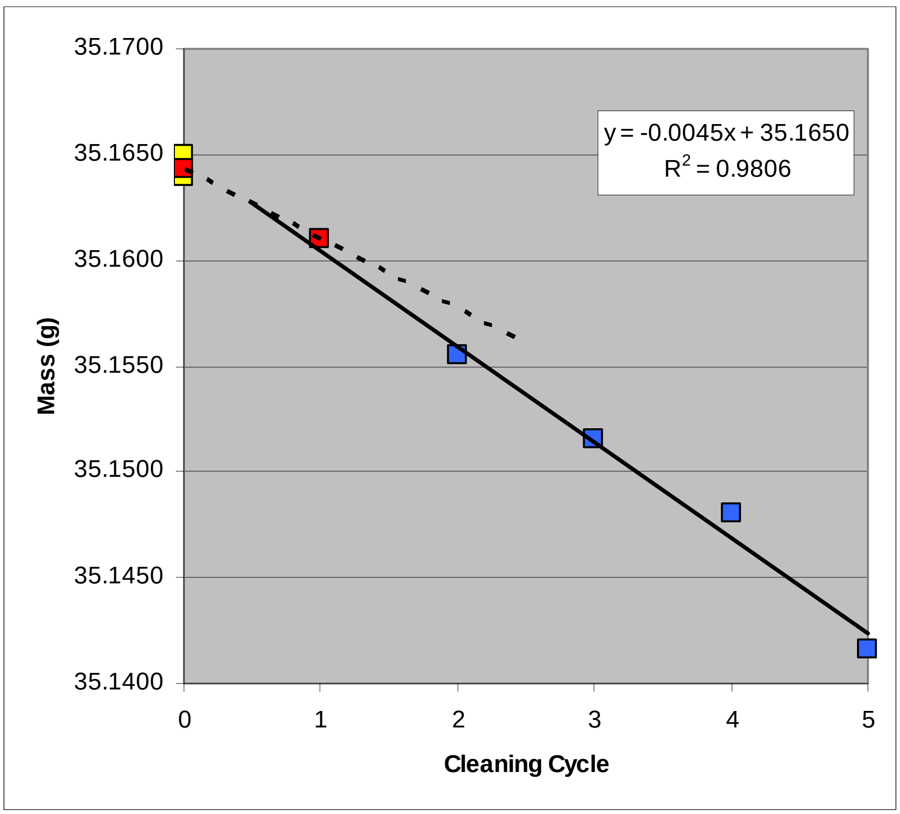

Coupon: L134
Test Matrix: Pb-Atm-0350-6-2
Initial wt (g) 35.3418
Removal wt (g) 35.3425

Calculated final wt (g) 35.3435
Total wt loss (g) -0.0017
Total wt loss (mg) -1.7

Cleaning Cycle	Wt (g)
0	35.3425
1	35.3399
2	35.3332
3	35.3268
4	35.3219
5	35.3169

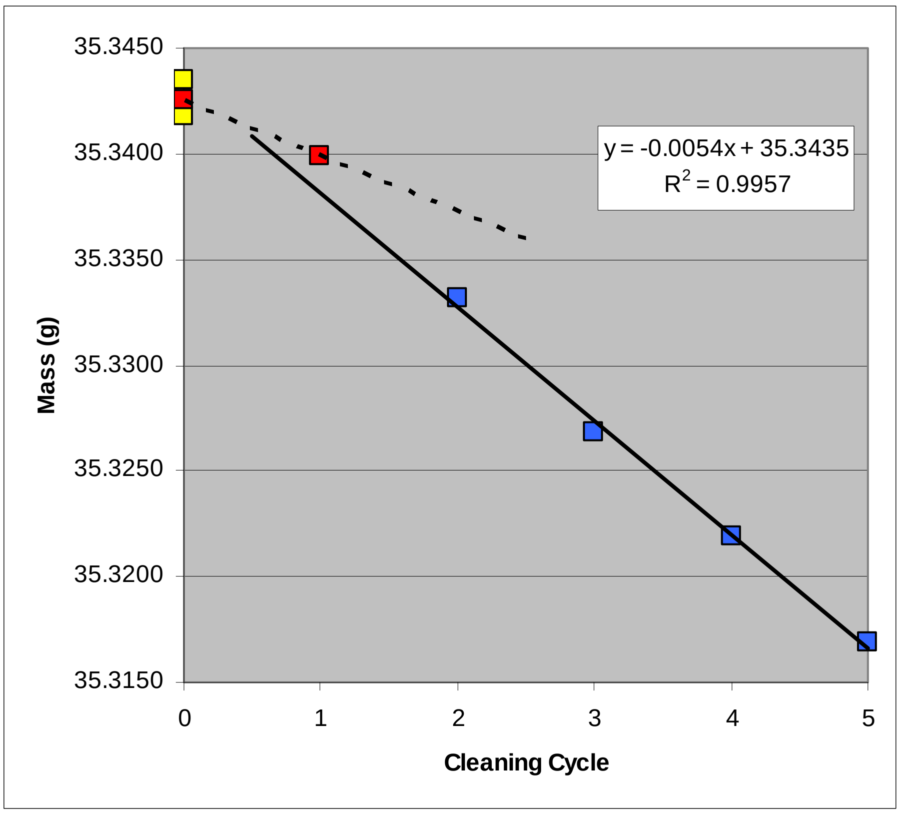

Coupon:	L299
Test Matrix:	Pb-G-1500-6-1f
Initial wt (g)	35.1086
Removal wt (g)	35.1027

Calculated final wt (g)	35.1001
Total wt loss (g)	0.0085
Total wt loss (mg)	8.5

Cleaning Cycle	Wt (g)
0	35.1027
1	35.0968
2	35.0917
3	35.0867
4	35.0825
5	35.0786

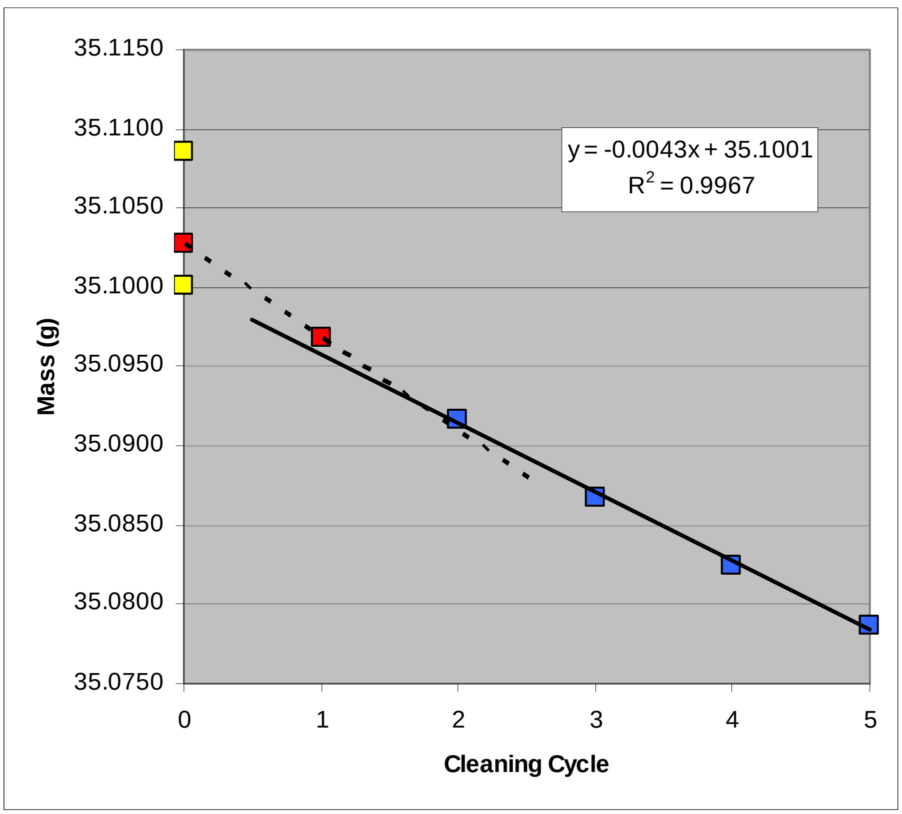

Coupon:	L300
Test Matrix:	Pb-G-1500-6-2f
Initial wt (g)	36.0213
Removal wt (g)	36.0258

Calculated final wt (g)	36.0137
Total wt loss (g)	0.0076
Total wt loss (mg)	7.6

Cleaning Cycle	Wt (g)
0	36.0258
1	36.0094
2	36.0051
3	35.9997
4	35.9953
5	35.9915

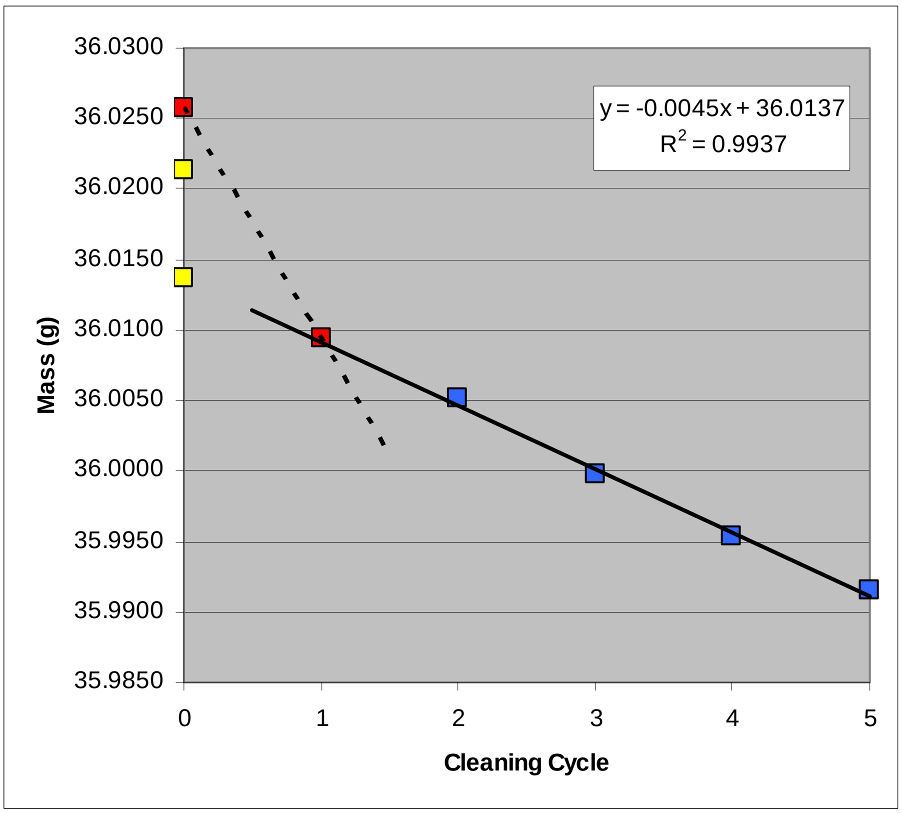

Coupon:	L302			
Test Matrix:	Pb-G-1500-6-1p			
Initial wt (g)	35.9088		**Calculated final wt (g)**	35.8793
Removal wt (g)	35.8967		**Total wt loss (g)**	0.0295
			Total wt loss (mg)	29.5

Cleaning Cycle	Wt (g)
0	35.8967
1	35.8754
2	35.8682
3	35.8632
4	35.8581
5	35.8518

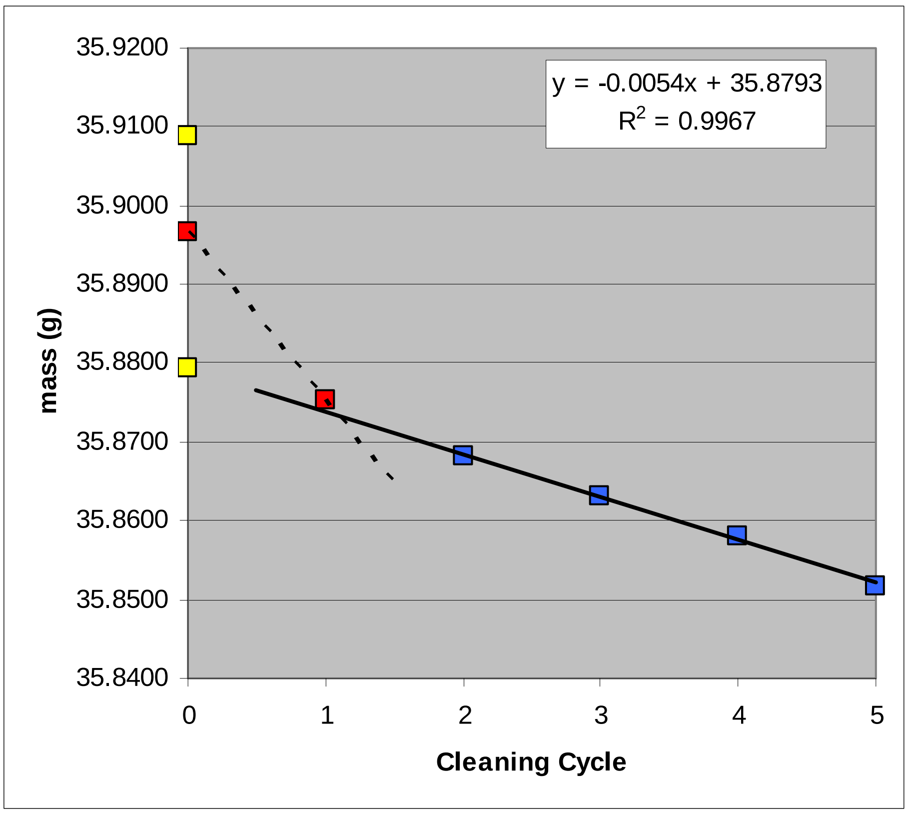

Coupon:	L303
Test Matrix:	Pb-G-1500-6-2p
Initial wt (g)	35.5716
Removal wt (g)	35.5709

Calculated final wt (g)	35.5546
Total wt loss (g)	0.017
Total wt loss (mg)	17

Cleaning Cycle	Wt (g)
0	35.5709
1	35.5504
2	35.5448
3	35.5398
4	35.5342
5	35.5301

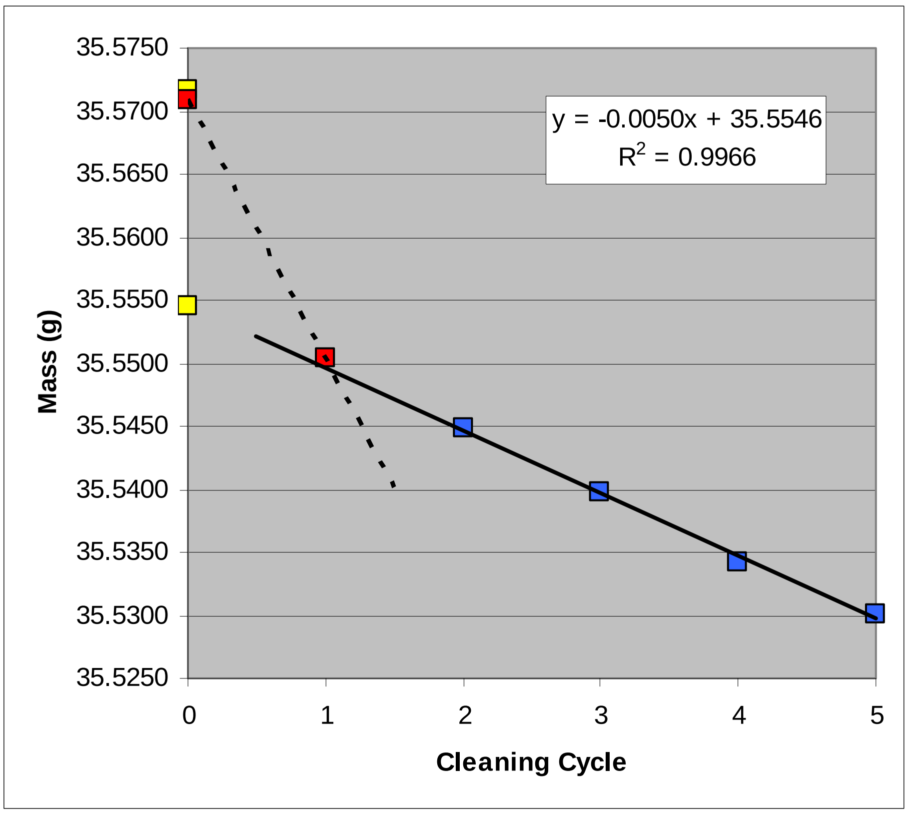

Coupon:	L305
Test Matrix:	Pb-Go-1500-6-1f
Initial wt (g)	34.6158
Removal wt (g)	34.6114

Calculated final wt (g)	34.6036
Total wt loss (g)	0.0122
Total wt loss (mg)	12.2

Cleaning Cycle	Wt (g)
0	34.6114
1	34.5994
2	34.5952
3	34.5912
4	34.5872
5	34.5827

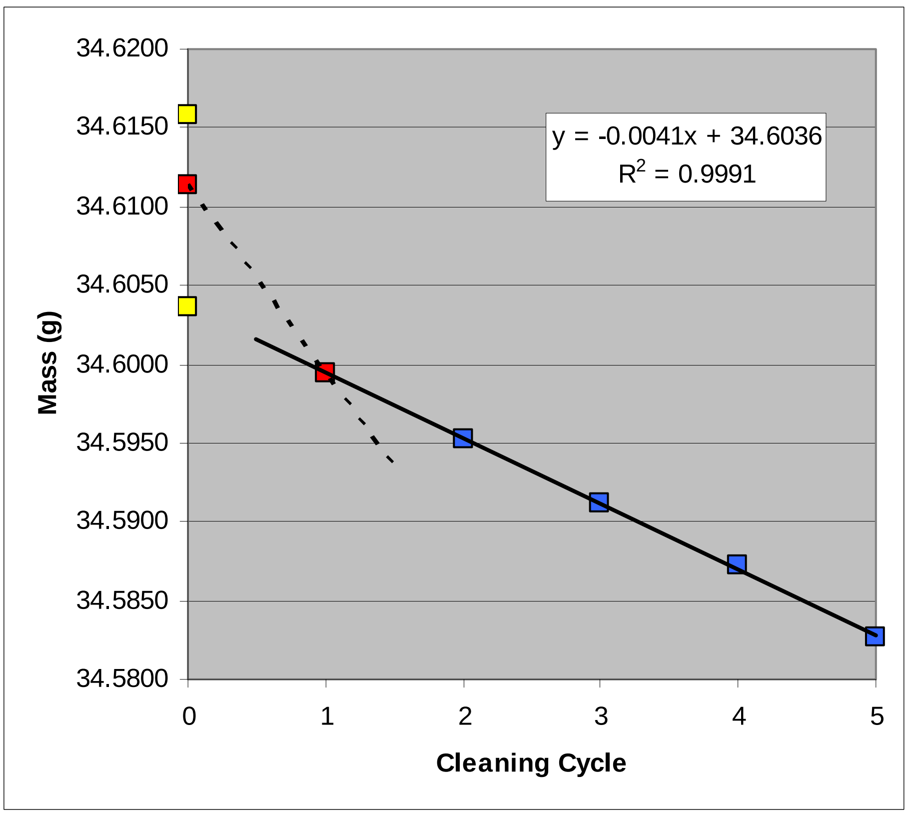

Coupon:	L306
Test Matrix:	Pb-Go-1500-6-2f
Initial wt (g)	34.8760
Removal wt (g)	34.8722

Calculated final wt (g)	34.8621
Total wt loss (g)	0.0139
Total wt loss (mg)	13.9

Cleaning Cycle	Wt (g)
0	34.8722
1	34.8598
2	34.8533
3	34.8487
4	34.8444
5	34.8400

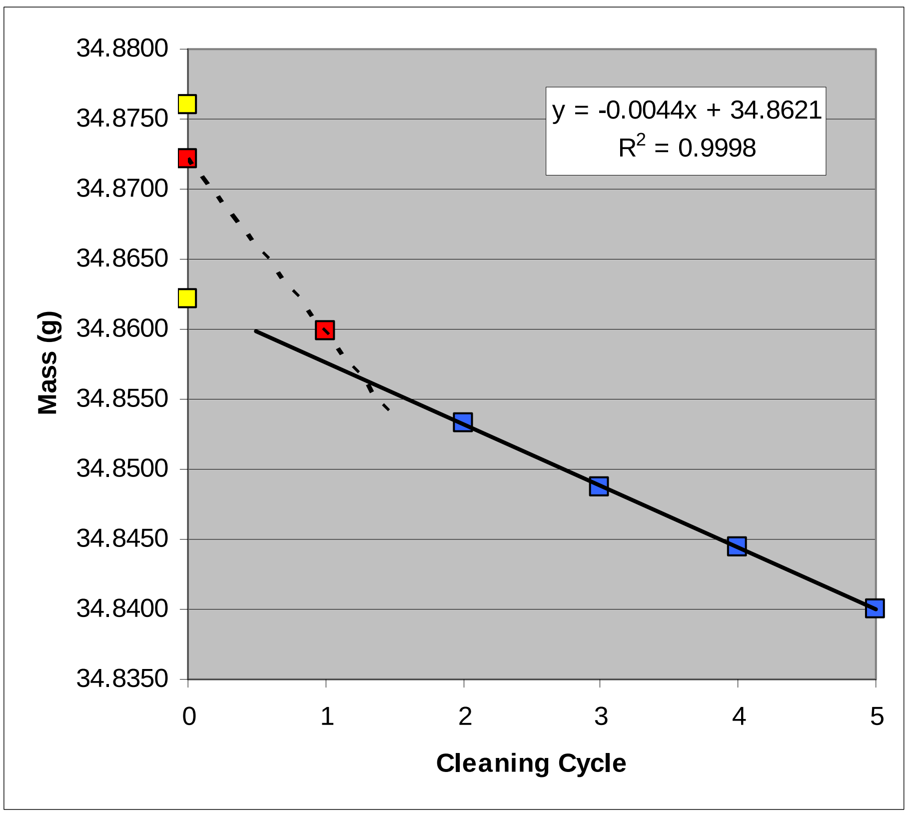

Coupon:	L308
Test Matrix:	Pb-Go-1500-6-1p
Initial wt (g)	35.0408
Removal wt (g)	35.0403

Calculated final wt (g)	35.0221
Total wt loss (g)	0.0187
Total wt loss (mg)	18.7

Cleaning Cycle	Wt (g)
0	35.0403
1	35.0159
2	35.0100
3	35.0040
4	34.9981
5	34.9919

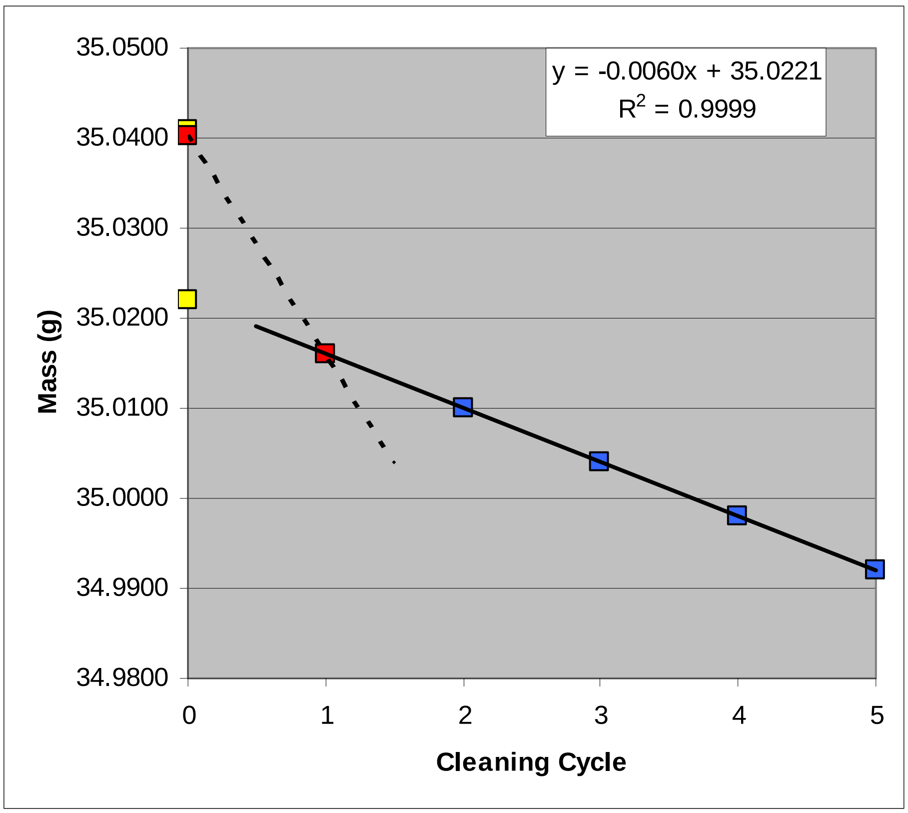

Coupon:	L309
Test Matrix:	Pb-Go-1500-6-2p
Initial wt (g)	34.8474
Removal wt (g)	34.8461

Calculated final wt (g)	34.8274
Total wt loss (g)	0.02
Total wt loss (mg)	20.0

Cleaning Cycle	Wt (g)
0	34.8461
1	34.8224
2	34.8175
3	34.8128
4	34.8082
5	34.8028

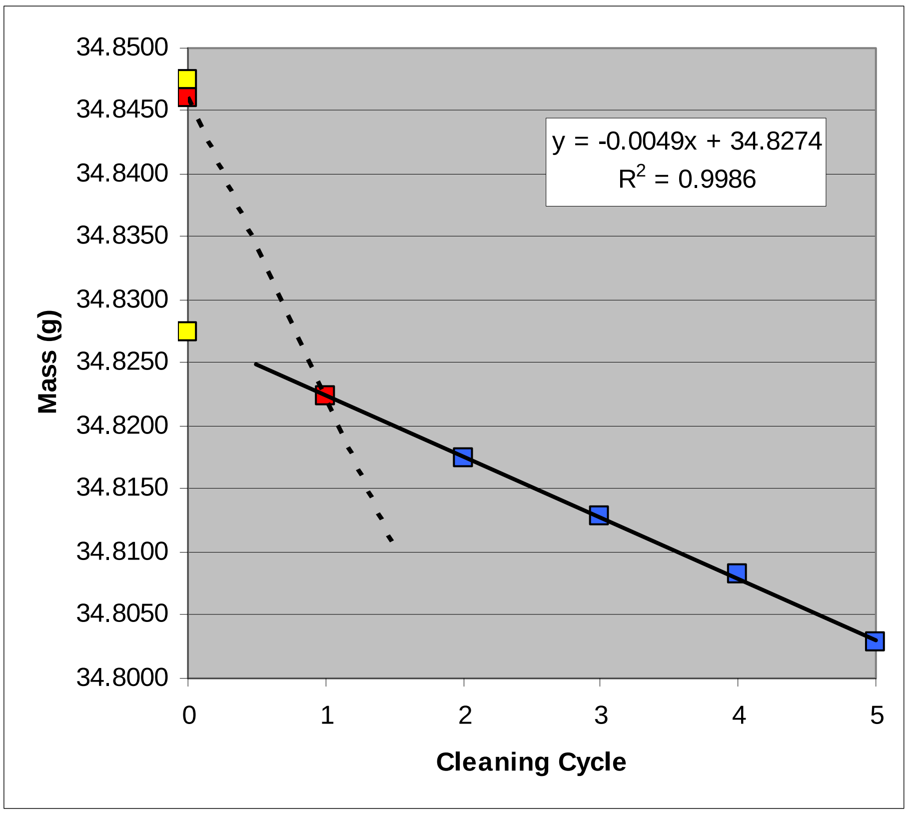

Coupon:	L311
Test Matrix:	Pb-E-1500-6-1f
Initial wt (g)	36.0171
Removal wt (g)	36.0644

Calculated final wt (g)	36.0132
Total wt loss (g)	0.0039
Total wt loss (mg)	3.9

Cleaning Cycle	Wt (g)
0	36.0644
1	36.0109
2	36.0050
3	36.0004
4	35.9965
5	35.9924

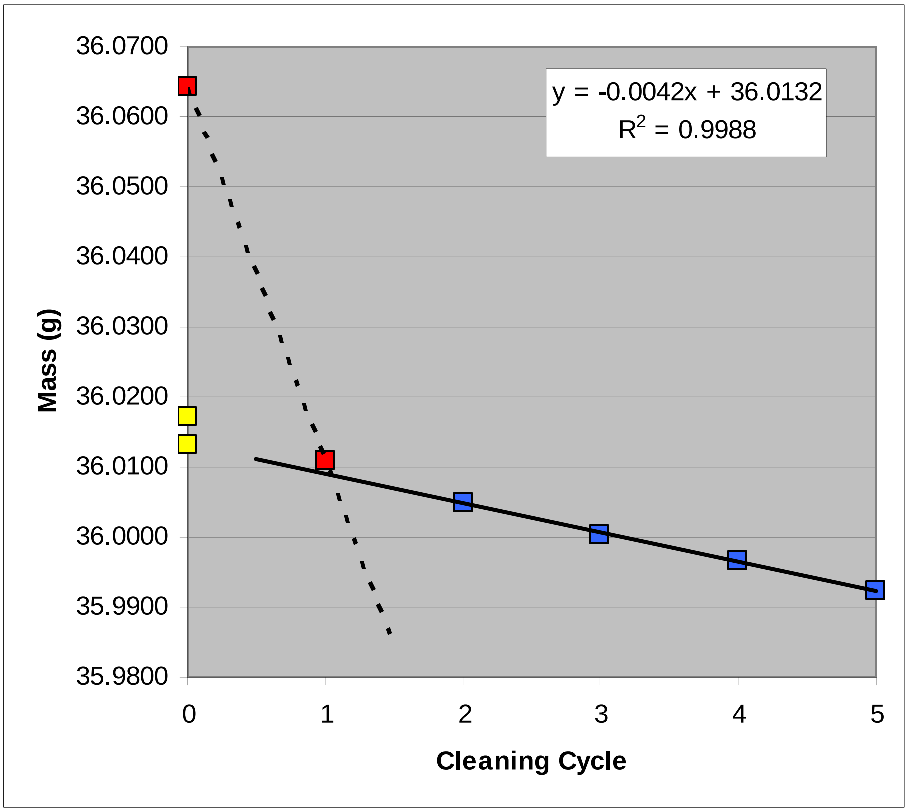

Coupon:	L312
Test Matrix:	Pb-E-1500-6-2f
Initial wt (g)	34.1353
Removal wt (g)	34.1589

Calculated final wt (g)	34.1305
Total wt loss (g)	0.0048
Total wt loss (mg)	4.8

Cleaning Cycle	Wt (g)
0	34.1589
1	34.1255
2	34.1207
3	34.1156
4	34.1102
5	34.1060

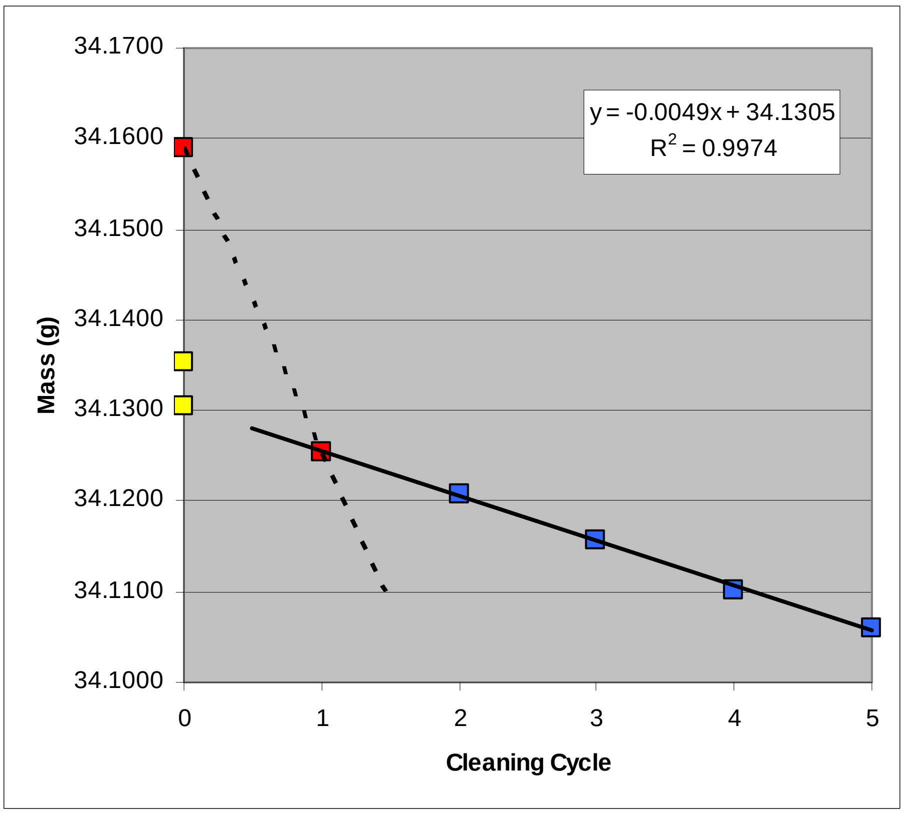

Coupon:	L314
Test Matrix:	Pb-E-1500-6-1p
Initial wt (g)	34.8270
Removal wt (g)	34.8406

Calculated final wt (g)	34.8128
Total wt loss (g)	0.0142
Total wt loss (mg)	14.2

Cleaning Cycle	Wt (g)
0	34.8406
1	34.8071
2	34.8018
3	34.7962
4	34.7900
5	34.7853

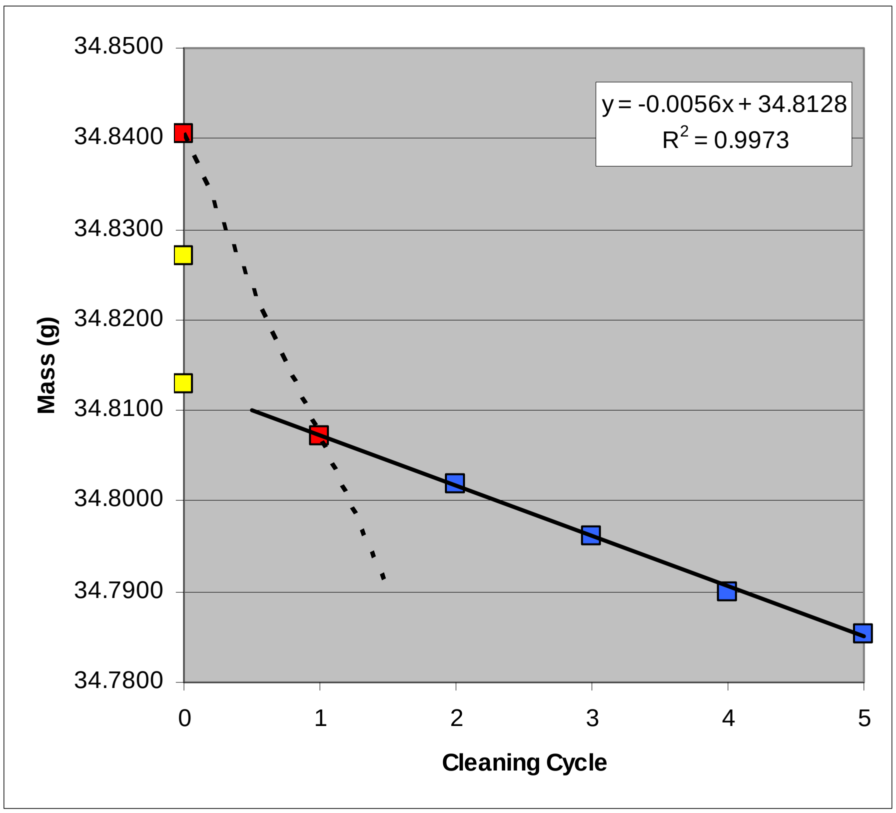

Coupon:	L315
Test Matrix:	Pb-E-1500-6-2p
Initial wt (g)	35.7921
Removal wt (g)	35.8138

Calculated final wt (g)	35.7813
Total wt loss (g)	0.0108
Total wt loss (mg)	10.8

Cleaning Cycle	Wt (g)
0	35.8138
1	35.7744
2	35.7675
3	35.7596
4	35.7555
5	35.7458

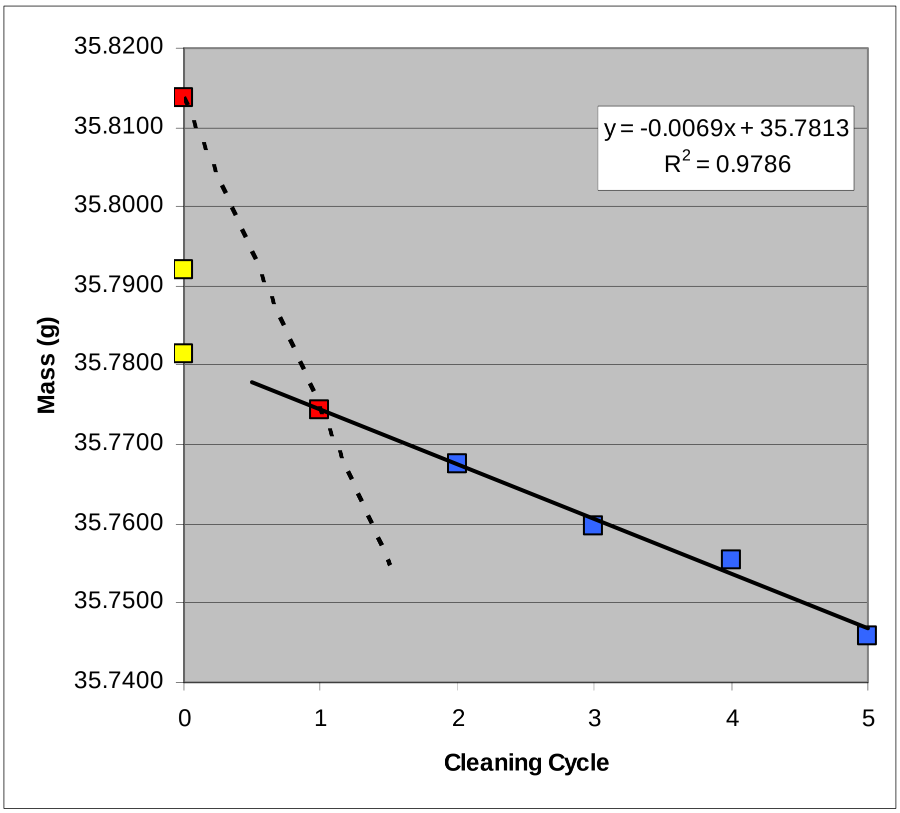

Coupon: L317
Test Matrix: Pb-Eo-1500-6-1f
Initial wt (g) 35.8858
Removal wt (g) 35.9051

Calculated final wt (g) 35.8788
Total wt loss (g) 0.0070
Total wt loss (mg) 7.0

Cleaning Cycle	Wt (g)
0	35.9051
1	35.8740
2	35.8703
3	35.8661
4	35.8617
5	35.8576

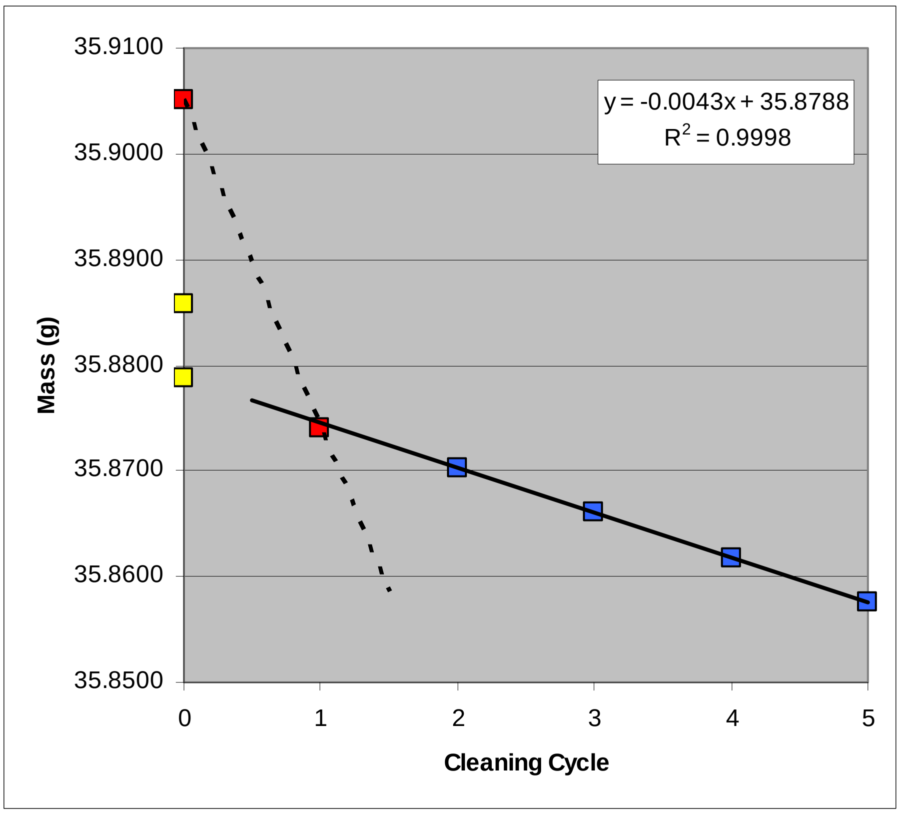

Coupon:	L318
Test Matrix:	Pb-Eo-1500-6-2f
Initial wt (g)	34.8114
Removal wt (g)	34.8365

Calculated final wt (g)	34.8040
Total wt loss (g)	0.0074
Total wt loss (mg)	7.4

Cleaning Cycle	Wt (g)
0	34.8365
1	34.7989
2	34.7940
3	34.7877
4	34.7830
5	34.7781

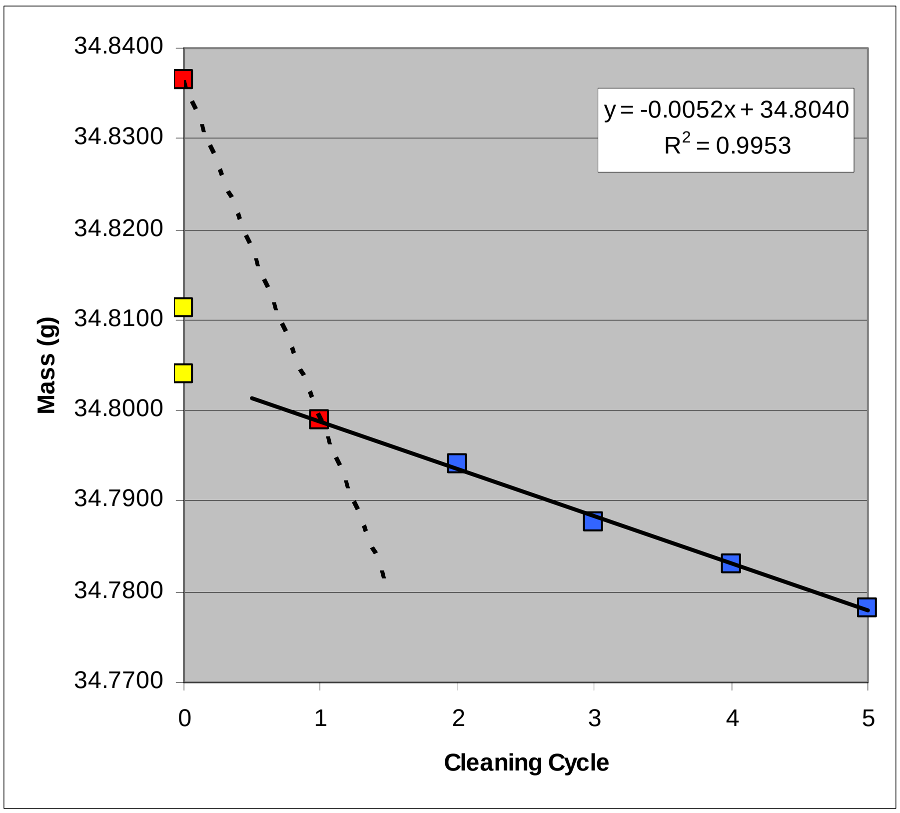

Coupon:	L320
Test Matrix:	Pb-Eo-1500-6-1p
Initial wt (g)	35.3177
Removal wt (g)	35.3248

Calculated final wt (g)	35.3072
Total wt loss (g)	0.0105
Total wt loss (mg)	10.5

Cleaning Cycle	Wt (g)
0	35.3248
1	35.3019
2	35.2966
3	35.2897
4	35.2843
5	35.2797

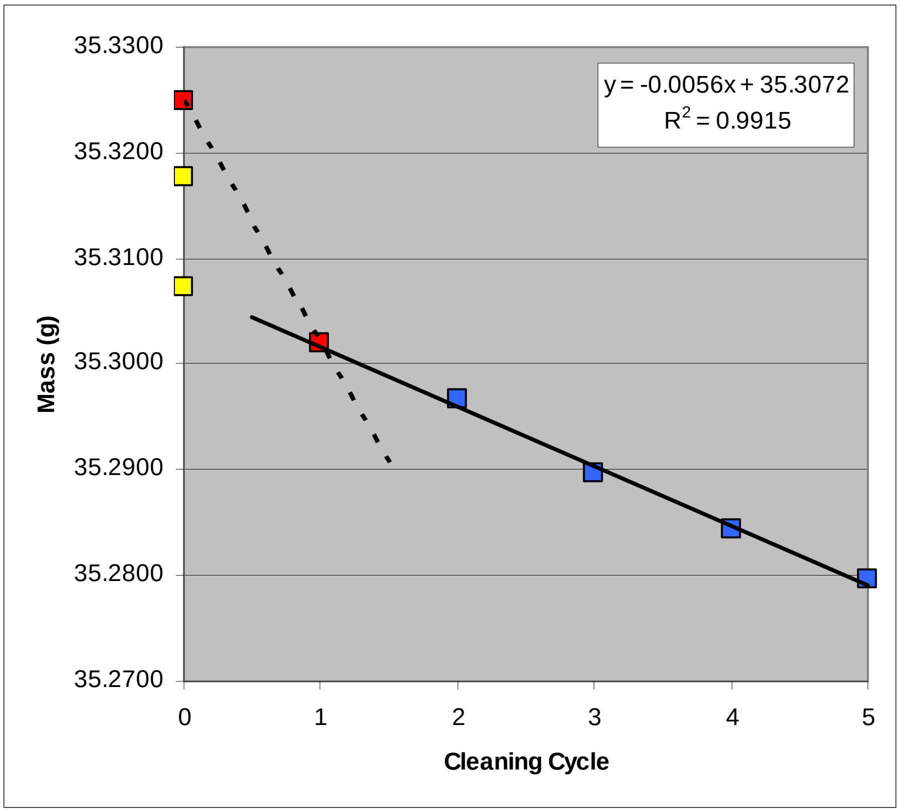

Coupon:	L321
Test Matrix:	Pb-Eo-1500-6-1p
Initial wt (g)	34.6691
Removal wt (g)	34.6774

Calculated final wt (g)	34.6548
Total wt loss (g)	0.0143
Total wt loss (mg)	14.3

Cleaning Cycle	Wt (g)
0	34.6774
1	34.6494
2	34.6441
3	34.6371
4	34.6321
5	34.6270

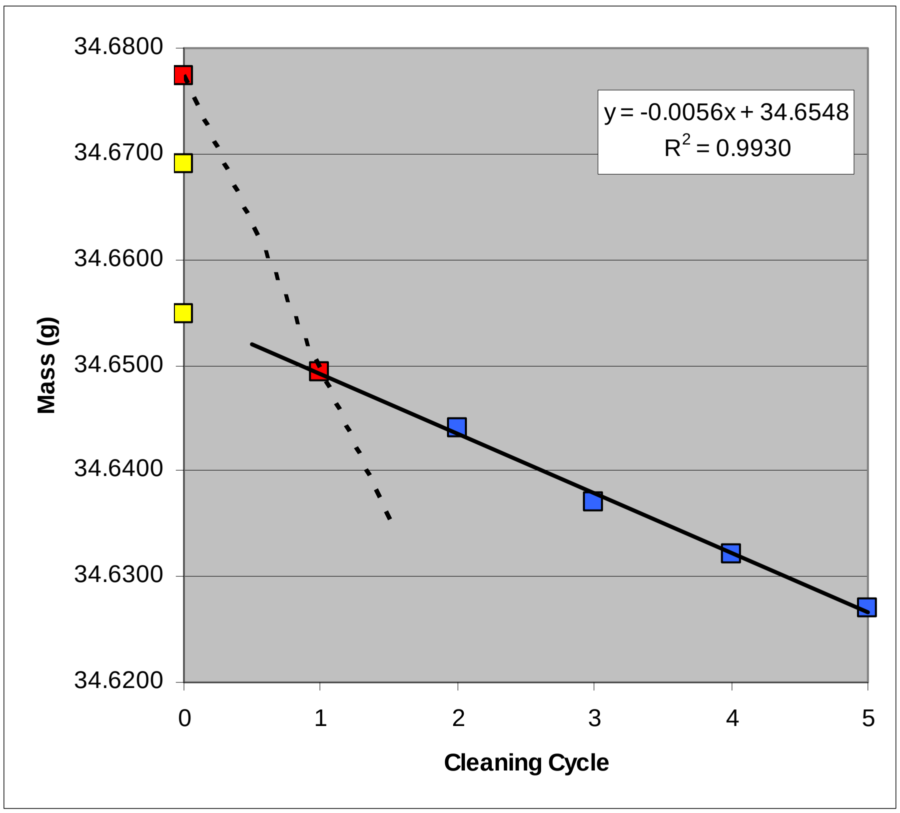

Coupon:	L323
Test Matrix:	Pb-Atm-1500-6-1
Initial wt (g)	35.0368
Removal wt (g)	35.0370

Calculated final wt (g)	35.0336
Total wt loss (g)	0.0032
Total wt loss (mg)	3.2

Cleaning Cycle	Wt (g)
0	35.0370
1	35.0318
2	35.0229
3	35.0181
4	35.0132
5	35.0072

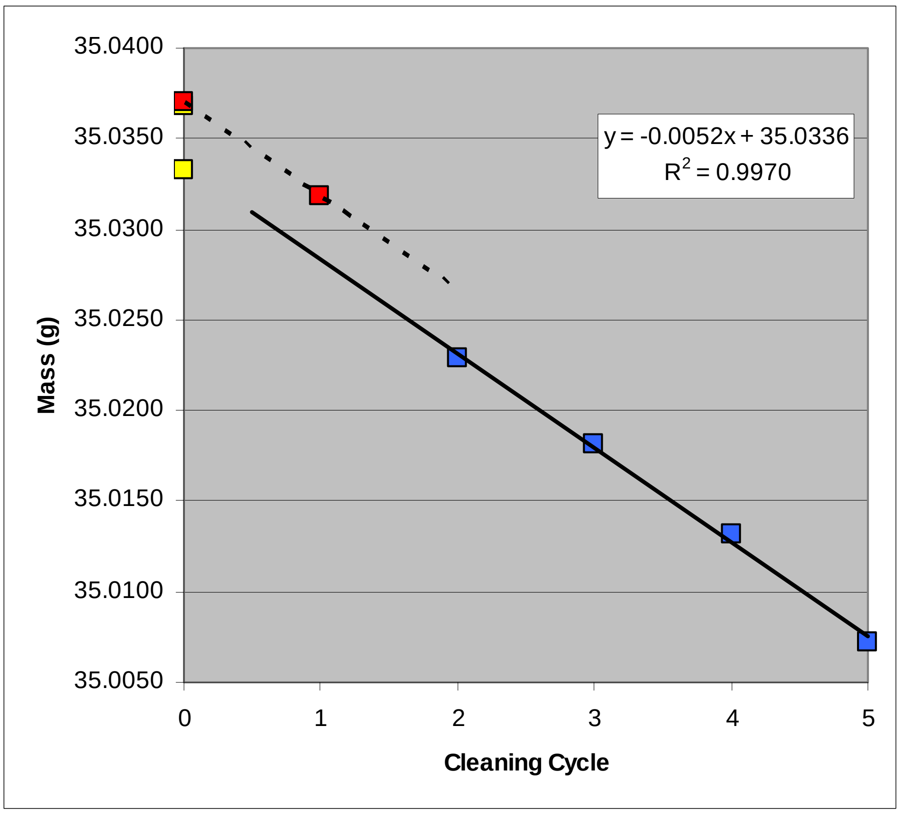

Coupon:	L324
Test Matrix:	Pb-Atm-1500-6-2
Initial wt (g)	35.1052
Removal wt (g)	35.1062

Calculated final wt (g)	35.1000
Total wt loss (g)	0.0052
Total wt loss (mg)	5.2

Cleaning Cycle	Wt (g)
0	35.1062
1	35.0972
2	35.0906
3	35.0853
4	35.0809
5	35.0761

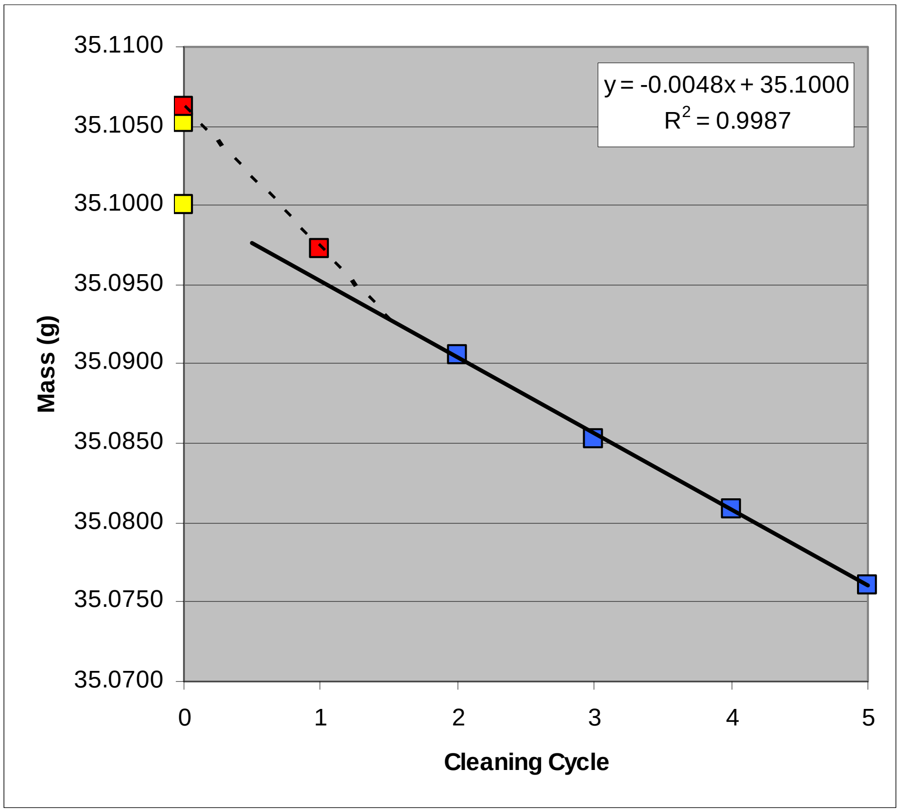

Coupon:	L413
Test Matrix:	Pb-G-3500-6-1f
Initial wt (g)	34.6030
Removal wt (g)	34.6236

Calculated final wt (g)	34.5922
Total wt loss (g)	0.0108
Total wt loss (mg)	10.8

Cleaning Cycle	Wt (g)
0	34.6236
1	34.5897
2	34.5845
3	34.5806
4	34.5767
5	34.5729

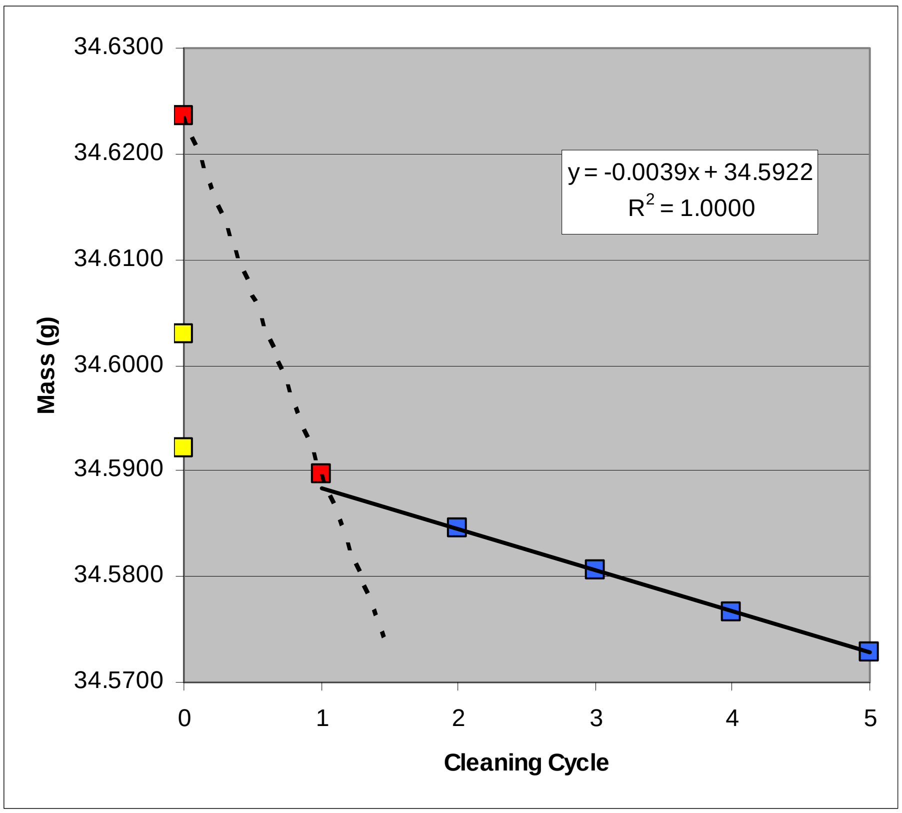

Coupon:	L414
Test Matrix:	Pb-G-3500-6-2f
Initial wt (g)	34.2356
Removal wt (g)	34.2576

Calculated final wt (g)	34.2262
Total wt loss (g)	0.0094
Total wt loss (mg)	9.4

Cleaning Cycle	Wt (g)
0	34.2576
1	34.2205
2	34.2170
3	34.2134
4	34.2084
5	34.2039

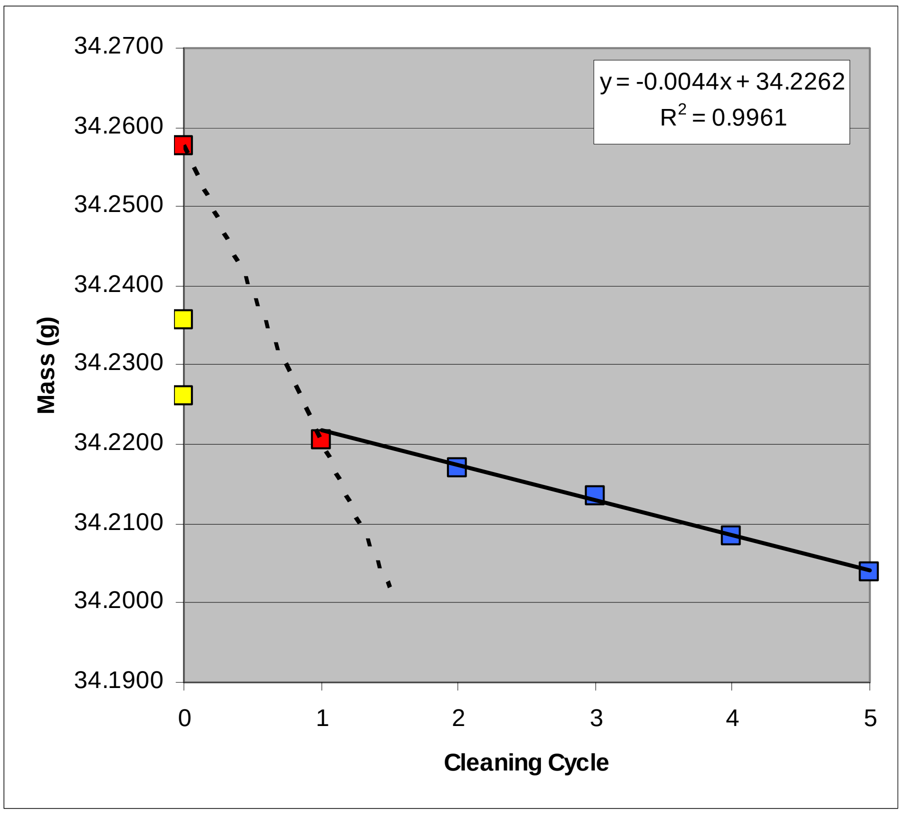

Coupon:	L417
Test Matrix:	Pb-G-3500-6-2p
Initial wt (g)	35.1097
Removal wt (g)	35.1034

Calculated final wt (g)	35.0965
Total wt loss (g)	0.0132
Total wt loss (mg)	13.2

Cleaning Cycle	**Wt (g)**
0	35.1034
1	35.0903
2	35.0860
3	35.0798
4	35.0751
5	35.0696

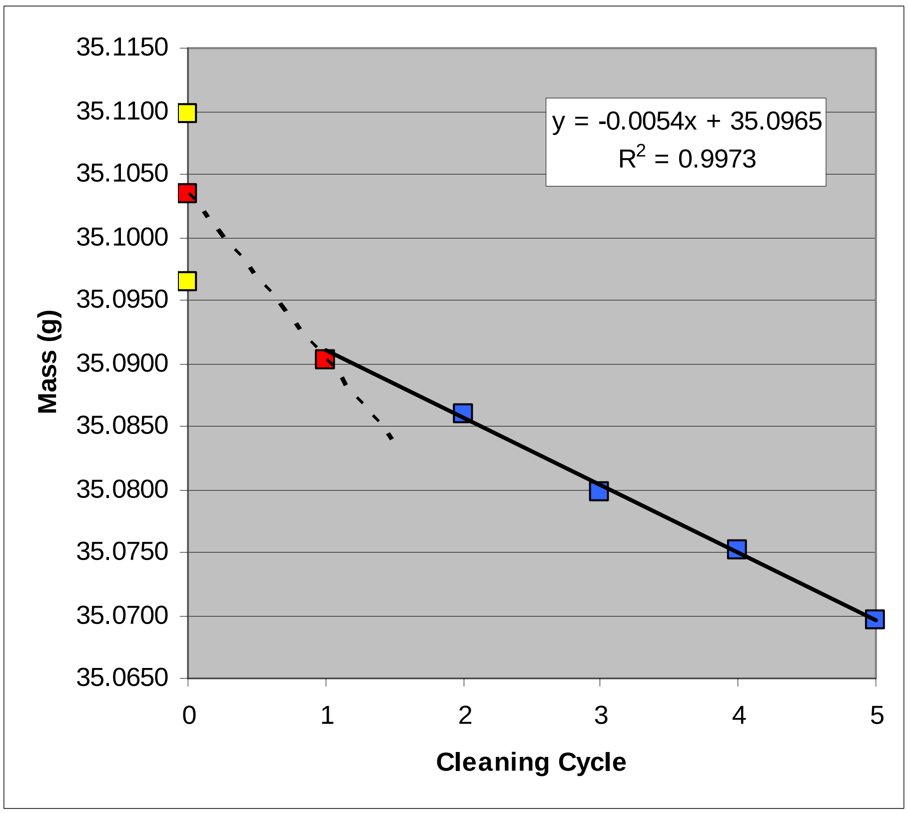

Coupon:	L418
Test Matrix:	Pb-G-3500-6-3p
Initial wt (g)	34.9317
Removal wt (g)	34.9275

Calculated final wt (g)	34.9201
Total wt loss (g)	0.0116
Total wt loss (mg)	11.6

Cleaning Cycle	Wt (g)
0	34.9275
1	34.9155
2	34.9109
3	34.9056
4	34.9013
5	34.8966

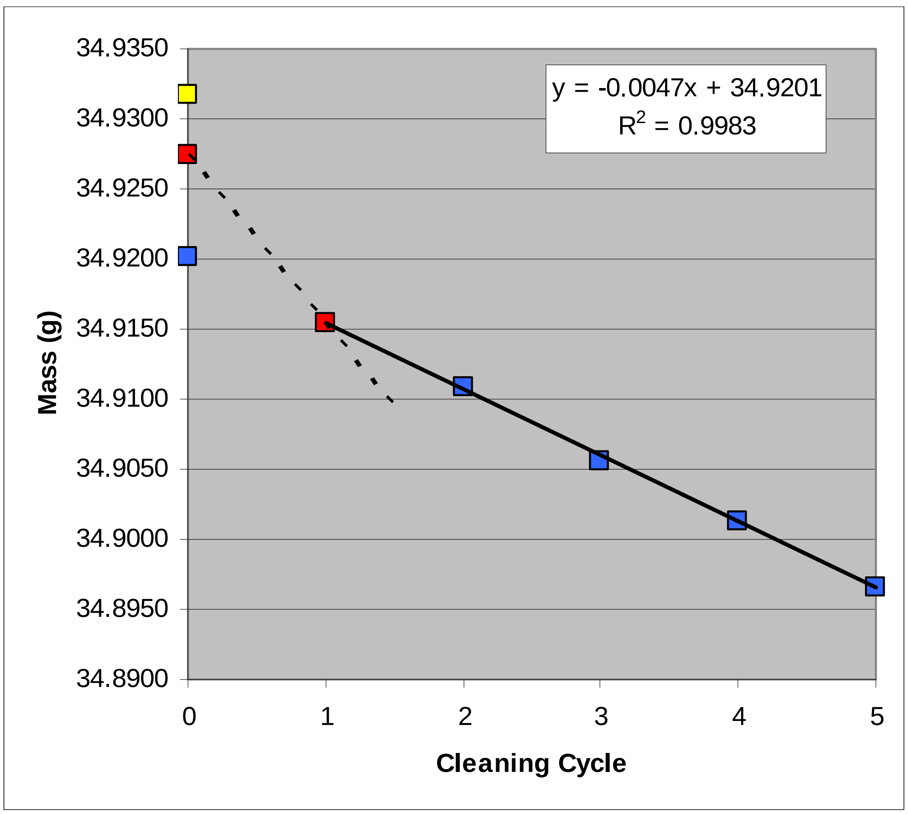

Coupon:	L419
Test Matrix:	Pb-Go-3500-6-1f
Initial wt (g)	34.9312
Removal wt (g)	34.9557

Calculated final wt (g)	34.9194
Total wt loss (g)	0.0118
Total wt loss (mg)	11.8

Cleaning Cycle	Wt (g)
0	34.9557
1	34.9158
2	34.9109
3	34.9057
4	34.9022
5	34.8975

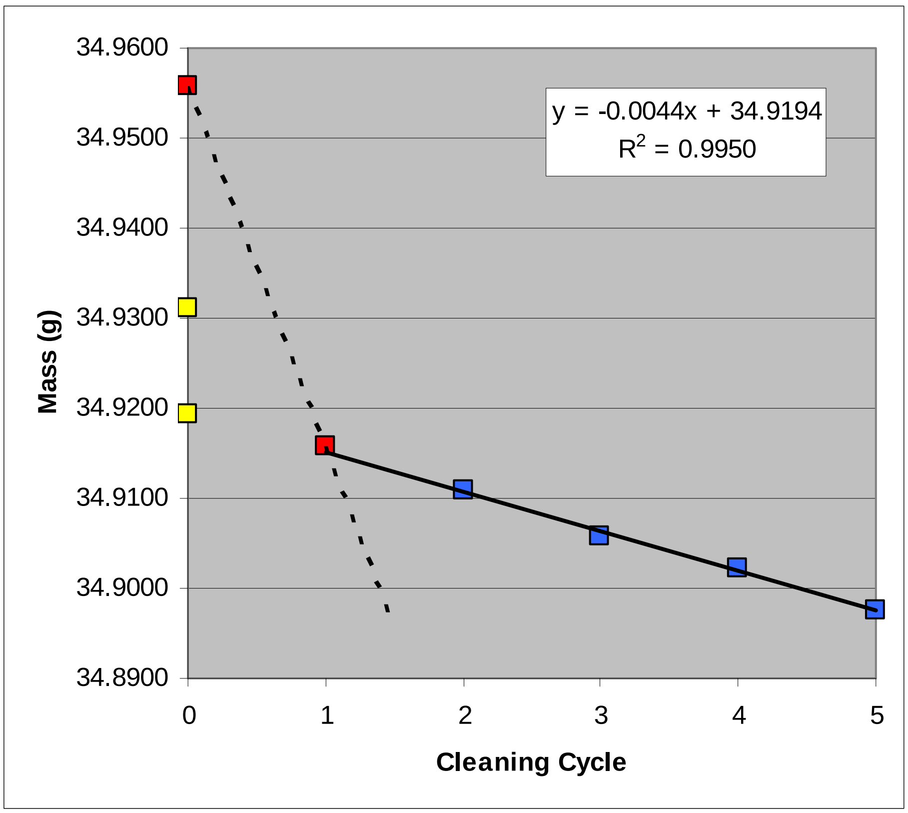

Coupon:	L420
Test Matrix:	Pb-Go-3500-6-2f
Initial wt (g)	34.1202
Removal wt (g)	34.1348

Calculated final wt (g)	34.1119
Total wt loss (g)	0.0083
Total wt loss (mg)	8.3

Cleaning Cycle	Wt (g)
0	34.1348
1	34.1062
2	34.1035
3	34.1000
4	34.0948
5	34.0914

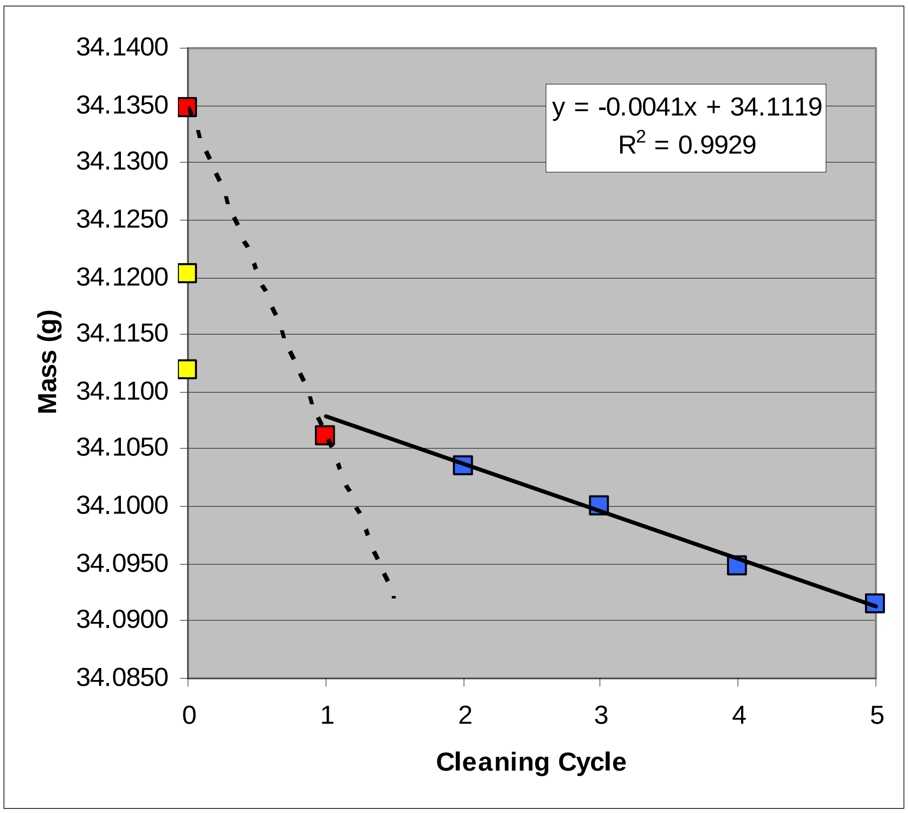

Coupon:	L422
Test Matrix:	Pb-Go-3500-6-1p
Initial wt (g)	34.7956
Removal wt (g)	34.7916

Calculated final wt (g)	34.7837
Total wt loss (g)	0.0119
Total wt loss (mg)	11.9

Cleaning Cycle	Wt (g)
0	34.7916
1	34.7786
2	34.7749
3	34.7714
4	34.7663
5	34.7624

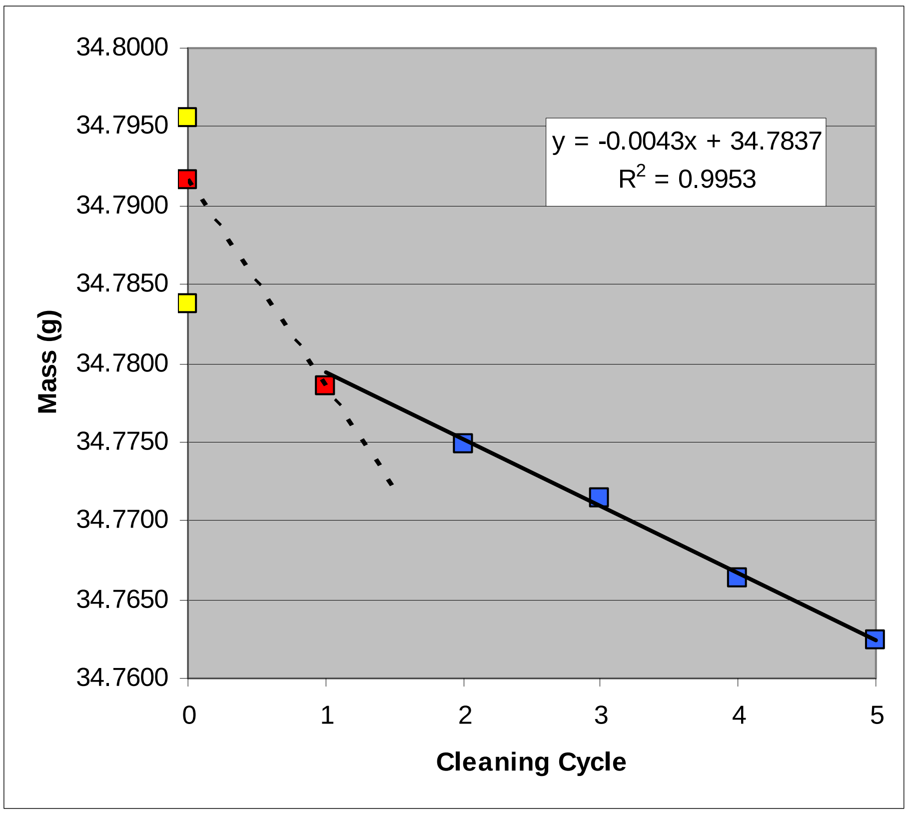

Coupon:	L423
Test Matrix:	Pb-Go-3500-6-2p
Initial wt (g)	35.1465
Removal wt (g)	35.1415

Calculated final wt (g)	35.1292
Total wt loss (g)	0.0173
Total wt loss (mg)	17.3

Cleaning Cycle	Wt (g)
0	35.1415
1	35.1246
2	35.1200
3	35.1138
4	35.1101
5	35.1051

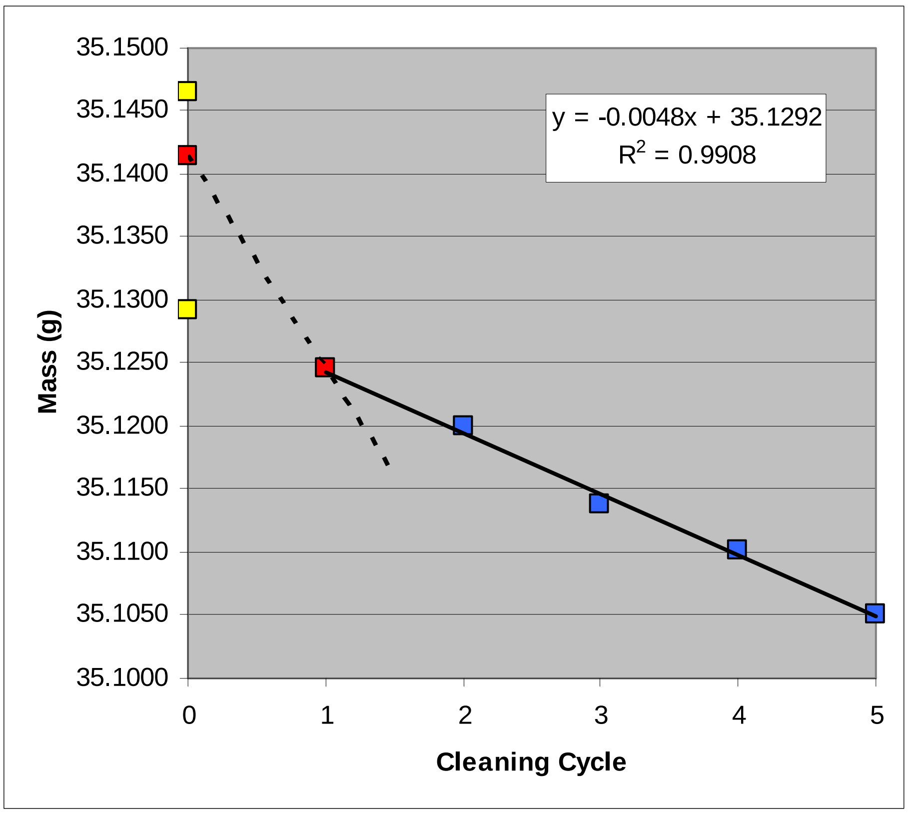

Coupon: L425
Test Matrix: Pb-E-3500-6-1f
Initial wt (g) 34.3943
Removal wt (g) 34.7063

Calculated final wt (g) 34.3891
Total wt loss (g) 0.0052
Total wt loss (mg) 5.2

Cleaning Cycle	Wt (g)
0	34.7063
1	34.4242
2	34.3859
3	34.3789
4	34.3760
5	34.3722

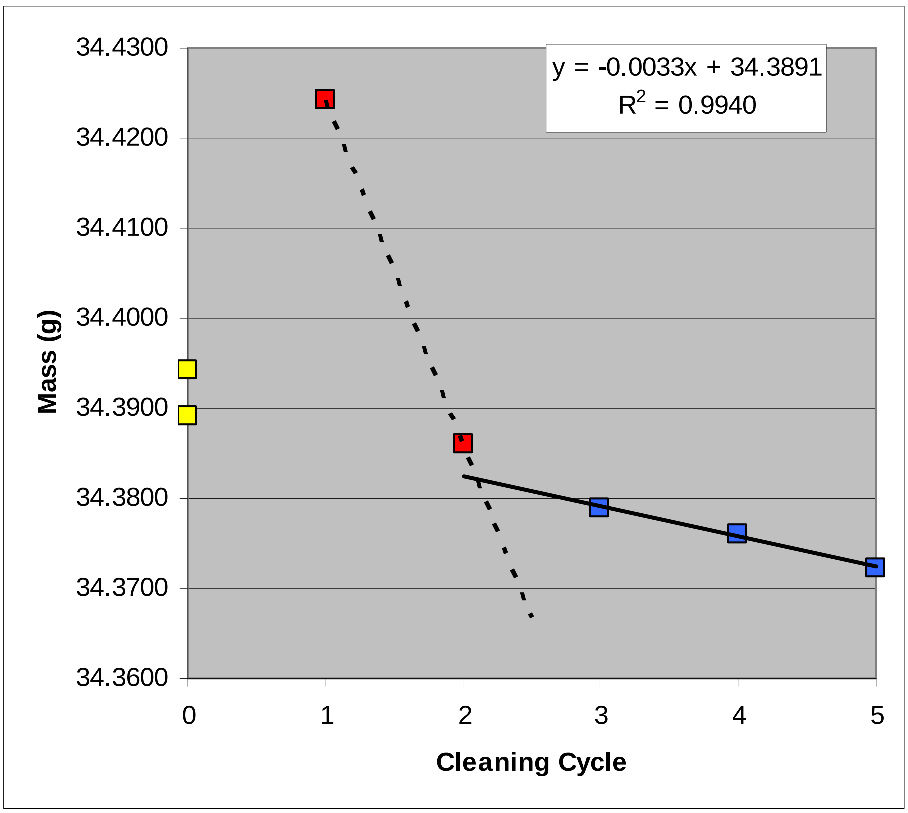

Coupon:	L426
Test Matrix:	Pb-E-3500-6-2f
Initial wt (g)	34.1568
Removal wt (g)	34.2169

Calculated final wt (g)	34.1452
Total wt loss (g)	0.0116
Total wt loss (mg)	11.6

Cleaning Cycle	**Wt (g)**
0	34.2169
1	34.1414
2	34.1368
3	34.1325
4	34.1282
5	34.1241

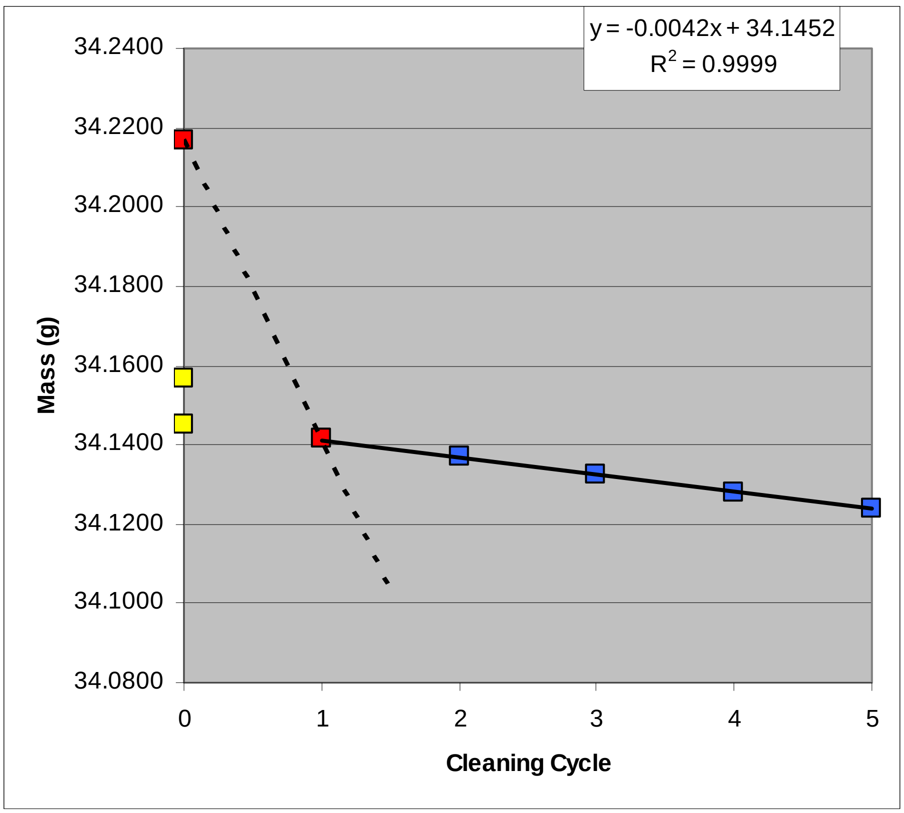

Coupon:	L428
Test Matrix:	Pb-E-3500-6-1p
Initial wt (g)	35.1248
Removal wt (g)	35.2062

Calculated final wt (g)	35.1098
Total wt loss (g)	0.0150
Total wt loss (mg)	15.0

Cleaning Cycle	Wt (g)
0	35.2062
1	35.1300
2	35.1046
3	35.0984
4	35.0942
5	35.0907

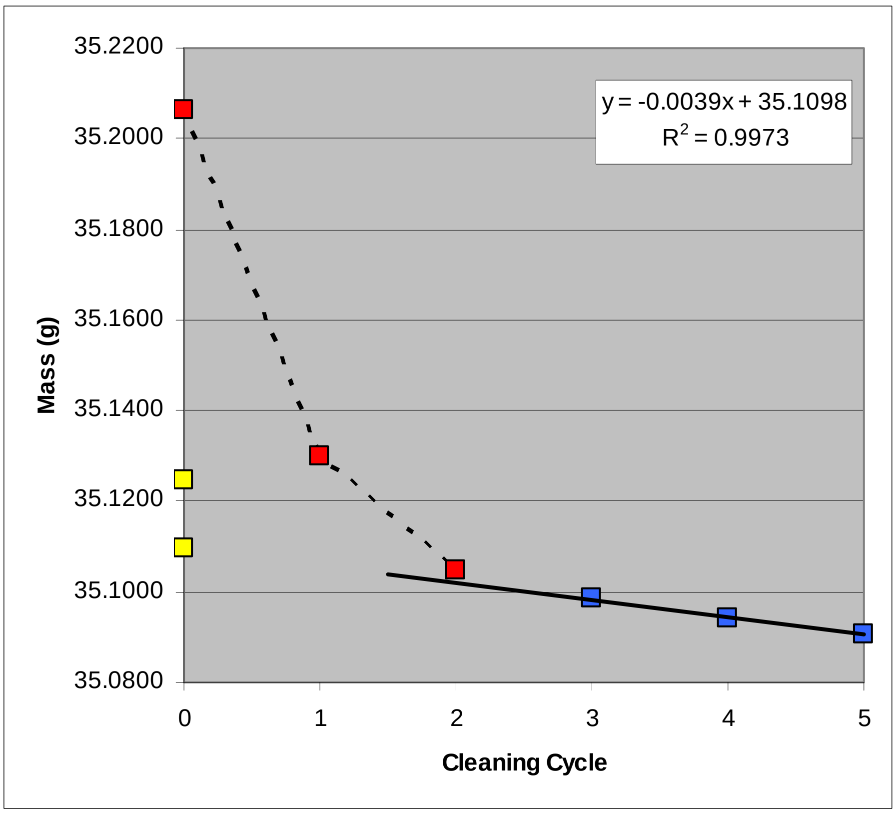

Coupon:	L429
Test Matrix:	Pb-E-3500-6-2p
Initial wt (g)	34.6425
Removal wt (g)	34.6596

Calculated final wt (g)	34.6245
Total wt loss (g)	0.0180
Total wt loss (mg)	18.0

Cleaning Cycle	Wt (g)
0	34.6596
1	34.6199
2	34.6147
3	34.6106
4	34.6053
5	34.6005

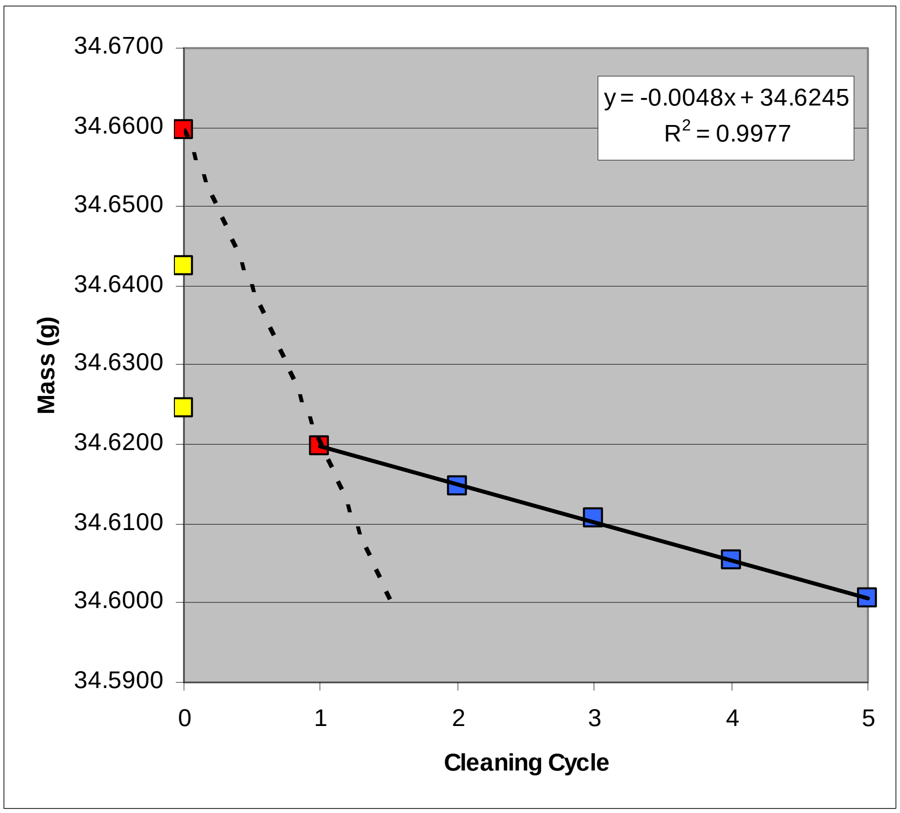

Coupon:	L431
Test Matrix:	Pb-Eo-3500-6-1f
Initial wt (g)	34.7844
Removal wt (g)	34.8063

Calculated final wt (g)	34.7754
Total wt loss (g)	0.0090
Total wt loss (mg)	9.0

Cleaning Cycle	Wt (g)
0	34.8063
1	34.7731
2	34.7691
3	34.7652
4	34.7619
5	34.7592

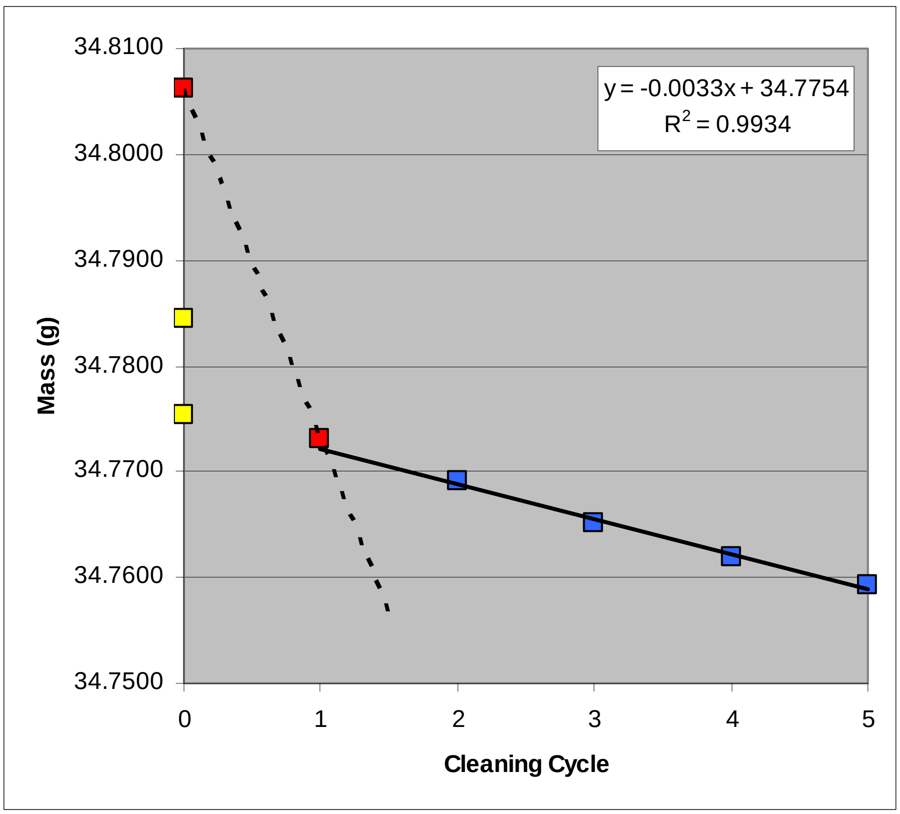

Coupon:	L432
Test Matrix:	Pb-Eo-3500-6-2f
Initial wt (g)	34.7211
Removal wt (g)	34.7537

Calculated final wt (g)	34.7132
Total wt loss (g)	0.0079
Total wt loss (mg)	7.9

Cleaning Cycle	Wt (g)
0	34.7537
1	34.7120
2	34.7058
3	34.7018
4	34.6982
5	34.6945

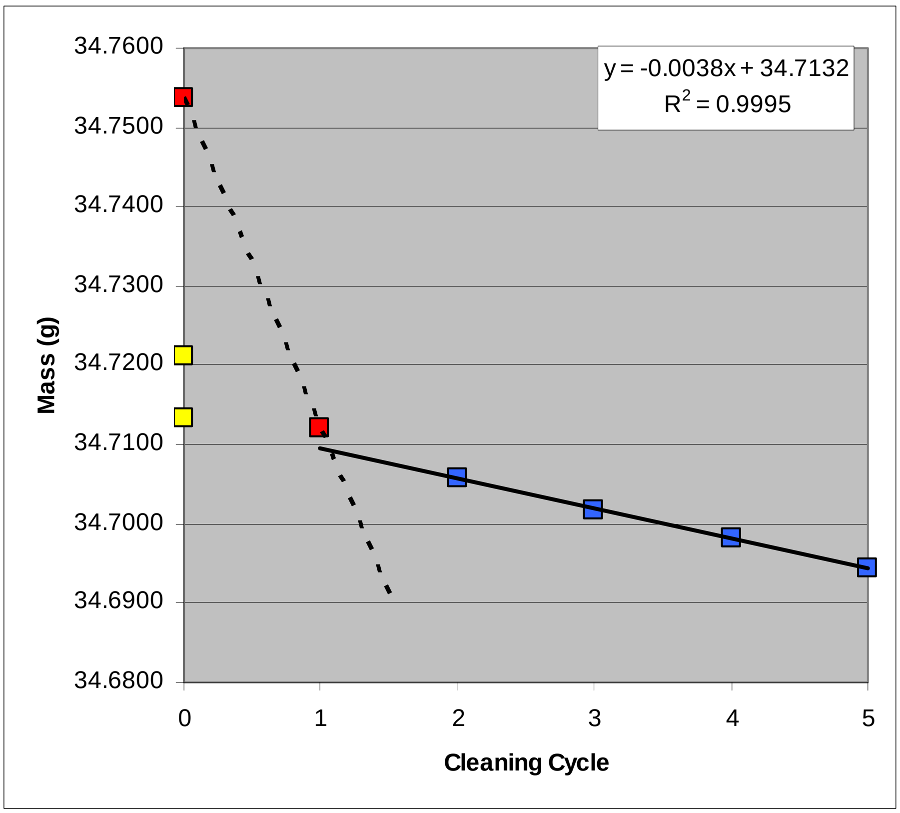

Coupon:	L434
Test Matrix:	Pb-Eo-3500-6-1pf
Initial wt (g)	34.8573
Removal wt (g)	34.8658

Calculated final wt (g)	34.8476
Total wt loss (g)	0.0097
Total wt loss (mg)	9.7

Cleaning Cycle	Wt (g)
0	34.8658
1	34.8450
2	34.8402
3	34.8364
4	34.8327
5	34.8290

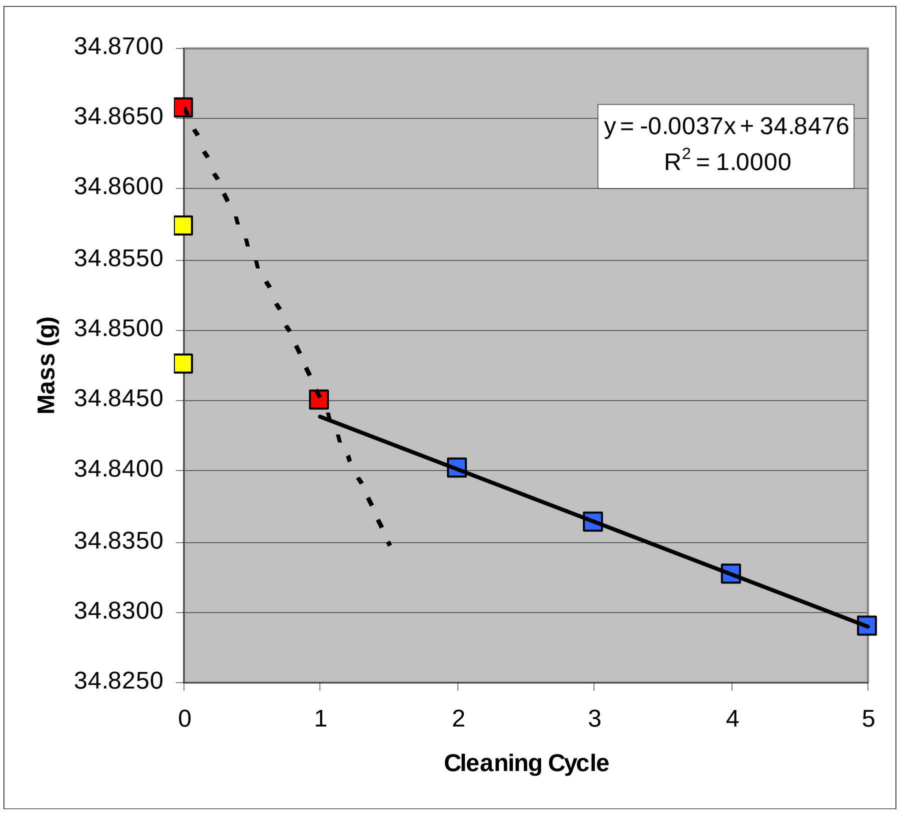

Coupon:	L435
Test Matrix:	Pb-Eo-3500-6-2p
Initial wt (g)	35.1251
Removal wt (g)	35.1781

Calculated final wt (g)	35.1154
Total wt loss (g)	0.0097
Total wt loss (mg)	9.7

Cleaning Cycle	Wt (g)
0	35.1781
1	35.1142
2	35.1077
3	35.1039
4	35.1004
5	35.0961

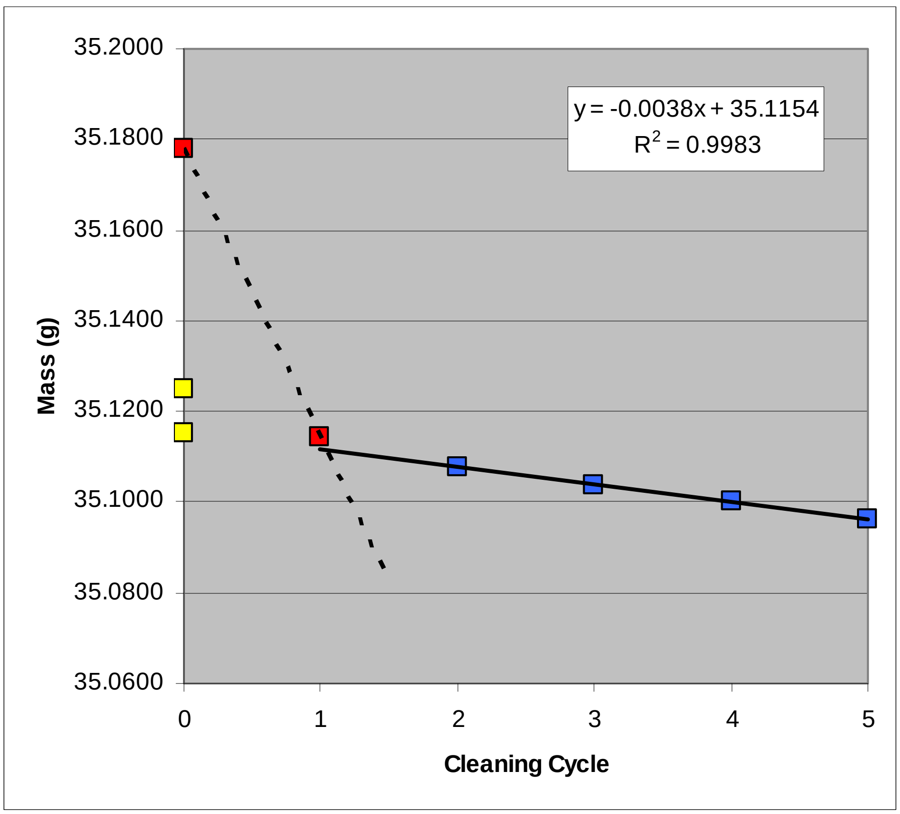

Coupon:	L453
Test Matrix:	Pb-Atm-3500-6-2
Initial wt (g)	34.9586
Removal wt (g)	34.9595

Calculated final wt (g)	34.9565
Total wt loss (g)	0.0021
Total wt loss (mg)	2.1

Cleaning Cycle	**Wt (g)**
0	34.9595
1	34.9509
2	34.9468
3	34.9408
4	34.9358
5	34.9316

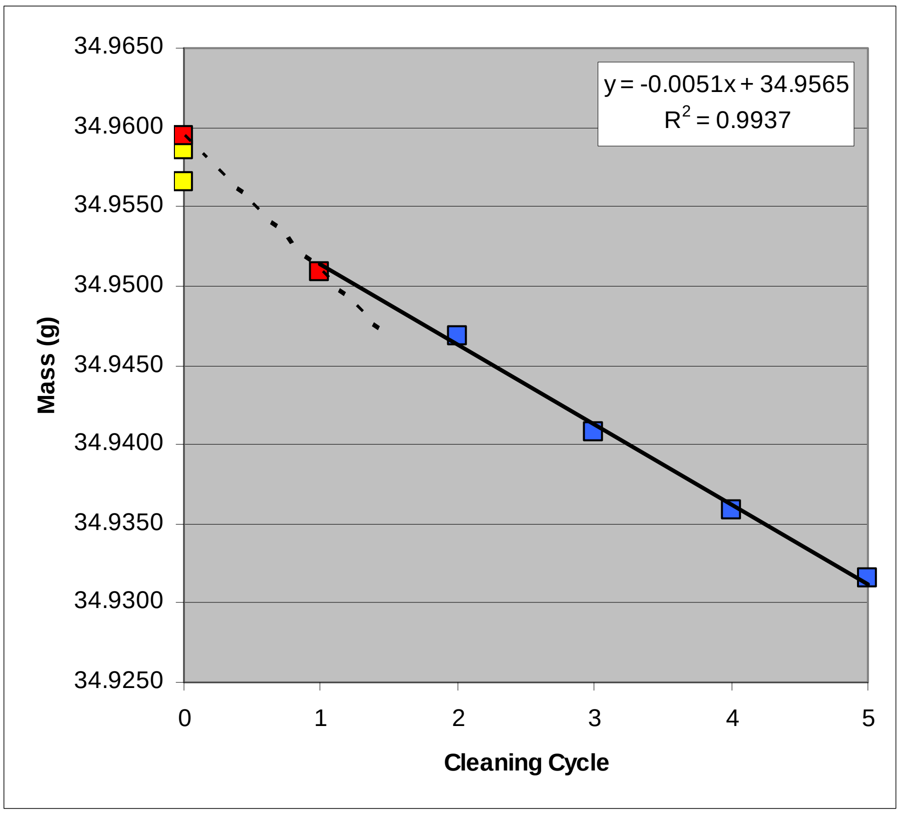

Coupon:	L454
Test Matrix:	Pb-Atm-3500-6-3
Initial wt (g)	34.7891
Removal wt (g)	34.7913

Calculated final wt (g)	34.7879
Total wt loss (g)	0.0012
Total wt loss (mg)	1.2

Cleaning Cycle	Wt (g)
0	34.7913
1	34.7838
2	34.7802
3	34.7754
4	34.7715
5	34.7681